Identification of regulatory mechanisms important to control the *Yersinia pseudotuberculosis* type III secretion and virulence

Von der Fakultät für Lebenswissenschaften

der Technischen Universität Carolo-Wilhelmina zu Braunschweig

zur Erlangung des Grades einer

Doktorin der Naturwissenschaften

(Dr. rer. nat.)

genehmigte

D i s s e r t a t i o n

von Maria Kusmierek
aus Moskau

1. Referentin: Professorin Dr. Petra Dersch
2. Referent: Professor Dr. Michael Steinert
eingereicht am: 24.09.2018
mündliche Prüfung (Disputation) am: 10.12.2018

Druckjahr 2019

Vorveröffentlichungen der Dissertation

Teilergebnisse aus dieser Arbeit wurden mit Genehmigung der Fakultät für Lebenswissenschaften, vertreten durch die Mentorin der Arbeit, in folgenden Beiträgen vorab veröffentlicht:

Publikationen

Kusmierek M, Hoßmann J, Steinmann R, Vollmer I, Volk M, Opitz W, Heroven AK, Wolf-Watz H, Dersch P. A bacterial translocator hijacks riboregulators to control type III secretion in response to host cell contact. PLoS pathog. *Expected to be submitted in September 2018.*

Nuss AM, Beckstette M, **Pimenova M**, Schmühl C, Opitz W, Pisano F, Heroven, A.K., Dersch, P. (2017) Tissue dual RNA-seq allows fast discovery of infection-specific functions and riboregulators shaping host-pathogen transcriptomes. Proc Natl Acad Sci U S A. 2017 Jan 31;114(5): E791-E800.

Tagungsbeiträge

Hoßmann J, **Pimenova M**, Steinmann R, Opitz W, Heroven AK, Dersch P: Thermal and secretion-dependent regulation of the master regulator LcrF in *Yersinia pseudotuberculosis*. (Poster). 4th National Yersinia Meeting, Hamburg, Germany (2014).

Pimenova M, Steinmann R, Hoßmann J, Heroven AK, Dersch P: Regulation of type III secretion by the *Yersinia pseudotuberculosis* carbon storage regulator system. (Talk). Follow-up meeting of the members of DFG priority program SPP1258: „Sensory and regulatory RNAs in Prokaryotes“, Jena, Germany (2014).

Pimenova M, Steinmann R, Opitz W, Heroven AK, Dersch P: Regulation of the major virulence activator LcrF by the *Yersinia pseudotuberculosis* carbon storage regulator system. (Poster). Follow-up meeting oft the members of DFG priority program SPP1258: „Sensory and regulatory RNAs in Prokaryotes CRISPR-Cas“, Braunschweig, Germany (2015).

Pimenova M, Steinmann R, Opitz W, Hoßmann J, Heroven AK, Dersch P: Regulation of the major virulence activator LcrF by the *Yersinia pseudotuberculosis* carbon storage regulator system. (Talk). 5th National Yersinia Meeting, Münster, Germany (2016).

Pimenova M, Hoßmann J, Steinmann R, Opitz W, Heroven AK, Dersch P: Regulation of the major virulence activator LcrF by the *Yersinia pseudotuberculosis* carbon storage

regulator system. (Poster). Follow-up meeting oft the members of DFG priority program SPP1258: „Sensory and regulatory RNAs in Prokaryotes CRISPR-Cas, Munich, Germany (2016).

Pimenova M, Hoßmann J, Steinmann R, Opitz W, Heroven AK, Dersch P: Identification of regulatory mechanisms important to control *Yersinia pseudotuberculosis* type III secretion and virulence. (Talk). Microbiology and Infection 2017 – 5th Joint Conference of DGHM & VAAM, Würzburg, Germany (2017).

Kusmierek M, Hoßmann J, Steinmann R, Opitz W, Heroven AK, Dersch P: Regulation of the major virulence activator LcrF by the *Yersinia pseudotuberculosis* carbon storage regulator system. (Poster). Annual Conference 2018 of the Association for General and Applied Microbiology, Wolfsburg, Germany (2018).

Kusmierek M, Hoßmann J, Steinmann R, Opitz W, Heroven AK, Dersch P: Identification of regulatory mechanisms important to control *Yersinia pseudotuberculosis* type III secretion and virulence. (Poster). RNA Meeting on Sensory and Regulatory RNA, Gießen, Germany (2018).

Kusmierek M, Hoßmann J, Steinmann R, Opitz W, Heroven AK, Dersch P: Identification of regulatory mechanisms important to control *Yersinia pseudotuberculosis* type III secretion and virulence. (Talk). Young Microbiologists Symposium 2018, Belfast, Northern Ireland (2018).

Table of contents

Abbreviations

%	per cent
°C	degree Celsius
A	adenine
Ap	ampicillin
APEC	avian pathogenic *E. coli*
APS	ammonium persulfate
approx.	approximately
ATP	adenosine triphosphate
asRNA	anti-sense RNA
aqua bidest	double-destilled water
ATP	adenosine triphosphate
BHI	brain-heart infusion
BSA	bovine serum albumin
bp	base pair
C	cytosine
CCD	charge-coupled device
Cb	carbenicillin
cDNA	complementary DNA
CDS	coding sequence
CIP	calf intestinal phosphatase
CLIP-seq	UV crosslinking-immunoprecipitation-high-throughput sequencing
Cm	chloramphenicol
CRP	cAMP receptor protein
Csr	carbon storage regulator
Ct	cycle threshold
Da	dalton
DNA	desoxyribonucleic acid
dNTP	deoxynucleotide triphosphate
DTT	dithiothreitol
DYT	double yeast tryptone
e.g.	*exampli gratia*
EDTA	ethylenediaminetetraacetic acid
ECM	extracellular matrix
EHEC	enterohemorrhagic *E. coli*
EMSA	electromobility shift assay
EPEC	enteropathogenic *E. coli*
ERCC	external RNA controls consortium
ESR	extracytoplasmatic stress responses
ESRS	extracytoplasmatic stress response system
et al.	*et alii*
EtBr	ethidium bromide
FC	fold change

G	guanine
g	gram
γ-^{32}P-ATP	ATP, labeled on the gamma phosphate group with ^{32}P
GGEP	global gene-expression profile
h	hour(s)
HF	high fidelity
HRP	horseradish peroxidase
HTH	helix-turn-helix (HTH)
i.e.	*id est*
InvA	invasin A
Kan	kanamycin
kb	kilobase
kDa	kilo-Dalton
KEGG	Kyoto Encyclopedia of genes and genomes
kV	kilovolt
lacZ	reporter gene encoding for β-galactosidase
l	liter
LB	Luria-Bertani medium
LCR	low calcium response
LPS	lipopolysaccharide
LRR	leucine-rich repeat
M	molar
mA	milliampere
M cell	microfold cell
µCi	microcurie
µF	microfarad
µg	microgram
mg	milligram
min	minute(s)
mJ	millijoule
µl	microliter
ml	milliliter
MLN	mesenteric lymph nodes
MOPS	3-(N-morpholino)propanesulfonic acid
mM	millimolare
MS	membrane and supramembrane
NaOx	disodium oxalate
NCBI	National Center for Biotechnology Information
NCS	newborn calf serum
NEB	New England Biolabs
ncRNA	non-coding RNA
ng	nanogram
nm	nanometer
nM	nanomolare

NMR	nuclear magnetic resonance
nt	nucleotides
OD	optical density
Ω	ohm
OM	outer membrane
OMVs	outer membrane vesicles
ONPG	o-nitrophenyl-β-D-galactosidase
PAGE	polyacrylamide gel electrophoresis
PBS	phosphate buffered saline
PCR	polymerase chain reaction
PNK	T4 polynucleotide kinase
PP	Peyer's patches
PRKs	protein kinase C-related kinases
PVDV	polyvinylidene fluoride
pYV	plasmid of *Yersinia* virulence
qRT-PCR	quantitative real-time PCR
R	resistance
RBS	ribosomal-binding site
RBP	RNA-binding protein
RIN	RNA integrity number
RIP-seq	RNA-binding protein immunoprecipitation sequencing
RLU	relative luminescence units
RNA	ribonucleic acid
RNA-seq	high-throughput RNA sequencing
RPKM	reads per kilobase million
RPMI	Roswell Park Memorial Institute
rpm	rotations per minute
rRNA	ribosomal RNA
RSK	ribosomal S6 kinase
Rsm	regulator of secondary metabolism
SD	Shine-Dalgarno
SDS	sodium dodecyl sulfate
SPI-1/2	*Salmonella* pathogenicity island-1/2
spp.	*Species pluralis*
Syc	specific Yop chaperone
t	time
T	thymine
T3S	type three secretion
T3SS	type three secretion system
T6SS	type VI secretion system
TAE	tris-acetate buffer
TAP	tobacco acid pyrophosphatase
Taq	DNA polymerase of *Thermus aquaticus*
TBE	Tris/Borate/EDTA

TCA	trichloroacetic acid
TCS	two component systems
TE	Tris-EDTA buffer
TEMED	tetramethylethylenediamine
TPRs	tetratricopeptide repeats
Tris	trishydroxymethylaminomethane
tRNA	transfer RNA
TSS	transcriptional start site
U	uridine or units
UV	ultra violet
UTR	untranslated region
V	volume
vs.	versus
v/v	volume per volume
v/w	weight per volume
WHO	World Health Organization
wt	wild type
XL	crosslinking
YadA	*Yersinia* adhesin A
YmoA	*Yersinia* modulator A
Yop	*Yersinia* outer proteins
Ysc	*Yersinia* secretion

Figures

Tables

1 Introduction

Bacteria represent a widespread group of microorganisms, whose members have conquered almost all conceivable habitats. Their success relies on the ability to rapidly adjust their metabolism in response to constantly varying environmental conditions and stressors. To do so, a precise regulation of gene expression is indispensable. One of the best examples demonstrating sophisticated regulation of gene expression under dramatically changing environmental conditions is the group of pathogenic bacteria. During infection, pathogens are confronted with severe alterations between outside and inside the host (temperature, pH, ion content, oxygen concentration as well as nutrition supply). Furthermore, they have to evade recognition by the host immune system and to compete with the host microbiota in order to survive and persist. Consequently, pathogenic bacteria are forced to judge numerous environmental parameters and to process this information to choose the gene expression program ideal for each stage of infection.

1.1 The genus *Yersinia*

The genus *Yersinia*, a member of the phylum of γ-Proteobacteria in the family *Enterobacteriaceae*, was named after the French bacteriologist Alexandre Yersin (1863-1943) (Bottone, 1997). In Hong Kong in June 1894, Yersin discovered a bacterial cause of the Chinese plague and named it *Pasteurella pestis*, after his mentor, Louis Pasteur. In 1970, *Pasteurella pestis* was renamed to *Yersinia pestis* in memory of its discoverer (Zietz & Dunkelberg, 2004; Hawgood, 2008; Butler, 2014). The members of the genus *Yersinia* are Gram-negative, non-sporeforming rods or coccobacilli that grow facultative aerobically. Although, yersiniae are psychrotolerant and able to grow in a temperature range between 4°C and 43°C, their growth optimum lies between 25-29°C (Bottone, 1999). The genus consists of 18 species, three of which are pathogenic for animals and humans (McNally *et al*., 2016). *Y. enterocolitica* and *Y. pseudotuberculosis* are enteric pathogens that have emerged 200 million years ago. *Y. pestis*, the causative agent of pneumonic, bubonic and septicaemic plague, is a recently evolved (1,500-20,000 years ago) clonal variant of *Y. pseudotuberculosis* with approximately 98% homology at the DNA level (Achtman *et al*., 1999; Achtman *et al*., 2004; Plano & Schesser, 2013; Wren, 2003). All three species are facultative intracellular pathogens with a zoonotic lifestyle, exhibit tropism for lymphoid tissue and are able to evade the host immune system (Bhunia, 2008; Koornhof *et al*., 1999; Smego *et al*., 1999). Furthermore, pathogenicity of these *Yersinia* spp. strongly depends on the presence of the ~70 kb virulence plasmid (pYV in *Y. enterocolitica*, pIB1/pYV in *Y. pseudotuberculosis* and pCD1 in *Y. pestis*), which encodes several factors crucial for survival and persistence in the host (Brubaker, 1991; Cornelis *et al*., 1989; Gemski *et al*., 1980; Portnoyt & Falkowt, 1981). Despite the aforementioned similarities between the pathogenic yersiniae, their transmission and infection routes as well as disease severity vary significantly (Fig. 1.1).

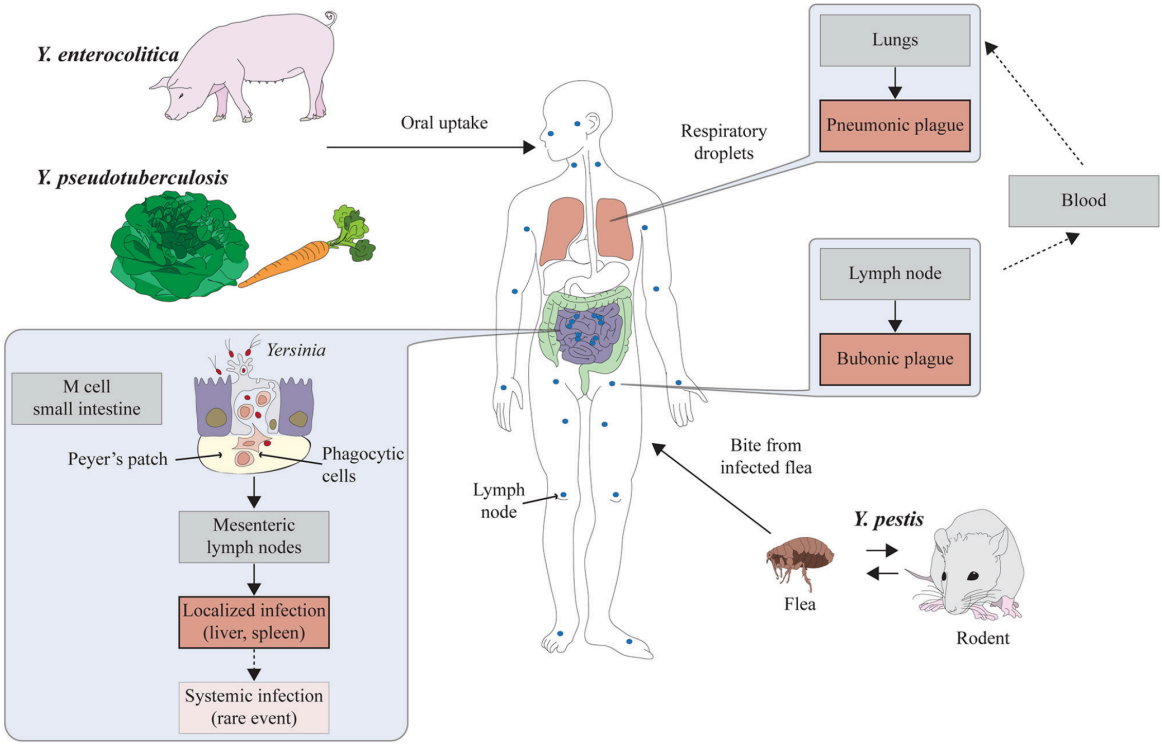

Figure 1.1. Life style and transmission ways of pathogenic yersiniae.
Y. pestis possesses a complex lifestyle with diverse rodent reservoirs in nature. Transmission occurs via flea bites, causing bubonic plague. Pneumonic plague is transmitted from person to person through respiratory droplets. In contrast to *Y. pestis,* the enteric pathogens *Y. enterocolitica* and *Y. pseudotuberculosis* enter the host by ingestion of contaminated food or water and invade the lymphatic system through the M cells of the small intestine. This results in localized or, in rare cases, in systemic infection (Heroven & Dersch, 2014)[1].

Both enteric *Yersinia* species are food-borne pathogens that are transmitted via the fecal-oral route through ingestion of contaminated food or water. Typically, they cause a self-limiting invasive gastrointestinal disease in humans and animals called Yersiniosis (Koornhof *et al*., 1999). Nevertheless, *Y. enterocolitica* and *Y. pseudotuberculosis* differ significantly, both pheno- and genotypically (Wren, 2003). *Y. enterocolitica* represents a heterogeneous group of bacteria based on biochemical, antigenic and virulence properties. For instance, in terms of their pathogenicity level *Y. enterocolitica* strains can be distinguished in nonpathogenic (Biotype 1A), weakly pathogenic (Biotypes 2-5) and highly pathogenic (Biotype 1B) biotypes (McNally *et al*., 2004). *Y. pseudotuberculosis* strains, in contrast, are less variable in biochemical reactions and can be divided into 21 serotypes according to their O-antigen structure (Bogdanovich *et al*., 2003; Kenyon *et al*., 2017). Remarkably, while the serotypes O1-O5 are almost exclusively pathogenic, serotypes O6-O15 were never been found in human clinical samples (Fukushima, 2003). However, even the biotypes isolated from animals and the environment (O6-O15) contain certain pathogenicity factors. Consequently, all *Y. pseudotuberculosis* strains are considered potentially pathogenic for humans (Carniel, 2001). Due to the heterogeneity of yersiniae populations, the sources of contamination are also extremely variable and include

[1] Heroven and Dersch (2014) is licensed under the terms of the Creative Commons Attribution License (CC BY).

soil, water, plants and a variety of animals (Langford, 1972; Frandölich *et al*., 2003; Jalava *et al*., 2004; Jalava *et al*., 2006; Muhldorfer *et al*., 2010; Fogelson *et al*., 2015).

Although enteropathogenic *Yersinia* species are distributed on all continents, Yersiniosis is most common in Europe, rather than in tropical or subtropical regions, with the highest incidence rate in Germany (Bottone, 1999; Rosner *et al*., 2010; Kamińska & Sadkowska-Todys, 2016). While Yersiniosis is primarily associated with *Y. enterocolitica* infection and less frequently with *Y. pseudotuberculosis*, several outbreaks of *Y. pseudotuberculosis* infection cases have been, nevertheless, reported in Finland, Russia, Korea and Japan (Fukushima *et al*., 1985; Koo *et al*., 1996; Voskressenskaya *et al*., 2004; Jalava *et al*., 2006). Yersiniosis is usually accompanied by several gut-associated symptoms ranging from mild diarrhea to mesenteric lymphadenitis with abdominal pain and fever. However, especially in immunocompromised individuals, Yersiniosis can invoke more severe post infection sequelae including Kawasaki disease, tubulointerstitial nephritis, urethritis, chronic prostatitis, inflammatory bowel disease and Grave's disease, pleurisy, cholecystitis, reactive arthritis, erythema nodosum and septicemia (Tertti *et al*., 1989; Fukumoto *et al*., 1995; Ljungberg *et al*., 1995; Naiel & Raul, 1998; Hannu *et al*., 2003; Jalava *et al*., 2006; Hargreaves *et al*., 2013; Horinouchi *et al*., 2015; Tuompo *et al*., 2017). Additionally, recent studies demonstrated that enterocolitis caused by *Y. pseudotuberculosis* can clinically mimic malignant lymphoma (Imataki *et al*., 2014). Occasionally, even patients lacking any immune disorders can acquire life-threatening *Yersinia*-associated sepsis via transfusion of *Y. enterocolitica*-contaminated blood (Tipple *et al*., 1990; Guinet *et al*., 2011).

In contrast to the enteric lifestyle of *Y. enterocolitica* and *Y. pseudotuberculosis*, *Y. pestis* has a mammalian blood-borne lifestyle and primarily uses infected rodent fleas as vectors for transmission (Zhou & Yang, 2009). Additionally, *Y. pestis* can spread through inhalation of bacteria-containing aerosols. In rare cases, *Y. pestis* infection can occur via direct contact or injection of infected animals (Perry & Fetherston, 1997). The extreme differences in lifestyle and virulence between enteropathogenic yersiniae and *Y. pestis* are a result of the few evolution-driven key changes in the genome (*e.g.* inactivation of *yadA* and O antigen cluster, gain of *pla* and *ymt* and loss of *ureD*, PDE2, *rcsA*, and PDE3) as well as acquisition of two additional plasmids by *Y. pestis* (pPCP1 and pMT1) (Atkinson & Williams, 2016; Hinnebusch *et al*., 2016; Reuter *et al*., 2014; Zhou & Yang, 2009). Although plague is considered to be an ancient disease, the World Health Organization (WHO) classified *Y. pestis* as a re-emerging pathogen (Guiyoule *et al*., 2001). Indeed, plague cases are still reported in China, in the United States (in Arizona in 2007 and in Chicago in 2009) and in Africa, mostly in Congo (Butler, 2013). Recently, two large outbreaks of pneumonic plague in Madagascar and Asia were stated (Butler, 2013). An unusually widespread outbreak of pneumonic and bubonic plague was reported in Madagascar (August 2017 through October 2017) ("WHO | Plague – Madagascar," 2017).

1.2 Infection process of enteropathogenic *Yersinia* species

The infection process of *Y. enterocolitica* and *Y. pseudotuberculosis* can be classified into two main acute phases. Those are the initial infection and the ongoing infection. Both acute infection phases are defined by expression of a distinct set of virulence factors (Fig. 1.2). The appropriate expression of these factors promotes an efficient colonization of specific host niches as well as resistance against host defense mechanisms.

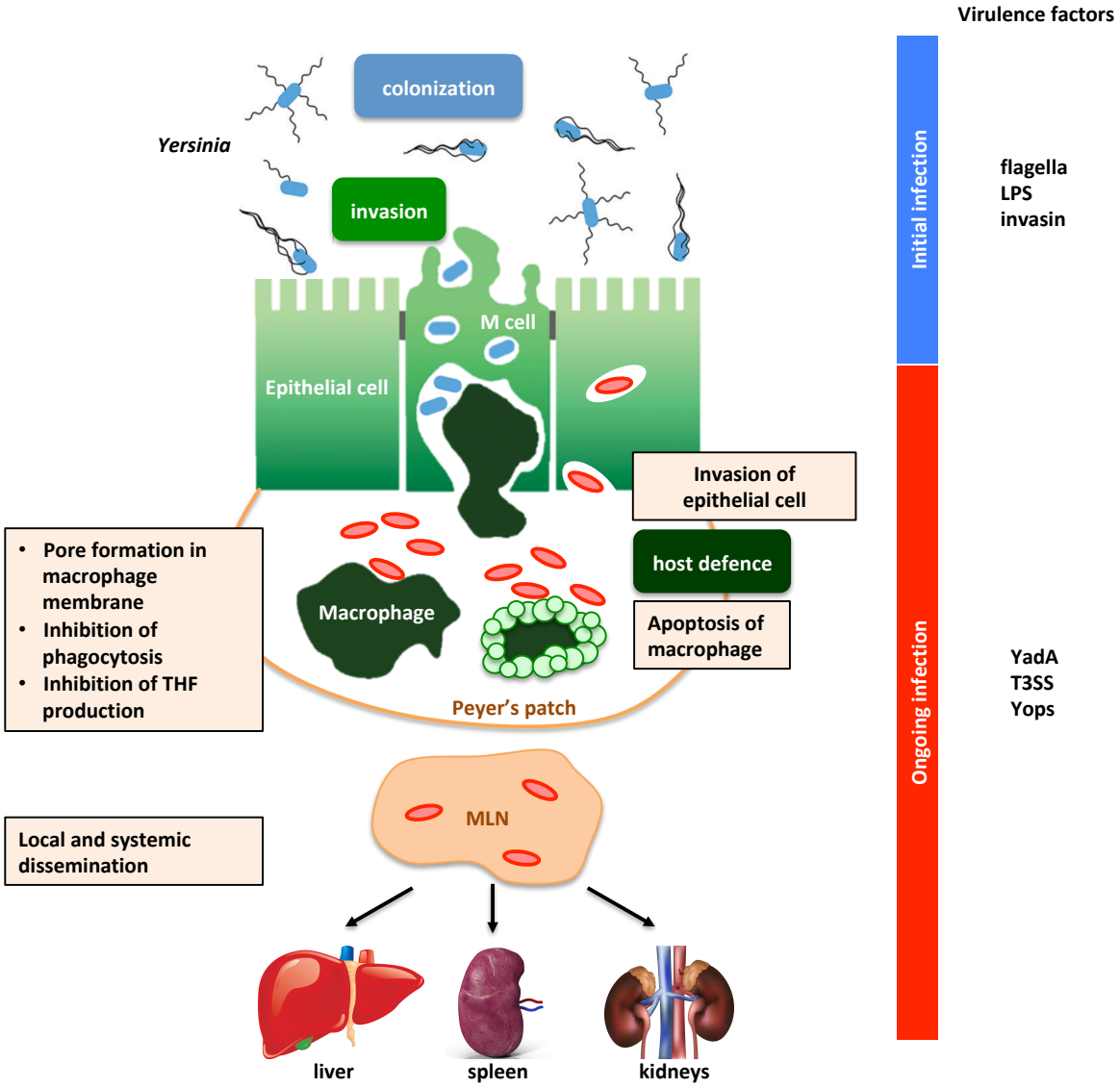

Figure 1.2. Infection process of enteropathogenic yersiniae.
Infection process of enteropathogenic yersiniae can be divided into two main phases: (i) Initial infection and (ii) Ongoing infection. (i) After ingestion, enteropathogenic *Yersinia* species pass through the gastrointestinal tract until they reach ileum. There, *Yersinia* are taken up by the M cells and enter the underlying lymphoid tissue (Peyer's patches). (ii) Once yersiniae reach lymphoid tissues, they are confronted with resident macrophages. Pathogens overcome the host immune system using the virulence plasmid-encoded factors: YadA, the T3SS and the effector proteins (Yops). Consequently, the bacteria are able to disseminate to the mesenteric lymph nodes (MLN)

and to systemic organs, such as liver, spleen, and kidney (modified after Sansonetti, 2004[2] and Erhardt & Dersch, 2015[3]).

Although in most cases the enteropathogenic *Yersinia* elicit acute infection, recent studies demonstrated their ability to develop a persistent infection (Fahlgren *et al.*, 2014, Avican *et al*., 2015). Moreover, the *Yersinia* persistent infection has been associated with several chronic inflammatory diseases, such as reactive arthritis, Crohn's disease, inflammatory bowel disease, and pseudoappendicitis (Girschick *et al*., 2008; Ternhag *et al*., 2008).

1.2.1 Initial infection phase

The two main aims of the enteropathogenic yersiniae during the initial infection phase are 'colonization' and 'invasion'. The initial infection begins with ingestion of the pathogen via consumption of contaminated food and water. Thereafter, the bacteria pass through the gastrointestinal tract until they reach the ileum. This terminal part of the small intestine is characterized by the presence of the microfold cells (M cells). These cells are preferentially found in the epithelia, overlying the organized lymphoid follicles of the gut-associated lymphoid tissue including the Peyer's patches. M cells possess unique morphological features, such as reduced glycocalyx, irregular brush border and reduced microvilli. Moreover, they are specialized for the sampling of the macromolecules, antigens and microorganisms within the gut lumen and their direct transport into the underlying lymphoid tissue. These exclusive properties make the M cells an excellent gateway for bacteria into the host (Jang *et al*., 2004; Mabbott *et al*., 2013). To initiate an active internalization and transmigration through the intestinal epithelial barrier via the M cells, enteropathogenic *Yersinia* harbor the chromosomally encoded protein invasin (Grutzkau *et al*., 1990). The *invA* gene encoding invasin is strongly expressed in stationary phase at 25 °C, pH 8 but shows poor expression at 37 °C, pH 8 (Nagel *et al*., 2001). This highlights that invasin expression prior to oral uptake might be beneficial for efficient transcytosis through the epithelial barrier (Pepe & Miller, 1993). Interestingly, under acidic conditions (pH 5.5), invasin expression in *Y. enterocolitica* occurs even at 37 °C (Grassl *et al*., 2003; Revell & Miller, 2000; Uliczka *et al*., 2011). Invasin is a surface-exposed outer membrane protein closely related to intimins and establishes an interaction with β_1-integrins (Isberg, 1990; Hamburger *et al*., 1999; Tsai *et al*., 2010). Remarkably, β_1-integrins are specific for the luminal side of M cells, but not for that of other enterocytes. Binding of *Yersinia* Invasin to the β_1-integrin triggers the actin polymerization at the contact site of the M cell, initiating uptake of the pathogen. Consequently, *Yersinia* is internalized by the so-called 'zipper' mechanism (Marra & Isberg, 1997; Sansonetti, 2002). Further virulence factors required for successful establishment of the initial infection are chromosomally encoded flagella, O-antigen coupled lipopolysaccharides (LPS) as well as several other adhesins (Young *et al*., 2000; Skurnik, 2004; Uliczka *et al*., 2011; Hoffman *et al*., 2017).

[2] Adapted by permission from Springer Nature: Springer Nature, Nature Reviews Immunology, War and peace at mucosal surfaces, Philippe J. Sansonetti, Copyright © 2004

[3] Heroven and Dersch (2014) is licensed under the terms of the Creative Commons Attribution License (CC BY).

1.2.2 Ongoing infection phase

After transmigration through the epithelial barrier, yersiniae invade the underlying lymphatic tissue, particularly Peyer's patches, followed by dissemination into mesenteric lymph nodes (MLNs), liver, spleen, and, occasionally, kidney (Autenrieth *et al*., 1996; Barnes *et al*., 2006; Heroven & Dersch, 2006), referred to as ongoing infection phase. Replication of *Yersinia* in these tissues and organs occurs extracellularly via formation of monoclonal microcolonies within necrotic microabscesses (Simonet *et al*., 1990; Oellerich *et al*., 2007; Trülzsch *et al*., 2007). Remarkably, *Yersinia* was also shown to survive and proliferate inside macrophages. During the ongoing infection, yersiniae are confronted with the host immune system. Thus, the primary goal of the pathogen in this phase is to evade a host's immune response. In order to survive and multiply in the lymphoid tissue as well as for dissemination into deeper organs, enteroinvasive *Yersinia* species require an additional set of virulence factors. The antiphagocytic defense system of *Yersinia* includes the virulence plasmid-encoded *Yersinia* adhesin A (YadA), the type III secretion system (T3SS), and the corresponding "anti-host" effector proteins (Yops) (Cornelis *et al*., 1998; Atkinson & Williams, 2016). Synthesis of these virulence factors prevents uptake and elimination of enteric *Yersinia* by professional phagocytes (Bliska *et al*., 2013). Furthermore, Yops were recently reported to impair the degranulation of neutrophils, which further increases *Yersinia* survival (Taheri *et al*., 2016). Transcription of the genes encoding for this integrated defense system is activated by the AraC-type regulator LcrF (VirF in *Y. enterocolitica*) in response to temperature and host cell contact (Bölin *et al*., 1988; Pettersson *et al*., 1996).

1.2.2.1 Plasmid-encoded virulence factors

Yersinia adhesin YadA

The *Yersinia* adhesin YadA represents a versatile virulence factor expressed in both enteric *Yesinia* species (Bölin & Wolf-Watz, 1982; Ackermann *et al*., 2008). This trimeric autotransporter adhesin (TAA) belongs to the family of oligomeric coiled-coil adhesins (Oca) (Hoiczyk *et al*., 2000; Linke *et al*., 2006). YadA forms a fibrous, lollipop-like structure of approximately 23 nm in length and densely covers the entire bacterial surface (Hoiczyk *et al*., 2000). Mature YadA harbors two functional regions, an N-terminal extracellular (passenger) domain and a C-terminal β-barrel (translocation) domain anchored in the outer membrane (Fig. 1.3).

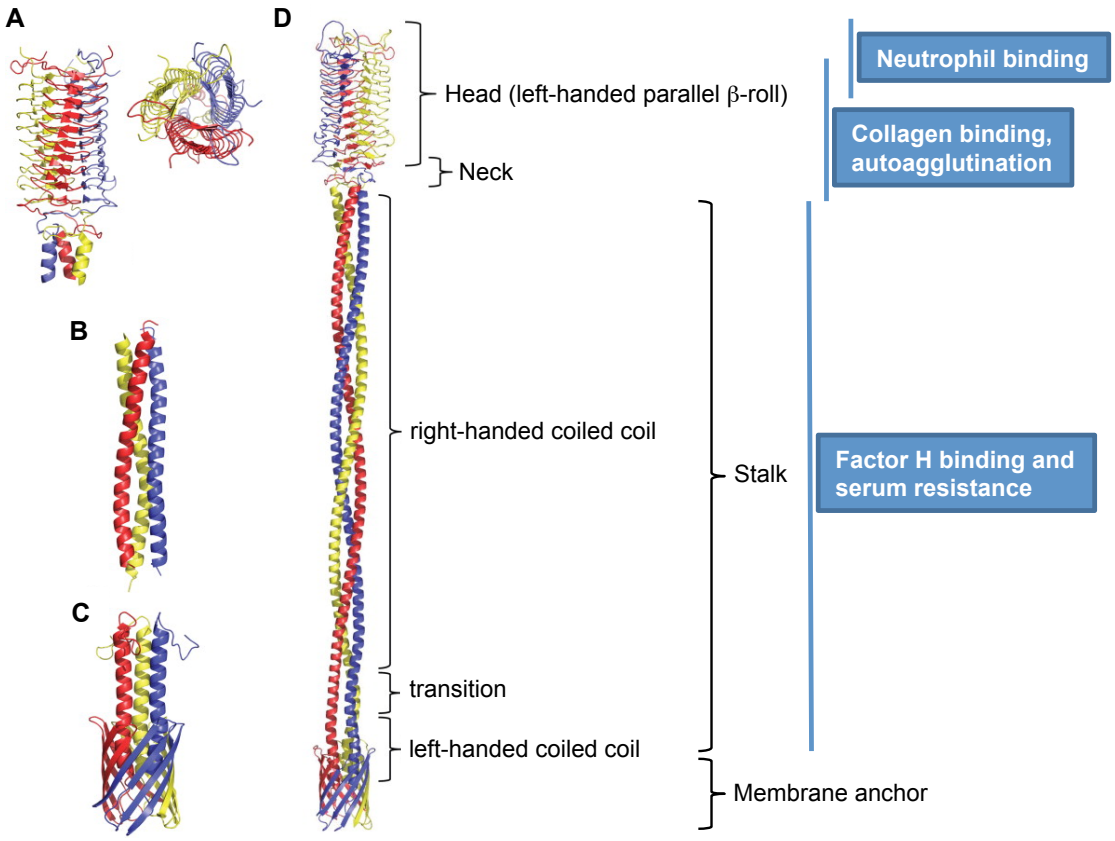

Figure 1.3. Structure of YadA from *Y. enterocolitica*.
A Crystal structure of the collagen-binding head domain in side view (left), representing the left-handed parallel β-roll, in top view (right), showing the trimeric organization. **B** Crystal structure of the transition zone from right- (upper region) to left-handed (lower region) supercoiling. **C** Solid-state nuclear magnetic resonance structure of the translocation domain, demonstrating the 12-stranded β-barrel linker within the pore of the barrel and the beginning of the stalk. **D** Model of the complete YadA structure with various elements and coiled-coil regions. Binding regions for different ligands are annotated (modified after Mikula *et al*., 2013[4] and Mühlenkamp *et al*., 2015[5]).

The passenger domain consists of three main parts: a pillar-like stalk made of right-handed coiled coils, a neck (connector), and a bulky head (Szczesny & Lupas, 2008). These regions are diverse and appear repetitively in various combinations. The translocation domain, in contrast, is more conserved. It performs type Vc secretion of the N-terminal domain through the outer membrane, defining this adhesin family as 'autotransporter' (Henderson *et al*., 2004; Leo *et al*., 2012).

YadA synthesis begins immediately after *Yersinia* cross the intestinal mucosa. It possesses a variety of activities, which contribute to successful establishment of infection (Mikula *et al*., 2013). These include: binding to the extracellular matrix (ECM) molecules collagen, fibronectin, and laminin (Schulze-Koops *et al*., 1992; Flügel *et al*., 1994; Heise & Dersch, 2006), adhesion to epithelial cells, neutrophils, and macrophages (Heesemann *et al*., 1987; Roggenkamp *et al*., 1996), invasion of epithelial cells and induction of pro-inflammatory

[4] Mikula *et al*., 2013 is licensed under the terms of the Creative Commons Attribution License.

[5] Adapted by permission from Elsevier GmbH: Elsevier, International Journal of Medical Microbiology, *Yersinia* adhesin A (YadA) – Beauty & beast, Mühlenkamp *et al*., Copyright © 2015.

cytokines (Eitel & Dersch, 2002; Eitel *et al*., 2004), serum resistance (Lambris *et al*., 2008; Biedzka-Sarek *et al*., 2005), and autoagglutination (Hoiczyk *et al*., 2000). Notably, YadA is indispensible for virulence in *Y. enterocolitica*, but not in *Y. pseudotuberculosis* (Pepe *et al*., 1995; Roggenkamp *et al*., 1995; Han & Miller, 1997). For instance, in *Y. enterocolitica* the YadA-mediated adhesion is an imperative prerequisite for an efficient translocation of effector proteins. In particular, the length of the T3SS injectisome and YadA are functionally coupled (Mota *et al*., 2005). Interestingly, although the *yadA* gene is present in *Y. pestis*, it is inactivated via a frame shift mutation caused by a single nucleotide deletion (Rosqvist *et al*., 1988). Moreover, expression of *Y. pseudotuberculosis* YadA is detrimental for *Y. pestis* and reduces its virulence (Skurnik & Wolf-Watz, 1989; Eitel & Dersch, 2002).

The *Yersinia* Ysc-Yop virulon

One of the most efficient strategies subverting the host defense is the direct injection of anti-phagocytic effector proteins into the cytosol of the host cell via a sophisticated nanomachine called T3SS (Fig. 1.4). The T3SS forms a cylindrical structure spanning the bacterial envelope with a hollow needle-like element, which protrudes from the outer surface of the basal body (Izoré *et al*., 2011). It is generally believed that the effector proteins are injected through the needle-like structure of the T3SS into the cytosol of the target cell after contact between the pathogen and the eukaryotic cell has been established (Cornelis & Van Gijsegem, 2000). This mechanism of 'toxin' delivery is highly conserved and has proven to be ubiquitous among a large number of Gram-negative mammalian and plant pathogens (e.g. pathogenic *Escherichia coli*, *Yersinia*, *Salmonella*, *Shigella*, *Bordetella*, *Chlamydia*, *Pseudomonas*, *Xanthomonas*, *Ralstonia*, and *Erwinia* species) (Cornelis & Van Gijsegem, 2000). All three pathogenic *Yersinia* species demand the plasmid-encoded Ysc (Yop secretion)-Yop machinery for virulence. In particular, the yersiniae T3SS-Yop apparatus is responsible for inactivation of phagocytosis (Cornelis & Wolf-Watz, 1997). Being injected in the host immune cell (mainly macrophages, dendritic cells, and neutrophils), the anti-phagocytic Yop effector proteins are able to destabilize the actin cytoskeleton, suppress cytokine production and induce apoptosis (Viboud & Bliska, 2005; Plano & Schesser, 2013).

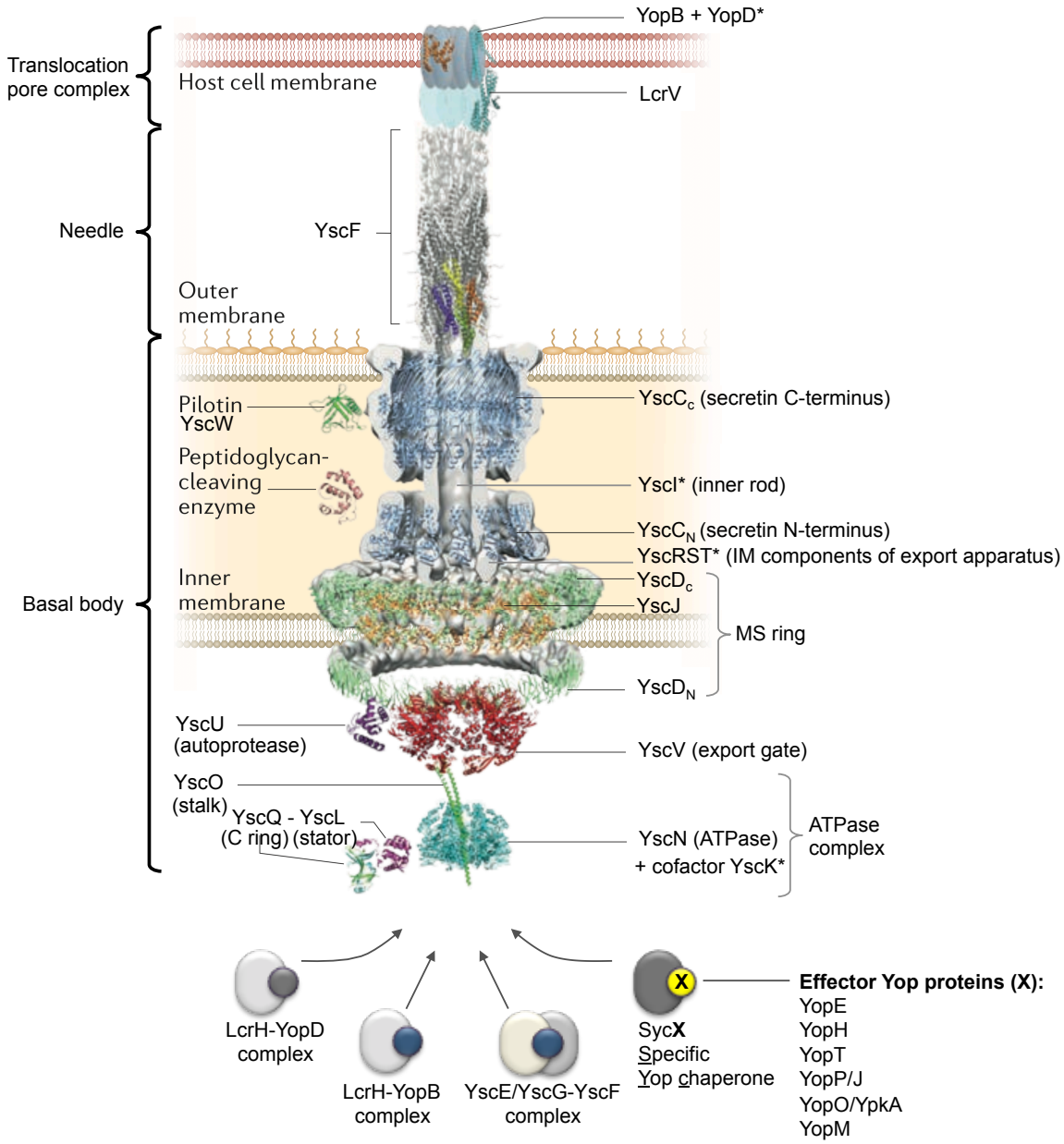

Figure 1.4. Model of the T3SS.
Model of T3SS, representing a hybrid of solved structures of individual T3SSs components from different bacteria and schematic view of the *Yersinia* injectisome compounds. Furthermore, the model schematically demonstrates the export of the translocator (LcrH-YopD and LcrH-YopB), structural (YscE/YscG-YscF) and effector proteins (Syc-effector Yops) with their corresponding chaperons. The *Yersinia* spp. nomenclature is applied. * - unknown structure. Scaffold proteins: YscC, YscD, YscJ; export apparatus proteins: YscR, YscS, YscT, YscU, YscV; cytoplasmic components: YscQ (C ring) and YscN, YscL, YscK (ATPase complex); channel-like structures: YscI (rod) and YscF (needle); pore complex: LcrV (needle tip) and YopB, YopD (translocation pore) (modified after Dewoody *et al*., 2013[6] and Deng *et al*., 2017[7]).

The *Yersinia* T3SS is composed of more than 20 structural proteins that can be divided into four major groups according to their functions: (1) structural proteins, assembling the injectisome, (2) the cytotoxic Yop effector proteins, (3) the translocators, which form the

[6] Dewoody *et al*., 2013 is licensed under the terms of the Creative Commons Attribution License.

[7] Adapted by permission from Springer Nature: Springer Nature, Nature Reviews Immunology, Assembly, structure, function and regulation of type III secretion systems, Deng *et al*., Copyright © 2017.

translocation pore in the host membrane, and (4) the chaperones that bind the effectors (class I chaperones, e.g. Syc chaperones), translocators (class II chaperones, e.g. LcrH), and structural proteins (class III chaperones, e.g. YscE/YscG for YscF needle protein) prior to their export to keep them in a secretion-competent state and to target them for secretion (Neyt & Cornelis, 1999; Stebbins & Galán, 2001; Akeda & Galán, 2005; Letzelter *et al*., 2006; Sun *et al*., 2008; Izoré *et al*., 2011). The injectisome is homologous to the bacterial flagellum and consists of basal body, needle and translocation pore complex that is formed in the eukaryotic cell membrane (Kudryashev *et al*., 2013).

The early stages of T3SS formation are assisted by the general secretory (Sec) pathway (Costa *et al*., 2015). In *Yersinia* spp., this process starts with an outside-in assembly of the **basal body**, which spans the bacterial double membrane as well as peptidoglycan layer (Diepold *et al*., 2010). In contrast, the basal body of the flagellum as well as the T3SSs of *Salmonella* SPI-1, enteropathogenic *E. coli* (EPEC) and enterohemorrhagic *E. coli* (EHEC) assemble in an inside-out manner (Kimbrough & Miller, 2000; Gauthier *et al*., 2003; Erhardt *et al*., 2010; Wagner *et al*., 2010; Deng *et al*., 2017). The basal body represents a series of ring structures connected by the rod (Portaliou *et al*., 2016). First, the peptidoglycan-cleaving enzyme locally removes the peptidoglycan layer in the periplasm to enable the access of secretin (YscC) to the outer membrane (Burkinshaw *et al*., 2015; Deng *et al*., 2017). Oligomerization of YcsC results in the assembly of the outer membrane ring (OM ring) (Koster *et al*., 1997; Kowal *et al*., 2013). This process is guided by a small lipoprotein YcsW, also called pilotin (Burghout *et al*., 2004). Acting as a molecular 'stapler', pilotin mediates the proper folding of the C-terminal S-domain, which is essential for the establishment of clamping interactions between two proceeding secretin protomers upon assembly (Worrall *et al*., 2016). Thereafter, the inner membrane ring (MS ring) of YscD is formed, bridging with the OM secretin ring (Spreter *et al*., 2009; Ross & Plano, 2011). Next, YscD recruits YscJ, its oligomerization completing the MS ring assembly (Yip *et al*., 2005; Diepold *et al*., 2010). Together these structures create a so-called scaffold (YscCDJ) embedded within the peptidoglycan layer (Dewoody *et al*., 2013). Once the basic channel through the bacterial envelope is generated, the export apparatus is docked to YscJ onto the base of the MS ring (Diepold *et al*., 2010). Remarkably, the export apparatus comprising the integral membrane proteins YscRSTUV assembles within the inner membrane independently of the scaffold (Diepold *et al*., 2011). Later on, the ATPase complex, consisting of YscNKL, and the cytoplasmatic ring (C ring), composed of YscQ, associate with the inner membrane rings and interact with the export apparatus (Jackson & Plano, 2000; Blaylock *et al*., 2006). Upon completion of the basal body, proteins essential for **needle** formation can be exported via the T3SS itself (Dewoody *et al*., 2013). At this point, the so-called "early" T3SS substrates (YscIFPXO and YopR) are secreted (Payne & Straley, 1998; Day & Plano, 2000; Agrain *et al*., 2005; Blaylock *et al*., 2010). First, the needle protein YscF is translocated through the inner rod (YscI), followed by YscF polymerization and, subsequently, needle formation (Marlovits *et al*., 2004; Diepold *et al*., 2012; Sal-Man *et al*., 2012). Notably, the autoprotease (YscU) and the needle-length ruler (YscP) are involved in the regulation of the needle length and the specificity switch from "early" to "middle" substrates (Journet *et al*., 2003; Mota *et al*., 2005; Erhardt *et al*., 2011).

Once the needle assembly is completed, secretion of the "middle" T3SS substrates starts. These are the **translocators** YopB, YopD, and LcrV. After secretion, LcrV polymerizes at the distal end of the needle and forms a pentameric needle-tip complex (Mueller *et al*., 2005; Broz *et al*., 2007). This LcrV tip complex is suggested to serve as a platform for insertion of the YopBD translocon into the eukaryotic cell membrane (Goure *et al*., 2005; Mueller *et al*., 2008). Furthermore, LcrV is indespensible for YopB insertion and translocon formation in mammalian membranes (Harmon *et al*., 2013). Moreover, LcrV was described to determine the translocation pore size (Holmstrom *et al*., 2001). Finally, environmental signals such as physical contact with the host cell *in vivo* or, calcium chelation from the growth medium *in vitro*, trigger the last specificity switch from "middle" to "late" substrates (effector proteins) (Lee *et al*., 1998). In the absence of these stimuli, the gatekeeper protein complex (TyeA-YopN) prevents effector protein secretion (Lee *et al*., 2001; Buttner, 2012; Plano & Schesser, 2013).

After assembly of the injectisome, six effectors are delivered into immune cells, mainly macrophages, dendritic cells, and neutrophils, where they interfere with multiple host signaling pathways (Fig. 1.5) (Cornelis, 2002). In general, this interference disturbs actin-based membrane remodeling, prevents phagocytosis and can cause cell death (Bliska *et al*., 2013).

The protein tyrosine phosphatase (PTPase) YopH represents a 50 kDa protein, which contains an N-terminal substrate binding domain and a C-terminal PTPase domain (Black *et al*., 1998). YopH is one of the most important effectors for *Yersinia* virulence especially in terms of phagocytosis prevention. The PTPase activity of YopH leads to inhibition of the early calcium signaling and ROS synthesis. Furthermore, YopH represses the production of proinflammatory cytokines, such as tumor necrosis factor alpha (TNF-α), interleukin (IL)-10, and IL-1β, as well as the chemokine MCP-1 (monocyte chemotactic protein 1) (Persson *et al*., 1997; Andersson *et al*., 1999; Persson *et al*., 1999; Sauvonnet *et al*., 2002; Adkins *et al*., 2007; Rolán *et al*., 2013). Moreover, when acting in concert with YopE, YopH was shown to repress integrin β1-mediated activation of the inflammasome in epithelial cells (Thinwa *et al*., 2014). Additionally, YopH disrupts the focal adhesion complex and thus prevents phagocytosis (Black *et al*., 2000; Aepfelbacher *et al*., 2007).

YopE is a 23 kDa GTPase activating protein (GAP), which structurally and biochemically resembles eukaryotic Rho GTPases (Evdokimov *et al*., 2009; Aepfelbacher *et al*., 2011). The Rho GTPases represent key signaling molecules implicated in rearrangement of the actin cytoskeleton to enable phagocytosis (Groves *et al*., 2008). YopE facilitates the GTPase activity of Rho GTPases, resulting in the loss of cell motility and suppression of phagocytosis (Roppenser *et al*., 2009). Furthermore, YopE inhibits production of reactive oxygen species (ROS). Notably, both activities of YopE are essential for *Yersinia* splenic colonization in infected mice (Songsungthong *et al*., 2010).

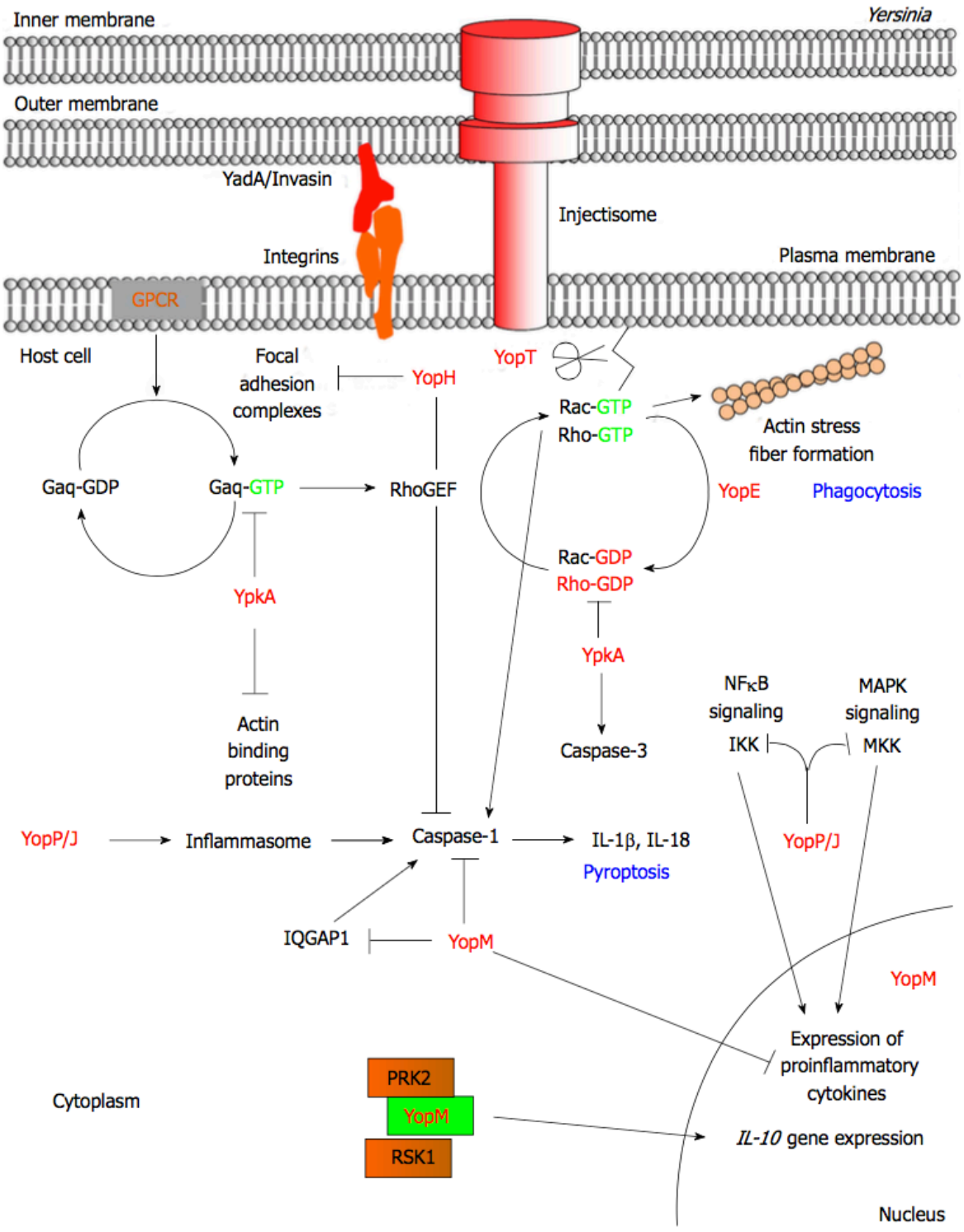

Figure 1.5. Interference of *Yersinia* effector proteins with the host signaling pathways. Contact of *Yersinia* with the eukaryotic host cell promotes the T3SS assembly and, subsequently, the secretion of Yops. Once inside the host cell, the effector proteins manipulate several host signaling cascades controlling cytoskeleton dynamics (YopE, YopT, YopH, YopO/YpkA) to inhibit phagocytosis. Furthermore, YopP/J and YopM inhibit proinflammatory cytokine production. Additionally, YopP/J activates the inflammasome complex resulting in the cell death process termed pyroptosis (Pha & Navarro, 2016[8]).

[8] Pha & Navarro, 2016 is licensed under the terms of the Creative Commons Attribution-Noncommercial (CC BY-NC 4.0) License.

YopT is a 35.5 kDa cysteine protease that also targets the Rho family of GTPases (Iriarte & Cornelis, 1998; Zumbihl *et al*., 1999). The catalytic action of YopT results in the mislocalization of the membrane-bound Rho GTPase and leads to the disruption of the actin cytoskeleton (Shao *et al*., 2003). Additionally, YopT affects the NFκB signaling pathway, thus abolishing NFκB-mediated proinflammatory responses (Dach *et al*., 2009; Köberle *et al*., 2012). Interestingly, not all pathogenic *Yersinia* spp. possess YopT. Some serotypes of *Y. pseudotuberculosis* harbor an internal deletion in the *yopT* gene (Bliska *et al*., 2006). Moreover, loss of *yopT* in *Yersinia* can be fully complemented by the activity of YopE effector, indicating that YopT is dispensable for *Yersinia* virulence (Viboud *et al*., 2006).

The *Yersinia* protein kinase A, YpkA (YopO in *Y. enterocolitica*), is an 80 kDa serine/threonine (Ser/Thr) kinase, which is involved in disruption of the actin cytoskeleton and prevention of phagocytosis (Håkansson *et al*., 1996). Interestingly, in addition to the Ser/Thr kinase domain, YpkA harbors a guanine nucleotide dissociation-like inhibitor (GDI) domain (Galyov *et al*., 1993; Prehna *et al*., 2006). Actions of both eukaryotic-like enzymatic domains influence the actin cytoskeleton by targeting the activation state of the Rho GTPases, RhoA and Rac1. Since the GDI domain of YpkA mimics the host GDI activity, it directly targets the Rho GTPases resulting in the inhibition of GTP loading. Moreover, the kinase domain binds to the alpha subunit of the heterotrimeric G protein complex, Galphaq, in order to abolish activation of downstream Rho proteins through the LARG RhoGEF (Prehna *et al*., 2006; Navarro *et al*., 2007). Studies on YpkA suggest that both enzymatic domains are essential for *Yersinia* virulence (Galyov *et al*., 1993; Prehna *et al*., 2006; Wiley *et al*., 2006; Navarro *et al*., 2007).

The acetyltransferase YopJ (YopP in *Y. enterocolitica*) is a 34 kDa protein with deubiquitinating and putative cysteine protease activity. YopP/J suppresses the synthesis of proinflammatory molecules. This effector downregulates the proinflammatory response through interference with the mitogen-activating protein kinase (MAPK) and the NFκB signaling pathways (Mukherjee *et al*., 2006; Sweet *et al*., 2007). Furthermore, in cooperation with other Yop effectors, YopP/J was reported to inhibit the production of chemoattractants and, consequently, to prevent the early recruitment of neutrophils to the site of infection (Denecker *et al*., 2002; Zhou *et al*., 2004; Vagima *et al*., 2015). Remarkably, secretion of YopJ by *Y. pseudotuberculosis* located within the macrophage phagosomes activates apoptosis or necrosis of macrophages (Zhang *et al*., 2011; Zheng *et al*., 2012).

YopM is a leucine-rich repeat (LRR)-containing protein that localizes to both the cytoplasm and the nucleus of the eukaryotic cell (Skrzypek *et al*., 1998; Benabdillah *et al*., 2004). YopM counteracts caspase-1 activation through arresting the pyrin inflammasome formation, which is triggered by the RhoA-inactivating enzymatic function of YopE and YopT (Chung *et al*., 2014; Chung *et al*., 2016; Park *et al*., 2016). Interestingly, since YopM lacks catalytic activity and interacts with multiple targets, it is suggested to act as a scaffold. Particularly, the LRR region binds to serine/threonine protein kinase C-related kinases (PRKs) and the C-terminal domain interacts with the ribosomal S6 kinase (RSK)

(McCoy *et al*., 2010; McPhee *et al*., 2010). Furthermore, YopM was shown to activate the anti-inflammatory cytokine, IL-10 (McPhee *et al*., 2012). Thus, YopM-mediated recruitment and activation of host kinases for downregulation of pyrin as well as the IL-10 induction promotes *Yersinia* virulence (Chung *et al*., 2016).

Recently, two different models of effector delivery were suggested: a direct injection model and a binary AB toxin-like delivery model. According to the direct injection model unfolded translocators and effector proteins are exported through the T3SS needle, followed by translocation pore assembly and finally the effector delivery into the host cell. Current observations of the T3SS substrates trapped in the needle strongly support this model (Dohlich *et al*., 2014; Radics *et al*., 2013). In the alternative binary AB toxin-like model unfolded translocators and effectors are also delivered through the T3SS needle, however, prior to host cell contact. After secretion, they localize to the bacterial cell surface. Upon contact with the host cell, which might be sensed by the needle, translocators and effectors migrate to the host cell membrane. At this step, the translocation pore is assembled enabling the 'injection-independent' effector delivery (Akopyan *et al*., 2011; Edgren *et al*., 2012). Additionally, a simultaneous transport of effectors into the host cell by both models was also suggested (Akopyan *et al*., 2011; Kendall, 2017). Remarkably, *Y. pseudotuberculosis* and EPEC seem to apply the same T3SS-dependent mechanism for delivery of extracellular proteins into the host cell, as YopH and EspC share the translocation motif (Tejeda-Dominguez *et al*., 2017).

1.3 Regulatory mechanisms controlling expression of the *Yersinia* YadA and the T3SS

The expression of the virulence plasmid-encoded genes in *Yersinia* is induced in response to environmental signals sensed during the transition from the gut lumen to lymphoid tissues. The initial signal that activates *yadA* and T3SS/*yop* gene transcription as well as synthesis of the corresponding proteins is a thermal upshift to temperatures above 30°C (Cornelis *et al*., 1989). An additional environmental signal that triggers the expression of the Yop virulon and YadA is contact with eukaryotic cells (Pettersson *et al*., 1996). Remarkably, *in vitro*, depletion of calcium from the growth medium in combination with a temperature shift to 37°C mimics the effect of the host cell contact and leads to massive expression and secretion of Yop effectors (Brubaker, 2007). This phenomenon was first described in *Y. pestis*, which is unable to grow at 37°C in the absence of calcium, and is known as the Low Calcium Response (LCR) (Kupferberg & Higuchi, 1958; Higuchi *et al*., 1959). However, there is still no mechanistic explanation for calcium-mediated regulation of Yop secretion and the growth arrest upon active T3S. Nevertheless, some T3SS-associated genes, mutations in which resulted in a calcium-blind *Yersinia* phenotype, were originally termed for the LCR (Perry *et al*., 1986; Yother & Goguen, 1985). Numerous factors were proposed to be involved in the temperature as well as the cell contact- and/or calcium-dependent control of the pYV-encoded virulence factors and will be described in the following.

1.3.1 Major virulence activator LcrF

The upregulation of the T3SS-associated genes at human body temperature is a direct consequence of temperature-dependent expression of the transcriptional regulator LcrF (VirF in *Y. enterocolitica*) (Fig. 1.6) (Cornelis *et al*., 1987). LcrF was first discovered in *Y. pestis* as a factor essential for thermal induction of several virulence plasmid-encoded genes (Yother *et al*., 1986). The 30 kDa LcrF protein is an AraC-like transcriptional activator, its carboxy-terminal region enabling DNA binding and sharing homology with that of the transcriptional regulator AraC in *E. coli* (Schleif, 2010). The carboxy-terminal domain of all AraC family members including LcrF harbours two helix-turn-helix (HTH) domains (King *et al*., 2013). The recognition helix interacts with specific DNA residues within the major groove (Rhee *et al*., 1998). Recently, LcrF and its homolog ExsA from *Pseudomonas aeruginosa* were shown to bind the consensus sequence AaAAAnwnMygrCynnnmYTGyaAk (W: A or T; M: A or C; Y: C or T; R: A or G; K: G or T; uppercase letters represent more highly conserved residues). Moreover, the activators of T3SS-related genes from *Photorhabdus luminescens*, *Aeromonas hydrophilus*, and *Vibrio parahaemolyticus* recognize the same nucleotide sequence motif (Brutinel *et al*., 2008; Diaz *et al*., 2011; King *et al*., 2013). The amino-terminal domain of AraC-like proteins is responsible for the dimer assembly. Furthermore, the N-terminal region of several AraC-like proteins binds cofactors, which affect the regulation of transcription (Schleif, 2010). Interestingly, in contrast to the *E. coli* AraC, no additional cofactors binding was shown for *Yersinia* LcrF (Schwiesow *et al*., 2015). LcrF is known to interact with its target DNA as a preformed dimer. However, a recent study demonstrated that LcrF defective for self-association can still bind DNA by sequential recruitment of two monomers to the promoter region (King *et al*., 2013). Furthermore, like the *E. coli* AraC, LcrF is thought to directly bind to RNA polymerase, facilitating the interaction between the polymerase and the promoter region. Thus, LcrF improves the transcription-initiation of virulence plasmid-encoded genes (Cornelis *et al*., 1989; Schleif, 2010). LcrF itself is also encoded on the *Yersinia* virulence plasmid and is transcribed in an operon with the pilotin YscW from the σ^{70}-dependent *yscW* promoter (Böhme *et al*., 2012; Schwiesow *et al*., 2015).

1.3.1.1 Regulation of *lcrF* transcription

Transcription of *lcrF* is abolished below 30°C by the inhibitory effect of the nucleoid-associated protein *Yersinia* modulator A (**YmoA**) (Böhme *et al*., 2012). The chromosomally-encoded YmoA protein forms a heterodimeric complex with the histone-like protein H-NS and binds to the sequence directly downstream of the *yscW* promoter (Nieto *et al*., 2002; Madrid *et al*., 2007; Böhme *et al*., 2012). This interaction inhibits *lcrF* transcription, thus repressing the T3SS expression at moderate temperatures (Cornelis *et al*., 1991; Böhme *et al*., 2012). Remarkably, H-NS can also interact as a homodimer with the *yscW-lcrF* promoter region. However, the effect of the H-NS homodimer on *lcrF* transcription is unclear (Böhme *et al*., 2012). Thermal upshift to 37°C leads to a conformational change in the virulence plasmid DNA topology, followed by significant derepression of LcrF expression (Cornelis *et al*., 1989; Michiels *et al*., 1991; Rohde *et al*.,

1994; Rohde *et al*., 1999). Consequently, it is possible that the DNA binding efficiency of the YmoA/H-NS heterodimer and H-NS homodimer is also temperature-dependent (Böhme *et al*., 2012). At mammalian body temperature (37°C) YmoA is rapidly degraded by ClpP and Lon proteases, which enables transcription of the *yscW-lcrF* operon (Jackson *et al*., 2004; Böhme *et al*., 2012).

Several additional environmental signals affecting *lcrF* transcription have been reported. For instance, during the course of infection yersiniae are confronted with oxygen stress and significant changes in iron bioavailability. Iron in turn is a crucial component for *Yersinia* virulence. Interestingly, oxidative stress/limitation as well as iron availability affect the expression and activity of the iron-sulphur cluster coordinating the transcription regulator **IscR**, which was recently characterized as an essential factor for T3S in *Yersinia* (Yeo *et al*., 2006; Mettert & Kiley, 2014; Miller *et al*., 2014). IscR is able to recognize two separate DNA binding motifs to control transcription of its target genes. Consequently, this protein is active in both the holo-IscR and the apo-IscR forms. Interestingly, type I motifs are recognized solely by holo-IscR, while type II motifs are bound by both apo-IscR an holo-IscR (Schwartz *et al*., 2001; Nesbit *et al*., 2009; Fleischhacker *et al*., 2012). In *Y. pseudotuberculosis* IscR regulates *lcrF* transcription via binding to the type II motif within the *yscW-lcrF* promoter. Thus, IscR controls the *Yersinia* T3SS through direct activation of *lcrF* transcription (Miller *et al*., 2014). Although both apo-IscR and holo-IscR are able to promote the T3SS gene transcription, the *Y. pseudotuberculosis* IscR in the apo-locked form causes a proton motive force defect that abolishes transcription and secretion of Yop effectors (Miller *et al*., 2014).

Additionally, the response regulator **RcsB** from the Rcs phosphorelay system was reported to activate the *lcrF* transcription (Li *et al*., 2014). The Rcs system is found exclusively in the family of *Enterobacteriaceae* and enables bacteria to maintain their membrane integrity during environmental alterations such as osmotic shock, dehydration, overproduction of envelope proteins, and perturbations in extracellular polysaccharide production under extracytoplasmatic stress conditions (Majdalani & Gottesman, 2005; Huang *et al*., 2006). Once phosphorylated, RscB can directly bind to a conserved RcsB box located upstream of the -35 promoter element of the *yscW-lcrF* operon. RcsB binding increases the *lcrF* mRNA level, thus enhancing T3SS protein expression and effector secretion (Li *et al*., 2014). Environmental factors and regulators involved in the transcriptional control of LcrF expression are summarized in Fig. 1.6.

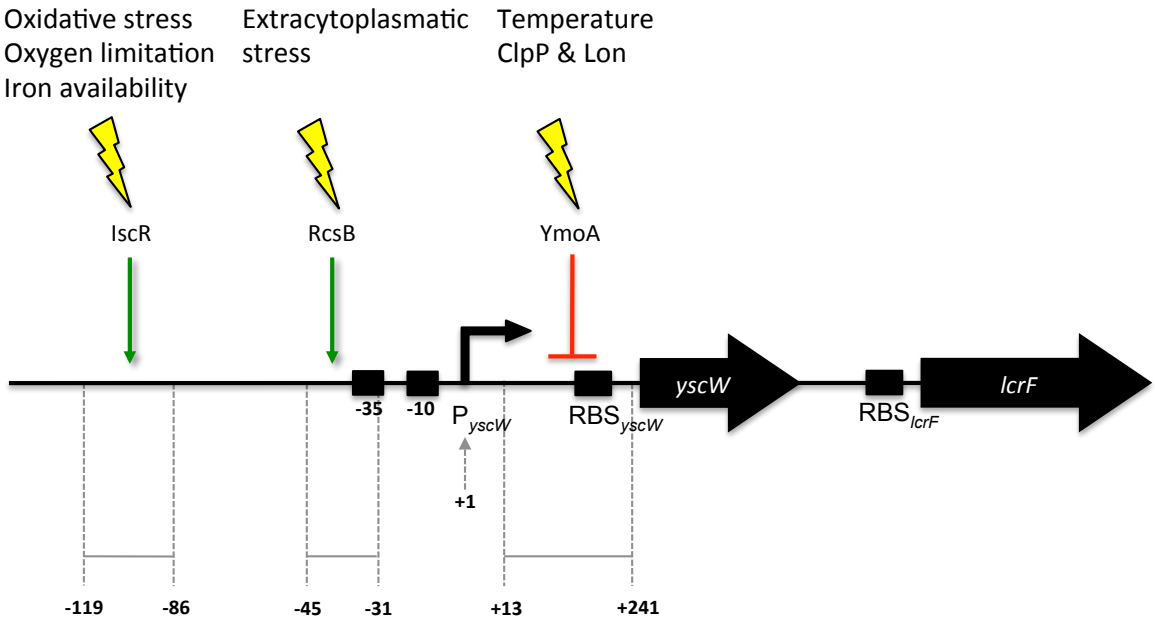

Figure 1.6. Regulators of *lcrF* transcription.
YmoA, IscR and RcsB control LcrF expression on the transcriptional level in response to various environmental signals such as temperature, oxidative stress/limitation, iron availability, and extracytoplasmatic stress. YmoA acts at moderate temperature as a transcriptional repressor of LcrF. At host temperature YmoA is degraded by ClpP and Lon proteases, and IscR and RcsB activate *lcrF* transcription. The numbers indicate the position of the IscR-, RcsB-, and YmoA-dependent regions with respect to the transcriptional start site of the *yscW-lcrF* operon.

1.3.1.2 Thermoregulation of LcrF translation

LcrF expression is also regulated on the post-transcriptional level through a 'fourU' RNA thermometer within the 5' untranslated region (5'-UTR) of the *lcrF* mRNA (Fig. 1.7) (Hoe & Goguen, 1993; Böhme *et al*., 2012). The *lcrF* 5'-UTR harbors a secondary structure composed of two stemloops (hairpin I and II). The hairpin II possesses the AGGA sequence of the *lcrF* ribosomal binding site (RBS) that pairs with the 'fourU' motif (a stretch of four uridines) located 26 to 29 nt upstream of the *lcrF* translational start site. The 'fourU' element was first described in the aggregation suppression A heat shock gene (*agsA*) from *Salmonella enterica* serovar Typhimurium (Waldminghaus *et al*., 2007). At moderate temperatures (25°C), the 'fourU'-RBS structure is stable and prevents access of the 30S ribosome to the Shine-Dalgarno (SD) sequence. Consequently, *lcrF* translation is abolished. Elevated temperatures destabilize intramolecular base pairing, which liberates the RBS and allows initiation of translation (Böhme *et al*., 2012). Notably, although the hairpin I is not essential for thermosensing, it is suggested to contribute to the appropriate folding and/or stability of the 'closed' thermo-labile RNA-element. Subsequently, this temperature-mediated post-transcriptional control mechanism guarantees an appropriate level of *lcrF* expression during infection and is indispensible for *Y. pseudotuberculosis* virulence in the BALB/C mouse infection model (Böhme *et al*., 2012).

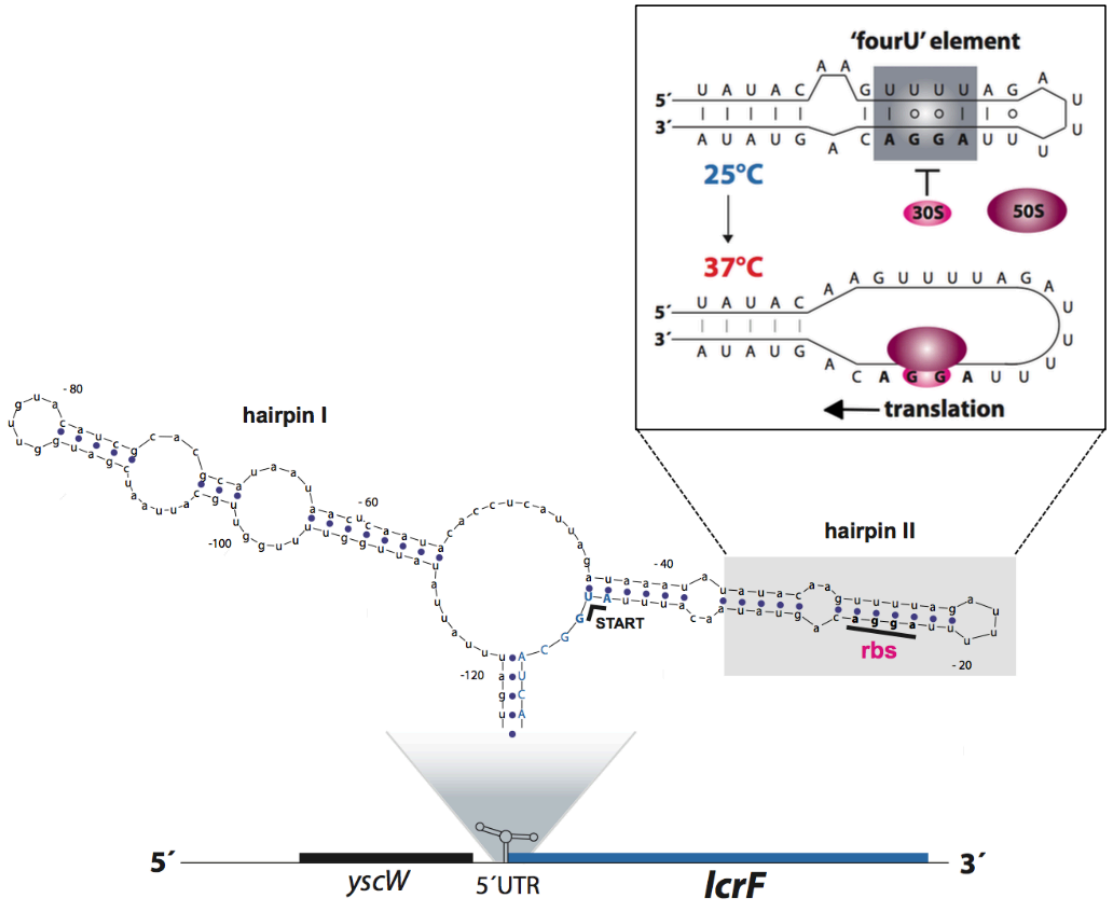

Figure 1.7. Temperature-dependent regulation of *lcrF* translation.
At moderate temperatures (25°C) the *lcrF* 5'-UTR forms a stable secondary structure made of two hairpins. Hairpin II includes the ribosomal binding site (RBS) that interacts with the 'fourU' element. Thus, binding of the 30S ribosomal subunit is prevented and translation initiation is abolished. The RBS-'fourU' base-pairing melts in response to the temperature upshift to 37°C. Consequently, the RBS becomes accessible for the ribosome, allowing the *lcrF* translation (Steinmann & Dersch, 2013[9]).

1.3.1.3 Cell contact and low calcium response

At 37°C expression of the virulence plasmid-encoded genes can be further enhanced by depletion of calcium from the growth medium. In *Y. pestis* LCR leads to a strong growth defect together with massive secretion of Yop effectors in Ca^{2+}-deprived medium (Higuchi *et al.*, 1959; Cornelis *et al.*, 1998; Brubaker, 2007; Fowler, 2009). Since LcrF is an exlusive activator of *yadA* and *ysc-yop* gene transcription, it was assumed that LcrF expression might also depend on contact with the host cell/depletion of calcium. Indeed, both the mRNA and protein levels of LcrF increase significantly upon cell contact or in calcium-deprived media (Opitz, 2013). Intriguingly, recent data revealed that contact with eukaryotic cells results in induction of LcrF expression and, subsequently, activation of the virulence plasmid encoded genes in *Y. pseudotuberculosis* even at moderate temperatures (25°C) (Opitz, 2013). However, depletion of calcium without a temperature upshift *in vitro* was insufficient to stimulate LcrF expression (Pimenova, 2014). Together, this strongly

[9] Steinmann & Dersch, 2013 is reproduced from Future Microbiol. (2013) 8(1), 85-105 with permission of Future Medicine Ltd.

suggests that the sensing and/or molecular mechanisms triggering the LcrF expression during cell contact and under calcium depletion conditions are different.

1.3.2 Yop-mediated negative feedback regulation

In order to prevent the energy intensive overproduction of T3SS-associated factors under non-secretion conditions (absence of the host cell contact *in vivo* or high calcium concentrations *in vitro*) *Yersinia* employs a so-called negative feedback loop. It acts at the post-transcriptional level and includes at least four proteins: the translocon component YopD (see 1.2.2.1) with its cognate chaperone LcrH, LcrQ, and the YopH chaperone SycH (Cambronne & Schneewind, 2002; Cambronne *et al*., 2004; Kopaskie *et al*., 2013).

So far, the bifunctional 33 kDa protein YopD is the only identified RNA-binding effector (Tawk *et al*., 2017). Moreover, secreted YopD establishes the translocation pore in the eukaryotic membrane, but on the other hand, when not secreted, YopD regulates T3SS genes by a direct binding to the short AU-rich sequences of bacterial mRNA (Cambronne & Schneewind, 2002; Chen & Anderson, 2011; Kopaskie *et al*., 2013). For both of these activities, YopD demands binding to its 19 kDa cognate chaperone LcrH (SycD in *Y. enterocolitica*), which is assumed to be essential for protein stability as well as for the secretion of YopD (Francis *et al*., 2000; Anderson *et al*., 2002). LcrH is the chaperone of both translocator proteins YopB and YopD and is classified as a class II chaperone from the T3SS. LcrH represents a homodimer with an all α-helical fold, which consists of three tandemly arrayed tetratricopeptide repeats (TPRs) (Büttner *et al*., 2008). TPRs are composed of 34 amino acid motifs that build a helix-turn-helix conformation and are stacked on top of each other to assemble elongated structures (Singh *et al*., 2013). LcrH is a weak dimer that harbors a very flexible and weakly folded C-terminus that is kept together by the dimeric interface at the N-terminus (Singh *et al*., 2013). This flexible structure is suggested to be crucial to effectively find the target peptide of the large cognate LcrH partners YopB and YopD. Thereafter, the chaperone folds and binds the translocator, assembling a more rigidly bound structure (Singh *et al*., 2013). This mechanism is termed ‘fly-casting’ and was already described for other proteins also harboring the TPRs (Shoemaker *et al*., 2000; Cliff *et al*., 2005; Perham *et al*., 2005; Lamboy *et al*., 2011).

According to recent studies, binding of the YopD-LcrH complex to the 5’-UTR of its target transcript results in a decrease of mRNA stability (Francis *et al*., 2001; Chen & Anderson, 2011). Excitingly, YopD was found to repress LcrF expression at the post-transcriptional level either directly, or through positive regulation of LcrF repressors such as YmoA (see 1.3.1.1), CsrA (see 1.3.3), and exoribonuclease PNPase (see 1.3.4) (Steinmann, 2013; Hoßmann, 2017). Additionally, YopD can interact with the 30S ribosomal subunit which prevents the 70S ribosome assembly (Kopaskie *et al*., 2013). Intriguingly, the full structure of YopD remains unsolved. Nevertheless, it was shown that YopD possesses a C-terminal amphipathic α-helix domain, which spans residues 278 to 292 (Tengel *et al*., 2002; Olsson *et al*., 2004; Costa *et al*., 2010). Furthermore, a putative C-terminal coiled-coil located immediately upstream of the amphipathic α-helix domain was reported (Pallen *et al*., 1997; Bröms *et al*., 2003; Costa *et al*., 2012). Moreover, a second putative coiled-coil motif that lies near to the YopD N-terminus was predicted.

This putative N-terminal coiled-coil motif seems to be unique to the *Yersinia* genus, as no similar motif could be predicted for the YopD-like structures from other bacterial members of the Ysc-Yop T3SS phylogenetic clade. In *Y. pseudotuberculosis* this putative N-terminal YopD coiled-coil domain is indispensible for full virulence (Costa *et al*., 2012). Notably, the N-terminal hydrophobic domain as well as the C-terminal amphipathic domain are essential for binding to LcrH (Francis *et al*., 2000; Olsson *et al*., 2004; Costa *et al*., 2012).

LcrQ is a 12 kDa LCR-associated protein, which is also involved in the negative feedback loop (Wulff-Strobel *et al*., 2002). Similar to the YopD-LcrH-mediated repression, LcrQ-dependent feedback regulation of *yop* genes requires AU-rich sequences in the 5'-UTRs (Cambronne & Schneewind, 2002; Cambronne *et al*., 2004). Recently, LcrQ was demonstrated to share the same targets with LcrF. Thus, it is able to block the activating role of LcrF (Li *et al*., 2014). LcrQ-mediated repression is abolished either by its secretion or, due to LcrQ homologies to the N-terminus of YopH, through binding to the YopH chaperone SycH (Rimpiläinen *et al*., 1992; Pettersson *et al*., 1996; Wulff-Strobel *et al*., 2002).

1.3.3 The carbon storage regulator system (Csr system)

The Csr/Rsm (Carbon storage regulator/Regulator of secondary metabolism) system represents a global post-transcriptional regulatory system, which is indispensible for adaptation of various proteobacterial human and plant pathogens to dramatically changing environmental conditions (Andrade *et al*., 2014; Kusmierek & Dersch, 2018). In general, the Csr/Rsm system includes the highly conserved, dimeric RNA-binding protein (RBP) CsrA/RsmA (18.6 kDa), and varying regulatory elements, which modulate the CsrA/RsmA activity (Gutierrez *et al*., 2005). In particular, the Csr system of *Y. pseudotuberculosis* consists of CsrA and two non-coding RNAs, CsrB and CsrC (Heroven *et al*., 2012). Each CsrA/RsmA monomer is composed of 5 antiparallel β-strands, and an α-helix at the C terminus (Fig. 1.8).

By dimerization, two CsrA monomers assemble a β-sandwich of two intertwined antiparallel β-sheets followed by the C-terminal α-helix. According to a NMR titration experiments, β1 and β5 of each subunit build a highly positively charged surface that enables RNA binding (Gutierrez *et al*., 2005; Schubert *et al*., 2007). This dimeric nature allows CsrA/RsmA to simultaneously bind two sites on a target RNA molecule, which are separated by 10–63 nucleotides (Mercante *et al*., 2009; Lapouge *et al*., 2013).

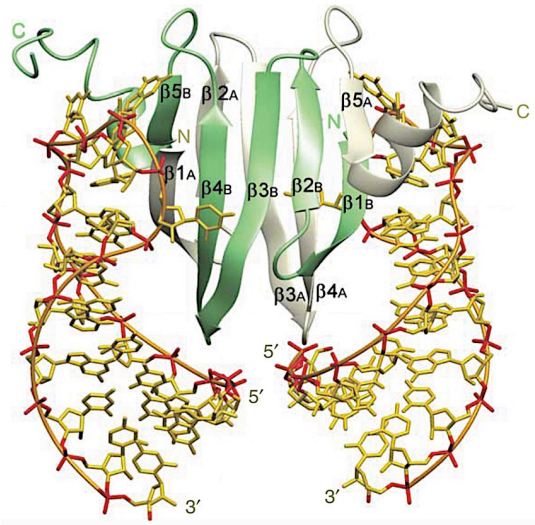

Figure 1.8. Structure of the CsrA homolog RsmE in complex with RNA.
RsmE dimer (green/grey), member of the CsrA/RsmA family from *Pseudomonas fluorescens*, interacts with 20-nucleotide sites (yellow/red) within the *hcnA* sequence (Schubert *et al*., 2007[10]).

Different biochemical and genetic approaches revealed that CsrA/RsmA most frequently interacts with GGA motifs in single-stranded loop regions of short hairpin structures in the 5′-untranslated regions (5′-UTRs) of their target RNAs (Dubey *et al*., 2005; Schubert *et al*., 2007; Duss *et al*., 2014). Subsequently, this bridging mechanism allows CsrA/RsmA to interact with specific RNAs, and to regulate gene expression at the transcriptional and post-transcriptional level. Generally, CsrA/RsmA interaction hinders ribosome access to the Shine-Dalgarno (SD) sequence, preventing translation. Consequently, the target transcript is predisposed to enhanced degradation. This scenario mostly occurs when one of the CsrA/RsmA-bound GGA motifs overlaps with the RBS (Fig. 1.9) (Baker *et al*., 2002; Dubey *et al*., 2003; Mercante *et al*., 2009). Alternatively, CsrA/RsmA binding can repress the expression of certain RNases or prevent their access to the target transcript. Furthermore, CsrA/RsmA can block the formation of inhibitory RNA structures. This, in turn, can improve transcript stability and activate translation by increasing ribosome accessibility (Fig. 1.9) (Patterson-Fortin *et al*., 2013; Yakhnin *et al*., 2013; Ren *et al*., 2014; Park *et al*., 2015). Excitingly, application of CLIP-seq (UV crosslinking-immunoprecipitation-high-throughput sequencing) for a transcriptome-wide investigation of CsrA targets revealed that CsrA binding sites are located not only within the 5'-UTRs, but also in the coding region as well as in the 3'-UTRs of transcripts (Holmqvist *et al*., 2016).

[10] Reprinted by permission from Springer Nature: Springer Nature, Nature Structural & Molecular Biology, Molecular basis of messenger RNA recognition by the specific bacterial repressing clamp RsmA/CsrA, Schubert *et al*., Copyright © 2007.

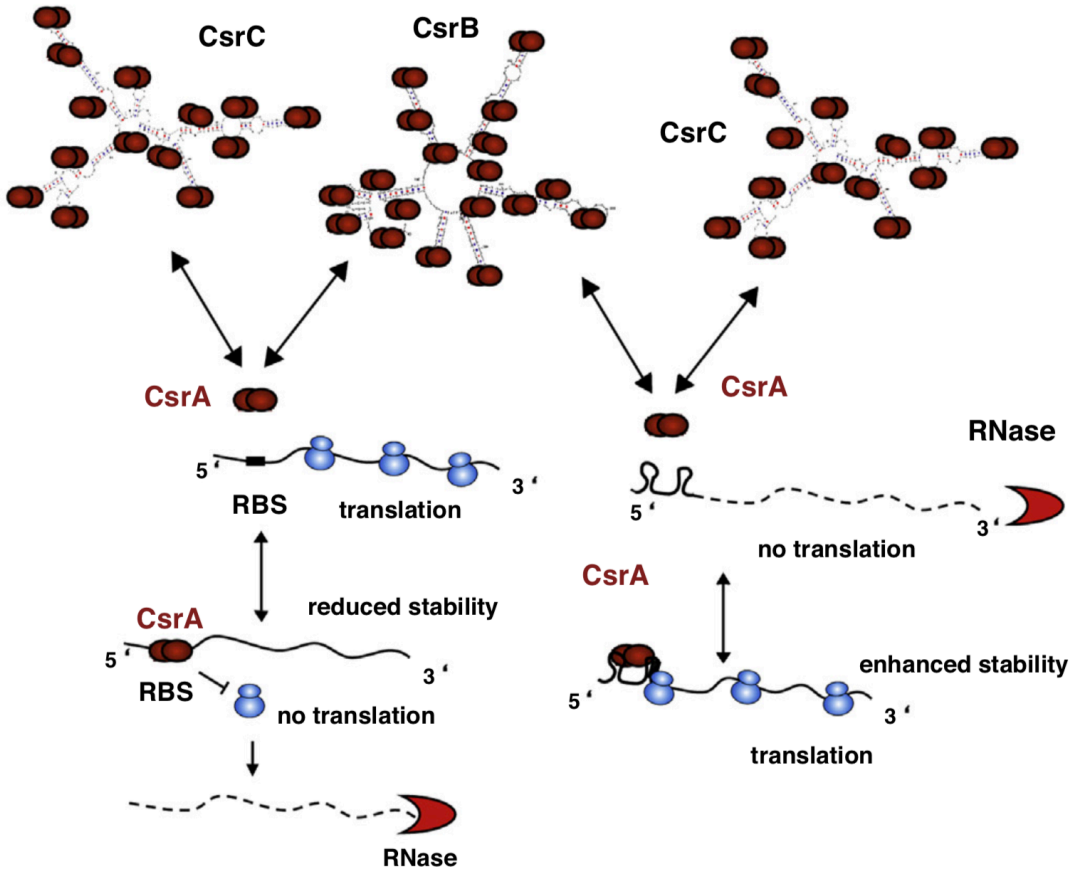

Figure 1.9. Mechanism of Csr system-mediated regulation of gene expression.
CsrA binding to its target transcript can either repress or activate translation. The CsrA dimer predominantly interacts with conserved GGA-containing motifs located in the 5'-UTR of target mRNAs near the ribosomal binding site (RBS). When a CsrA-bound GGA motif covers the Shine-Dalgarno (SD) sequence, translation is abolished. Alternatively, CsrA binding can increase ribosome accessibility to the SD sequence by preventing the formation of inhibitory RNA structures. Furthermore, CsrA can protect its target transcript from certain RNases, thus increasing transcript stability. The non-coding RNAs CsrB and CsrC possess numerous GGA-motifs in single-stranded regions of their hairpins. Subsequently, when present in adequate amounts, CsrB and CsrC can sequester CsrA from its target mRNA, thus antagonizing CsrA activity (Kusmierek & Dersch, 2018[11]).

Regulation of the Csr/Rsm system is extremely complex and multilayered. The activity of CsrA/RsmA of γ-proteobacteria is primarily controlled by two or more analogous, non-coding, highly structured Csr/Rsm-type RNAs (Kulkarni *et al.*, 2006). In *Y. pseudotuberculosis* these are the CsrB and CsrC RNAs, which harbor multiple GGA-containing stem-loops (18 and 14, respectively) (Heroven *et al.*, 2008; Vakulskas *et al.*, 2015). Consequently, the regulatory Csr/Rsm-type RNAs can sequester CsrA/RsmA from its target transcript and antagonize its function (Romeo, 1998; Weilbacher *et al.*, 2003). Moreover, CsrA enhances the stability of the CsrB and CsrC RNAs. Furthermore, the CsrB and CsrC RNAs are counter-controlled meaning that the overproduction of one Csr-RNA leads to downregulation of the other (Heroven *et al.*, 2008; Heroven *et al.*, 2012). Non-coding RNAs (ncRNAs) other than the typical

[11] Reprinted by permission from Elsevier Ltd.: Elsevier, Current Opinion in Microbiology, Regulation of host–pathogen interactions via the post-transcriptional Csr/Rsm system, Kusmierek & Dersch, Copyright © 2017.

Csr/Rsm RNAs, such as the *E. coli* ncRNA McaS/IsrA, can also serve as functional CsrA binding partners (Jorgensen *et al*., 2013; van Nues *et al*., 2016; Holmqvist *et al*., 2016). Moreover, not only ncRNAs but also highly abundant mRNA elements, such as the 5′-UTR region of the *fimAICDHF* mRNA encoding type I fimbriae of *S.* Typhimurium, are able to compete with Csr/Rsm-type RNAs and antagonize CsrA function (Sterzenbach *et al*., 2013). CsrA can also simultaneously activate its own transcription (indirect effect) and inhibit its translation (direct effect) (Yakhnin *et al*., 2011). In flagellated bacterial clades of eubacteria other than γ-proteobacteria, CsrA activity is allosterically controlled via interaction with different proteins (Altegoer *et al*., 2016; Mukherjee *et al*., 2016). For instance, the flagellar assembly factor FliW from the enteric pathogen *Campylobacter jejuni* forms a CsrA-FliW heterodimer, antagonizing the CsrA-dependent repression of FlaA (flagellar filament protein) synthesis. Reciprocal binding of FliW to flagellins counteracts this process (Radomska *et al*., 2016). Additionally, *flaA* mRNA possesses two GGA motifs in adjacent hexaloops. Thus, *flaA* itself can titrate CsrA activity (Dugar *et al*., 2016). These two mechanisms provide *C. jejuni* with a sophisticated feedback regulation strategy for effective adjustment of the cytosolic flagellin copy number.

Studies with several bacterial pathogens demonstrated that the Csr/Rsm system forms a large regulon and has an immense influence on the bacterial transcriptome (Potts *et al*., 2017). Implementation of RIP-seq and CLIP-seq for investigation of the CsrA interactome revealed that CsrA directly targets the transcripts of a large number of CsrA-dependent genes (Esquerré *et al*., 2016; Holmqvist *et al*., 2016; Sahr *et al*., 2017; Sowa *et al*., 2017). The majority of CsrA/RsmA-dependent genes are involved in fundamental bacterial processes including metabolic functions, stress responses, and numerous physiological processes (Wei *et al*., 2001; Molofsky & Swanson, 2003; Dubey *et al*., 2003; Heroven *et al*., 2012; Bücker *et al*., 2014; Oliva *et al*., 2015; Morin *et al*., 2016; Godfrey *et al*., 2017). Consequently, a CsrA/RsmA-mediated control of genes crucial for the pathogens biological fitness contributes to bacterial virulence (Kusmierek & Dersch, 2018). A recent work on enteropathogenic yersiniae revealed that CsrA/RsmA affects the virulence plasmid-encoded T3SS (*ysc/yop*). This CsrA-dependent regulation of the Ysc/Yop T3SS is suggested to be crucial for the switch between the acute and chronic lifestyle of yersiniae (Avican *et al*., 2015). In *Y. enterocolitica* CsrA/RsmA improves secretion of Yop effectors. Intriguingly, the loss of CsrA in *Y. pseudotuberculosis* fully abolishes Yop effector secretion and makes the pathogen avirulent (Nuss *et al*., 2017).

1.3.4 The RNA degradosome

The bacterial RNA degradosome represents a highly structured multi-enzyme complex that is responsible for the processing and degradation of RNA substrates. This multi-protein assembly plays an important role in the RNA turnover in various bacterial species including pathogens (Bruce *et al*., 2017). The most extensive investigation of the degradosome was performed in *E. coli* and revealed detailed information about its structure and function. The *E. coli* degradosome includes the endoribonuclease RNase E, the phosphorylytic exoribonuclease polynucleotide phosphorylase (PNPase), the DEAD-box helicase RhlB, and the glycolytic enzyme enolase (Fig. 1.10) (Carpousis, 2007). Generally,

RNase E performs the initial cleavage of substrate transcripts, followed by RhlB-mediated RNA unfolding and, finally, degradation of the remaining single-stranded RNA fragments by PNPase (Hui *et al*., 2014).

RNase E is the central enzyme of the RNA metabolism and RNA-based regulation (riboregulation) in *E. coli* (Carpousis, 2007). This endoribonuclease forms a large multidomain homotetramer, wherein each protomer consists of 1061 amino acids and possesses both catalytic and scaffolding regions. The N-terminal domain of each RNase E monomer is highly conserved and provides the degradosome with a hydrolytic endoribonuclease activity. RNase E targets and cleaves single-stranded RNAs and is activated via the 5'-monophosphate group of the substrate transcript (Callaghan *et al*., 2005; Koslover *et al*., 2008). The C-terminal part of the enzyme is more variable compared to the N-terminal part and serves as a scaffold for degradosome assembly. Interestingly, the scaffolding domain of RNase E is predicted to be natively disordered. The small linear recognition motifs interact with the canonical degradosome enzymes, RNA, as well as the cytoplasmic membrane. The latter results in the localization of the degradosome assembly to the cytoplasmic periphery (Callaghan *et al*., 2004; Khemici *et al*., 2008; Aït-Bara & Carpousis, 2015; Strahl *et al*., 2015; Moffitt *et al*., 2016). Remarkably, the C-terminal domain of RNase E interacts with the global small RNA chaperone Hfq, which is an essential player in the post-transcriptional regulation of gene expression (Morita *et al*., 2005; Aiba, 2007). This Hfq-degradosome interaction may contribute to the cooperation of Hfq with the RNA-binding activity of the RNase E C-terminal domain, thus facilitating the mRNA target recognition and handover to the catalytic centres of degradosome (Bruce *et al*., 2017).

PNPase is an 80 kDa homo-trimeric 3' to 5' exoribonuclease that only poorly degrades structured RNA molecules (Guarneros & Portier, 1990; Symmons *et al*., 2000). This enzyme catalyzes the RNA degradation into nucleotide diphosphates through phosphorylation of the phosphodiester backbone with an inorganic phosphate (Carpousis, 2007; Worrall & Luisi, 2007). However, when the nucleotide di-phosphate concentration is higher than those of inorganic phosphate, PNPase can also act as a polymerase (Deutscher & Li, 2001). Each PNPase protomer consists of four domains: two N-terminal catalytic PH domains and two conserved RNA-binding domains, KH and S1 (Rosenzweig & Chopra, 2013). Remarkably, both RNA-binding domains are not necessary for the degradosome assembly (Symmons *et al*., 2000; Stickney *et al*., 2005). The PH domains build a small catalytic channel of ~14 Å, into which only the single-stranded and unfolded substrate RNAs can enter (Symmons *et al*., 2000; Shi *et al*., 2008). Thus, physical association with RhlB, which is independent of the degradosome-assembling region of RNase E, is necessary for this activity of PNPase (Liou *et al*., 2002; Tseng *et al*., 2015). In addition to its role in RNA cleavage, PNPase can stabilize regulatory non-coding sRNAs, protecting them from RNase E-mediated premature degradation (De Lay & Gottesman, 2011).

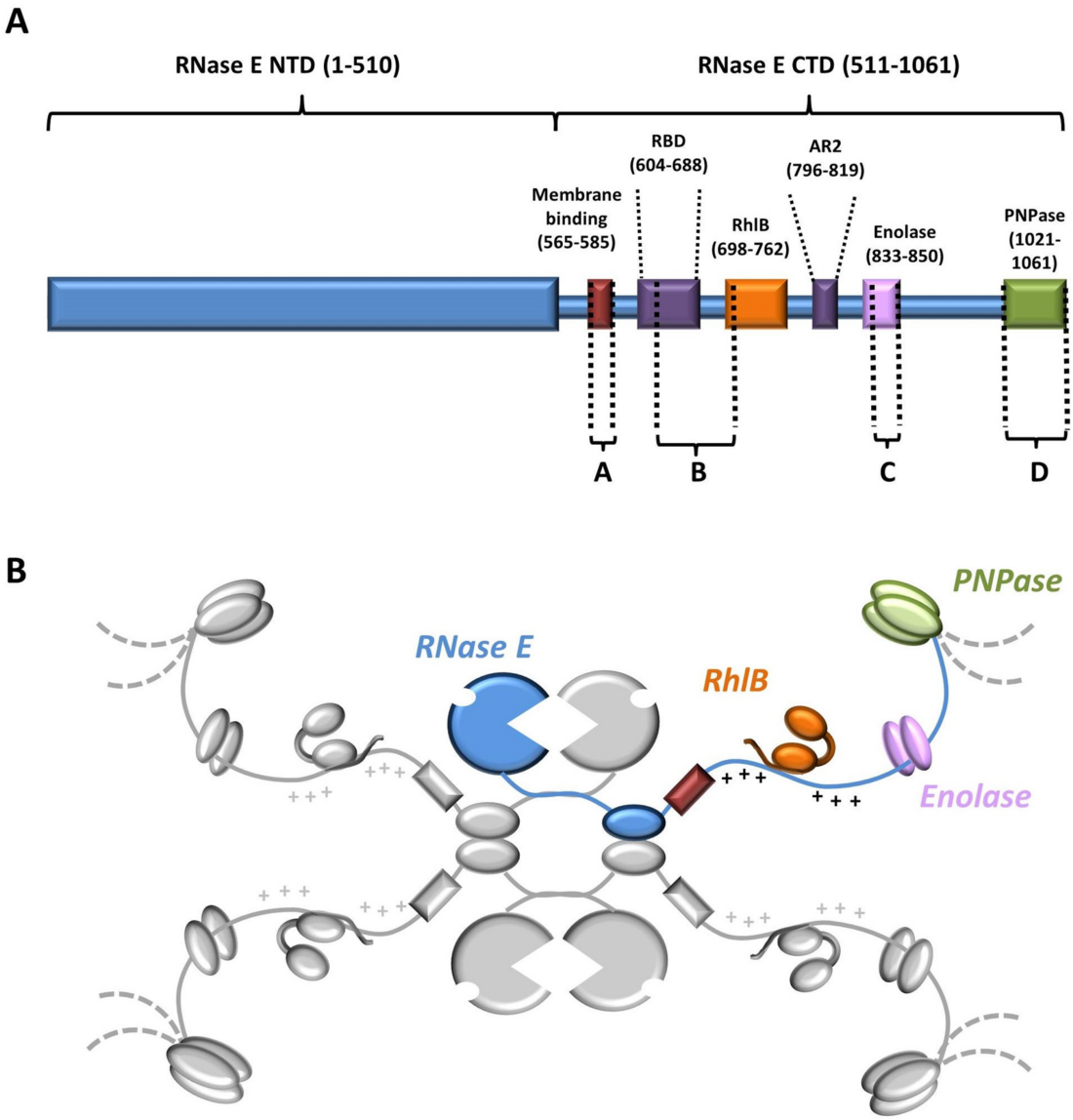

Figure 1.10. Schematic composition of the *E. coli* RNA degradosome.
A RNase E with its N- and C-terminal domains and the relative positions of RNA-, protein- and membrane binding domains (red). The letters (A-D) indicate the regions that have structural propensity according to the bioinformatics and biophysical analyses. **B** Tetrameric organization of RNase E (one monomer in blue and the others in gray). The other canonical degradosome components are demonstrated in their relative positions on the C-terminal domain of RNase E: PNPase (green), RhlB (orange), and enolase (pink). Additionally, the RhlB-binding site is flanked by two arginine rich RNA binding domains RBD and AR2, shown in lilac on the linear view and marked with + due to their high density of positively charged residues (Bruce *et al*., 2017[12]).

The DEAD box helicase **RhlB** is indispensible in the RNA degradation process. RhlB possesses ATPase and RNA-unwinding activities that are boosted through the interaction with RNase E (Khemici *et al*., 2005; Chandran *et al*., 2007). The ATPase domain harbors a Mg-ATP-binding Walker II motif, containing the D-E-A-D amino sequence, and is structurally conserved among the DEAD-box protein family. RhlB consists of an N- and C-terminal RecA-like domain and a dynamic, positively charged C-terminal tail, which

[12] Bruce *et al*., 2017 is licensed under the terms of the Creative Commons Attribution License (http://creativecommons.org/licenses/by/4.0/).

contributes to RNA binding (Chandran *et al*., 2007; Worrall *et al*., 2008). Interestingly, interaction with RNase E occurs solely within the C-terminal RecA-like domain (Chandran *et al*., 2007). The RhlB-binding site in the degradosome complex is located in the RNase E region corresponding to the residues 698-762 (Górna *et al*., 2012). Remarkably, the natively unstructured C-terminal domain of RNase E gains some structural order upon interaction with RhlB (Bruce *et al*., 2017).

Enolase is a 48 kDa enzyme of the glycolytic metabolism that is present in all three domains of life (archaea, eubacteria and eukaryotes). This enzyme is responsible for the interconversion of phosphoenolpyruvate and 2-phospho-D-glycerate, which proceeds by the reversible elimination of water (Chandran & Luisi, 2006). The exact role of enolase in the degradosome remains unclear. Nevertheless, a recent study revealed a positive effect of enolase on the RNA-binding affinity of the AR2 domain of RNase E (Bruce *et al*., 2017). This fact supports the hypothesis that enolase in the degradosome may link cellular metabolic state with gene regulation at the post-transcriptional level (Chandran & Luisi, 2006).

Intriguingly, in *Yersinia* RNase E and PNPase regulate the Ysc-Yop T3SS at the post-transcriptional level (Rosenzweig *et al*., 2005; Yang *et al*., 2008). The *Y. pseudotuberculosis* dominant-negative RNase E mutant failed to secrete Yop effectors, although their expression level was not affected (Yang *et al*., 2008). PNPase is also essential for the proper secretion of Yops, with only the RNA-binding domain and not the catalytic domain of PNPase required for regulation of T3S. It is proposed that RNase E and PNPase control the T3S via a common mechanism (Yang *et al*., 2008). Taken together, this highlights the relevance of the degradation-based regulation for bacterial virulence.

The so far identified regulatory network underlying T3SS regulation is summarised in Fig. 1.11.

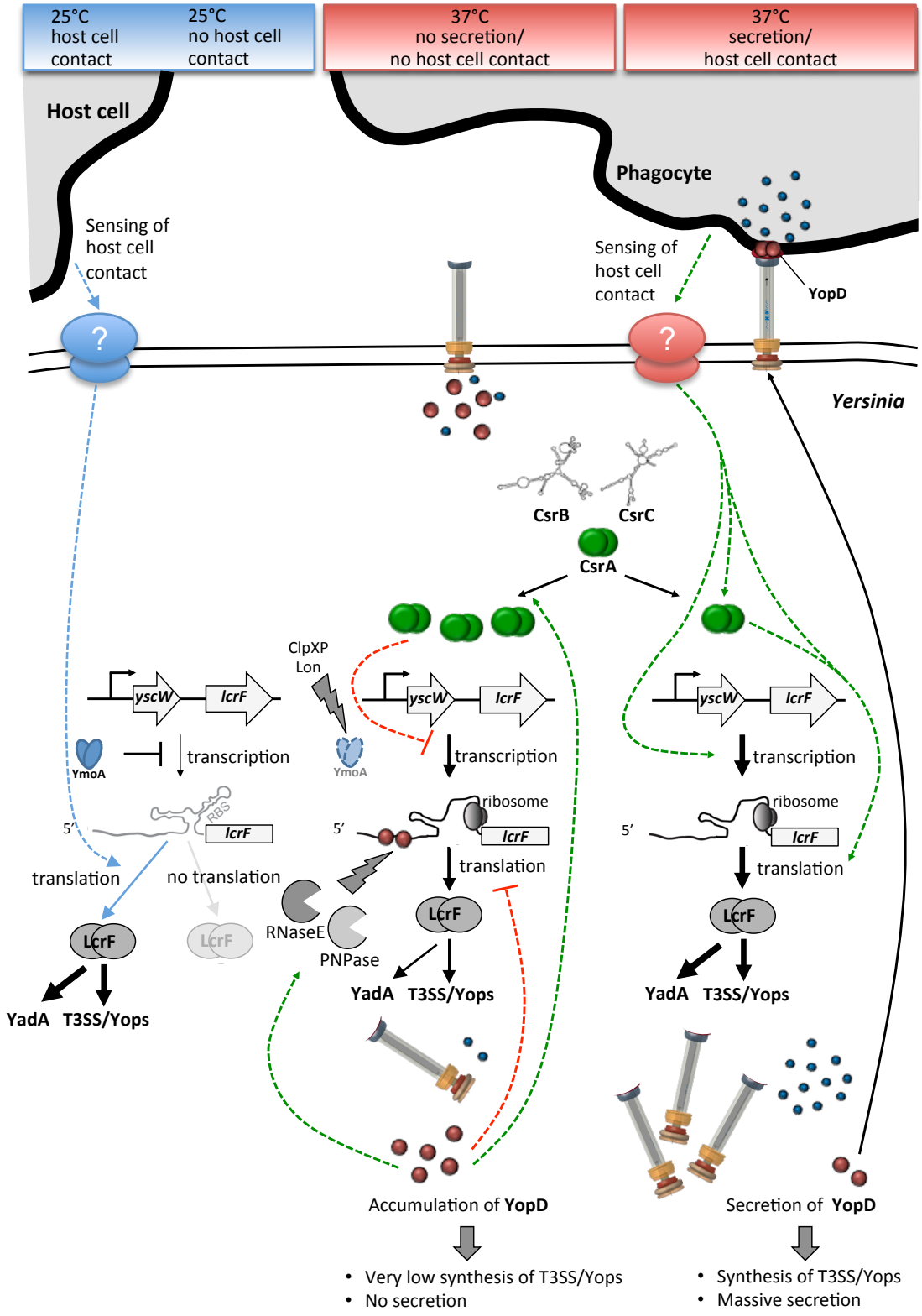

Figure 1.11. Working model of cell contact-/secretion-dependent regulation of the T3SS. LcrF expression is abolished at moderate temperatures by the transcriptional regulator YmoA and the LcrF RNA-thermometer. However, contact with the host cell is able to overcome this repression of LcrF via an unknown mechanism. At 37°C, *lcrF* synthesis is slightly induced and results in the expression of the T3SS genes. In the absence of cell contact, YopD downregulates *lcrF* via a negative feedback loop. Firstly, YopD might affect *lcrF* transcript stability. Secondly, YopD negatively affects T3SS expression by the activation of LcrF repressors (CsrA, RNase E, PNPase). Moreover, inhibition of *lcrF* transcription is also CsrA-dependent, but the mechanism is

unknown. Contact with the eukaryotic cell promotes secretion of Yops, including the T3SS inhibitor YopD. Remarkably, the transcriptional inhibitor of *lcrF*, CsrA, is absolutely essential for *lcrF* translation under secretion conditions. Preliminary data suggest that CsrA has "upstream" interaction partners, which sense the cell contact signal (blue complex with question mark), with potential "downstream" interaction partners transmitting this signal to the T3SS. Red lines indicate repressive effects. Green lines indicate positive effects. Blue lines indicate temperature-independent cell contact-mediated activation of LcrF expression.

1.4 Aim of this work

Bacterial type III secretion systems (T3SS) are complex nanomachines and major virulence determinants of animal and plant pathogens. The T3SS enables direct injection of effector proteins into host cells, where they interfere with crucial cellular functions. Although much is known about the structure and function of T3SSs, the regulatory principles promoting the expression of the delivery machinery during infection are poorly understood.

The major goal of this work is to elucidate the regulatory network that controls expression of T3SS components in *Y. pseudotuberculosis* in response to host cell contact and/or under secretion conditions. This includes (i) bacterial factors that sense host cell contact and transmit the signal into the cytosol, (ii) control elements involved in signal transduction, and (iii) factors that regulate the synthesis of the major virulence activator LcrF on both the transcriptional and post-transcriptional level.

According to previous studies, the RNA-binding proteins CsrA and YopD are some of the key factors involved in this regulatory network (Opitz, 2013; Steinmann, 2013; Pimenova, 2014; Hoßmann, 2017). Moreover, the components of the RNA degradosome, RNase E and PNPase, were also reported to control the *Yersinia* T3SS (Rosenzweig *et al*., 2005; Yang *et al*., 2008; Steinmann, 2013; Hoßmann, 2017). The interplay and the molecular mechanisms by which these and additional factors control LcrF expression will be a main focus of the study. The global influence of CsrA and YopD on the gene expression of *Y. pseudotuberculosis* will be analyzed by transcriptional profiling using comparative high-throughput RNA-Seq. Furthermore, the novel RNA-Seq based technique called CLIP-Seq will be applied for identification of genes, which are directly affected by CsrA-binding under secretion conditions.

2 Material and methods

2.1 Material

2.1.1 Equipment and material

Equipment and material used in this study were obtained from the following companies: Amersham, BD Bioscience, BD Falcon, Biometra, BioRad, Biospec, Biozym, Conrad Electronic, Covaris, Difco, Eppendorf, Fermentas, GE Healthcare, G. Heinemann, Heraeus, Infors AG, Invitrogen, LIFE Technologies, Macherey-Nagel, Millipore, Neolab, PeqLab, Promega, QIAGEN, Roth, Sarstedt, Sartorius, Schott, Sorvall, Thermo Fisher Scientific, T.H. Geyer, VWR International, Vilber and Whatman Schleicher & Schüll GmbH if not mentioned otherwise.

2.1.2 Buffers and solutions

Chemicals used for buffers and solutions were purchased from the following manufacturers: Ambion, Applichem, BD Biosciences, Bioline, Epicentre, Fermentas, Fisher Scientific, GIBCO, Hartmann Analytic, Invitrogen, Macherey-Nagel, Merck, Metabion, New England Biolabs (NEB), Oxoid, Promega, QIAGEN, Roche, Roth, Sigma-Aldrich, T.H. Geyer and VWR. The composition of the employed buffers and solutions is listed in Table 2.1. All buffers and solutions were prepared with H_2O_{dest}, if not indicated otherwise.

Table 2.1. Buffers and solutions

Buffer/solution	Composition
Anode buffer	0.1 M Tris, 0.0225 M HCl
Cathode buffer	0.1 M Tris, 0.1 M tricine, 0.1 % SDS
CDP* detection buffer	100 mM Tris-HCl, 100 mM NaCl
CDP* maleic acid buffer	100 mM maleic acid, 150 mM NaCl, pH 7
CDP* wash buffer	100 mM maleic acid, 150 mM NaCl, 0.3 % Tween 20, pH 7
CDP* blocking reagent (10x)	10 % blocking reagent (Roche) in CDP* maleic acid buffer
CIP buffer	100 mM NaCl, 50 mM Tris-HCl pH 7.4, 10 mM $MgCl_2$
Coomassie staining solution	20 % isopropanol, 10 % acetic acid, 0.05 % Coomassie™ Brilliant Blue G250
CsrA bandshift buffer	20 mM Na_2HPO_4/ NaH_2PO_4 pH 8.0, 100 mM KCl; 2 mM DTT; 5 % glycerol
CsrA elution buffer	0.1 M Tris-HCl pH 7.5, 0.3 M NaCl, 40 mM imidazole
CsrA lysis buffer	0.1 M Tris-HCl pH 7.5, 0.3 M NaCl, 20 mM imidazole
CsrA washing buffer	0.1 M Tris-HCl pH 7.5, 0.3 M NaCl, 250 mM imidazole
GLII buffer	95 % formamide, 18 mM EDTA, 0.025 % xylene cyanol, 0.025 % bromphenol blue

Buffer/solution	Composition
High-Salt buffer	50 mM NaH_2PO_4, 1 M NaCl, 0.05 % Tween 20, pH 8.0
Hybridization buffer	1x blocking reagent in maleic acid buffer
Lysis buffer	2 % SDS, 0.01 M NaOAc, pH 4.5
Lysozyme-TE-buffer	50 mg/ml lysozyme in TE buffer
MOPS (20x)	200 mM MOPS, 50 mM sodium acetate, 10 mM EDTA
MOPS agarose gel	1.2 % agarose, 1.1 % MOPS
NP-T buffer	50 mM NaH_2PO_4, 300 mM NaCl, 0.05 % Tween 20, pH 8.0
ONPG solution	4 mg/ml ONPG
10x PBS	80 g/l NaCl, 2 g/l KCl, 6.1 g/l Na_2HPO_4, 2 g/l KH_2PO_4, pH 7.3
2x PK buffer	100 mM Tris-HCl pH 7.9, 10 mM EDTA, 1 % SDS
PNK buffer	50 mM Tris-HCl pH 7.4, 10 mM $MgCl_2$, 0.1 mM spermidine
Resuspension buffer	0.3 M sucrose, 0.01 M NaOAc, pH 4.5
Rifampicin solution	30 mg/ml in MeOH
RNA loading buffer (5x)	31 % formamide, 2.7 % formaldehyde, 0.1 mg/ml EtBr, 4 mM EDTA (pH 8.0), 0.03 % bromphenol blue and 20 % glycerol in 4x MOPS buffer
SDS running buffer	33 mM Tris-HCl pH 8.3, 192 mM glycine, 0.1 % SDS
SDS sample buffer (1x)	60 mM Tris pH 6.8, 10 % glycerol, 2 % SDS, 3 % DTT, 0.02 % bromphenol blue
SDS separating buffer (4x)	1.5 M Tris-HCl pH 8.8, 4 % SDS
SDS stacking buffer (4x)	0.5 M Tris-HCl pH 6.8, 4 % SDS
SSC (20x)	3 M NaCl, 0.3 M sodium citrate, pH 7
Stop solution (5%)	5 % Roti®-aqua-phenol, 95 % EtOH
Stop solution (10%)	10 % Roti®-aqua-phenol, 90 % EtOH
TAE (50x)	2 M Tris, 100 mM EDTA, pH 8.0
TBE (10x)	900 mM Tris-HCl, 900 mM boric acid, 25 mM EDTA, pH 8.0
TBST buffer	20 mM Tris-HCl pH 7.5, 150 mM NaCl, 0.05 %Tween-20
TBSTM buffer	5 % powdered milk in TBST
TE	10 mM Tris-HCl, 1 mM EDTA, pH 7.5
Transblot buffer	25 mM Tris, 192 mM glycine, 20 % MeOH
Transformation buffer	272 mM sucrose, 15 % glycerol, sterile filtrated
Wash buffer 1	2x SSC, 0.1 % SDS
Wash buffer 2	0.1x SSC, 0.1 % SDS
YopD bandshift buffer	50 mM Na_2HPO_4/ NaH_2PO_4 pH 8.0, 150 mM KCl; 2 mM DTT; 5% glycerol
YopD elution buffer	50 mM Na_2HPO_4/ NaH_2PO_4 pH 8.0, 150 mM NaCl, 80 mM imidazole
YopD lysis buffer	50 mM Na_2HPO_4/ NaH_2PO_4 pH 8.0, 150 mM NaCl, 40 mM imidazole
YopD washing buffer	50 mM Na_2HPO_4/ NaH_2PO_4 pH 8.0, 150 mM NaCl, 250 mM imidazole
Z-buffer	100 mK sodium phosphate buffer pH 7, 1 mM Mg_2SO_4

2.1.3 Media and medium supplements

Media used in this work were prepared with dest. water, if not indicated otherwise, and are listed in Table 2.2. For the preparation of solid media 15 g of agar were added to 1 L of liquid media (except for *Yersinia* selective agar).

Table 2.2. Media

Medium	Composition
BHI (Brain-Heart Infusion) broth	37 g/l BHI
DYT (Double Yeast Tryptone) (J. H. Miller, 1992)	10 g/L yeast extract, 5 g/l NaCl, 16 g/L tryptone
LB (Luria-Bertani) broth (Sambrook & Russell, 2001)	5 g/l NaCl, 5 g/l yeast extract, 10 g/l tryptone
RPMI 1640 + GlutaMax-I (Roswell Park Memorial Institute) supplemented with 5 µg/ml Newborn calf serum (NCS)	Gibco (Life Technologies)
Yersinia selective medium	*Yersinia* selective agar base with *Yersinia* selective supplement (Oxoid)

Specific selection for resistant bacteria was achieved by addition of sterile filtrated antibiotics to the media (Table 2.3).

Table 2.3. Final concentrations of antibiotics

Antibiotic	Final concentration
Carbenicillin (Cb)	100 µg/ml
Chloramphenicol (Cm)	30 µg/ml
Kanamycin (Kan)	50 µg/ml
Rifampicin	1 mg/ml

2.1.4 Enzymes, antibodies and kits

Enzymes, antibodies and commercial kits exploited in this study are listed in Table 2.4, 2.5 and 2.6 respectively.

Table 2.4. Enzymes

Enzyme	Manufacturer
Antarctic phosphatase	NEB
Benzonase	Sigma-Aldrich
CIP (Calf Intestinal Phosphatase)	NEB
Lysozyme	NEB
Mango*Taq*™ DNA Polymerase	Bioline
Phusion® High-Fidelity DNA Polymerase	NEB
PNK (T4 Polynucleotide Kinase)	Fisher Scientific

Enzyme	Manufacturer
5' Polyphosphatase	Epicentre
Restriction enzymes	NEB
TAP (Tobacco Acid Pyrophosphatase)	Epicentre
TURBO™ DNase	Ambion
T4 DNA Ligase	Promega
T4 RNA Ligase I	NEB

Table 2.5. Antibodies

Antibody	Manufacturer
Primary antibodies	
Anti-FLAG (1:1000)	Sigma
Anti-CsrA (1:5000)	Davids Biotechnology
Anti-H-NS (1:150000)	Davids Biotechnology
Anti-LcrF (1:8000)	Greg Plano
Secondary antibodies	
Anti-mouse Immunoglobulin HRP conjugate	NEB
Anti-rabbit Immunoglobulin HRP conjugate	Cell Signaling

Table 2.6. Kits

Kit	Manufacturer
ERCC RNA spike-in control mixes	Ambion
Biotin RNA Labeling Mix	Roche
Chemiluminescent Nucleic Acid Detection Module	Thermo Fisher Scientific
CloneJET PCR Cloning Kit	Thermo Scientific
DIG DNA Labeling Mix	Roche
DIG luminescent detection	Roche
Mango Mix™	Bioline
MICROB*Express*™ Kit	Ambion
MinElute PCR Purification Kit	QIAGEN
NEBNext® Multiplex Small RNA Library Prep Set for Illumina®	NEB
NucleoSpin® Gel and PCR Clean-up	Macherey-Nagel
NucleoSpin® Plasmid	Macherey-Nagel
PURExpress® *in vitro* Protein Synthesis	NEB
QIAprep® Spin Miniprep kit	QIAGEN
QIAquick® Gel Extraction kit	QIAGEN
QIAquick® PCR purification kit	QIAGEN
SensiFastTM SYBR® No-ROX One-Step kit	Bioline
SV Total RNA Isolation System kit	Promega

Kit	Manufacturer
TranscriptAid™ High Yield	Fermentas
TURBO™ DNase	Ambion
T4 DNA Ligase	Promega
T4 RNA Ligase I	NEB

2.1.5 Oligonucleotides and plasmids

Oligonucleotides were obtained from Metabion and shipped at 100 µM in dest. water (Table 2.7).

Table 2.7. Oligonucleotides

Name	Sequence (5'-3')	Restriction site
555	CGGCGCGGATCCCTCTCACACCAGCTGTG	*BamH*I
556	GGGGGCGTCGACGGCAAACTCAATATCCTG	*Sal*I
583	GGGCGCGGATCCGATTGGGCCGGAATCTAGC	*BamH*I
714	GCGATCGGCATAACCACCACG	
I82	GCAATCAGCTAGTCAATTTG	
I214	GCGGCGTCTAGACCATTGAATCTTCACAATCTAATCCCG	*Xba*I
I303	GCGCGCTGCAGGATTTTTAGGACAGTATAAC	*Pts*I
I404	TTTGAATTCGCCATCTTGTGAATGCTCAAC	*EcoR*I
I515	GCAGTTCATTTGGATCAATAC	
III44	GAGACAACTCCACACCCA	
III45	GCAAAAGCAGTAATTCCT	
III393	CCGACGTAAAGCCGCGATAC	
III394	CCTCGTTCATAAGCACTCGTC	
III731	GAATAAGCATTCTTTGCTCC	
IV527	TTGCTGACTCCGATTATTCG	
IV528	GAAGACGACCGCGCCCAAC	
IV529	CGCGACTCAGCAAGAAGAG	
IV530	GCCGATGTCTGGGCGCAG	
V4	TGATTGGCGATGAGGTTACGG	
V5	TTCTGCTTGGATGCGCTGGT	
V066	GGGCGCGTAATACGACTCACTATAGGAATGTAATGGCTTAC GTTTTC	
V516	GGGCGCGCTAGCTTACTCTCGAACTTTCCCCTC	*Nhe*I
V700	GGGCGCGTAATACGACTCACTATAGCAACAATACCGTGAAA TGC	
V941	GAGCATGCGGCCGCTAAGAACAGTGAA	
VI085	CGGAGTCAGCAAAATTGTACC	

Name	Sequence (5'-3')	Restriction site
VI086	GGGCGCCTCGAGTCCCTATCAGTGATAGAGATTGACATCCCTATCAGTGATAGAGATACTGAGCACGTTTGCTGATTCCGATTCTAACC	*Xho*I
VI203	GCGGCGGAGCTCTAACTGTTGCTCGGCGGCGGG	*Sac*I
VI204	**GAAGCAGCTCCAGCCTACAC**ATGAGTACATTCTCTTTTAATCAGATC	
VI205	**ACTAAGGAGGATATTCATATG**CGCATAAAAATTCCTCAGCCTTATT	
VI206	GCGGCGGAGCTCTTATTGCTACAAAGCGTTGGTCTG	*Sac*I
VI207	GCACGGGTTGTCAAAAGAGAGC	
VI208	GACCCTACTAATTTGGGCCG	
VI249	GCGGCGCTCGAGCACTCATCTAATTAGCCATTGC	*Xho*I
VI251	GCGGCGGCTAGCAAGAGAGATGCAATCTAACTAAT	*Nhe*I
VI252	ACCATCCAATTGTTTTGTTTGGC	
VI253	CTAATGGTCTTGATACTGCGG	
VI254	CCTTTCTTCCAAGTGGGTACC	
VI255	CCGGCTGCTGGCCCCGC	
VI256	GGAGATCATTACCAACCTACCGC	
VI257	GCCAATCTTGTGTTTCCAGCTTAG	
VI388	GATTACGCCAAGCTTGGCTGC	
VI389	GACGGCCAGTGAATTCCCGG	
VI497	GCGGCGGGTAACCTCCCTATCAGTGATAGAGATTGACATCCCTATCAGTGATAGAGATACTGAGCACGTGATTTATTATATTGGTTTTGGTTG	*BstE*II
VI560	GGCTAATACGACTCACTATAGCGTTGATTCTCGTTAGACC	
VI561	CGCTAATTGCTTGATTTCAC	
VI562	GGCTAATACGACTCACTATAGGTGAAATCAAGCAATTAGCG	
VI563	AGGGGCGCATTATTTCG	
VI564	GGCTAATACGACTCACTATAGGGCTTACCGAAATAATGCG	
VI565	CATTCTTTTCATCTTTAACTTACTCG	
VI593	GCGGCGGAATTCGGCTATTAGAAGATAACGTTTGCG	*Eco*RI
VI594	GCGGCGCTGCAGACAATAACTTCCTGGCCTTCACG	*Pst*I
VI595	GCGGCGGAGCTCTGTTAGCGGCTCTCATTACTCC	*Sac*I
VI596	**GAAGCAGCTCCAGCCTACAC**AGTGTGGTAGAATATCAGCTAAC	
VI597	**ACTAAGGAGGATATTCATATG**TAAATGATGCTAAGTTCCACCTC	
VI598	GCGGCGGAGCTCCACAACCCATTGATAGGCTGAC	*Sac*I
VI599	CTTCTTTGCAGGCGTCTAGCGG	
VI600	CTTGATCATCTCATGAGCGGCC	
VI614	GGAAGCTAAGCAAATTTGCGCGAG	

Name	Sequence (5'-3')	Restriction site
VI618	CCCACGGAGAATCCGACGGG	*Sac*I
VI729	GCGGCGGAATTCTAATACGACTCACTATAGTGATTTATT ATATTGGTTTTGGTTG	*EcoR*I
VI950	GCGCGTAATACGACTCACTATAGGTTCGCGCGGCTAATGAG AG	
VII593	AATGATACGGCGACCACCG	
VII594	CAAGCAGAAGACGGCATACG	
VII836	GAGTTTGTAGAAACGCAAAAAGG	

Underlined – restriction sites
Dotted underlined – T7 promoter
Dashed underlined – P_{tet} promoter
Bold – sequences homologous to kanamycin resistance gene (pKD4)

The plasmids used in this study are listed in Table 2.8.

Table 2.8. Plasmids

Name	Description	Reference
pAKH3	pGP704, *sacB*$^+$, ori R6K, Ap^R	(Heroven *et al*., 2012)
pAKH172	pET28a, *csrA*$^+$, ori (3286), Kan^R	A.K. Heroven
pFU98	promoterless *luxCDABE* operon, ori pSC101*, Cm^R	(Uliczka *et al*., 2011)
pGP20	promoterless *lacZ* gene, ori pSC101, Tet^R	P. Gerlach
pHSG576	cloning vector, ori pSC101, Cm^R	(Takeshita *et al*., 1987)
pJH12	pET28a, *yopD*$^+$, *lcrH*$^+$, ori M13, Kan^R	J. Hoßmann
pJH35	pHSG576, P_{csrA}::*csrA*:3xFLAG$^+$ (-298/+183), ori pSC101, Cm^R	J. Hoßmann
pKB14	pBAD18-*lacZ*(481), pBAD::*lcrF'-'lacZ* (-124 to +74)[a], ori pMB1, Ap^R	K. Böhme
pKB60	pHSG576, *csrA*$^+$, ori pSC101, Cm^R	K. Böhme
pKB98	pBAD18-*lacZ*(481), pBAD::*lcrF'-'lacZ* (-124 to +74)[a] (mutation AG-46/-45CC), ori pMB1, Kan^R, Ap^R	K. Böhme
pKB99	pBAD18-*lacZ*(481), pBAD::*lcrF'-'lacZ* (-124 to +74)[a] (mutation GUU-30/-28AAA), ori pMB1, Kan^R, Ap^R	K. Böhme
pKD4	kanamycin cassette template	(Datsenko & Wanner, 2000)
pMK46	pFU98, P_{yscW} (-42 to +428)[b], ori SC101*, Cm^R	M. Kroll
pMP1	pBAD33-RBS$_{lcrF}$; 3´UTR, ori M13, Cm^R	M. Pimenova
pMP2	pBAD33-RBS$_{lcrF}$; Δ3´UTR, ori M13, Cm^R	M. Pimenova
pMP14	pFU98, P_{lac}::*yscW* (+28 to +428)[b] , ori SC101, Cm^R	M. Pimenova
pMP26	pAKH3, Δ*rcsF*, ori R6K, Kan^R, Ap^R	this study
pMP27	pFU98-P$_{tet}$::*yscW* (+28 to +428)[b], ori pSC101*, Cm^R	
pMP28	pFU98-P$_{rprA}$::*rprA* (-158 to -1)[c], ori pSC101*, Cm^R	this study
pMP30	pKB14, P$_{tet}$::*lcrF'-'lacZ* (-124 to +74)[a], ori pMB1, Ap^R	this study

Name	Description	Reference
pMP31	pGP20, P_{rne}::*rne'-'lacZ* (-508 to +305)[d], ori SC101, Tet^R	this study
pMP35	pAKH3, Δ*rhlB*, ori R6K, Kan^R, Ap^R	this study
pRS15	pRS1, ori p15A, Cm^R	R. Steinmann
pRS16	pRS1, ori p15A, *yopD*$^+$, Cm^R	R. Steinmann
pRS40	pBAD33, P_{BAD}::*rne* (-15 to +1395)[d], ori p15A, Cm^R	R. Steinmann
pTS31	pFU98, *yadA-luxCDABE* +RBS, ori SC101*, Cm^R	(Uliczka *et al*., 2011)
pWO41	pTS31, *yadA-luxCDABE* +RBS, ori SC101*, Ap^R	W. Opitz
pWO42	pTS34, *yscWlcrF-luxCDABE* +RBS, ori SC101*, Ap^R	W. Opitz

[a] – relative to translational start codon of *lcrF*
[b] – relative to transcriptional start of *yscW*
[c, d] – relative to translational start codon of *rprA* and *rne* respectively

2.1.6 Bacterial strains and cell lines

Bacterial strains and eukaryotic cell lines employed in this work are mentioned in Table 2.9.

Table 2.9. Strains and cell lines

Strain/cell line	Description	Reference
***Escherichia coli* K12**		
BL21(DE3)	F^- *gal met* r^-m^- *lon hsdS* λLysp*lac*UV5-T7 gene1p*lacI*^{q} *lacI*	(Studier & Moffatt, 1986)
S17-1λpir	*recA*, *thi*, *pro*, *hsdR*$^-$M$^+$ (RP4-2 Tc::Mu-Km::Tn7), λpir	(Simon *et al*., 1983)
Yersinia pseudotuberculosis		
YPIII	pIB1, wild-type	(Bölin *et al*., 1982)
YPIII (pIB68)	YPIII pIB102, Δ*yscS*, Kan^R	(Bergman *et al*., 1994)
YPIII (pIB102)	YPIII, pIB102, (*yadA*::Tn5), Kan^R	(Bölin *et al*., 1982)
YPIII (pIB604)	YPIII pIB102, Δ*yopB*, Kan^R	(Håkansson *et al*., 1996)
YP12	ΔpIB1	(Dersch & Isberg, 1999)
YP53	YPIII, pIB1, Δ*csrA*, Kan^R	(Heroven *et al*., 2008)
YP66	YPIII, pIB1, Δ*lcrF*, Ap^R	(Böhme *et al*., 2012)
YP90	YPIII, *yscW-lcrF* (UU-28/-27CC)[a]	(Böhme *et al*., 2012)
YP91	YPIII, pIB1, Δ*yopD*	R. Steinmann
YP95	YPIII, *yscW-lcrF* (GUU-30/-28AAA)[a]	(Böhme *et al*., 2012)
YP101	YPIII, pIB1, Δ*yscS*	R. Steinmann
YP138	YPIII, pIB1, Δ*pnp*	R. Steinmann
YP145	YPIII, pIB1, Δ*csrA* Δ*yopD*, Kan^R	R. Steinmann
YP179	YPIII, pIB1, Δ*lcrF*	R. Steinmann
YP155	YPIII, ΔpIB1, pWO14 (*yscWlcrF*$^+$), Ap^R	(Opitz, 2013)

Strain/cell line	Description	Reference
Yersinia pseudotuberculosis		
YP280	YPIII, pIB1, Δ*csrA*Δ*lcrF,* Kan^R	M. Pimenova
YP284	YPIII, pIB1, Δ*csrA lcrF* (GUU-30/-28AAA) open thermoloop, Kan^R	R. Steinmann
YP300	YPIII, pIB1, Δ*ompR/envZ*, Kan^R	M. Pimenova
YP310	YPIII, pIB1, Δ*rcsBC*, Kan^R	this study
YP323	YPIII pIB1, Δ*rcsF*, Kan^R	this study
YP342	YPIII, pIB1, Δ*rhlB*, Kan^R	this study
Eukaryotic cell line		
HEp-2	Human carcinoma larynx epithelial cell line	(Toolan, 1954)

[a] – relative to translational start codon of *lcrF*

2.1.7 Software and databases

The following applications were used in this work: Adobe Illustrator CS4 (Adobe Systems Software Ireland Ltd.), Adobe Photoshop CS4 (Adobe Systems Software Ireland Ltd.), A plasmid Editor (ApE), Graph Pad PRISM 6.0 (Graphpad Software, Inc.), Image J (Schneider *et al*., 2012), Image Lab 2.0.1 (BioRad), Microsoft® Excel® 14.4.1 (Microsoft), Rotor-Gene Q Series Software 2.0.2 (QIAGEN), SkanIt Software 2.4.3 Research edition Varioskan Flash (Thermo Scientific), National Center for Biotechnology Information (NCBI).

2.2 Methods

2.2.1 Microbiological methods

2.2.1.1 Sterilization

Liquid and solid media was moist heat sterilized for 20 minutes at 121 °C and 1 bar overpressure in an autoclave. Non-autoclaveable solutions (*e.g.* antibiotics or sucrose) were sterile filtered using filters with a pore diameter of 0.2 µm. Glass equipment such as pipettes or flasks was heat-sterilized at 180 °C in a compartment dryer.

2.2.1.2 Growth conditions

E. coli strains (Table 2.9) were grown overnight under aerobic conditions at 37 °C in liquid LB medium in a shaking incubator at 200 rpm and on solid LB medium. *Y. pseudotuberculosis* strains (Table 2.9) were aerobically cultivated at 25 °C on solid LB or *Yersinia* agar plates for 2 days or in liquid LB_{BD} medium in a shaking incubator at 200 rpm. Over day cultures were incubated at 25 °C for 2 hours and then 20 mM NaOx and 20 mM $MgCl_2$ was added (secretion conditions) or not (non-secretion conditions), followed by shift to 37 °C for 4 hours. Flasks and glass test tubes were used for liquid

cultivation and petri dishes for cultivation on solid medium. For selective growth of the bacteria, antibiotics were added to the medium.

2.2.1.3 Determination of cell density

The cell density of a liquid bacterial culture was determined spectrophotometrically by measurement of the optical density at a wavelength of 600 nm (OD_{600}). An OD_{600} of 1 corresponds to a cell density of $1x10^9$ cells/ml (Sambrook & Russell, 2001) with a protein content of 150 µg (Miller, 1992). Cultures with an OD_{600} exceeding 1 were diluted 1:10 to ensure measurements within the linear range. The corresponding growth medium was used as a reference.

2.2.1.4 Storage of bacteria

Short and middle term (up to 14 days) storage of bacteria was carried out on agar plates at 4 °C. For the long-term storage 1.25 ml of an overnight culture were mixed with 750 µl glycerol (end concentration 30 % glycerol) and stored at -80 °C.

2.2.2 Molecular biological and genetic methods for DNA

2.2.2.1 Determination of DNA concentration and quality

Nucleic acid concentration was determined by measuring the absorbance with a NanoDrop photospectrometer. Since the wavelength of maximum absorption for both DNA and RNA is 260 nm, A_{260} was measured. The calculation of the nucleic acid concentration was conducted using the following equation:

$$Concentration\ (\mu g/ml) = (A_{260} - A_{320}) \times diluting\ factor \times 50\ \mu g/ml$$

To test the DNA purity A_{260}/A_{280} and A_{260}/A_{230} ratios were measured. An A_{260}/A_{280} ratio lower then 1.8 indicates protein contamination. The A_{260}/A_{230} ratio refers to the presence of organic compounds or chaotropic salts in the sample and should be higher than 1.5, ideally close to 1.8. The A_{260} measurement was also adjusted for turbidity, another indication of possible contamination, which is measured at an absorbance of A_{320}.

2.2.2.2 Polymerase chain reaction (PCR)

Polymerase chain reaction was performed to specifically amplify DNA fragments (Saiki *et al*., 1988). PCR requires four essential components: DNA template, DNA polymerase, primers and nucleotides. Initially, the reaction is heated up to 95 °C to separate the double stranded DNA into single strands (denaturation step). After that, the mixture is cooled down so that the primers, short fragments of single stranded DNA that are complementary to the target sequence, can bind to the DNA template) (annealing step). Annealing temperature depends on the nucleotide composition of the primers and is calculated using the formula T_a (°C) = 4(G+C) + 2(A+T) (Suggs *et al*., 1981). Subsequently, the reaction is heated to 72 °C and the DNA polymerase begins to synthesize new DNA from the end of the primers in 5' to 3' direction (elongation step). The elongation time depends on the polymerase and the size of the amplified DNA fragment. This cycle can be repeated 30 to 40 times, which allows the DNA target to be exponentially amplified.

Two different DNA-polymerases were used in this study: Mango *Taq* polymerase (from *Thermus aquaticus*) for colony- and test PCRs and Phusion-HF polymerase (from *Pyrococcus furiosus*) for cloning, mutagenesis and sequencing because of its higher fidelity when copying DNA. Phusion® and Mango*Taq*™ PCRs were performed in 50 µl or 20 µl aliquots respectively according to the manufacturer's instructions using T3000 Thermocycler (PeqLab) or a gradient cycler (Eppendorf).

2.2.2.3 DNA agarose gel electrophoresis

Agarose gel electrophoresis was conducted to separate double stranded DNA fragments of varying sizes. For this purpose DNA samples were loaded into pre-cast wells of the agarose gel and an electric field was applied. The phosphate backbone of the DNA molecule is negatively charged. Consequently, when placed in an electric field, DNA fragments will move from negatively charged cathode to the positively charged anode. The migration rate of DNA through a gel primarily depends on the size and conformation of the molecule, the percentage of agarose as well as on the voltage applied. In this work DNA separation was performed depending on the fragment size with 0.8 % to 2.5 % agarose gels at a voltage of 100 V to 120 V for approximately 45 min in 1x TAE buffer. To facilitate the application of the DNA samples to the gel they were mixed with 6x loading dye. For estimation of the size and approximate quantification of the separated DNA fragments, 4 µl DNA ladder mix (Fermentas, USA) were used. Subsequently the separated DNA molecules were visualized under 226 nm UV light after staining with ethidium bromide (1 µg/ml in water) and photographed with a CCD (charge-coupled device) camera of the gel documentation system (BioRad, USA).

2.2.2.4 DNA extraction from agarose gels

For isolation and purification of a DNA molecule of interest from a mixture of nucleic acids with different sizes, the DNA fragments were separated by agarose gel electrophoresis and stained with ethidium bromide. Visualization of the DNA fragment of interest was performed under 315 nm UV light, which renders a less destructive effect on the DNA compared to 226 nm UV light, used for the routine visualization. Thereafter, the DNA fragment of interest was isolated from the agarose gel and purified using the 'QIAquick Gel Extraction Kit' (QIAGEN, Germany). DNA fragments less then 100 bp were purified with 'NucleoSpin® Gel and PCR Clean-up Kit' (Macherey-Nagel, Germany) according to the manufacturer's instructions. The DNA was eluted with 30 µl nuclease-free water.

2.2.2.5 Isolation of plasmid DNA

Isolation of plasmid DNA from bacterial cells was carried out using the 'QIAGEN Plasmid Mini Kit' or 'QIAGEN Plasmid Midi Kit' (QIAGEN, Germany) according to the manufacturers instructions. For this purpose, an overnight culture of bacteria harboring the plasmid of interest was grown in BHI medium supplemented with appropriate antibiotics. Finally, plasmid DNA was eluted with 30 µl (for 'Mini Kit') or 100 µl (for 'Midi Kit') nuclease-free water.

2.2.2.6 DNA purification

Purification of DNA was performed after PCR reactions or restriction digests to remove enzymes, salts, and dNTPs using the 'PCR Purification Kit' (QIAGEN, Germany). For purification of DNA fragments less then 100 bp 'NucleoSpin® Gel and PCR Clean-up Kit' (Macherey-Nagel, Germany) was applied. The DNA was eluted with 30 µl nuclease-free water.

2.2.2.7 DNA sequencing

Sequencing of plasmids or PCR products was performed by the in-house facility, the Department of Genome Analysis, GMAK (HZI, Germany).

2.2.2.8 Cloning techniques

2.2.2.8.1 Restriction digest

For insertion of DNA fragments into a specific site of a vector, both molecules need to have compatible 3' and 5' ends. To gain these compatible sites, the insert and the vector were digested with the same restriction enzymes (NEB, England). Restriction enzymes recognize specific palindromic DNA sequences of four to eight base pairs and produce 'sticky' or 'blunt' ends, which can be re-ligated. The optimal reaction setup in terms of temperature, incubation time, and buffer composition is provided by the manufacturer. A typical reaction of 50 µl contained the following ingredients:

plasmid DNA (2 µg)	5	µl
enzyme 1	0.5	µl
enzyme 2	0.5	µl
BSA (10x)	5	µl
buffer (10x)	5	µl
Nuclease-free water	34	µl

The restriction digest was generally performed at 37 °C for 1 to 2 hours.

2.2.2.8.2 Dephosphorylation of plasmid DNA

In order to decrease the religation rate, the phosphate groups at the 5' end of linearized vector DNA were removed by adding 'Antarctic Phosphatase' (NEB, USA). The enzyme was applied directly to the restriction digest. 1 µl of the phosphatase was typically added to a 50 µl digest reaction. The enzyme was incubated at 37 °C for 15 min and inactivated at 65 °C for 5 min.

2.2.2.8.3 Ligation

The final step for construction of a plasmid is the integration of the DNA fragment of interest (insert) into the desired vector. In a ligation reaction, the enzyme T4 DNA ligase (Promega, USA) catalyzes the formation of phosphodiester bonds between the 5'-phosphate and the 3'-hydroxyl groups of two DNA strands (i.e., insert and vector) with compatible restriction sites. A 10 µl standard ligation reaction was composed of:

DNA fragment (insert)	8	µl
vector DNA	0.5	µl
T4 DNA ligase	0.5	µl
ligation buffer (10x)	1	µl

The ligation was performed overnight at 4 °C. To calculate the religation rate of the linearized vector, a control ligation reaction with nuclease free water instead of the insert was performed in parallel.

2.2.2.9 Plasmid construction

2.2.2.9.1 Construction of plasmid pMP27

pMP27 represents P_{tet}*::yscW-luxCDABE* transcriptional reporter gene fusions, that was used to confirm the negative effect of CsrA on *yscW-lcrF* transcription. The plasmids pMP27 was derived from low copy *lux-CDABE* reporter vector pFU98. Insert for pMP27 was generated with primer pair VI086/V516 (table 2.7.), digested with *Xho*I and *Nhe*I and ligated into *Xho*I/*Nhe*I site of pFU98.

2.2.2.9.1 Construction of plasmid pMP28

pMP28 represents *rprA'-luxCDABE* transcriptional reporter gene fusions. It was employed as readout for investigation of the CsrA effect on *rcsB* expression. The plasmid pMP28 and was derived from low copy *lux-CDABE* reporter vector pFU98. Insert for pMP28 was generated with primer pair VI249/VI251 (table 2.7.), digested with *Xho*I and *Nhe*I and ligated into *Xho*I/*Nhe*I site of pFU98.

2.2.2.9.2 Construction of plasmid pMP30

pMP30 was constructed to confirm the previously identified positive effect of CsrA on *lcrF* translation. For this purpose, P_{BAD} promoter from pKB14 was exchanged against P_{tet} promoter. Insert P_{tet}*::lcrF'* (-123 to +75 relative to the translational start of *lcrF*) was amplified with primer pair VI497/I404 (table 2.7.) and digested with *BstE*II and *Eco*RI. pKB14 was also digested with *BstE*II and *Eco*RI and separated from the insert P_{BAD}::*lcrF'* (-123 to +75 relative to the translational start of *lcrF*) by gel extraction (see 2.2.2.4.). Finally, the P_{tet}*::lcrF'* insert was ligated into *BstEII*/*EcoRI* site of linearized pKB14.

2.2.2.9.4 Construction of plasmid pMP31

pMP31 encodes an *rne'-'lacZ* reporter gene fusion, that was employed to determine the cellular RNase E activity (Yang *et al*., 2008). The insert, 5' UTR of *rne* mRNA (-465 to -1 relative to the translational start of *rne*) fused to *lacZ* reporter gene, was amplified with primer pair VI593 and VI594 (837 bp) and digested with *Eco*RI and *Pst*I. Finally, the insert was ligated into *Eco*RI and *Pst*I site of linearized pGP20.

2.2.2.9.5 Construction of mutagenesis plasmids

Mutant strains of the *Y. pseudotuberculosis* wild type strain YPIII with gene deletions were constructed by homologous recombination using suicide plasmids derived from pAKH3 (pMP26, and pMP35). Construction of plasmids was based on an overlapping three step PCR. In the first and second PCR reaction the region (i.e., 300-500 bp) upstream respectively downstream of the loci to be mutated was amplified. For gene deletion, the reverse primer (B) of the upstream region as well as the forward primer (C) of downstream region possessed additional 20 nt at the 5' end that were homologous to the start or to the end of the kanamycin resistance gene, respectively. The third PCR reaction was performed with 5' forward primer (A) of the upstream region and the 3' reverse primer (D) of the downstream region, both harboring restriction sites at their 5' ends, using the upstream and downstream PCR products of the target sequence as templates as well as the kanamycin cassette. Mutagenesis plasmids and corresponding primer combinations used in this study are listed in Table 2.10. A description of the mutagenesis plasmids constructed in this study is given in Table 2.8.

Table 2.10. Mutagenesis plasmids and primer combinations

Mutagenesis plasmid	Primer			
	A	B	C	D
pMP26	VI203	VI204	VI205	VI206
pMP35	VI595	VI596	VI597	VI598

2.2.2.10 Transformation

Transformation was applied in order to introduce DNA fragments into bacterial cells. Both *Y. pseudotuberculosis* and *E. coli* cells were transformed by electroporation.

2.2.2.10.1 Preparation of electrocompetent *E. coli* cells

For the production of electrocompetent *E. coli* cells a sufficient volume of BHI medium (approx. 100 ml) was inoculated 1:100 from overnight culture. The bacteria were grown at 37 °C to an OD_{600} between 0.5 to 0.8 and then chilled on ice for 10 min. All following steps were performed at 4 °C or on ice. Cells were harvested by centrifugation in a Sigma 3-18 K centrifuge using 19776-H rotor at 6,000 rpm for 5 min. The bacterial pellet was washed in 30 ml ice-cold 10 % glycerol and centrifuged as described above. This washing step was repeated once. After final centrifugation, the cells were resuspended in 10 % glycerol using 1/1000 volume of the original culture volume. Finally, the electrocompetent *E. coli* cells were used for transformation immediately or stored in 40 µl aliquots at -40 °C.

2.2.2.10.2 Preparation of electrocompetent *Yersinia* cells

To prepare electrocompetent *Yersinia* cells sufficient for approximately 6 transformations, 20 ml BHI medium were inoculated 1:50 or 1:20 from overnight culture. The cells were cultivated at 25 °C to an OD_{600} of approximately 0.8. The bacteria were harvested and the pellet was washed twice with ice-cold *Yersinia* transformation buffer. The bacterial pellet was finally resuspended in transformation buffer using 1/500 volume of the original

culture volume. 40 µl aliquots were used for transformation. Competent *Yersinia* cells were always prepared freshly and immediately applied to electroporation.

2.2.2.10.3 Electroporation

To introduce exogenous DNA fragments into bacterial cells by electroporation, 1-4 µl of the desired purified plasmid DNA was added to one aliquot of electrocompetent bacteria and transferred to a precooled 2 mm electroporation cuvettes (Peqlab, Germany). Ligation reactions were dialyzed before application using a 0.025 filter membrane (Millipore, Germany). For transformation, the cells were treated with an electric pulse of 2.2 kV, a capacity of 25 µF and a resistance of 200 Ω. After electroporation, the bacteria were directly resuspended in 1 ml BHI medium. For phenotypic expression of the resistance genes, *E. coli* was cultivated for 1 hour at 37 °C shaking and *Y. pseudotuberculosis* for 2 hours at 25 °C shaking. Thereafter, the bacteria were plated on solid LB medium with appropriate antibiotics and cultivated as described in 2.2.1.2.

2.2.2.11 Conjugation

Conjugation was carried out in order to construct the mutant strains of *Y. pseudotuberculosis* using suicide plasmids, which were integrated into the genome by homologous recombination. The *E. coli* S17-1λpir strain served as a donor of the mutagenesis plasmid. This strain carries a chromosomal sequence called the fertility factor, which allows the production of an F-pilus enabling the transfer of the plasmid to the recipient bacterium. For conjugation a required volume of BHI medium (5 ml per conjugation) with appropriate antibiotics was inoculated 1:100 from an overnight culture of the suicide plasmid donor (*E. coli*) and 1:50 for the recipient strains (*Y. pseudotuberculosis*). The donor culture was incubated for 2.5 hours at 37 °C shaking followed by another 30 min at 37 °C without shaking to promote the formation of F-pili. The recipient *Yersinia* strain was incubated for 3 hours at 25 °C. An important prerequisite for conjugation is the close contact (mating) between donor and recipient strains. For this purpose, 1 ml of the donor culture was applied onto a 0.22 µm GSWP filter membrane (Millipore, Germany). To remove the remaining antibiotics, the filter was washed with 2 ml of BHI medium. Next, 3-4 ml of *Yersinia* recipient culture were added onto the filter. After every application the liquid medium was withdrawn. To allow mating, the filter was incubated on LB agar plate at 25 °C for at least 4 hours. Subsequently, cells were washed down from the filter by rinsing with BHI medium and plated on *Yersinia* selective agar (Oxoid, UK) with appropriate antibiotics to avoid growth of the donor *E. coli* strain. The recombination of the plasmid into the *Yersinia* genome yielded a merodiploid strain, including the wild type and the mutant copy of the loci of interest. A second homologous recombination to remove the integrated sequences of the suicide vector was enforced by plating the merodiploid strain on LB plates containing 10 % sucrose. Sucrose induces expression of the *sacB* gene encoded on the integrated plasmid. Its gene product converts sucrose to levan, a toxic substance accumulating in the periplasm and preventing bacterial growth (Gay *et al*., 1985). A spontaneous second recombination process is therefore advantageous. 50 fast growing colonies were selected and screened for respective

antibiotic sensitivity to prove the loss of the integrated vector. Positive mutants were verified by PCR and DNA sequencing.

2.2.3 Molecular biological methods for RNA

2.2.3.1 RNA isolation and purification

To test the regulatory influences on the transcript level of different virulence factors, total RNA was isolated from the *Y. pseudotuberculosis* strain of interest. Depending on the downstream analysis, different RNA isolation approaches were applied.

2.2.3.1.1 RNA isolation with SV Total RNA Isolation System

In order to detect the transcript of interest via Northern blot, total RNA was isolated using the SV Total RNA Isolation Kit (Promega, USA). For this, bacterial cells were grown under the desired conditions. After that, 4 ml of the culture were harvested by centrifugation in a microcentrifuge 5415 R (Eppendorf, Germany) at 9000 rpm for 3 min, resuspended in 0.4 volume stop solution (800 µl) and immediately frozen in liquid nitrogen for at least 2 min. To remove the stop solution, cells were centrifuged at 12,000 rpm for 1 min and the supernatant was discarded. Subsequently, cells were either stored at -20 °C or RNA was prepared directly. For this, pellet was treated with 200 µl lysozyme-TE-buffer for 7-10 min at RT in order to lyse the cells. Further, RNA isolation was performed using the SV Total RNA Isolation Kit according to the manufacturers instructions. The RNA was eluted in 50-100 µl nuclease-free water and stored at -20 °C. Total RNA was quantified by micro-spectrophotometry (see 2.2.2.3).

2.2.3.1.2 Hot-phenol RNA extraction

High quality and high quantity of the total RNA is crucial for RNA sequencing. To yield intact high quality RNA, the hot phenol isolation technique was applied. For this purpose, bacterial cells of 5-25 ml culture were harvested by centrifugation in a Sigma 3-18 K centrifuge using 19776-H rotor at 4,000 rpm for 2-3 min. Centrifugation steps were performed at the temperature at which the bacterial cells were grown. Thereafter, the supernatant was discarded and bacterial pellets were snap frozen in liquid nitrogen for at least 2 min. Subsequently, the cells were either stored at -80 °C or RNA was prepared directly. Bacterial pellets were resuspended in 250 µl RNA resuspension buffer (Table 2.1.) on ice and transferred into 2 ml safe-lock tubes. After the pellets were resuspended, 250 µl RNA lysis buffer (Table 2.1.) were added, the samples were mixed and incubated at 65 °C for 90 s. Next, 500 µl pre-heated (65 °C) saturated aqua-phenol was mixed with the lysate. After incubation for 3 min, the samples were immediately frozen in liquid nitrogen for at least 1 min. Thereafter, the samples were centrifuged at 13,000 rpm for 10 min at room temperature and the aqueous layer was carefully transferred to a 2 ml safe-lock tube (Eppendorf, Germany). Treatment of the samples with aqua-phenol, described above, was performed three times. For extraction of phenol, 300 µl chloroform/isoamyl-alcohol (24:1) were added, samples were vortexed for 30 s and centrifuged for 10 min at 13,000 rpm at room temperature. Subsequently, the aqueous

supernatant was transferred to a fresh reaction tube. The extraction step was repeated. Thereafter, the RNA extract in the watery supernatant was ethanol precipitated by adding 1/10 volume of 3 M sodium acetate (pH 4.5) and 2.5 volumes ice-cold ethanol to each sample. The samples were mixed and incubated at -20 °C overnight or at -80 °C for 1 hour. The RNA was recovered by centrifugation at 13,000 rpm for 30 min at 4 °C. Pellets were washed with ice cold 70 % (v/v) ethanol and centrifuged at 13,000 rpm for 10 min at 4 °C. The washing step was performed two times. Afterwards, ethanol was carefully removed and the RNA pellets were air dried for 5 min in a fume hood. Finally, the pellets from each sample were resuspended in a total of 100-180 µl (depending on pellet size) of nuclease free water.

2.2.3.1.3 Phenol/chloroform/isoamyl alcohol purification

For removal and inactivation of proteins from RNA solutions, the RNA solution volume was increased to 300 µl with RNase-free water. Subsequently, 1 volume of phenol/chloroform/isoamyl alcohol (25:24:1) was added, vortexed for 30 s and centrifuged at 13,000 rpm for 10 min at 4 °C. Thereafter, the RNA containing supernatant was extracted twice with 1 volume of chloroform/isoamyl alcohol. Next, the RNA was precipitated with 0.1 volumes of 3 M sodium acetate and 2.5 volumes of ethanol at -20 °C overnight or at -80 °C for 1 hour. Subsequently, the RNA was pelleted by centrifugation at 13,000 rpm for 10 min at 4 °C, washed with 70 % (v/v) ethanol, air-dried and resuspended in 50-100 µl of nuclease-free water.

2.2.3.2 Determination of RNA concentration and quality

Total RNA concentration was measured using micro-spectrophotometry with a NanoDrop (PEQLAB, Germany) at 260 nm (see 2.2.2.1). An A_{260} of 1 corresponds to 40 µg/ml RNA. To check the purity of isolated RNA, the A_{260}/A_{280} ratio was calculated. The A_{260}/A_{280} ratio of ~2.0 represents pure RNA. For RNA sequencing RNA integrity and quality was additionally analyzed at the in-house genome analytics platform with the Agilent 2100 Bioanalyzer using either the Agilent RNA 6000 Nano kit or Pico kit. The quality of the RNA (RNA integrity number, RIN) was calculated by the obtained electropherograms (Figure 2.1) utilizing the Expert Software B02.08 (Agilent Technologies).

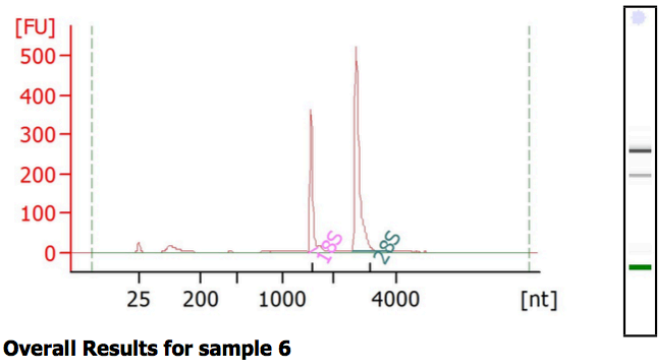

Overall Results for sample 6

RNA Area:	1.125,8
RNA Concentration:	409 ng/µl
rRNA Ratio [28s / 18s]:	2,3
RNA Integrity Number (RIN):	10 (B.02.08, Anomaly Threshold(s) manually adapted)
Result Flagging Color:	
Result Flagging Label:	RIN:10

Fragment table for sample 6

Name	Start Size [nt]	End Size [nt]	Area	% of total Area
18S	1.498	1.684	287,3	25,5
28S	2.621	3.767	654,3	58,1

Figure 2.1 RNA electropherogram.
RNA profile obtained from an Agilent RNA 6000 Nano Kit with Expert Software B02.08 (Agilent Technologies).

2.2.3.3 DNA digestion

The TURBO™ DNase (Ambion) is a genetically engineered DNA endonuclease derived from the bovine DNase I that possesses an increased catalytic efficiency at higher salt and lower DNA concentrations. The TURBO™ DNase treatment was employed to remove contaminating traces of DNA from RNA total extracts for qRT-PCR or RNA sequencing. A 240 µl standard DNA digestion reaction for 50 µg total RNA was composed of:

TURBO™ DNase	2	µl
10x TURBO™ DNase buffer	24	µl
RiboLock™ RNase Inhibitor (40 U/µl)	1	µl
RNA	213	µl

The digestion was incubated at 37 °C for 1 h. To inactivate the TURBO™ DNase phenol/chloroform/isoamyl alcohol extraction (2.4.5) was carried out.

2.2.3.4 Quantitative real-time PCR

Quantitative real-time PCR (qRT-PCR) was applied to estimate bacterial expression patterns using the SensiFastTM SYBR® No-ROX One-Step kit (Bioline). During qRT-PCR, total RNA was reverse-transcribed by a reverse transcriptase into complementary DNA (cDNA). Subsequently, the desired cDNA was amplified via PCR. After each PCR-cycle, fluorescence intensity of the green fluorescent dye SYBR®, which intercalates into double-stranded DNA, was monitored. The measured fluorescence intensity was used for relative quantification of transcript abundance. A 12.5 µl standard qRT-PCR reaction for DNA-free RNA (2.2.3.2) with a final concentration of 25 ng/µl was composed of:

2x SensiFast™ SYBR No-ROX One-Step Mix	6.25	µl
10 µM forward primer	0.5	µl
10 µM reverse primer	0.5	µl
Reverse transcriptase	0.125	µl
RiboSafe RNase inhibitor	0.25	µl
Nuclease-free water	2.375	µl
RNA (25 ng/µl)	2.5	µl

Reverse transcription and subsequent qRT-PCRs were carried out in the Rotor-Gene Q real-time PCR cycler (QIAGEN) in technical duplicates. A 3-step-cycling program with subsequent melt-profile analysis to monitor product specificity was applied (Table 2.11). The acquired data was further processed with the Gene-Rotor Q Series software. The normalization method was typically set to dynamic tube normalization and normalization was user-defined starting from cycle 1-10. The cycle threshold (Ct) was determined by setting the threshold routinely to 0.010. This threshold reflects the lower fluorescence detection limit of the instrument and creates the baseline of the amplification plot. Fluorescence above the threshold indicates the accumulation of PCR product and determines the Ct of the sample.

Table 2.11. qRT-PCR program

Step	Cycles	T °C	Time	Description
cDNA generation	1	45	20 min	Reverse transcription
Polymerase activation	1	95	5 min	
PCR	<50	95	10 s	Denaturation
		52-62	20 s	Annealing
		72	10-30 s	Extension and acquisition
	1	72	5 min	Final extension
Melt profile analysis		58-99		Ramp heating and fluorescence detection

The melt profile was analyzed by setting the threshold to >2. The obtained melt profile and PCR product melt temperatures were used to estimate the product specificity and to exclude the abundance of primer dimers. To calculate the relative expression of a target gene compared to a reference gene, the relative quantification method described by was applied Pfaffl, 2001 was applied (Equation 1 to 4). According to equation 4, an ideal primer efficiency of 2 (one duplication per cycle) was assumed. The total RNA samples were normalized to *sopB* in order to get more stable normalization of relative gene expression. Finally, the mean of the determined $\Delta Ct_{\text{reference gene}}$ (Equation 2) was calculated (Equation 3).

$$\Delta Ct_{gene\ of\ interest} = mean\ Ct_{gene\ of\ interest_{reference\ condition}} - Ct_{gene\ of\ interest_{test\ condition}} \quad (1)$$

$$\Delta Ct_{reference\ gene} = mean\ Ct_{reference\ gene_{reference\ condition}} - Ct_{referencegene_{test\ condition}} \quad (2)$$

$$\Delta Ct_{reference\ gene} = mean\ \Delta Ct_{reference\ gene\ 1\&2} \quad (3)$$

$$relative\ expression = \frac{2^{\Delta Ct_{gene\ of\ interest}}}{2^{\Delta Ct_{reference\ gene}}} \quad (4)$$

Specific primer pairs for the transcripts of interest used in this study are listed in table 2.12.

Table 2.12. Target mRNA and primer combinations

Transcript of interest	Primer combination
lcrF	III44 / III45
csrA	V4 / V5
sopB	III393 / III394

2.2.3.5 RNA agarose gel electrophoresis

Agarose gel electrophoresis was performed to analyze a specific transcript. The negative charge of RNA molecules allows to separate them in the electric field according to their size, due to the different migration velocity. To resolve the secondary structure of RNA molecules, which could also affect their motility in the agarose gel, RNA samples (20-50 µg of total RNA) were mixed with RNA-loading buffer containing EtBr and denaturated at 70 °C for 10 min. Thereafter samples were chilled on ice for 2 min to prevent rebuilding of the secondary structures. The denaturated RNA was applied to a 1.2 % MOPS-agarose gel in 1x MOPS buffer (Table 2.1) and separated for 75 min at a voltage of 120V. For estimation of the RNA size, digoxigenin labeled 'RNA Molecular weight Marker I' (Roche, Germany) was loaded. To assess the RNA quality and as a loading control, the 23S and 16S rRNAs were visualized at the gel documentation system with UV light (BioRad, USA) via ethidium bromide in the RNA loading buffer.

2.2.3.6 Northern blot analysis

To detect a transcript of interest northern blot analysis was performed. Therefore, a complementary digoxigenin-labeled DNA-probe was amplified with the *Taq* polymerase (NEB) and applied for hybridization with the target mRNA. A 100 µl PCR labeling reaction contained the following ingredients:

ThermoPol buffer (10x)	10	µl
DIG DNA labeling Mix (10x)	10	µl
$MgSO_4$	10	µl
10 µM forward primer	3	µl
10 µM reverse primer	3	µl
template	1	µl
Taq polymerase (1U/µl)	1	µl
H_2O	62	µl

Probes for the indicated transcripts used in this study were synthesized with the primers listed in table 2.13.

Table 2.13. DNA probes and primer combinations for Northern blot

Transcript of interest	Primer combination
lcrF	I214 / I303
csrA	V4 / V5
csrB	555 / 556
csrC	I82 / 583
pnp	IV527 / IV528
rne	IV529 / IV530
rcsB	VI252 / VI253
lacZ	VI618 / 714

After separating by gel electrophoresis, the total RNA was transferred onto a positively charged nylon membrane by vacuum blotting at 5 bar for 1.5 hours in 10x SSC blotting buffer. In the next step, the RNA was crosslinked to the membrane with an UV-crosslinker (Stratagene, USA) 3 times using an autocrosslink modus (3 min, 120,000 µJ). Prehybridisation, hybridisation with Dig-labeled DNA-probes and membrane washing was performed with the 'DIG Luminescent Detection Kit' (Roche, Germany) according to the manufacturer's instructions. Subsequently, the Dig-labeled probe-RNA complex was visualized using the CDP-Star system (Roche, Germany). After incubation with the chemiluminescent substrate the membrane was exposed to X-ray films CL-Xposure (Thermo Scientific, USA).

Following strategy was applied to estimate the translation efficiency of *lcrF* based on the results of Northern and Western blot results. Quantification of translation efficiency of the band intensities was performed with the image-processing program ImageJ. First, the intensities of the loading controls were estimated. The one of the wild type strain under non-secretion conditions was taken as a reference value equal to one. Afterwards, the intensities of the loading controls of the other samples were normalized to this reference. Additionally, the LcrF protein and transcript levels were determined densitometrically and normalized to those from the wild type under non-secretion conditions. After that, relative protein and transcript levels were calculated as a normalized protein/normalized loading control or normalized mRNA/normalized loading control ratio. Subsequently, translation efficiency of *lcrF* was determined as a relative protein/relative mRNA ratio. Consequently, the relative protein/relative mRNA ratio of the wild type strain under non-secretion conditions was set to 1. Thereafter, the *lcrF* translation efficiency of each strain under secretion conditions was normalized to those under non-secretion conditions. The *lcrF* translation efficiency induction of the wild type strain was taken as a reference value equal to one.

2.2.3.7 RNA stability assay

To estimate the half-life of a transcript in different *Y. pseudotuberculosis* strains, the decay of the mRNA was monitored over a period of time. The bacteria were cultivated under the desired growth conditions. To stop continuous transcription, rifampicin was added to the

cells at a final concentration of 1 mg/ml. Subsequently, 3.6 ml of the culture were split between two 2 ml safe-lock tubes (Eppendorf, Germany) with 0.2 ml 10 % stop solution, and snap-frozen in liquid nitrogen. Due to the short time intervals, samples to detect the stability of the transcript of interest were taken from each strain separately at time points 0, 0.5, 1, 2, 3, 5, and 7.5 min after addition of rifampicin. Total RNA was isolated (see 2.2.3.1.1) and northern blotting was performed as described above (see 2.2.3.5 – 2.2.3.6). To assess the degradation rate of a transcript, relative mRNA concentrations were determined for the indicated time points. For this purpose, northern blots were documented with a gel documentation system (BioRad, USA) and analyzed densitometrically with the Image J Software (Schneider *et al*., 2012). The relative mRNA concentrations were normalized to the relative concentrations of the 23S and 16S rRNA loading controls. Relative mRNA concentrations were plotted on a half-logarithmic scale and an exponential regression line was applied to calculate the half-life of a specific transcript.

2.2.3.8 RNA electrophoretic mobility shift assay (RNA-EMSA)

RNA-EMSA is a powerful method for rapid detection and quantification of the direct interactions between an RNA binding protein (RBP) and the transcript of interest. This technique is based on the fact that the RBP-RNA complex is less mobile when separated on the gel then the unbound RNA. RNA-EMSA approach was employed in this study to investigate possible targets of CsrA and YopD proteins. Prior to the assay synthesis of the target RNA fragment (2.2.3.7.1), labeling of RNA with biotin (2.2.3.7.2) as well as production of the RBP of interest (2.2.4.10) were performed.

2.2.3.8.1 *In vitro* transcription

In vitro transcription was applied for template-directed generation of RNA molecules of interest (Beckert & Masquida, 2011). For this purpose, a template harboring a T7 coliphage promoter sequence upstream of the desired sequence was designed. Primer pairs employed in this study for synthesis of the T7 promoter containing DNA template are listed in table 2.14. PCR reaction was performed with the Phusion-HF polymerase (NEB).

Table 2.14. DNA probes and primer combinations for *in vitro* transcription

Transcript of interest [a]	Primer combination
csrA (-91 to +10)	V066 / III731
hns (+175 to +226)	V700 / I515
rne up (-356 to -250)	VI560 / VI561
rne mid (-270 to -124)	VI562 / VI563
rne down (-148 to +12)	VI564 / VI565
pnp (-141 to +12)	VI950 / VI085

[a] – all coordinates are relative to translational start codon of particular gene

For purification of PCR products the NucleoSpin® Gel and PCR Clean-up kit (Macherey-Nagel, Germany) was applied. A crucial advantage of this Kit is the ability to clean-up even very small DNA fragments (down to 50 bp). The following *in vitro* transcription was

performed using the TranscriptAid T7 High Yield Transcription Kit (Thermo Scientific, USA) according to the manufactures instruction. Subsequently, RNA was purified by phenol/chloroform/isoamyl alcohol extraction (see 2.2.3.1.3).

2.2.3.8.2 3'-Biotinilation of RNA

In order to detect the RNA of interest on the nondenaturating gel upon RNA-EMSA, the RNAs obtained via *in vitro* transcription were 3'-end labeled with pCp-Biotin (Jena Bioscience, Germany). For this purpose, a 60 µl ligation reaction with the following components was performed:

T4 RNA ligase buffer (10x)	6	µl
10 mM ATP	6	µl
10 % DMSO (w/v)	6	µl
10 µM pCp-Biotin	6	µl
50 % PEG-8000	18	µl
RNA	2	µg
T4 RNA Ligase I	2	µl
Nuclease-free water	x	µl

The reaction was incubated at 18 °C for 2 h or overnight. Thereafter, the biotin-labeled RNA was purified via phenol/chloroform/isoamyl alcohol extraction (see 2.2.3.1.3) and the RNA concentration was estimated using NanoDrop™ ND-1000 UV spectrometer (Thermo Scientific, USA).

2.2.3.8.3 Detection of Biotin-labeled RNA

To examine the biotinilation efficiency as well as the quality of the biotin-labeled RNAs the Chemiluminescent Nucleic Acid Detection Module (Thermo Scientific) was employed. To do so, 2 nM RNA was applied on the native 4 % TBE polyacrylamide gel that consists of:

10x TBE	8	ml
40 % (w/v) polyacrylamide	1	ml
nuclease free water	8	ml
TEMED	10	µl
10 % APS	100	µl

Electrophoresis was conducted at a constant voltage of 80 V per gel and a maximum current for approximately 50 min. After separation samples were transferred from the polyacrylamide gel onto a positively charged nylon membrane (Roche, Switzerland) via semi-dry blotting. Therefore, the membrane was activated in 1x TBE and placed between the gel surface and the positive electrode in a sandwich, which additionally includes two whatman papers, both soaked in 1x TBE buffer, at each side. The sandwich was thereafter placed in a Trans-Blot® SD Semi-Dry Transfer Cell (BioRad, Germany) and the transfer was performed for 30 min at 20 V and 4 °C. Afterward, the RNA was crosslinked to the membrane with an UV-crosslinker (Stratagene, USA) for 3 min at 120,000 µJ. For the fallowing steps, which were performed using the Chemiluminescent Nucleic Acid Detection Module (Thermo Scientific), the membrane was placed in a 50 ml Falcon tube to

allow the incubation on a tube roller. Since only small volumes of buffer were used, it was crucial to completely remove it after every incubation step. Before usage, an aliquot of 5 ml 1x blocking buffer and 4x wash buffer was pre-warmed in a water bath (37-50 °C) until precipitates were solubilized. Thereafter, the membrane was blocked for 15 min in 5 ml blocking solution. Next, the membrane was incubated with the stabilized Streptavidin-HRP conjugates (1:300) for 30 min. The washing step was carried out in 5 ml of 1x wash buffer for 5 min four times. Finally, the membrane was equilibrated in 5 ml substrate equilibration buffer, followed by incubation with 1 mL Chemiluminescent Substrate Working Solution (500 µl Luminol/Enhancer Solution and 500 µL Stable Peroxide Solution) in a foil for 5 min. During this incubation step the chemiluminescence reaction occurs. The oxidation of the chemiluminescence substrate, luminol, results in the emission of light. This reaction is catalyzed by HRP. Since the HRP is associated with the biotin-labeled RNA of interest on the membrane, the amount and location of light on the membrane is directly correlated with those of the targeted RNA. For detection of RNAs the ChemiDoc™ XRS+ (Bio-Rad, USA) imaging system was employed.

2.2.3.8.4 RNA-EMSA

During the gel mobility shift assay RBP-RNA complexes are separated from the unbound RNA. After synthesis of the RBP of interest and generation of the biotin-labeled RNA, RBP and RNA were incubated together to allow RBP-RNA complex formation. Prior to this binding reaction, the biotin-labeled target RNA was diluted in 1x band-shift buffer (Table 2.1), followed by the incubation for 10 min at 70 °C to achieve linearization of RNA. To capture the linearized RNA conformation, samples were quick-chilled on ice. The RBP of interest was purified as described in section 2.2.4.10. Thereafter, serial RBP dilutions were prepared (0 to 10,000 fmol) in the corresponding 1x band-shift buffer (Table 2.1.). A standard 10 µl binding reaction included 0-1,000 nM RBP of interest and 2 nM of the linearized biotin-labeled target RNA. Consequently, the binding reaction was incubated for 30 min on ice and then immediately loaded onto a 4 % TBE polyacrylamide gel. Electrophoresis and detection of the RBP-RNA complexes was carried out as described in section 2.2.3.8.3.

2.2.3.9 3'-RACE

To map the 3' end of *lcrF* mRNA 3'-RACE (rapid amplification of cDNA ends) was performed as described in Argaman *et al*., 2001. In brief, 3'-RACE analysis was carried out by the ligation of an adaptor to the 3' hydroxyl group of the RNA, followed by *lcrF*- and adapter- specific amplification.

2.2.3.9.1 Deprotection of 2'-ACE protected 3' RNA adapter

3' RNA adapter (5' (5'-P) UUC ACU GUU CUU AGC GGC CGC AUG CUC (idT-3') 3') was ordered from Dharmacon research and delivered in 2'-ACE protected form (Argaman *et al*., 2001). For further ligation reaction 3' RNA adapter was deprotected according to the manufacturers instructions.

2.2.3.9.2 RNA isolation

Isolation and purification of total RNA was performed using SV Total RNA Isolation Kit (Promega, USA) (see 2.2.3.1.1), followed by DNA digestion with TURBO™ DNase (Ambion) (see 2.2.3.3). Thereafter, RNA was purified with SV Total RNA Isolation Kit (Promega, USA) as described in section 2.2.3.1.1, starting with addition of the RNA Dilution Buffer (Promega, USA). RNA was eluted in 25 µl nuclease-free water.

2.2.3.9.3 Dephosphorylation of the total RNA

To enable RNA – 3' RNA adapter ligation, the RNA was dephosphorylated with the Calf Intestinal Alkaline Phosphatase (CIP, NEB). A standard 20 µl CIP treatment reaction was composed of:

RNA	10	µg
CIP buffer (10x)	2	µl
CIP (1 U/µl)	2	µl
Ribolock	1	µl
Nuclease-free water	to 20	µl

The reaction was incubated at 37 °C for 60 min. Thereafter, RNA was purified with the SV Total RNA Isolation Kit (Promega, USA) as described in section 2.2.3.1.1, starting with addition of the RNA Dilution Buffer (Promega, USA). RNA was eluted in 25 µl nuclease-free water.

2.2.3.9.4 3' RNA adapter ligation

For RNA – 3' RNA adapter ligation, 1 µg of dephosphorylated RNA was mixed with 500 pmol 3' RNA adapter, followed by heat-denaturation for 5 min at 95 °C. Thereafter, samples were quick-chilled on ice. A standard 20 µl ligation reaction with T4 RNA ligase (NEB) included the following components:

RNA + 3' RNA adapter mix	x	µl
T4 RNA Ligase buffer (10x)	2	µl
ATP (10 mM)	1	µl
DMSO (100%)	2	µl
PEG (50%)	6	µl
T4 RNA Ligase (20 U/µl)	1	µl
Nuclease-free water	to 20	µl

Reaction was incubated for at least 12 hours at 18 °C. RNA purification was carried out with SV Total RNA Isolation Kit (Promega, USA) as described in section 2.2.3.1.1, starting with addition of the RNA Dilution Buffer (Promega, USA). Purified RNA was eluted in 15 µl nuclease-free water.

2.2.3.9.5 First strand cDNA synthesis

Generation of the first strand cDNA was performed with the 5'/3' RACE Kit (Roche). A 20 µl cDNA synthesis reaction consisted of the following ingredients:

cDNA synthesis buffer (Vial 1)	4	µl
Deoxynucleotide Mixture (Vial 3)	2	µl
V941 (complementary to the 3' RNA adapter) (10 µM)	0.9	µl
RNA – 3' RNA adapter complex	0.5-2	µg
Transcriptor reverse transcriptase (Vial 2)	1	µl
Nuclease-free water	to 20	µl

To confirm the Kit's functionality, the cDNA synthesis reaction with the control neo-RNA (Vial 2) was carried out according to the manufacturer's manifestations. cDNA synthesis reactions were conducted in a Thermocycler using the following program: 20 min at 55 °C, 20 min at 60 °C, 20 min at 65 °C, 5 min at 85 °C.

2.2.3.9.6 PCR amplification of cDNA

Amplification of cDNA was carried out with Phusion-HF DNA polymerase (NEB). A 100 µl PCR included the following components:

cDNA product	1	µl
V941 (10 µM)	5	µl
Gene specific primer (10 µM)	5	µl
Deoxynucleotide Mixture (Vial 3)	2	µl
5x HF buffer	20	µl
Phusion HF polymerase	1	µl
Nuclease-free water	66	µl

The control reaction was conducted according to the manufacturers instructions. The reaction was performed in a thermal block cycler using the following parameters: annealing temperature – 63 °C, elongation time – 32 s, cycles number – 45. Thereafter, 20 µl PCR product were separated on 1.5 % agarose gel. 3'-RACE was classified as successful if a strong band of 1062 bp (for control reaction) was detected. Consequently, 100 µl PCR Product were applied on the 1.5 % agarose gel for gel extraction (see 2.2.2.4). The DNA was eluted with 20-30 µl nuclease-free water. To estimate the concentration of DNA 5 µl gel-extracted DNA was analyzed on 1.5 % agarose.

2.2.3.9.7 Cloning of the PCR products into pJET1.2/blunt vector

Gel-extracted products were cloned into the pJET1.2/blunt vector (Thermo Scientific) according to the manufacturer's instructions. After dialysis for 15 min at room temperature, 10 µl of the ligation mixture were introduced into electrocompetent *E. coli* S17-1λpir via electroporation (see 2.2.2.10.3). Colonies were screened for the presence of inserts via colony PCR with MangoMix (Bioline) using pJET1.2 sequencing primers. The reaction was performed in a thermal block cycler using the following parameters: annealing temperature – 60 °C, elongation time – length dependent, cycles number – 30. 5 µl PCR product were used for analysis on an agarose gel. Finally, the PCR products were purified with the 'PCR Purification Kit' (QIAGEN, Germany) and sequenced by the in-house facility, the Department of Genome Analysis, GMAK (HZI, Germany) using pJET1.2 sequencing primers.

2.2.3.10 RNA sequencing

To gain a global insight into the gene expression profile in *Y. pseudotuberculosis* as well as to specify the role of CsrA and YopD under secretion conditions, RNA sequencing (RNA-seq) was applied.

2.2.3.10.1 Bacterial growth

For each biological replicate, 5x 10 ml LB medium were inoculated 1:50 (wild type (YPIII)) or 1:20 (*csrA* deficient strain (YP53), Δ*yopD* (YP91) strain and *csrA*/*yopD* double mutant (YP145)) with an overnight culture of *Y. pseudotuberculosis* strain of interest and incubated under the conditions described in Table 2.15.

Table 2.15. Growth conditions for *Y. pseudotuberculosis* transcriptome analysis

Growth condition	Description
2 h at 25 °C followed by depletion of Ca^{2+} and shift to 37 °C for 4 h	Investigation of *Y. pstb.* transcriptome under Ca^{2+} depletion conditions (Yop secretion conditions)
2 h at 25 °C followed by 4 h at 37 °C	Investigation of *Y. pstb.* transcriptome under non-secretion conditions
2 h at 25 °C followed by depletion of Ca^{2+} and shift to 37 °C for 10 min	Investigation of the first changes in *Y. pstb.* transcriptome induced by temperature shift and Ca^{2+} depletion
2 h at 25 °C followed by 10 min at 37 °C	Investigation of the first changes in *Y. pstb.* transcriptome induced by temperature shift

2.2.3.10.2 RNA extraction

To extract total RNA for RNA-seq, the hot phenol isolation technique was applied (see 2.2.3.1.2). Concentration and quality of the purified RNA was estimated as described above (see 2.2.3.2).

2.2.3.10.3 DNase digestion

To remove DNA from the sample, DNase digestion was carried out (see 2.2.3.3). Finally, DNase free total RNA was eluted in 50-100 µl nuclease-free water.

2.2.3.10.4 Depletion of the ribosomal RNA

Ribosomal RNA (rRNA) represents the most dominant RNA species in the cell (between 80 % and 90 %). To improve the efficiency of the RNA-seq capacity rRNA depletion was performed (O'Neil *et al*., 2013). For this purpose, the MICROB*Express*™ Bacterial mRNA Enrichment Kit (Ambion, US), which uses capture oligonucleotides targeting specific regions of the 16S and 23S rRNAs, was employed according to the manufacture's specifications (with 8 µg total RNA as template). Thereafter, rRNA depleted total RNA was resuspended in 20 µl nuclease-free water. rRNA depletion was classified as efficient if no 16S and 23S rRNA peaks were visible on the Bioanalyzer profile.

2.2.3.10.5 TAP treatment

To enable the ligation reaction between the sequencing adapter and the 5'end of RNA, tobacco acid pyrophosphatase (TAP) treatment was performed. TAP converts the

5′ triphosphate structure of intact transcripts to a monophosphate. A standard 50 µl TAP treatment reaction consists of the following ingredients:

RNA	1	µg
TAP buffer (10x)	5	µl
TAP (10 U/µl)	0.5	µl
Ribolock	0.5	µl
Nuclease-free water	to 50	µl

The reaction was incubated at 37 °C for 90 min. Thereafter, RNA was purified via phenol/chloroform/isoamyl alcohol extraction (see 2.2.3.1.3). For ethanol precipitation 2 µl glycogen were added.

2.2.3.10.6 RNA fragmentation

In the next step, the RNA was fragmented by the in-house facility the Department of Genome Analysis, GMAK (HZI, Germany), using ultrasound (Covaris, USA). For this purpose, 300 ng RNA were resuspended in TE-buffer (Table 2.1) to reach a final volume of 130 µl. The following parameters were applied:

processing time	150	s
fragment size range	200	bases
intensity	5	
duty cycle	10	%

The fragmented RNA was ethanol precipitated and the RNA pellet was resuspended in 20 µl nuclease free water. Concentration and quality of the purified RNA was examined as described above (see 2.2.3.2). The RNA fragments should be in a size range of 150 – 600 bp.

2.2.3.10.7 RNA phosphorylation

Phosphorylation of the RNA 5’ ends was performed with the Thermo Scientific™ T4 Polynucleotide Kinase (T4 PNK). This enzyme catalyzes the transfer of γ-phosphate from ATP to the 5’-OH group of RNA what is essential for the following adapter ligation reaction. A standard 20 µl phosphorylation reaction included the following components:

RNA	15	µl
10x reaction buffer A for T4 PNK	2	µl
ATP (10 mM)	1.8	µl
T4 PNK	1	µl
Nuclease-free water	to 20	µl

The reaction was incubated for 25 min at 37 °C, followed by RNA purification via phenol/chloroform/isoamyl alcohol extraction (see 2.2.3.1.3). For ethanol precipitation 2 µl glycogen were added. Concentration and quality of the purified RNA was examined as described above (see 2.2.3.2.).

2.2.3.10.7 cDNA library preparation

cDNA library preparation was performed with NEBNext® Multiplex Small RNA Library Prep Set for Illumina® according to the manufacturers instructions.

2.2.3.10.8 Sequencing

The finalized libraries were sequenced with an Illumina cluster station (HiSeq, single-end mode, short reads, strand specific). The obtained data was processed as described in Nuss *et al*., 2015 and Nuss *et al*., 2017. After processing, the remaining reads were mapped to the *Y. pseudotuberculosis* YPIII genome.

2.2.3.11 CLIP sequencing

Combination of *in vivo* UV-crosslinking with RNA deep sequencing (CLIP-seq) is a powerful approach that enables the transcriptome-wide investigation of RNA-RBP interactions. Moreover, CLIP-Seq allows identification of the RBP target sites at single-nucleotide resolution (Holmqvist *et al*., 2016). In this work CLIP-seq was applied to explore the CsrA interactome in *Y. pseudotuberculosis* under secretion conditions. CLIP-seq was performed as described in Holmqvist *et al*., 2016.

2.2.3.11.1 Bacterial growth and UV crosslinking

To enable a selective purification of the RBP of interest, the RBP was tagged. In this study, the *in trans* expression of the 3xFLAG-tagged CsrA protein in *Y. pseudotuberculosis* Δ*csrA* strain (YP53) was performed. To do so, the *Y. pseudotuberculosis csrA* mutant was transformed with the 3xFLAG-tagged CsrA expression vector (pJH35). Thereafter, for each biological replicate, 200 ml LB medium were inoculated 1:50 from an overnight culture of *Y. pseudotuberculosis* YP53 harboring pJH35 and grown at 25 °C for 2 hours. Subsequently, secretion was induced by addition of 20 mM $MgCl_2$ as well as 20 mM sodium oxalate. The cultures were shifted to 37 °C and cultivated for another 4 hours. Next, 100 ml of the culture were poured in a 22x22 cm plastic tray and irradiated in the UV-crosslinker BLX-254 (Vilber, Germany) with UV-C light (254 nm) at 800 mJ/cm^2. Thereafter, the irradiated culture was harvested by pipetting and split between two 50 ml pre-cooled falcon tubes on ice. The remaining 100 ml culture were directly split between two 50 ml pre-cooled falcon tubes on ice. In the next step, the cells were pelleted by centrifugation for 40 min at 4700 rpm and 4 °C. After that, the supernatant was discarded and the pellets were either stored at -80 °C or cell lysis was performed.

2.2.3.11.2 Lysis

The pellets were resuspended in 800 µl ice-cold NP-T buffer (Table 2.1). The cell suspension was then placed into pre-cooled 2 ml safe-lock tubes (Eppendorf) containing 1 ml of 0.1 mm glass beads (Biospec, USA). The tubes were thereafter placed into pre-cooled plastic blocks and bacterial cells were disrupted using the bead beater (TissueLyser II, QIAGEN) by shaking at 30 Hz for 10 min. After a centrifugation steps (15 min at 13000 rpm and 4 °C), the cell lysates were transferred to the new tubes and centrifuged again. Clear cell lysates were diluted 1:4 in ice-cold NP-T buffer.

2.2.3.11.3 Anti-FLAG beads preparation and protein binding to antibody

Prior to use, anti-FLAG magnetic beads (Sigma-Aldrich) were prepared as described below. 30 µl 50 % bead suspension per lysate from a 100 ml bacterial culture were washed three times in 1600 µl NP-T buffer. After the washing step, magnetic beads were resuspended in the desired volume of the ice-cold NP-T buffer (400 µl per 100 ml bacterial culture). To pool-down the 3xFLAG-tagged CsrA from the cell lysates, 400 µl bead suspension were added to each lysate, and the mixture was incubated in the disk roller (Biozym, Germany) for one hour at 4 °C. Subsequently, beads were collected by a short centrifugation step (1 min at 1000 rpm and 4 °C) and resuspended in 1 ml ice-cold NP-T buffer.

2.2.3.10.4 Benzonase treatment

The on bead benzonase treatment was applied in order to remove all free, not CsrA-protected RNA molecules. For this purpose, the bead suspension was transferred to new 2 ml tubes (Eppendorf) and was washed twice with 1000 µl High-Salt buffer (Table 2.1) and twice with ice-cold NP-T buffer. Thereafter, beads were resuspended in 100 µl NP-T buffer, supplied with 1 mM $MgCl_2$ and 2.5 U benzonase nuclease (Sigma-Aldrich) and incubated for 10 min at 800 rpm and 37 °C. After benzonase treatment, the samples were chilled on ice for 2 min, followed by one washing step with 500 µl High-Salt buffer and two washing steps with 500 µl CIP buffer (Table 2.1).

2.2.3.11.5 Dephosphorylation

In the next step, the samples were treated with CIP (NEB). To do so, the beads were resuspended in 100 µl CIP buffer containing 10 U CIP and incubated for 30 min at 800 rpm and 37 °C. Thereafter, beads were washed one time with 500 µl High-Salt buffer and two times with PNK buffer (Table 2.1). To compare the protein amounts obtained from UV irradiated and non-irradiated samples from each biological replicate, 50 µl bead suspension were removed for subsequent Western blot analysis (see 2.2.3.10.6).

2.2.3.11.6 Radioactive labeling

After dephosphorylation, the remaining beads were resuspended in 100 µl PNK buffer with 10 U T4 Polynucleotide Kinase (Thermo Fisher Scientific, USA) and 10 µCi γ-^{32}P-ATP and incubated for 30 min at 37 °C. To increase the phosphorylation rate of the RNA 5' ends, the samples were additionally supplied with 20 µl of 10 mM ATP and further incubated for 10 min at 37 °C. After one washing step with 500 µl High-Salt buffer and two washing steps with 500 µl PNK buffer, the beads were resuspended in 20 µl 2x SDS sample buffer and incubated for 5 min at 95 °C. Finally, the magnetic beads were collected on a magnetic separator (DynaMag-2, Thermo Fisher Scientific, USA) and the supernatant was moved to new 1.5 ml tube (Eppendorf).

2.2.3.11.7 SDS-PAGE

The supernatant was loaded on 15 % SDS-polyacrylamide gel. To avoid cross-contamination, the samples were loaded in every second well. Electrophoresis was carried

out at 60 mA per gel until the front of loading dye reached the bottom of the gel. Thereafter, RNA-CsrA complexes were transferred to a nitrocellulose membrane (Amersham Protran Supported 0.45 µl NC, GE Healthcare). After blotting, the membrane edges as well as the protein marker were highlighted with a radioactively labeled pen and exposed to a phosphor screen for 30 min. The autoradiogram was applied as a template to cut out the labeled RNA-protein complexes from the membrane. Each membrane piece was further cut into 8 smaller pieces, placed into 2 ml LoBind tube (Eppendorf), and either stored at -20 °C or directly treated with Proteinase K.

2.2.3.10.8 Proteinase K treatment

To remove the CsrA protein, the membrane pieces were incubated in 400 µl PK buffer supplemented with 10 U SUPERaseIN (LifeTechnologies) and 0.4 mg Proteinase K (ThermoScientific) for one hour at 1000 rpm and 37 °C. Thereafter, 100 µl 9 M urea was added and the incubation was continued for another hour.

2.2.3.11.9 RNA extraction

For RNA purification, 450 µl RNA containing supernatant were mixed with 450 µl phenol/chloroform/isoamyl alcohol in a PhaseLock tube (Eppendorf) and incubated for 5 min at 13,000 rpm and 30 °C. Thereafter, the samples were centrifuged for 12 min at 13,000 rpm and 4 °C. The aqueous phase was precipitated with 3 volumes of ice-cold ethanol, 1/10 volume of 3 M NaOAc pH 5.2, and 1 µl of GlycoBlue (Life Technologies) in LoBind tubes (Eppendorf). The precipitate was collected by centrifugation for 30 minutes, 13,000 rpm and 4 °C, washed with 80 % ethanol, centrifuged again for 15 minutes at 13,000 rpm and 4 °C, dried 2 minutes at room temperature and resuspended in 10 µl sterile nuclease-free water.

2.2.3.11.10 cDNA library preparation

cDNA library preparation was carried out with the NEBNext® Multiplex Small RNA Library Prep Set for Illumina® as described above (see 2.2.3.9.7). However, concentration of the purified RNA that can be extracted using the CLIP-seq protocol is significantly lower in comparison to those obtained with the conventional RNA-seq protocol. Consequently, there are some differences in the cDNA library preparation for CLIP-seq. 0.5 µl 1:10 diluted 3’ SR Adaptor was mixed with 2.5 µl purified RNA or nuclease-free water (as a negative control), incubated for 2 min at 70 °C and chilled on ice. Thereafter, 5 µl 3’ Ligation Reaction Buffer and 1.5 µl 3’ Ligation Enzyme Mix were added, and the samples were incubated for 60 min at 25 °C. After addition of 0.25 µl of the SR RT Primer and 2.5 µl Nuclease Free Water the samples were incubated for 5 min at 75 °C, 15 min at 37 °C, and 15 min at 25 °C. Prior to the 5’ adaptor ligation, 0.5 µl 1:10 diluted 5’ SR Adaptor was denatured for 2 min at 70 °C. Thereafter, denatured 5’ SR Adaptor, 0.5 µl 10x Ligation Reaction Buffer and 1.24 µl 3’ Ligation Enzyme Mix were added to the sample followed by incubation for 60 min at 25 °C. In the next step, cDNA was synthetized. To do so, 4 µl First Strand Synthesis Reaction buffer, 0.5 µl Murine RNase Inhibitor, and 0.5 µl ProtoScript Reverse Transcriptase were added and the samples were

incubated for 60 min at 25 °C. To stop the reverse transcription, 15 min incubation at 70 °C was performed. Subsequently, the cDNA was amplified via PCR using the following program: 30 s at 94 °C, 22 cycles of 15 s at 94 °C, 30 s at 62 °C and 15 s at 70 °C. A 50 µl PCR reaction included the following components:

LongAmp Taq 2x Master mix	25	µl
SR Primer	1.25	µl
Index Primer	1.25	µl
Nuclease Free Water	12.5	µl
cDNA	10	µl

The PCR products were purified using the MinElute PCR Purification Kit (QIAGEN) according to the manufacturers instructions, and eluted in 10 µl nuclease-free water. After addition of 10 µl GLII buffer (Table 2.1) the samples were loaded on 6 % polyacrylamide gel with 7 M Urea:

Urea	7	M
TBE (10x)	8	ml
acryl/bisacrylamide (30 %)	12	ml
TEMED	40	µl
APS (105)	400	µl
aqua bidest	to 80	ml

Electrophoresis was carried out at 300 V for approximately 2 hours. Thereafter, gels were stained with SYBRGold (Life technologies) and the DNA fragments between 140-250 bp were excised from the gel. Each gel piece was further cut into 8 smaller pieces and placed into a 2 ml LoBind tube (Eppendorf). DNA was eluted in 500 µl DNA elution buffer (NEB) over night at 1000 rpm and 16 °C. After EtOH precipitation, the pellets were resuspended in 10 µl nuclease-free water. In the next step, the gel-extracted cDNA was reamplified. To do so, 2 µl DNA were mixed with 25 µl 2xLongAmp Taq PCR Master Mix, 2 µl each of primer VII593 and VII594 (10 µM), 19 µl nuclease-free water and amplified using the PCR program applied for the primary cDNA amplification. However, the cycle number was reduced to 4. Reamplified libraries were purified with the MinElute PCR Purification Kit (QIAGEN) following the manufacturer's specifications, and eluted in 15 µl nuclease-free water.

2.2.3.11.11 Sequencing

The finalized libraries were sequenced with an Illumina cluster station (HiSeq, paired-end mode (2x100 cycles), strand specific). The obtained data was processed as described in Holmqvist *et al*., 2016. After processing, the remaining reads were mapped to the *Y. pseudotuberculosis* YPIII genome.

2.2.4 Biochemical methods

2.2.4.1 Luciferase activity assay

A widely used reporter system for investigating the gene expression is the *lux* system. The *luxAB* genes encode for the enzyme luciferase whereas the *luxCDE* genes provide the

synthesis of the aldehyde substrate. An important disadvantage of this system is that the luciferase enzyme requires the cell energy (ATP). Consequently, *lux* assays can only be performed with bacterial cultures in the exponential growth phase. For expression analysis, the *luxCDABE* operon was fused to the promoter of the gene of interest, thus the intensity of the emitted light corresponds to the promoter activity. For this purpose, *Y. pseudotuberculosis* strains were transformed with the desired *luxCDABE* fusion plasmid. After incubation of the transformants (3 clones per plasmid) under the conditions of interest, 200 µl of each bacterial culture were directly transferred into microtiter plates and bioluminescence as well as cell densities were measured with the Varioscan Flash and SkanIt RE software (Thermo Scientific).

2.2.4.2 β-Galactosidase activity assay

Another biochemical system for gene expression analysis applied in this work is the *lacZ* reporter system. The *lacZ* gene encodes the enzyme β-galactosidase, which recognizes the synthetic compound o-nitrophenyl-β-D-galactopiranoside (ONPG) as a substrate. The β-galactosidase cleaves ONPG into galactose and the yellow colored o-nitrophenol. The color intensity corresponds to the enzyme concentration, which in turn directly correlates with the expression rate of the gene of interest. To perform the assay, *Y. pseudotuberculosis* strains were transformed with the reporter gene fusion plasmid and the transformants (3 clones per plasmid) were grown under the desired conditions. At the end of the cultivation the bacterial culture was diluted 1:10 with the growth medium (LB_{BD}) in the cuvette and cell density was measured via OD_{600}. 200 µl of each cell culture were transferred to 2 separate glass tubes directly from the cuvette and lysed by the addition of 50 µl 0.1 % SDS and 50 µl chloroform. After incubation for 10 min at room temperature, 1.8 ml Z-buffer were added and the reaction was started with 400 µl ONPG. When the samples were colored to a sufficient extent the reaction was stopped with 1 ml of 1 M $NaCl_2$ and the reaction time was recorded. Subsequently, 200 µl of the supernatant were transferred into a microtiter plate and the absorbance at a wavelength of 405 nm was measured in the Sunrise™ microplate absorbance reader (Tecan, Switzerland). The specific enzyme activity was calculated using the following equation:

$$specific\ activity = OD_{415} \times 6.75 / (OD_{600} \times \Delta t \times V)$$

specific activity	[µmol cleaved substrate/(mg protein x min)] or [U x mg protein]
OD_{415}	optical density of the sample after reaction
6.75	extinction coefficient of cleaved ONPG [µmol/(min x mg protein)]
OD_{600}	optical density of bacterial culture
V	used culture volume [ml]
Dt	reaction time [min]

2.2.4.3 Preparation of whole cell extracts

For the analysis of protein levels in different strains under various conditions, the cell densities (OD_{600}) of the bacterial cultures were adjusted to an OD equivalent of 1. An appropriate culture volume was centrifuged for 3 min at 11,000 rpm in a microcentrifuge Mini-Spin plus (Eppendorf, Germany) and the supernatant was removed. The pellets were

resuspended in 30 µl H_2O. After that, the samples were mixed with 30 µl 1x sample buffer and heated at 95°C for 5 min (Sambrook & Russell, 2001). Depending on the protein to be analyzed, between 5 and 20 µl of the whole cell extracts were applied on polyacrylamide gels.

2.2.4.4 Glycine-SDS-PAGE

SDS polyacrylamide gel electrophoresis enables the separation of proteins based on their ability to move within an electrical current, which is a function of their molecular weight (Laemmli, 1970). Polypeptide chains bind amounts of the anionic detergent SDS proportionally to their relative molecular mass, become negatively charged and are strongly attracted towards the positively charged anode in the electric field. SDS-PAGE system requires gels with two different acrylamide layers. The upper layer (stacking gel) is slightly acidic (pH 6.8) and has lower acrylamide concentration. It is designed to compress (stack) the proteins into a thin, sharply defined band when they reach the lower layer. The lower gel (separating, or resolving gel) is basic (pH 8.8), has a higher polyacrylamide content, making the gel pores narrower and is responsible for separating polypeptides by size (Yang & Mahmood, 2012). Glycine-SDS polacrylamide gels were used for discontinuous electrophoretic analysis of proteins with a molecular weight above 30 kDA. The polyacrylamide concentration of the stacking gel was individually adjusted depending on the molecular weight of the protein of interest. A 15 % SDS separating gel, used for analysis of 30 kDa proteins consists of (Sambrook & Russell, 2001):

acryl/bisacrylamide (30 %)	5	ml
separating gel buffer	2.5	ml
aqua bidest	2.5	ml
TEMED	50	µl
APS (105)	50	µl

The separating gel was covered with isopropanol in order to straighten the gel surface. As the separation gel was polymerized, the isopropanol was removed and the stacking gel was prepared:

acryl/bisacrylamide (30 %)	1.1	ml
stacking gel buffer	2.5	ml
aqua bidest	6.5	ml
TEMED	40	µl
APS (10 %)	80	µl

The stacking gel was poured on top of the separation gel and a comb was inserted. After polymerization the gel was transferred into a Mini-Protean II electrophoresis chamber (Biorad, USA) or PerfectBlue™ Doppel-Gelsystem Twin ExW S (VWR Peqlab, Germany) filled with SDS running buffer. Whole cell extract samples were applied onto the gel and SDS-PAGE was performed at a constant current of 30 mA per gel and maximum voltage for about 45 min. For size discrimination of the proteins, the molecular weight marker 'PageRuler™ Prestained Protein Ladder' (Fermentas) was loaded in a separate well. After electrophoresis, the polyacrylamide gels were either stained with

Coomassie™ Brilliant Blue G250 to visualize the separated proteins or further used for western blot analysis.

2.2.4.5 Tricine-SDS-PAGE

Polyacrylamide gel electrophoresis using a Tricine-Tris based buffer system was performed to achieve best separation and resolution of proteins smaller than 30 kDa (Schägger, 2006). This system consists of a cathode buffer for the cathode chamber and an anode buffer for the anode chamber. A standard 0.75 mm 18 % separating gel used for analysis of CsrA protein contained following ingredients:

acryl/bisacrylamide (30 %)	3.75	ml
3x gel buffer	2.5	ml
glycerol (100 %)	0.75	ml
aqua bidest	0.75	ml
TEMED	7.5	µl
APS (10 %)	75	µl

The stacking gel was composed of:

acryl/bisacrylamide (30 %)	0.53	ml
3x gel buffer	1	ml
aqua bidest	2.5	ml
TEMED	5	µl
APS (10 %)	50	µl

Electrophoresis was conducted at a constant current of 30 mA per gel and a maximum voltage for approximately 2 hours.

2.2.4.6 Coomassie staining

An easy and quick method to visualize proteins after separation by SDS-PAGE is staining of the gels with Coomassie™ Brilliant Blue G250. To do so, gels were incubated in Coomassie stain (Table 2.1) shaking for approximately 30 min until they were colored in dark blue. Thereafter, the staining solution was discarded and the gels were destained via several washing steps with ddH_2O until the protein bands were visible. To accelerate the staining and washing processes, the gels in staining solution/water were heated in a microwave oven. The staining solution was recycled several times.

2.2.4.7 Western blot analysis

The western blot technique was applied for the detection of a protein of interest (Towbin *et al*., 1979). After separation via SDS-PAGE, proteins were transferred from the polyacrylamide gel onto a polyvinylidene difluoride (PVDF) membrane. Thereafter, blotting was carried out using the equipment of the Mini Trans-Blot electrophoretic transfer cell (BioRad, USA) or PerfectBlue™ Semi-Dry Electroblotter Sedec™ M (VWR Peqlab, Germany). Firstly, the membrane was activated in methanol and placed between the gel surface and the positive electrode in a sandwich, which additionally includes a fiber pad and whatman papers, both soaked in transblot buffer, at each side. This construction protects the gel and the membrane during the blotting process. The sandwich was

thereafter enclosed in the blotting cassette, which in turn was placed into the blotting gasket. The whole system was then transferred to the blotting tank and filled with transblot buffer. Blotting was performed at a voltage of 100 V and maximum current for 1 hour. After blotting, the membrane was incubated with 5 % TBSTM for 1 hour or over night in order to block unspecific binding sites of the antibodies. Subsequently, the primary polyclonal antibody, which specifically binds to the protein of interest, was diluted in TBST buffer and applied to the membrane. The membrane was incubated with the primary antibody for 1 hour or overnight, followed by three washing steps with TBST for 10 min. Afterwards, the membrane was incubated with the secondary antibody, an anti-rabbit horseradish peroxidase (HRP) conjugate, for 1 hour. Thereafter, the membrane was washed three times with TBST for 10 min and incubated for 1 min with Pierce ECL western blotting substrate (Thermo Scientific, USA). In order to detect these signals, the membrane was exposed to X-ray films CL-Xposure (Thermo Scientific, USA).

2.2.4.8 Yop secretion assay

Contact with the host cell triggers the expression of the virulence plasmid encoded genes in *Y. pseudotuberculosis* and leads to secretion of a set of Yop effector proteins. To mimic cell contact for *in vitro* analysis of the profile and amount of these effector proteins in different strains, secretion is induced by calcium depletion (Cornelis *et al*., 1987). For a Yop secretion assay, about 50 ml LB medium were inoculated 1:50 with an overnight culture of the strain of interest and grown at 25 °C for 2 hours. Subsequently, secretion was induced by addition of 20 mM $MgCl_2$ as well as 20 mM sodium oxalate. The cultures were shifted to 37 °C and cultivated for another 4 hours. Cell quantities of the different bacterial cultures were adjusted according to their OD_{600}. The bacteria were harvested in falcon tubes by centrifugation in a Sigma 3-18 K centrifuge using 19776-H rotor at 9,000 rpm for 10 min. The supernatant was filtered through a 0.2 µm Filtropur S plus filter (Millipore, USA) and the proteins were precipitated with 1/10 volume of 100 % trichloroacetic acid (TCA). After incubation for 20 min on ice, the proteins were pelleted by centrifugation at 14,000 rpm and 4°C for 10 min. Thereafter, the pellets were resuspended in 2 ml acetone-SDS solution and incubated on ice for 20 min. The pellets were collected by centrifugation at 14,000 and 4 °C for 10 min in a microcentrifuge Mini-Spin plus (Eppendorf, Germany) and the supernatant was discarded. Afterwards, the protein pellets were washed with 500 µl 100 % acetone. After a last centrifugation step for 10 min at 14,000 rpm and 4 °C, the precipitated proteins were resuspended in equal amounts of sample buffer and applied on 15% SDS polyacrylamide gels for electrophoretic separation. For protein visualization Coomassie™ Brilliant Blue was employed.

2.2.4.9 *In vitro* transcription/translation

For the investigation of a direct effect of CsrA and YopD on *lcrF* translation efficiency *in vitro* translation was carried out using the PURExpress® *In Vitro* Protein Synthesis Kit (NEB) according to the manufacturer's instructions with minor modifications. pMP1 was used as a template for synthesis of the T7 promoter containing *lcrF* DNA fragment with primers VI729/VII836. To further generate the *lcrF* mRNA, *in vitro* transcription was

performed according to the TranscriptAid T7 High Yield Transcription Kit (Thermo Scientific, USA) user handbook. After phenol/chloroform/isoamyl alcohol extraction, 500 ng of the template *lcrF* mRNA were applied for LcrF *in vitro* translation in presence or absence of 100 nM CsrA/YopD protein.

2.2.4.10 Expression and purification of recombinant proteins

2.2.4.10.1 Expression

For the investigation of interactions between RBPs (CsrA, YopD) and the transcripts of interest via REMSA, recombinant RBPs were produced. To do so, the expression vectors pAKH172 and pJH12, carrying the His_6-CsrA (C-terminal tag) and His_6-YopD/LcrH complex respectively, were transformed into electrocompetent *E. coli* BL21 (DE3) (see 2.2.2.10). For protein expression, 500 ml DYT medium supplemented with kanamycin were inoculated 1:100 from an overnight culture and grown at 37 °C to an OD_{600} of approximately 0.5. Thereafter, 1 mM IPTG was added to induce the expression of recombinant proteins and the bacterial culture was shifted to 18 °C. Subsequently, the bacteria were pelleted by centrifugation at 6,000 rpm and 4 °C for 10 min in a SLA-3000 rotor. The pellets were either stored at -20 °C or the protein was directly extracted.

2.2.4.10.2 Purification

For extraction of recombinant proteins, the cell pellet was resuspended in 10 ml CsrA/YopD lysis buffer (Table 2.1) supplemented with the cOmplete™ EDTA-free protease inhibitor cocktail (Roche, Switzerland) and 4 µl benzonase. Cell lysis was performed with a French Press cell disruptor (G. Heinemann, Germany) at 18,000 psi for four times. To remove cell debris, the cell lysate was cleared by centrifugation in a Sigma 3-18 K centrifuge using 19776-H rotor at 14,000 rpm and 4 °C for 30 min. Thereafter, His_6-CsrA as well as His_6-YopD/LcrH complex were purified by flow-through Ni-NTA affinity chromatography with a bed volume of 0.5 Protino Ni-NTA agarose (Macherey-Nagel, Germany). For this purpose, the column was washed prior to use with 10 ml ddH_2O to remove traces of the ethanol from the storage solution and equilibrated thereafter with 10 ml CsrA/YopD lysis buffer (Table 2.1). Subsequently, 10 ml lysate were applied on the column and run by gravity flow. Afterwards, the column was washed two times with 10 ml of CsrA/YopD washing buffer (Table 2.1). Elution of the bound protein was achieved by adding six bed volumes of CsrA/YopD elution buffer (Table 2.1). To estimate the purification efficiency, supernatant-, flow through-, wash- and elution- fractions were analyzed by SDS-PAGE and Coomassie staining. The fraction with the highest purity and, for His_6-YopD/LcrH complex, also with the equal ratio of YopD to LcrH were dialyzed overnight in CsrA/YopD bandshift buffer (Table 2.1) at 4 °C. The dialyzed protein solution was stored at 4 °C for one to two weeks. To reuse the column, the residual bound protein was removed by washing with 10x column volumes of CsrA/YopD elution buffer. After that, the columns were equilibrated in 20 % ethanol and stored at 4 °C.

2.2.4.10.3 Bradford assay

Concentration of the purified recombinant protein was estimated via Bradford assay (Bradford, 1976). This assay relies on the protein-dye binding principle. In this study, Coomassie Brilliant Blue G250 was employed. Hydrophobic and ionic interactions of Coomassie dye with the protein stabilize the anionic form of the dye, resulting in a color change from brown (absorbance maximum 465 nm) to blue (absorbance maximum 595 nm). Consequently, the protein concentration can be quantified by measuring the amount of Coomassie dye in the blue form. For this purpose, 5 µL of protein solution were mixed with 250 µL of Bradford reagent in a 96-well microplate, followed by incubation for 5 min at room temperature. The absorbance was measured in a Sunrise^{TM} microplate reader (Tecan, Switzerland). After determining the extinction of a BSA calibration curve (25-1000 ng/µL), the protein concentration was calculated.

2.2.5 Cell culture methods

To find a possible sensor of the host cell contact or factors crucial for the host cell contact sensing in *Y. pseudotuberculosis*, the HEp-2 cell line (human epidermoid carcinoma cells, larynx) was used.

2.2.5.1 Cultivation of HEp-2 cells

HEp-2 cells were cultivated in a humidified atmosphere with 5% CO_2 at 37 °C (HERA cell 150 incubator, Thermo Scientific) in 75 cm^3 cell culture flasks in RPMI-1640+Glutamax medium supplemented with 7.5 % NCS as a growth factor. When the cells were approximately 80 % confluent (80 % of the flask surface was covered by cell monolayer) they were splitted (every 2 days). For this purpose, HEp-2 cells were washed with 6 ml PBS, followed by an incubation with 2 ml trypsin for 5 min at 37 °C. This step was performed to detach cells from the surface of the culture flask. To stop the cell trypsinisation, 8 ml of culture medium was added and cells were resuspended by pipetting (10 times). For a 1:25 split ratio, 1 ml of cell suspension was transferred into a new cell culture flask and filled up with 24 ml culture medium.

2.2.5.2 Determination of the cell number

The number of live cells was determined using an improved Neubauer chamber. To do so, the cell suspension was diluted in trypan blue at a ratio 1:10. Since the live cells possess an intact membrane, they are able to exclude trypan blue, whereas dead cells do not. In this way viable cells with a clear cytoplasm could be distinguished from non-viable cells with a blue colored cytoplasm, allowing to count only the live cells (Strober, 2001). The viable cell number per ml was calculated using the following equation:

$$cells/ml = total\ count \cdot 10^4 \cdot dilution\ factor$$

total count	average live cell number of four primary squares
dilution factor dilution	ratio with trypan blue

2.2.5.3 Cell contact assay

The cell contact assay was carried out in order to identify factors involved in the cell contact dependent activation of *lcrF* expression in *Y. pseudotuberculosis*. This model system is based on the work of Pettersson et al., 1996 but was advanced and complemented in the Dersch group (Opitz, 2013). *Y. pseudotuberculosis* strains were transformed with *yscWlcrF*- or *yadA* promoter- *luxCDABE* fusion plasmids (pWO42 and pWO41/pTS31, respectively) in order to provide a reporter system for monitoring of virulence gene expression. Three independent clones per each *Y. pseudotuberculosis* strain were grown at 25 °C overnight to stationary growth phase. In parallel 3 x 10^4 HEp-2 cells were seeded in 200 µl RPMI in 96 well lux microtiter plates (white, flat clear bottom, Corning Incorporated) and grown overnight. 1 well per replicate was always left empty for the cell contact negative sample. Cells were washed three times with 200 µl PBS. After the last washing step, 200 µl PBS were added to the wells with or without HEp-2 cells. The OD_{600} of the bacterial overnight culture was determined and adjusted to an OD_{600} of 0.1. Thereafter, 10 µl of the diluted bacterial suspension were applied onto the HEp-2 cells. Subsequently, the assay plate was centrifuged for 3 min at 1000 rpm, covered with a Breath-Easy® sealing membrane (Sigma-Aldrich) and incubated for 2.5 hours at 25 °C in a Varioscan plate reader (Thermo Scientific). Light emission was measured every 10 min via the Varioscan Flash and ScanIt RE software (Thermo Scientific). Curves of relative luminescence units (RLU) per time were calculated by counting the mean value out of the triplicates and were visualized by GraphPad Prism.

3 Results

After transmigration through the intestinal epithelial layer via the M-cells, enteropathogenic *Yersinia* species are confronted with the innate immune system of the host. In order to survive and immediately propagate the infection, *Yersinia* possesses a set of virulence factors that enable the pathogen to circumvent an attack by resident and recruited phagocytic cells (Galindo *et al*., 2011). These factors are encoded on the *Yersinia* virulence plasmid (pYV) and include the *Yersinia* adhesin A (YadA), which provides close contact between the pathogen and the host cell, and the T3SS with its corresponding anti-phagocytic effector proteins (Yops) (Cornelis *et al*., 1998). However, the synthesis of the aforementioned virulence factors is a high-energy consuming process. Additionally, these virulence determinants serve as perfect targets for the humoral immune response. Consequently, expression of the virulence plasmid-encoded factors should be tightly controlled. Transcription of *yadA* and the *ysc-yop* genes is activated by the major virulence regulator LcrF (Cornelis *et al*., 1998). The most essential environmental signals regulating LcrF synthesis are temperature and host cell contact (Böhme *et al*., 2012; Opitz, 2013). Furthermore, recent studies highlight the crucial role of the global regulator CsrA, the moonlighting protein YopD, as well as the RNA degradosome in regulation of *lcrF* expression (Steinmann, 2013; Hoßmann, 2017).

3.1 Regulation of later-stage virulence factors under non-secretion conditions

The temperature upshift to 37°C indicates to the *Yersinia* the entrance into the warm-blooded host environment. This signal leads to activation of LcrF synthesis, which in turn induces the transcription of *yadA* and the *ysc-yop* genes. However, the expression of the virulence plasmid-encoded genes remains low until secretion is triggered either by host cell contact *in vivo* or by depletion of Ca^{2+} from the growth medium *in vitro*. This "standby" mode is achieved via a sophisticated feedback mechanism preventing unnecessary *ysc-yop* gene expression. The key player in this regulatory cascade is the effector protein YopD. Under non-secretion conditions it accumulates inside the bacterial cell and represses the LcrF synthesis (Steinmann, 2013; Hoßmann, 2017). Consequently, the transcription of the T3SS associated genes is also downregulated. Moreover, one of the major RNA degradosome components, PNPase, was indicated to be involved in the YopD-dependent downregulation of *lcrF* expression (Steinmann, 2013). Although the negative effect of YopD on LcrF synthesis was already described, the detailed mechanism of the mode of action of YopD remained unclear. Additionally, under non-secretion conditions the RNA binding protein CsrA was also identified as a negative regulator of *lcrF* transcription (Opitz, 2013; Pimenova, 2014). Therefore, the mechanism of YopD- and CsrA-mediated repression of LcrF synthesis under conditions non-permissive for Yop secretion was investigated.

3.1.1 YopD-dependent regulation of LcrF translation

Previous studies demonstrated the negative effect of YopD on LcrF synthesis, as well as the ability of YopD to directly bind the *lcrF* transcript (Steinmann, 2013; Hoßmann, 2017). In order to unravel the mechanism of YopD-mediated post-transcriptional regulation of *lcrF* expression, the effect of YopD on *lcrF* mRNA translation initiation as well as on the *lcrF* transcript stability was analyzed.

The effect of YopD on *lcrF* translation initiation under non-secretion conditions was investigated using a translational pBAD::*lcrF'*$_{(-123\ to\ +75\ nt)}$-*'lacZ* reporter gene fusion (pKB14) introduced into the wild type strain YPIII and the *yopD* mutant YP91 (Fig. 3.1 A).

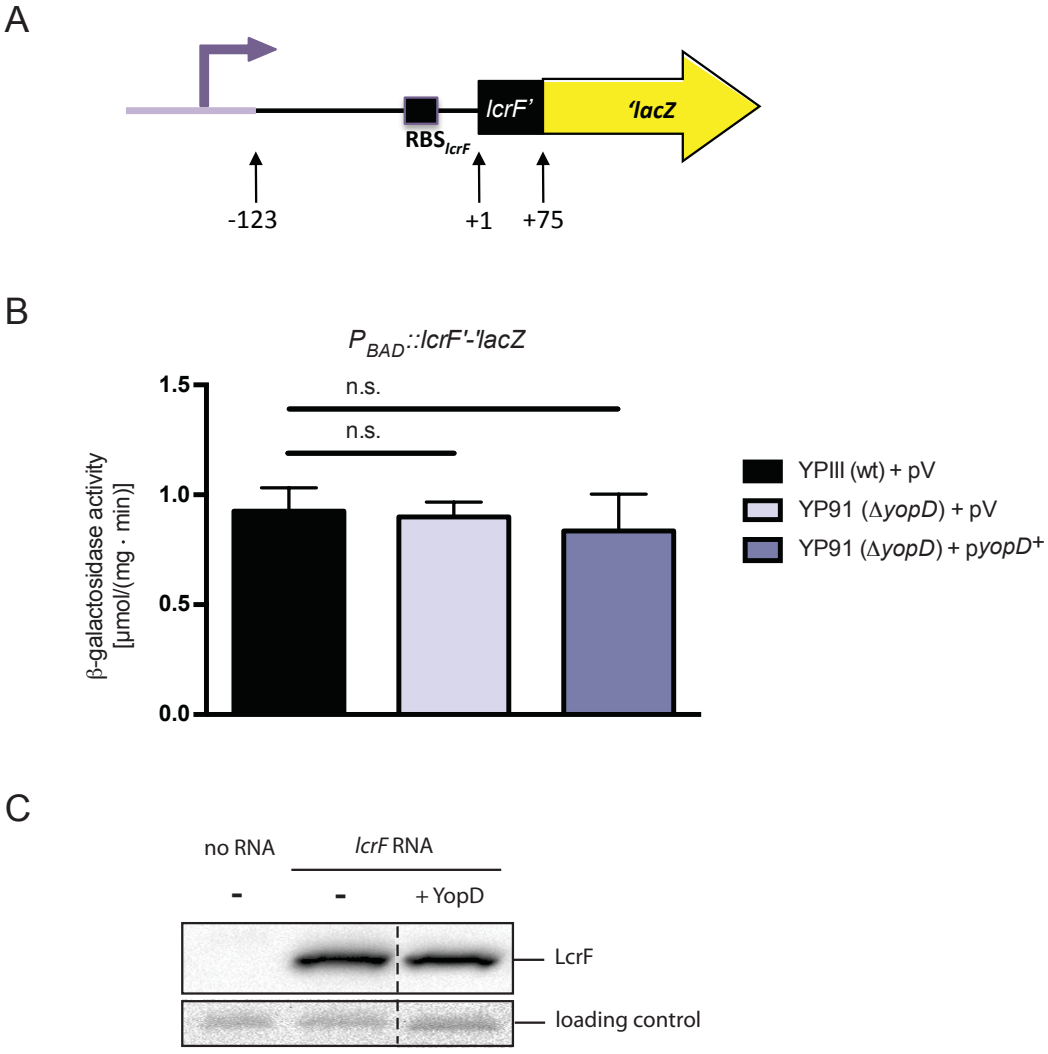

Figure 3.1. YopD does not affect translation initiation of *lcrF*.
A Schematic overview of the translational P_{BAD}::*lcrF'-'lacZ* reporter gene fusion (pKB14). The numbers indicate the nucleotides relative to the translational start site of the *lcrF* gene. The P_{BAD} promoter is colored in purple. **B** *Y. pseudotuberculosis* strains YPIII (wt), and YP91 (Δ*yopD*) harboring the translational reporter gene fusion pBAD::*lcrF'–'lacZ* (pKB14) and the empty vector pRS15 (pV) or the *yopD*+ plasmid (pRS16) were grown in LB_{BD} medium (1:50 diluted from overnight cultures for YPIII, or 1:25 for YP91) for two hours at 25°C. Expression of the pBAD promoter was activated by addition of 0.1% arabinose. Bacteria were further cultivated for four hours at 37°C. The β-galactosidase activity was determined and is given in µmol · mg^{-1} · min^{-1} for

comparison. The data represent the mean ± standard deviation of three independent experiments each performed in duplicates. Data were analyzed by the Student's t-test. Asterisks indicate the results that differed significantly from each other with **(P<0.01), n.s. (P>0.05). **C** The *in vitro* transcription/translation was performed as described in 2.2.4.9. Thereafter, samples were prepared for SDS-PAGE and transferred onto an Immobilon membrane. LcrF was detected by immunoblotting with a polyclonal α-LcrF antibody. The reaction, performed without *lcrF* RNA template but with YopD protein served as a negative control.

Furthermore, a *yopD*$^{+}$ plasmid (pRS15) was introduced into the YP91 strain to complement the *yopD* deletion. The cultures were grown in LB medium for 2 hours at 25 °C and for another 4 hours at 37°C. Expression of the pBAD::*lcrF'*$_{(-123 \text{ to } +75 \text{ nt})}$-*'lacZ* fusion was determined by β-galactosidase activity assay. As shown in Fig. 3.1 B, β-galactosidase activity of the pBAD::*lcrF'*$_{(-123 \text{ to } +75 \text{ nt})}$-*'lacZ* fusion remained unchanged, both in the absence of YopD and during the overexpression of *yopD* in YP91. To confirm that the translation initiation of *lcrF* is YopD-independent, the *in vitro* coupled transcription-translation PURExpress system was applied. The translation efficiency of *lcrF* in the presence or absence of YopD was examined by Western blot analysis. Addition of YopD to the system caused no difference in the LcrF synthesis (Fig. 3.1 C). Taken together, these results rule out a negative effect of YopD on translation initiation of *lcrF*.

Further, it was analyzed whether YopD negatively affects LcrF synthesis by decreasing the *lcrF* transcript stability. To monitor the degradation of the *lcrF* mRNA, RNA stability assays were performed with the wild type strain YPIII and the *yopD* mutant YP91. Cultures were grown under non-secretion conditions (see 2.2.1.2). In order to stop transcription, rifampicin was added to a final concentration of 1 mg/ml. Subsequently, samples were withdrawn at time points 0, 1, 2, 3, and 5 minutes after transcriptional arrest and *lcrF* mRNA levels were estimated via Northern blotting (Fig. 3.2 A). The degradation of *lcrF* transcript for each strain was assessed by quantification of detected signals using the gel analysis tool of the image-processing software ImageJ (Schneider *et al.*, 2012). Relative amounts of RNA were calculated and *lcrF* mRNA values are shown as percentages of the time point 0 value (Fig. 3.2 B). The quantitative analysis revealed an increased stability of the *lcrF* transcript in the *yopD* mutant strain with a half-life of 13.1 min compared to the wild type, where the half-life of *lcrF* was only 1.64 min (Fig. 3.2 B).

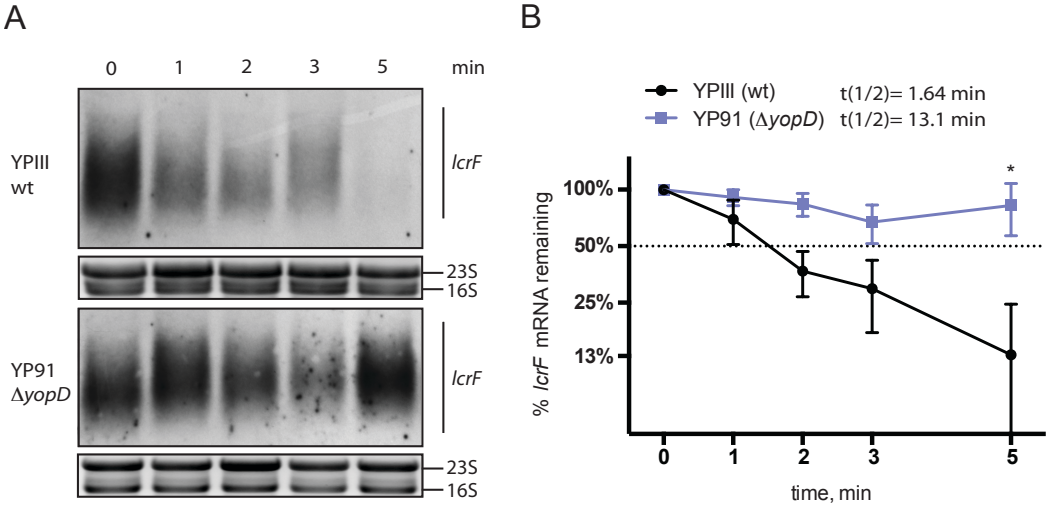

Figure 3.2. YopD decreases *lcrF* transcript stability.

A To determine the stability of the *lcrF* transcript in the YPIII wt strain compared to YP91 (Δ*yopD*), an RNA stability assay was performed after the cells were grown in LB_{BD} medium (1:50 diluted from overnight cultures) under non-secretion conditions (see 2.2.3.7). Total RNA was isolated and analyzed by northern blotting (see 2.2.3.5 – 2.2.3.6). **B** Northern blots were documented and densitometrically verified using the ImageJ software. The graph represents the relative *lcrF* mRNA concentration (y-axis) plotted against the time (x-axis) using a half-logarithmic scale. The half-life of *lcrF* mRNA in the different strains was calculated via exponential regression. The data represent the mean ± standard deviation of three independent experiments each performed in duplicates. Data were analyzed by the Student's t-test. Asterisks indicate the results that differed significantly from each other with *($P<0.05$).

Taken together, these results suggest that, although YopD has no effect on *lcrF* translation initiation, it represses LcrF synthesis at the post-transcriptional level decreasing the *lcrF* transcript stability.

3.1.1.1 Degradosome components repress *lcrF* expression

YopD was shown to positively affect the expression of genes encoding for the major RNA degradosome components, RNase E and PNPase (Steinmann, 2013; Hoßmann, 2017). Remarkably, both were previously described to be required for ideal functioning of the T3SS in *Y. pseudotuberculosis* and *Y. pestis* (Rosenzweig *et al*., 2005; Yang *et al*., 2008). Furthermore, a negative effect of PNPase on LcrF synthesis was demonstrated (Steinmann, 2013). Consequently, it is reasonable that YopD might interfere with components of the degradosome, thus indirectly decreasing the *lcrF* transcript stability (Steinmann, 2013). Therefore, it was intriguing to investigate the role of both degradosome components in the complex regulation of LcrF production.

3.1.1.1.1 *In trans* expression of C-terminally truncated RNase E is suitable for mimicking an *rne* deletion

Since a deletion of the gene encoding for RNase E (*rne*) is lethal for *Y. pseudotuberculosis*, a plasmid carrying the carboxyl-terminally truncated (dominant-negative) RNase E variant under the control of an inducible promoter (pRS40) was constructed (Fig. 3.3 A) as described by Yang *et al*. (2008).

Expression of this C-terminally truncated RNase E variant in the wild type strain confers a dominant-negative phenotype, enabling elucidation of the role of RNase E in the regulation of LcrF synthesis. The fact that RNase E controls its own synthesis by degrading the *rne* mRNA was used to estimate the cellular RNase E functionality in the presence or absence of the stably expressed C-terminally truncated RNase E (Yang *et al*., 2008). For this purpose, a plasmid harboring the 5' untranslated region of *rne* mRNA, which is responsible for the autoregulatory activity of RNase E, fused to the *lacZ* reporter was constructed (pMP31; Fig. 3.3 A) and introduced into the wild type YPIII carrying either a control plasmid (pBAD33) or pBAD-$rne_{1\text{-}465}$ (pRS40) (Jain & Belasco, 1995; Yang *et al*., 2008). Cultures were grown for two hours at 25°C followed by 4 hours at 37°C. Expression of the $rne'_{(-508 \text{ to } +305 \text{ nt})}$-*'lacZ* fusion was determined by a β-galactosidase activity assay. As shown in Fig. 3.3 B, β-galactosidase activity of the $rne'_{(-508 \text{ to } +305 \text{ nt})}$-*'lacZ* fusion was increased when the carboxyl-terminally truncated RNase E variant was expressed.

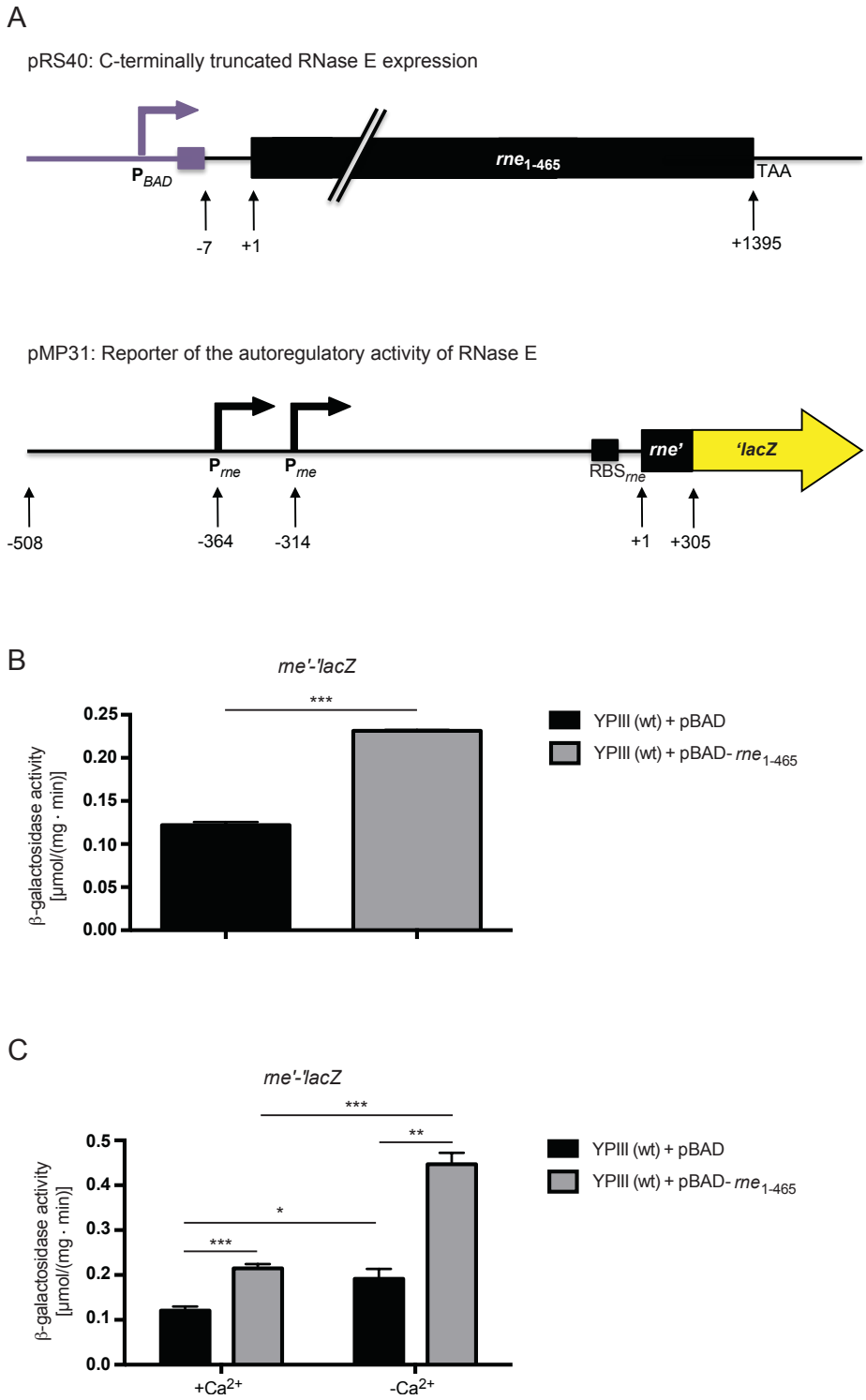

Figure 3.3. *In trans* expression of C-terminally truncated RNase E is suitable for mimicking an *rne* deletion ("Δ*rne*") in *Y. pseudotuberculosis*.

A Schematic overview of the RNase E expression plasmid pBAD-rne_{1-465} (pRS40), which harbors the first 465 codons of the *Y. pseudotuberculosis rne* gene, and the plasmid reporting on the autoregulatory activity of RNase E (pMP31) that contains 508 nucleotides of the upstream promoter region as well as the first 305 nucleotides of the *Y. pseudotuberculosis rne* gene fused in frame with *lacZ*. **B** *Y. pseudotuberculosis* strains were cotransformed with the *rne'-'lacZ* reporter and either the control or RNase E_{1-465} expression plasmid and grown in LB_{BD} medium (1:50 diluted from overnight cultures) for 2 hours at 25°C. Thereafter, arabinose was added to the final concentration of 0.1% and bacterial cultures were further incubated for 4 hours at 37 °C. Subsequently, β-galactosidase activity was determined and is given in $\mu mol \cdot mg^{-1} \cdot ml^{-1}$ for

comparison. **C** *Y. pseudotuberculosis* strains were cotransformed with the *rne'-'lacZ* reporter and either the control or RNase E_{1-465} expression plasmid and grown in LB medium (1:50 diluted from overnight cultures) for 2 hours at 25°C. Thereafter arabinose was added to the final concentration of 0.1 % and secretion was induced followed by 4 hours at 37°C (see 2.2.1.2). Consequently, β-galactosidase activity was determined and is given in $\mu mol \cdot mg^{-1} \cdot ml^{-1}$ for comparison. The data (**B-C**) represent the mean ± standard deviation of three independent experiments each performed in duplicates. Data were analyzed by the Student's t-test. Stars indicate the results that differed significantly from each other with *(P<0.05), **(P<0.01), ***(P<0.001).

This result confirms that expression of the carboxyl-terminally truncated dominant-negative RNase E variant downregulates the cellular RNase E activity and is suitable to mimic the *rne* gene deletion. Remarkably, comparative analysis of the *rne'*$_{(-508 \text{ to } +305 \text{ nt})}$-*'lacZ* expression under non-secretion (+Ca^{2+}) and secretion (-Ca^{2+}) conditions revealed a generally decreased RNase E activity upon depletion of Ca^{2+} (Fig. 3.3 C). This effect was even more pronounced in presence of the carboxyl-terminally truncated RNase E variant (Fig. 3.3 C). These data show the negative effect of Yops secretion on RNase E cellular functionality and support the results demonstrating the positive effect of intracellular YopD on RNase E expression (Steinmann, 2013).

3.1.1.2.2 RNase E, PNPase and RNA helicase B inhibit LcrF synthesis

Next, the involvement of RNase E as well as PNPase in the regulation of LcrF synthesis was analyzed. Furthermore, another degradosome component, RNA helicase B (RhlB), was shown to facilitate mRNA exonucleolytic degradation by PNPase and endoribonucleolytic cleavage by RNase E. This demonstrates the involvement of RhlB in PNPase- and RNase E-mediated regulation (Py *et al*., 1996; Khemici *et al*., 2005). However, deletion of the gene encoding for the last major degradosome enzyme, enolase, was shown to have almost no effect on PNPase- and RNase E-mediated degradation (Khemici *et al*., 2005). Based on these data, the *Y. pseudotuberculosis rhlB* mutant strain YP342 was constructed and also examined for its ability to influence LcrF production.

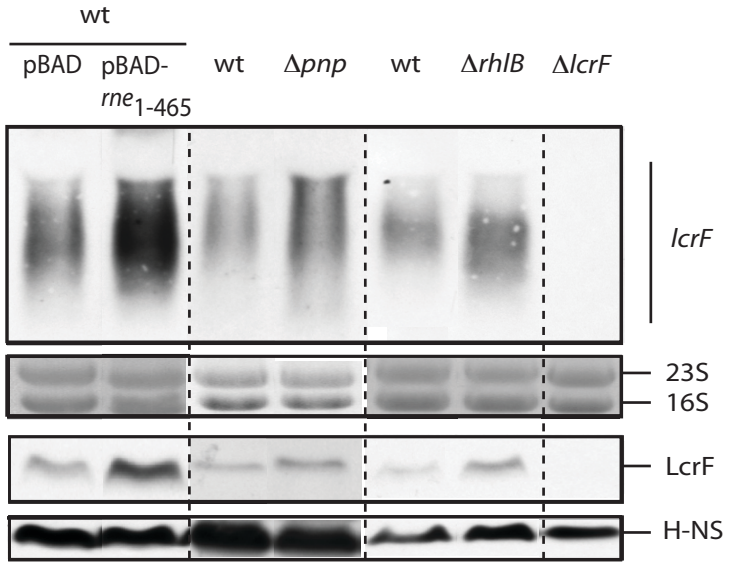

Figure 3.4. RNase E, PNPase and RNA helicase B inhibit LcrF synthesis.
Northern blot (upper panel) and western blot (lower panel) showing *lcrF* transcript and protein levels in *Y. pseudotuberculosis* strains. Wild type: *Y. pseudotuberculosis* YPIII (control for "Δ*rne*": YPIII transformed with the empty vector, pBAD33); "Δ*rne*": *Y. pseudotuberculosis* YPIII

transformed with RNase E_{1-465} expression plasmid, pRS40; Δ*pnp*: YP138; Δ*rhlB*: YP342. Overnight cultures were diluted 1:50 in fresh LB_{BD} medium and grown at 25 °C for two hours. Thereafter, bacterial cultures were incubated for 4 hours at 37 °C (for wild type transformed with pBAD33/pRS40 arabinose was added to a final concentration of 0.1% prior to the temperature shift). Northern blot analysis was carried out as described in 2.2.3.5 – 2.2.3.6. *lcrF* mRNA was specifically detected by a Dig-labeled *lcrF* DNA probe. *lcrF* transcript is indicated on the right. Furthermore, whole cell extracts of equal cell densities (OD_{600}=1) were prepared for Tricine-SDS-PAGE and transferred onto an Immobilon membrane. LcrF was detected by immunoblotting with a polyclonal α-LcrF antibody (loading control: α-H-NS). The *lcrF* mutant strain YP179 was used as negative control.

The wild type strain YPIII, transformed with the pBAD33 empty vector, YPIII carrying the carboxyl-terminally truncated RNase E expression plasmid, as well as the *pnp*-deficient strain YP138 and the *rhlB* mutant YP342 were cultured in LB medium for 2 hours at 25 °C and an additional 4 hours at 37 °C. Total RNA was isolated from each bacterial strain and the *lcrF* transcript was specifically detected with DNA probe against *lcrF*. Additionally, whole cell extracts were collected for analysis of LcrF protein levels by Western blotting. In agreement with the previous data, showing the negative effect of PNPase on LcrF protein synthesis (Steinmann, 2013), the loss of all tested degradosome components led to an enhanced *lcrF* mRNA and LcrF protein levels compared to the wild type (Fig. 3.4).

3.1.1.2 YopD indirectly controls LcrF expression via regulation of the major degradosome components

It is known that YopD, together with its cognate chaperone LcrH, affects gene expression by interacting with RNA (Chen & Anderson, 2011). Aiming to get deeper insight into YopD-mediated positive regulation of RNase E and PNPase expression, the ability of YopD to bind directly to the 5'-UTRs of *rne* and *pnp* mRNAs was investigated. Since LcrH is absolutely required for YopD stabilization, both the N-terminally His-tagged YopD and LcrH were overexpressed in *E. coli* and the His_6-YopD/LcrH protein complex was co-purified using Ni-NTA affinity chromatography (Fig. S1). Three biotinylated RNA fragments, covering the large 5'-UTR of the *rne* transcript ("*rne-up*": -365 to -251 nt; "*rne-mid*": -270 to -125 nt; "*rne-down*": -148 to +12 nt relative to the translational start site; Fig. 3.5 A), and one biotinylated RNA fragment for the whole 5'-UTR of the *pnp* transcript ("*pnp*": -141 to +12 relative to the translational start site; Fig. 3.6 A) were *in vitro* transcribed and analyzed for their ability to target the YopD/LcrH complex via RNA electrophoretic mobility shift assay (RNA-EMSA). The *in vitro* transcribed *hns* RNA fragment (+175 to +226 nt relative to the translational start site) was used as a negative control. 2 nM of RNA were incubated with increasing amounts of YopD/LcrH protein complex for 30 min at 4 °C.

As shown in Fig. 3.5 B, all three fragments of the *rne* 5'-UTR bound to YopD/LcrH. The "*rne up*" fragment (-365 to -251 nt relative to the translational start site) was shifted at 250 nM already, while the other two fragments were bound with a lower affinity of approx. 500 nM. This indicates that the YopD/LcrH complex is able to directly interact with the 5'-UTR of *rne*.

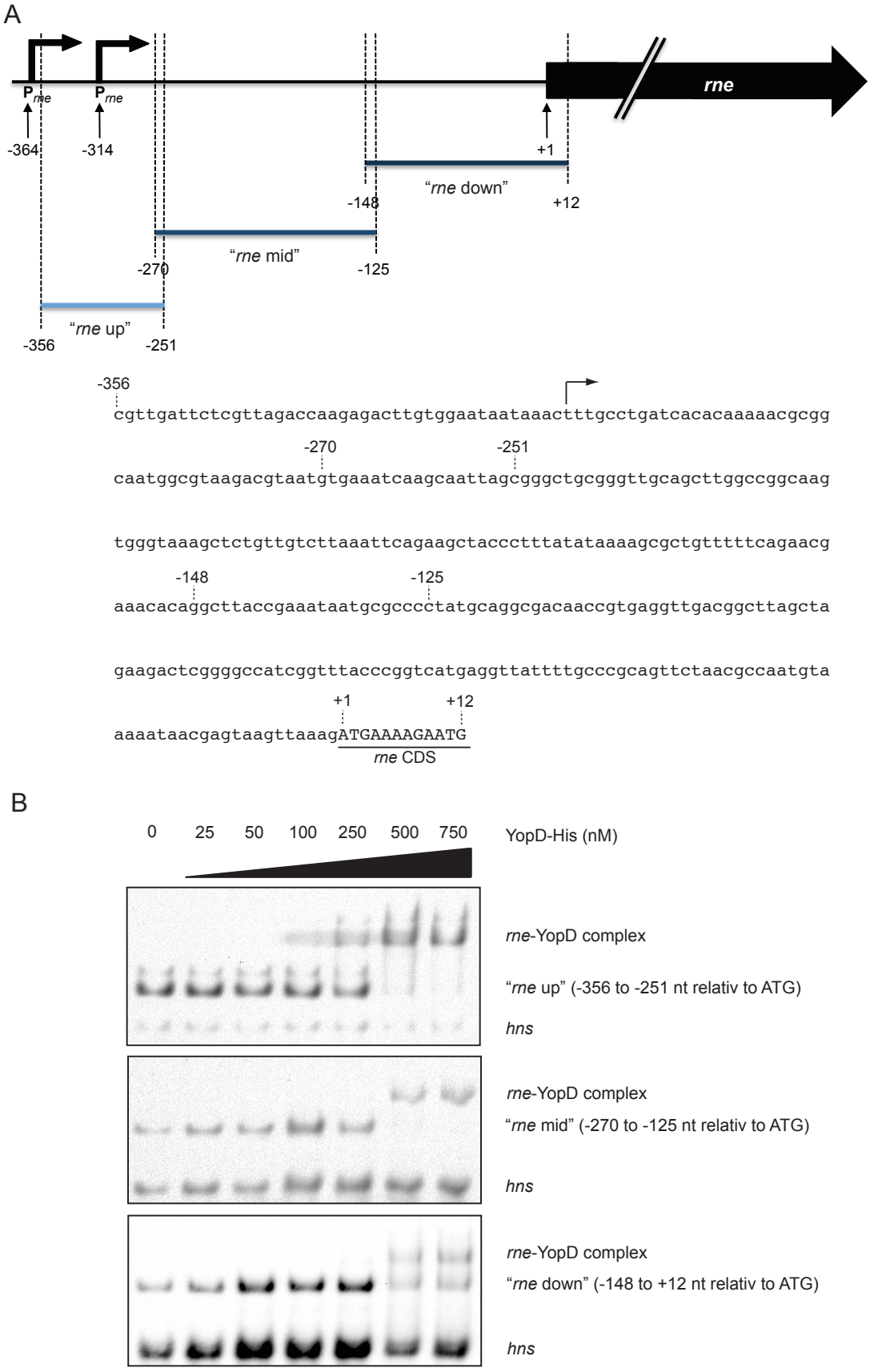

Figure 3.5. YopD binds the 5'-UTR of *rne* mRNA.
A Schematic overview of the *rne* gene locus of *Y. pseudotuberculosis* showing the transcriptional start sites (TSS; broken arrows) and the *rne* gene (black arrow). The *in vitro* transcribed RNA fragments applied for RNA-EMSA are given below. The region of the RNA fragments is indicated

relative to the translational start site. **B** Binding of YopD to the *rne* leader transcript was analyzed by RNA-EMSAs. Fragments of the *rne* 5'-UTR as well as the *hns* control fragment were *in vitro* transcribed, followed by labeling with biotin. 2 nM of the resulting *rne* 5'-UTR and the *hns* control fragment were incubated with increasing concentrations of YopD, separated by the native 7 % TBE-PAA gel, and transferred onto a nitrocellulose membrane. Thereafter, the biotin-labeled RNAs were visualized. Higher molecular bands represent the *rne*-YopD complexes.

Similar to the 5'-UTR of the *rne* mRNA, the fragment encoding for the 5'-UTR of the *pnp* transcript also bound the YopD/LcrH complex with an affinity of 500 nM (Fig. 3.6 B).

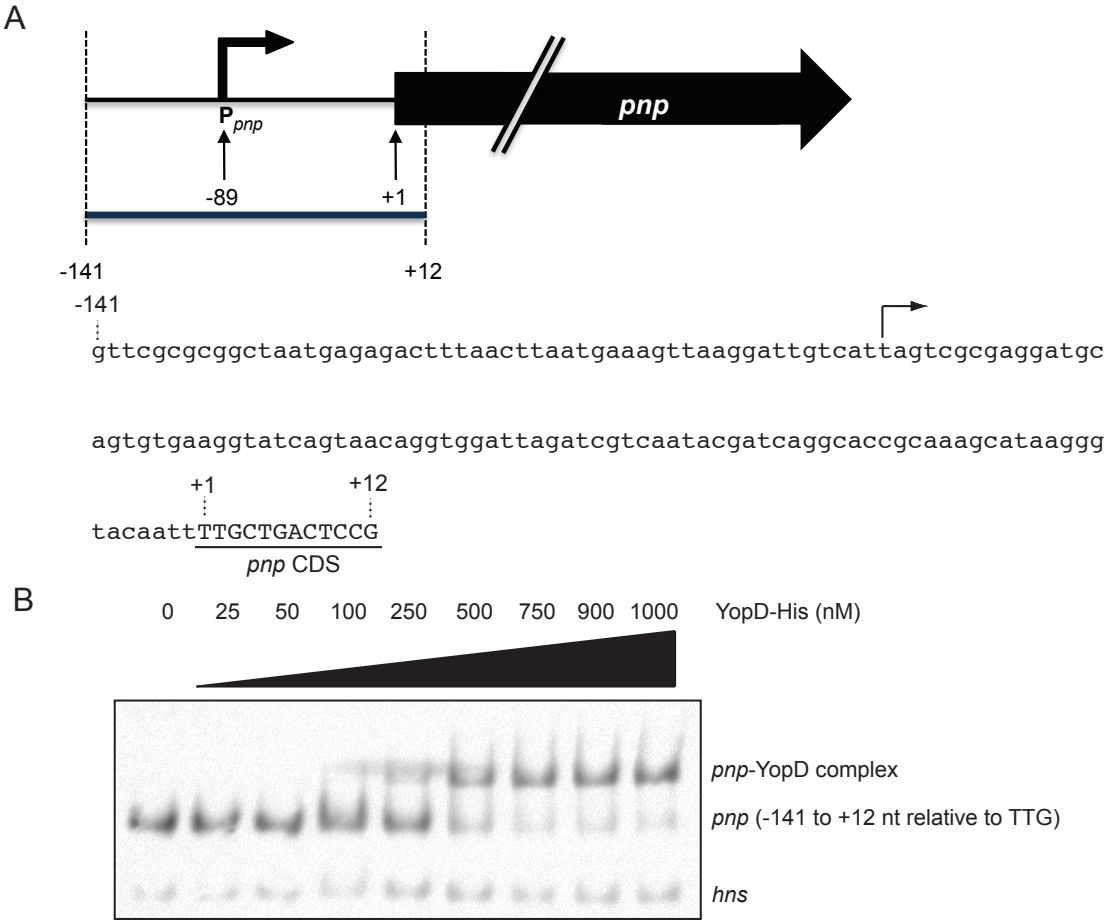

Figure 3.6. YopD binds the 5'-UTR of *pnp* mRNA.
A Schematic overview of the *pnp* gene locus of *Y. pseudotuberculosis* showing the transcriptional start site (TSS; broken arrow) and the *pnp* gene (black arrow). The *in vitro* transcribed RNA fragments applied for RNA-EMSA are shown below. The region of the RNA fragments is indicated relative to the translational start site. **B** Binding of YopD to the *pnp* leader transcript was analyzed by RNA-EMSAs. Fragments of the *pnp* 5'-UTR as well as the *hns* control fragment were *in vitro* transcribed, followed by labeling with biotin. 2 nM of the resulting *pnp* 5'-UTR and the *hns* control fragment were incubated with increasing concentrations of YopD, separated by the native 7% TBE-PAA gel, and transferred onto a nitrocellulose membrane. Thereafter, the biotin-labeled RNAs were visualized. Higher molecular bands represent the *pnp*-YopD complexes.

Taken together, it is likely that the direct binding of YopD to the 5'-UTR of the *rne* and *pnp* transcripts exerts a stabilizing effect on their mRNA, resulting in elevated expression of RNase E and PNPase in presence of YopD. This, in turn, might lead to enhanced degradation of *lcrF* transcript in the presence of YopD.

3.1.2 CsrA-dependent regulation of *lcrF* transcription

In *Y. pseudotuberculosis*, the RNA-binding protein CsrA, a component of the global post-transcriptional regulatory Csr system, was originally shown to control the synthesis of virulence genes essential for the initial infection process (Heroven *et al*., 2008). Recent data revealed that CsrA is also involved in the complex regulation of the major virulence activator LcrF. Moreover, a comparative microarray analysis demonstrated a differential expression level of numerous LcrF-dependent T3SS/*yop* genes in the absence of the CsrA protein (Opitz, 2013). Remarkably, under non-secretion conditions CsrA was shown to act as a negative regulator of *lcrF* transcription (Opitz, 2013; Pimenova, 2014). Therefore, the detailed mechanism of how CsrA affects *lcrF* transcription under non-secretion conditions was analyzed.

3.1.2.1 CsrA inhibits *lcrF* transcription indirectly by influencing the promoter region of the *yscW-lcrF* operon.

The global RNA-binding protein CsrA was shown to downregulate *lcrF* transcription under non-secretion conditions (Opitz, 2013; Steinmann, 2013; Pimenova, 2014). To confirm this data, a transcriptional P_{yscW}::*yscW'*$_{(-42\ to\ +428\ nt)}$-*luxCDABE* (pMK46) reporter gene fusion was introduced into the wild type strain YPIII and the *csrA* mutant YP53 (Fig. 3.7 A). Furthermore, a *csrA*$^+$ plasmid (pKB60) was introduced into the Δ*csrA* strain to test complementation. For this purpose, YPIII and YP53 carrying the P_{yscW}::*yscW'*$_{(-42\ to\ +428\ nt)}$-*luxCDABE* (pMK46) and either the control (pHSG576) or *csrA*$^+$ (pKB60) expression plasmid were inoculated from 25 °C overnight cultures and grown in LB_{BD} medium two hours at 25 °C followed by four hours at 37 °C. Expression of the P_{yscW}::*yscW'*$_{(-42\ to\ +428\ nt)}$-*luxCDABE* fusion was determined by luciferase activity assay. As shown in Fig. 3.7 B, luciferase activity of the P_{yscW}::*yscW'*$_{(-42\ to\ +428\ nt)}$-*luxCDABE* fusion was significantly increased in the *csrA*-deficient strain compared to the wild type. Overexpression of *csrA* in YP53 was able to restore the luciferase activity to wild type levels (Fig. 3.7 B). This confirms that CsrA is a negative regulator of *lcrF* transcription.

Additionally, preliminary data suggested the promoter region of the *yscW-lcrF* operon to be required for CsrA-mediated repression of *lcrF* transcription (Pimenova, 2014). To further confirm the role of the *yscW* promoter (P_{yscW}) region for CsrA-dependent negative regulation of *lcrF* transcription, expression of three *yscW'-luxCDABE* fusions under the control of the natural P_{yscW} promoter as well as two artificial promoters P_{lac} and P_{tet} was analyzed in *Y. pseudotuberculosis* wild-type (YPIII) and the *csrA* mutant (YP53) (Fig. 3.7). For this purpose, the overnight cultures of YPIII and YP53 carrying the P_{yscW}::*yscW'*$_{(-42\ to\ +428\ nt)}$-*luxCDABE* (pMK46), P_{lac}::*yscW'*$_{(+28\ to\ +428\ nt)}$-*luxCDABE* (pMP14) and P_{tet}::*yscW'*$_{(+28\ to\ +428\ nt)}$-*luxCDABE* (pMP27) reporter plasmids were inoculated in fresh LB_{BD} medium and grown at 25 °C for two hours. Thereafter, the cultures were shifted to 37 °C for additional four hours. Promoter activity was measured and compared between the wild type and the *csrA* mutant (Fig. 3.7 C). Under non-secretion conditions, the *yscW-lcrF* promoter was significantly upregulated in the absence of CsrA compared to the wild type. However, an exchange of the *yscW* promoter by the P_{lac} or P_{tet} abolished CsrA-mediated regulation of *yscW-lcrF* operon transcription. Taken together, these results

support the role of the *yscW* promoter region for CsrA-dependent repression of *lcrF* transcription.

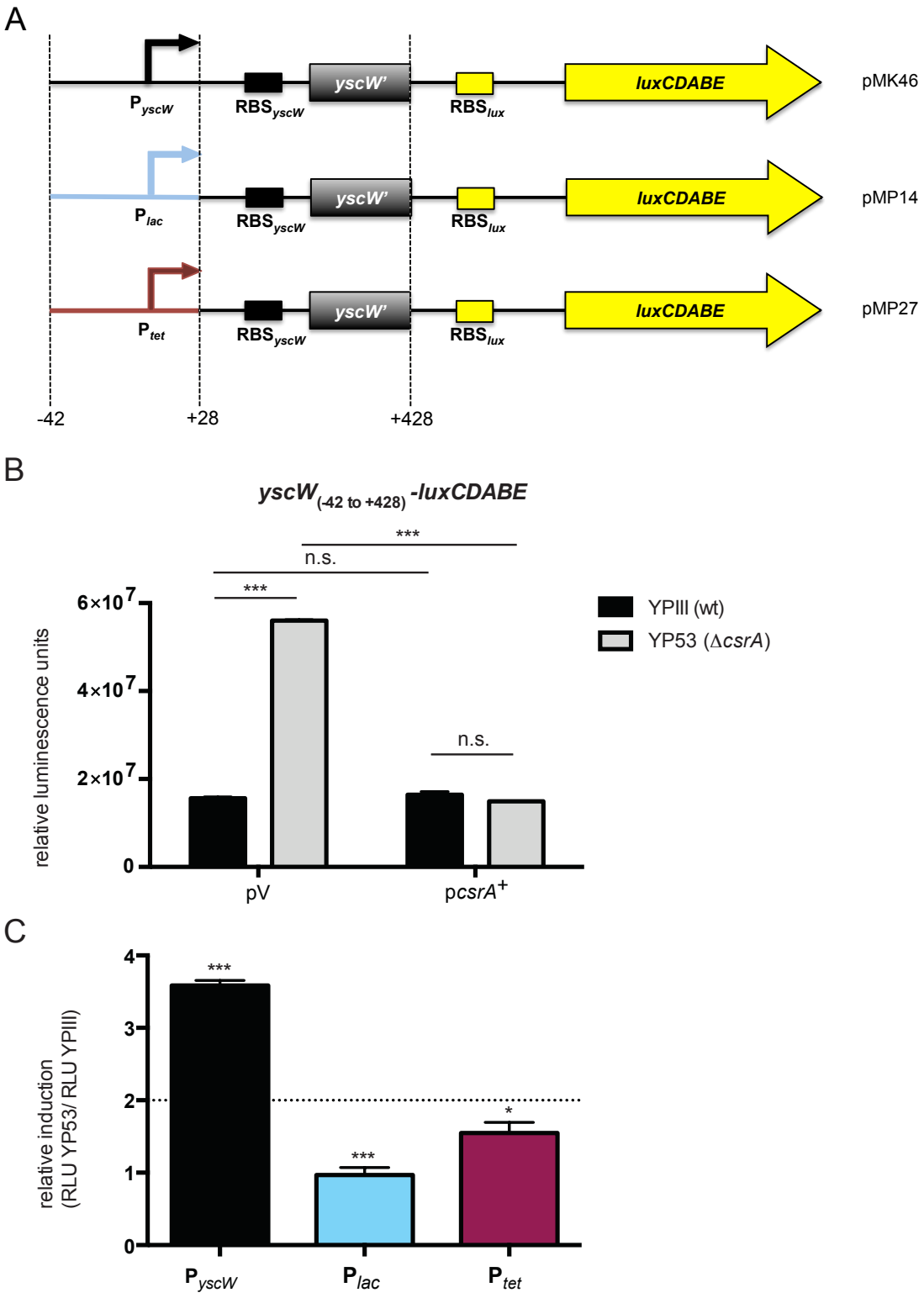

Figure 3.7. CsrA indirectly represses *lcrF* transcription via the *yscW* promoter region.
A Schematic overview of the P_{yscW}-*yscW'-luxCDABE* (pMK46), P_{lac}-*yscW'-luxCDABE* (pMP14), and P_{tet}-*yscW'-luxCDABE* (pMP27) transcriptional reporter gene fusions applied for the investigation of the CsrA-dependent regulation of *lcrF* transcription. The numbers indicate the 5' ends and the 3' ends of the *yscW* upstream region fragments fused to *luxCDABE* as well as the

5' ends of each promoter region with respect to the transcriptional start site of the *yscW* gene. **B** YPIII and YP53 overnight cultures carrying the pMK46 reporter construct and either the control (pHSG576) or *csrA*$^{+}$ (pKB60) expression plasmid were inoculated in LB_{BD} medium 1:50 (wt) or 1:20 (Δ*csrA*) and grown under non-secretion conditions. Thereafter, luciferase activity was measured. The relative luminescence units (luciferase activity) are indicated on the left. **C** YPIII and YP53 overnight cultures carrying the pMK46, pMP14 or pMP30 reporter constructs were inoculated in LB_{BD} medium 1:50 (wt) or 1:20 (Δ*csrA*) and grown under non-secretion conditions. Thereafter, luciferase activity was measured. The relative induction of each reporter gene fusion was calculated as luciferase activity in the *csrA* mutant normalized to those in the wild type and is indicated on the left. The relative induction >2 was classified as a significant induction. The data (**B-C**) represent the mean ± standard deviation of three independent experiments each performed in triplicates. Statistical significance was analyzed by the Student's t-test. Stars indicate the results that differed significantly from each other with *(P<0.05), **(P<0.01), ***(P<0.001), n.s. (P>0.05).

3.1.2.2 CsrA represses *lcrF* transcription via negative regulation of the transcriptional activator RcsB.

Since CsrA is exclusively an RNA binding protein, its negative effect on *lcrF* transcription was suggested to be indirect, apparently by repression of an unknown transcriptional activator or activation of an undiscovered transcriptional repressor. Comparative analysis of the sequences targeted by the already known *lcrF* transcriptional regulators revealed that the binding box of RcsB, the response regulator of the RCS phosphorelay system, is overlapping with the CsrA-dependent region (Fig. 3.8).

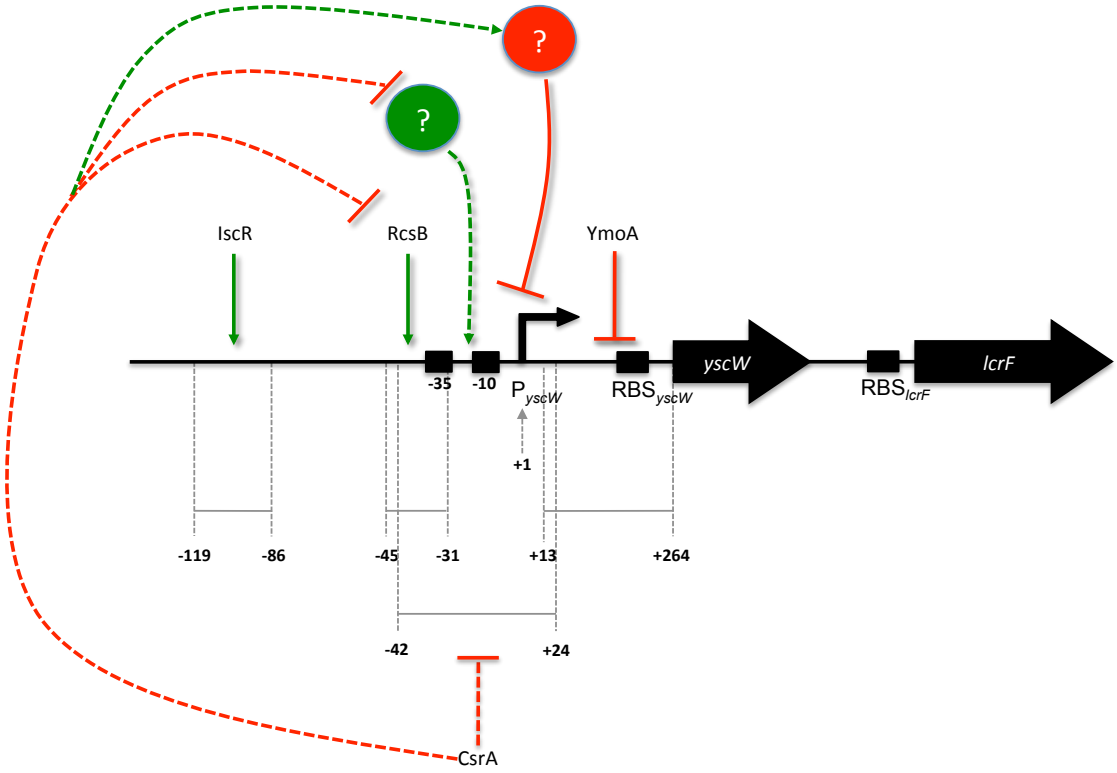

Figure 3.8. Proposed model of the CsrA-mediated indirect repression of *lcrF* transcription. Schematic overview of the IscR-, RcsB-, and YmoA-controlled DNA regions upstream to the *yscW-lcrF* operon. The RcsB-targeted site overlaps with the CsrA-dependent sequence. The numbers indicate the nucleotide positions with respect to the transcriptional start site of the *yscW-lcrF* operon (Böhme *et al*., 2012; Li *et al*., 2014; Miller *et al*., 2014).

This led to the assumption, that RcsB could be the missing link in CsrA-mediated negative regulation of *lcrF* transcription. To prove this hypothesis, the effect of CsrA on RcsB activity and expression was investigated. Since the synthesis of a small regulatory RNA, RprA, which was reported to control the level of σ^s in *E. coli*, is solely controlled by RcsB, a plasmid carrying the putative *rprA* promoter P_{rprA} (-158 to +1 nt) fused to the *luxCDABE* reporter was constructed (pMP28; Fig. 3.9 A) and used as a sensitive read-out of the RscB activity (Majdalani *et al*., 2002; Majdalani & Gottesman, 2005).

Luciferase activity of the P_{rprA}*::rprA'-luxCDABE* reporter gene fusion was determined in the *Y. pseudotuberculosis* wild type strain YPIII and the *csrA* mutant strain YP53 under non-secretion conditions (Fig. 3.9 A). Furthermore, complementation of the *csrA* deletion was tested by introduction of a $csrA^+$ plasmid (pKB60). The promoter activity of P_{rprA}*::rprA'-luxCDABE* reporter fusion was strongly upregulated in the absence of CsrA. Complementation of *csrA* mutant restored the luciferase activity to wild type levels (Fig. 3.9 A). According to this result, RcsB activity is repressed by CsrA.

In order to unravel the mechanism of CsrA-mediated regulation of RcsB, the influence of CsrA on *rcsB* transcription was analyzed. To do so, total RNA of YPIII and YP53 was isolated after cultivation in LB medium for 2 hours at 25 °C and another 4 hours at 37 °C in the presence of calcium. The yield of *rcsB* mRNA in these strains was assessed by Northern blotting analysis with an *rcsB* specific probe. As represented in Fig. 3.9 B the *rcsB* transcript amounts were significantly increased in the *csrA* mutant compared to the wild type. Overexpression of *csrA* in YP53 reduced the *rcsB* transcript level almost to the wild type levels (Fig. 3.9 B). This corresponds to the transcriptional upregulation of RcsB-dependent *rprA* promoter (P_{rprA}) activity in the *csrA* mutant (Fig. 3.9 A). Considering the fact that CsrA acts post-transcriptionally, it appeared likely that the *rcsB* transcript stability is affected by CsrA.

To further elucidate, whether the degradation of *rcsB* mRNA plays a role in the negative regulation by CsrA, RNA stability assays were performed with the wild type strain YPIII and the *csrA* mutant strain YP53. Cultures were grown in LB medium under non-secretion conditions. To stop transcription, rifampicin was added to a final concentration of 1 mg/ml. Thereafter, samples were withdrawn at indicated time points and *rcsB* mRNA levels were examined by Northern blot analysis (Fig. 3.9 C). The decay of the *rcsB* transcript for each strain was assessed by estimating the intensities of the detected signals. Relative amounts of RNA were calculated and the *rcsB* transcript values were expressed as percentages of the value at time point 0 min as shown in the diagram (Fig. 3.9 C right panel). As displayed in Fig. 3.9 C, the half-life of the *rcsB* transcript in the wild type strain YPIII was about 1.7 min in contrast to the extended half-life of approx. 4.3 min in the *csrA*-deficient strain.

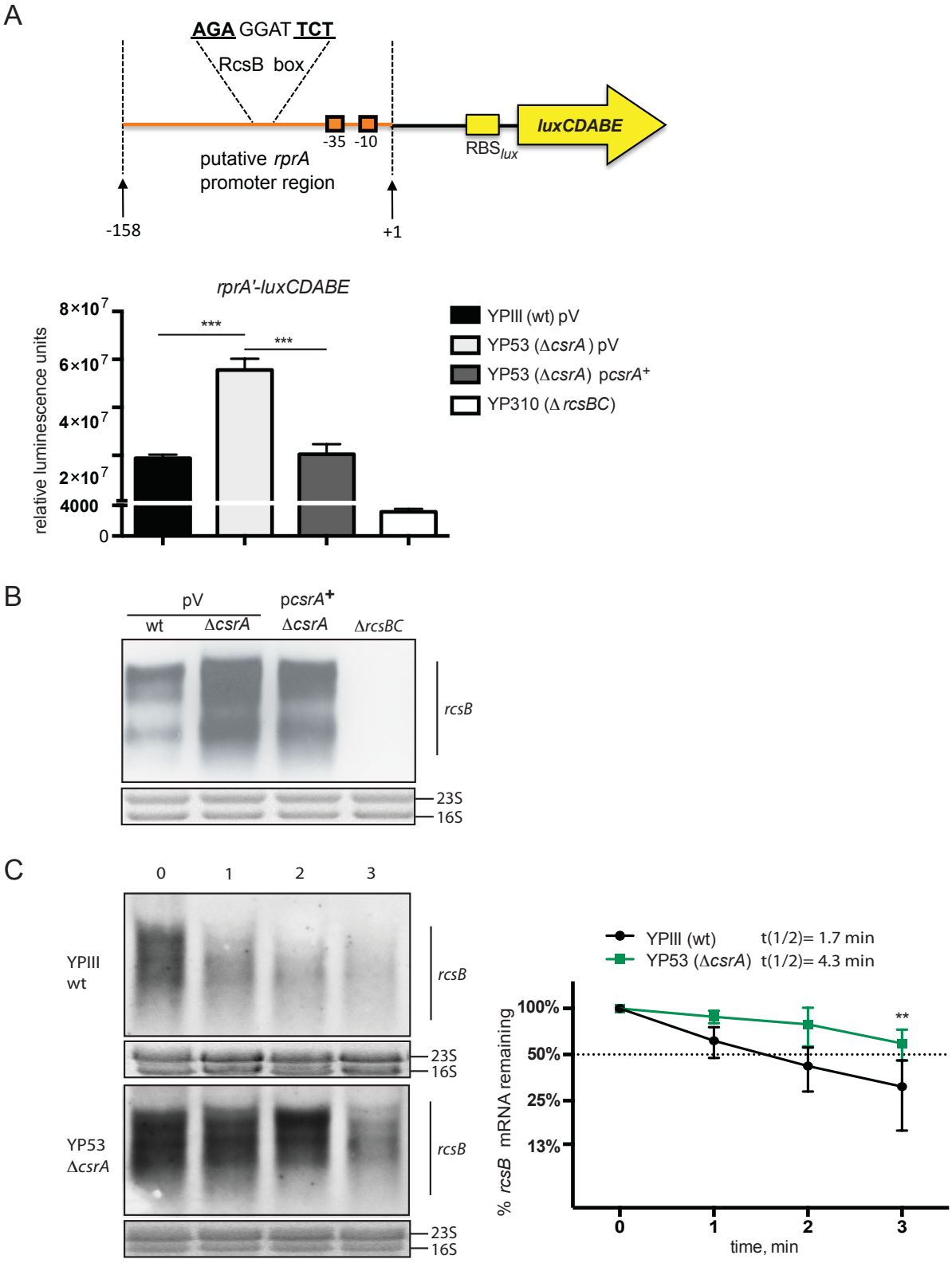

Figure 3.9. CsrA is a negative regulator of the transcriptional activator RcsB.
A Schematic overview of the P_{rprA}::*rprA'-luxCDABE* (pMP28) transcriptional reporter gene fusion for investigation of the effect of CsrA on RcsB. The numbers indicate the 5' ends and the 3' ends of the *rprA* upstream (putative promoter) region fused to *luxCDABE* with respect to the transcriptional start site of the *rprA* gene. The RcsB binding site (RcsB box) as well as the -35 and -10 boxes are indicated. YPIII and YP53 overnight cultures carrying the pMP28 reporter construct and the empty vector pHSG576 (pV) or the *csrA*$^+$ plasmid (pKB60) were inoculated in LB_{BD} medium 1:50 (wt) or 1:20 (Δ*csrA*) and grown under non-secretion conditions. Thereafter, luciferase

activity was measured. The relative luminescence units (luciferase activity) are indicated on the left. The *rcsBC* mutant strain YP310 was used as negative control. Statistical significance was analyzed by the Student's t-test. Asterisks indicate the results that differed significantly from each other with ***(P<0.001). **B** Northern blot analysis was performed as described in 2.2.3.5 – 2.2.3.6. The *rcsB* transcript is indicated on the right. The *rcsBC* mutant strain YP310 was used as negative control. **C** To estimate the stability of *rcsB* transcript in YPIII compared to YP53 (Δ*csrA*), an RNA stability assay was performed (see 2.2.3.7) after the cells were grown under non-secretion conditions. Northern blots were documented and densiometrically verified using the ImageJ software. The graph represents the relative *rcsB* mRNA concentration (y-axis) plotted against the time (x-axis) on a half-logarithmic scale. The data represent the mean ± standard deviation of three independent experiments each performed in duplicates. Data were analyzed by the Student's t-test. Asterisks indicate the results that differed significantly from each other with **(P<0.01).

Taken together CsrA inhibits RscB production post-transcriptionally by stimulating the degradation process of *rcsB* mRNA. CsrA-mediated downregulation of RcsB synthesis in turn leads to the repression of *lcrF* transcription.

3.2 Regulation of later-stage virulence factors under secretion conditions

Depletion of Ca^{2+} from the growth medium *in vitro* leads to the secretion of Yops, including the LcrF-repressor YopD. Consequently, Yop secretion further triggers LcrF synthesis leading to enhanced transcription of *yadA* and the *ysc-yop* genes and, subsequently, to elevated secretion of effector proteins. Apart from YopD secretion, the riboregulator CsrA was shown to be indispensible for the upregulation of the T3SS upon Ca^{2+}-depletion *in vitro* and host cell contact *in vivo* (Nuss *et al*., 2017). Furthermore, according to preliminary data, CsrA positively affects LcrF synthesis under secretion conditions at the post-transcriptional level (Opitz, 2013; Pimenova, 2014). Our interest was therefore unraveling the detailed mechanism of CsrA-mediated positive regulation of *lcrF* translation upon Yop secretion.

3.2.1 CsrA positively affects *lcrF* translation

In *Y. pseudotuberculosis* wild type strain YPIII grown under secretion conditions both the *lcrF* mRNA and LcrF protein levels increase. Remarkably, previous observations demonstrated that this is not the case in the *csrA*-deficient strain (Opitz, 2013; Pimenova, 2014). Despite the fact that similar *lcrF* mRNA level exist in the wild type strain and in the *csrA* mutant under Ca^{2+}-depletion conditions, no induction of LcrF protein level could be observed in the absence of CsrA (Opitz, 2013; Pimenova, 2014). This data suggest that *lcrF* translation is impaired due to the lack of the CsrA protein. The following inquiry was performed to confirm the previously documented impact of CsrA on LcrF synthesis under secretion conditions. For that, complementation analysis, which ensures that the influence on LcrF seen in the *csrA* mutant strain is due to the loss of CsrA and not due to polar effects, was conducted by introducing a $csrA^+$ plasmid (pKB60) into the YP53. The empty vector pHSG576 (pV) was introduced into YPIII and YP53 to exclude any unspecific effects by the plasmid backbone. The strains were grown in LB medium under secretion conditions. The *lcrF* mRNA and LcrF protein amounts were assessed via Northern blotting

and Western blotting, respectively, and compared between the wild type, the *csrA* mutant, and the *csrA* mutant with p*csrA*$^+$ (Fig. 3.10 A).

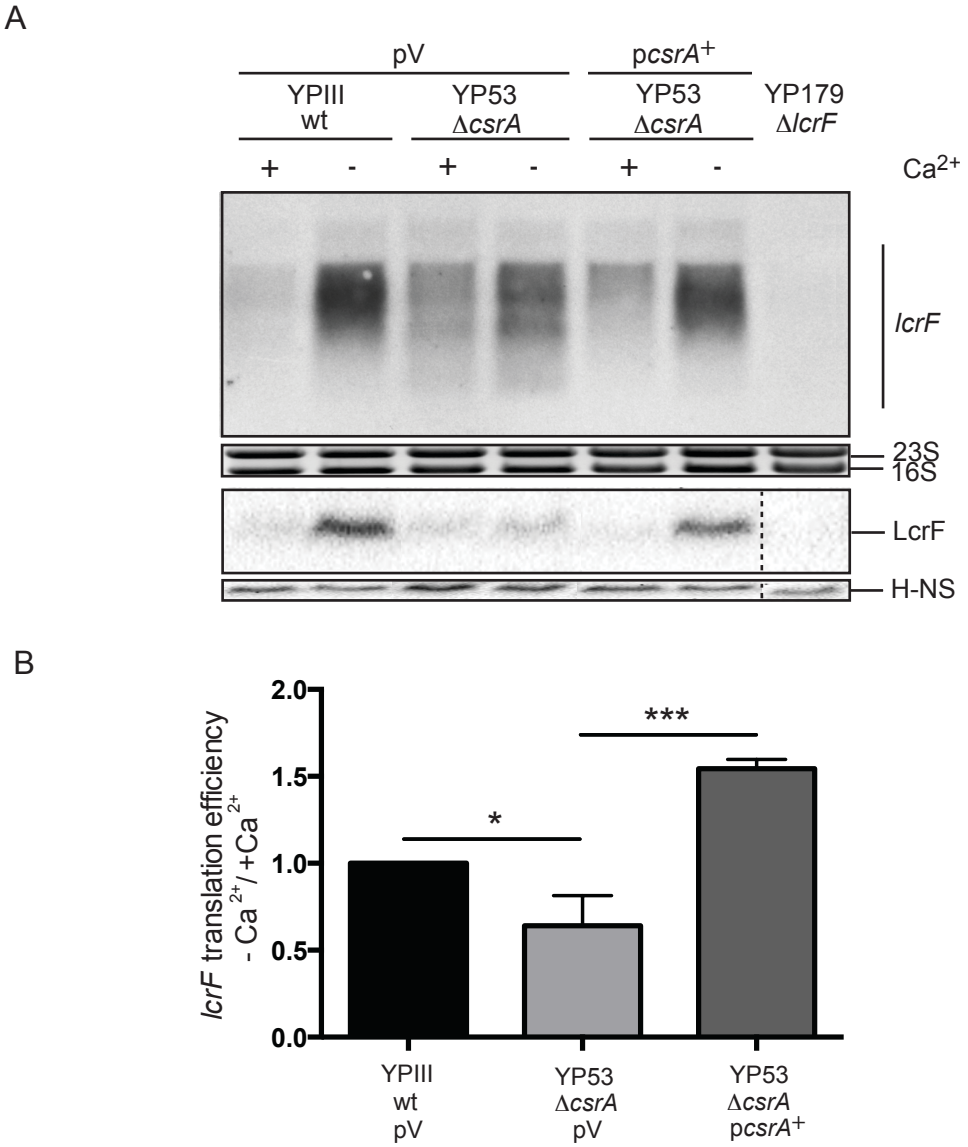

Figure 3.10. CsrA positively affects *lcrF* translation under secretion conditions.
YPIII and YP53 carrying the empty vector pHSG576 (pV) or the *csrA*$^+$ plasmid (pKB60) were grown in LB_{BD} under non-secretion or secretion conditions. Thereafter, *lcrF* transcript and LcrF protein levels were analyzed with Northern blot (upper panel) and Western blot (lower panel), respectively. **A** Northern blot analysis was performed as described in 2.2.3.5 – 2.2.3.6. *lcrF* transcript is indicated on the right. Furthermore, whole cell extracts of equal cell densities (OD_{600}=1) were prepared for Tricine-SDS-PAGE and transferred onto an Immobilon membrane. LcrF was detected by immunoblotting with a polyclonal α-LcrF antibody (loading control: α-H-NS). The *lcrF* mutant strain YP179 was used as negative control. **B** Northern blot and Western blot data obtained from three independent investigations of CsrA- and Ca^{2+}-dependent LcrF expression were analyzed. Quantification the *lcrF* translation efficiency was carried out as described in 2.2.3.6. Statistical significance was analyzed by the Student's t-test. Asterisks indicate the results that differed significantly from each other with *($P<0.05$), ***($P<0.001$).

In agreement with the previous observations, the *lcrF* mRNA level was significantly elevated in the Δ*csrA* strain (YP53) under non-secretion conditions, compared to the wild type (YPIII) (Fig. 3.10 A). This corresponds to the transcriptional upregulation of

luciferase activity detected in the *csrA*-deficient strain (Fig. 3.7 B). However, the LcrF protein level under these conditions was only slightly increased in the absence of CsrA. In the wild type the elevated amount of the *lcrF* mRNA reflected the strongly upregulated LcrF protein level under Ca^{2+} depletion conditions. This confirms the data showing an enhanced translation efficiency of *lcrF* under secretion conditions (Pimenova, 2014). In contrast to the wild type, the *lcrF* transcript level was only slightly increased and LcrF protein amounts remained almost unchanged under secretion conditions in the Δ*csrA* strain (Fig. 3.10 A). Ectopically expression of *csrA* in YP53 could restore the wild type *lcrF* transcript and LcrF protein level.

To assess the CsrA effect on the secretion-dependent increase of *lcrF* translation efficiency, defined as protein/mRNA ratio under secretion conditions *versus* protein/mRNA ratio under non-secretion conditions, the Northern blot and Western blot data were quantitatively evaluated (Fig. 3.10 B). For this purpose, the gel analysis tool of the image-processing software ImageJ was applied (Schneider *et al*., 2012). The Ca^{2+} depletion-dependent *lcrF* translation efficiency in the wild type was used as reference value equal to one. Secretion-dependent changes of *lcrF* translation efficiency in the *csrA* mutant and in YP53 carrying the p*csrA*$^+$ plasmid were calculated relative to the reference value. As demonstrated in Fig. 3.10 B, translation efficiency of *lcrF* was significantly less increased upon Ca^{2+} depletion in the Δ*csrA* strain compared to the wild type. Overexpression of *csrA* in YP53 strongly improved *lcrF* translation efficiency (Fig. 3.10 B).

Taken together, these results further highlight the crucial role of CsrA in positive regulation of LcrF synthesis at the post-transcriptional level. Thus, it is possible that CsrA promotes the *lcrF* translation initiation and/or positively affects the *lcrF* transcript stability.

3.2.1.1 CsrA promotes translation initiation of *lcrF*

In the following, it was further investigated, whether CsrA enhances LcrF synthesis by affecting the translation initiation of *lcrF*. For that, expression of the translational pBAD::*lcrF'*$_{(-123\ to\ +75\ nt)}$-*'lacZ* reporter gene fusion (pKB14) was examined in the wild type strain YPIII, the *csrA* mutant YP53 as well as in the Δ*csrA*Δ*yopD* double mutant strain YP145 (Fig. 3.11). The Δ*csrA*Δ*yopD* double mutant strain YP145 was included in the analysis to confirm the result of this work, which demonstrated that YopD has no effect on *lcrF* translation initiation (Fig. 3.1 B, C). Additionally, a *csrA*$^+$ plasmid (pKB60) was introduced into the YP53 and YP145 to test complementation of the *csrA* deletion. A possible CsrA-dependency of the P_{BAD} promoter was excluded by measuring the activity of P_{tet}::*lcrF'*$_{(-123\ to\ +75\ nt)}$-*'lacZ* (pMP30) in the wild type strain and the Δ*csrA* strain (Fig. S2). Bacterial strains were cultivated in LB medium for 2 hours at 25 °C, followed by depletion of Ca^{2+} from the growth medium and additional incubation at 37 °C for 4 hours. Expression level of the pBAD::*lcrF'*$_{(-123\ to\ +75\ nt)}$-*'lacZ* fusion was estimated by β-galactosidase activity assay.

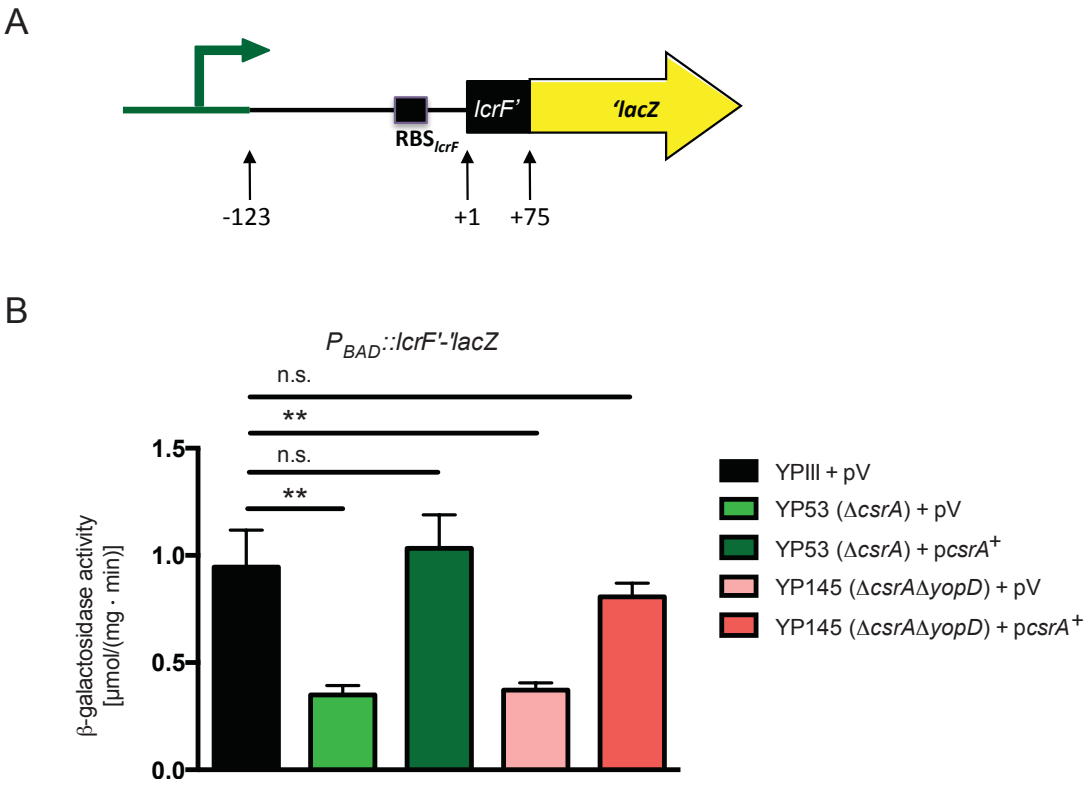

Figure 3.11. CsrA promotes translation initiation of *lcrF*.
A Schematic representation of the translational P_{BAD}::*lcrF'*-*'lacZ* reporter gene fusion (pKB14). The numbers indicate the nucleotides with respect to the translational start site of the *lcrF* gene. The P_{BAD} promoter is colored in green. **B** *Y. pseudotuberculosis* strains YPIII (wt), YP53 (Δ*csrA*), and YP145 (Δ*csrA*Δ*yopD*) harboring the translational reporter gene fusion pBAD::*lcrF'*–*'lacZ* (pKB14) and the empty vector pHSG576 (pV) or the *csrA*+ plasmid (pKB60) were grown in LB_{BD} medium (1:50 diluted from overnight cultures for YPIII, or 1:20 for YP53) for two hours at 25 °C. Expression of the pBAD promoter was activated by the addition of 0.1 % arabinose. Secretion conditions were induced, followed by further cultivation for four hours at 37 °C. The β-galactosidase activity was determined and is given in µmol · mg^{-1} · min^{-1} for comparison. The data represent the mean ± standard deviation of three independent experiments each performed in duplicates. Data were analyzed by the Student's t-test. Asterisks indicate the results that differed significantly from each other with **($P<0.01$), n.s. ($P>0.05$).

As shown in Fig. 3.11 B, expression of the pBAD::*lcrF'*$_{(-123\ to\ +75\ nt)}$-*'lacZ* fusion was significantly reduced in the *csrA* mutant compared to the wild type strain. The same effect was observed for the Δ*csrA*Δ*yopD* double mutant strain. Overexpression of *csrA* in YP53 and YP145 resulted in wild type levels of β-galactosidase activity (Fig. 3.11 B). Together, these results strongly suggest a positive, YopD-independent effect of CsrA on *lcrF* translation initiation.

Considering previous studies demonstrating the importance of the *lcrF* RNA thermometer structure in post-transcriptional activation of LcrF synthesis, as well as the ability of CsrA to bind the GGA motif within the thermoloop, the possible involvement of CsrA in maintenance of the "opened" stemloop structure was investigated (Böhme *et al.*, 2012; Hoßmann, 2017). Hence, expression of three pBAD::*lcrF'*$_{(-123\ to\ +75\ nt)}$-*'lacZ* translational reporter gene fusions harboring either the "wild type" (pKB14), or stabilized "closed" (pKB98) and destabilized "opened" (pKB99) thermoloop structures was determined in

Y. pseudotuberculosis wild type strain YPIII and compared to those in the *csrA* mutant YP53 (Fig. 3.12).

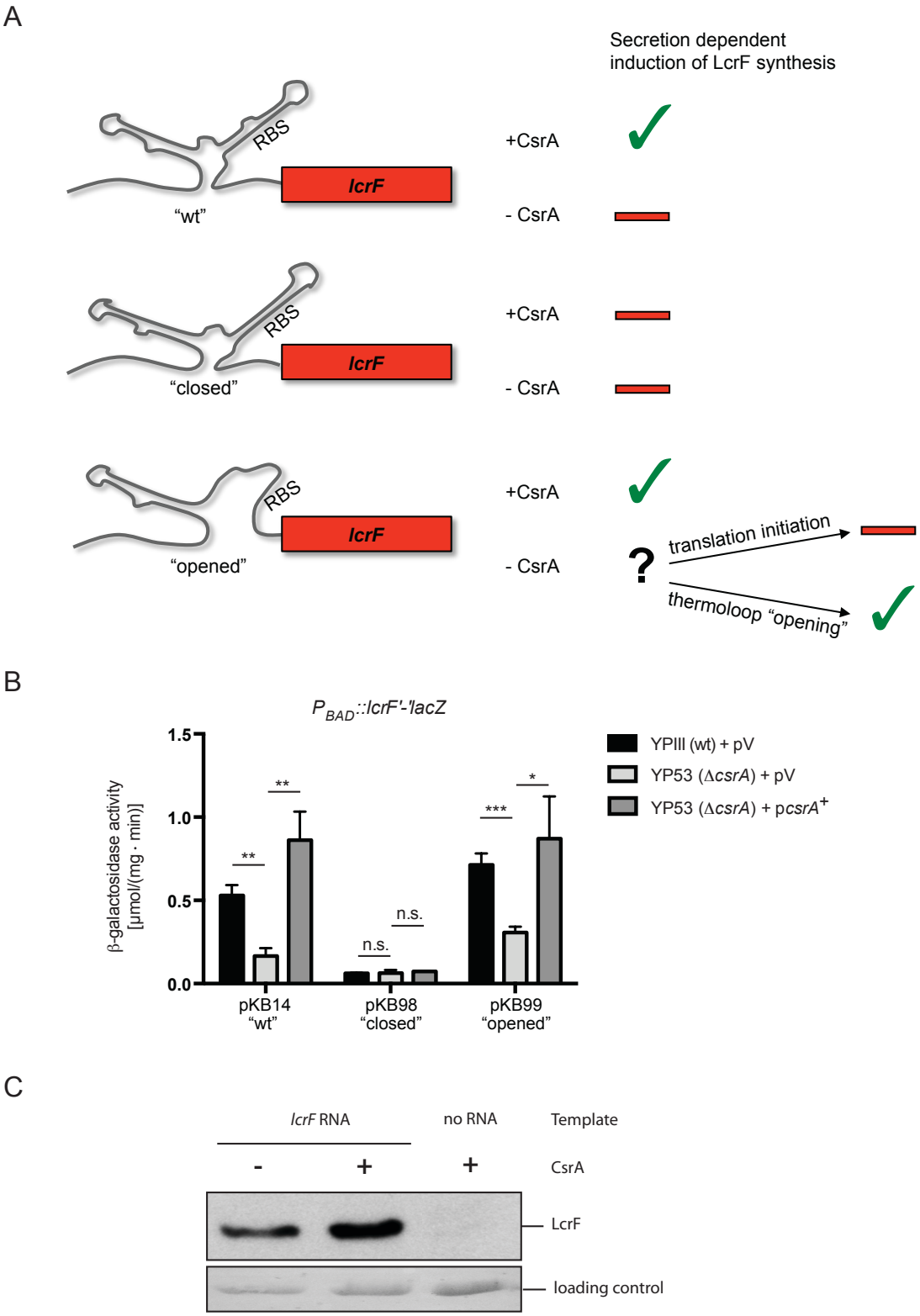

Figure 3.12. CsrA enhances *lcrF* translation initiation by stabilizing the *lcrF* thermoloop in an "opened" conformation.

A Proposed model of the CsrA effect on *lcrF* induction under secretion conditions dependent on the *lcrF* thermoloop conformation. **B** *Y. pseudotuberculosis* strains YPIII (wt) and YP53 (Δ*csrA*) harboring the translational reporter gene fusion pBAD::*lcrF'–'lacZ* carrying either the wild type

lcrF thermoloop (pKB14), or *lcrF* thermoloop in "closed" (pKB98) or in "opened" (pKB99) conformation, and the empty vector pHSG576 (pV) or the *csrA*+ plasmid (pKB60) were grown in LB_{BD} medium for two hours at 25 °C. Expression of the pBAD promoter was activated by addition of 0.1 % arabinose and secretion conditions were induced. Bacteria were further cultivated for four hours at 37 °C. The β-galactosidase activity was determined and is given in $\mu mol \cdot mg^{-1} \cdot min^{-1}$ for comparison. The data represent the mean ± standard deviation of three independent experiments each performed in duplicates. Data were analyzed by the Student's t-test. Asterisks indicate the results that differed significantly from each other with *(P<0.05), **(P<0.01), ***(P<0.001), n.s. (P>0.05). **C** The *in vitro* transcription/translation was performed as described in 2.2.4.9. LcrF was detected by immunoblotting with a polyclonal α-LcrF antibody. The reaction, performed without *lcrF* RNA template but with CsrA protein served as a negative control.

Stabilization of the stemloop structure was achieved by exchange of the nucleotides AG at position -46 to -45, relative to the *lcrF* translational start site, to CC. These substitutions improve complementarity and boost the base pairing interactions in the thermoloop structure. For destabilization of the second hairpin structure, the nucleotides GUU at position -30 to -28, relative to the *lcrF* translational start site, were exchanged to AAA.

It was assumed, that if CsrA is essential for *lcrF* translation initiation, CsrA-dependency of the secretion-mediated LcrF synthesis would still be present even when the thermoloop structure is "opened" (Fig. 3.12 A). To test this hypothesis, the wild type strain YPIII and the *csrA*-deficient strain YP53 carrying one of the three aforementioned variations of the *lcrF* stemloop structure were grown in LB medium for 2 hours at 25 °C. Thereafter, depletion of Ca^{2+} from the growth medium was induced and bacterial cultures were incubated for additional 4 hours at 37 °C. Moreover, complementation of the *csrA* deletion was examined by introducing a $csrA^{+}$ plasmid (pKB60) into YP53. The impact of these mutations on CsrA-dependent LcrF synthesis was estimated by β-galactosidase activity assay (Fig 3.12 B).

As expected, almost no β-galactosidase activity was observed, when the stemloop structure in the *lcrF* 5'-UTR was stabilized. Excitingly, although expression of the pBAD::*lcrF'*$_{(-123\ to\ +75\ nt)}$-*'lacZ* fusion harboring the "opened" thermoloop structure was generally higher than those of the reporter fusion with the "wild type" *lcrF* 5'-UTR, it was still CsrA-dependent. Furthermore, overexpression of *csrA* in YP53 restored the wild type levels of β-galactosidase activity (Fig. 3.12 B). The data indicate that CsrA is indispensible for *lcrF* translation initiation. Thereby, CsrA may stabilize the opened stemloop conformation thus making the Shine-Dalgarno sequence more accessible for the ribosome (Kusmierek & Dersch, 2018).

To further assess whether *lcrF* translation initiation is enhanced in presence of CsrA, the *in vitro* coupled transcription-translation PURExpress system was employed. The translation efficiency of *lcrF* in presence or absence of CsrA was investigated by Western blot analysis. In consistency with previous results, addition of CsrA to the system led to increased LcrF protein amount (Fig. 3.12 C). Taken together, these results emphasize that CsrA positively affects the translation initiation of *lcrF*.

3.2.1.2 CsrA increases *lcrF* transcript stability

By performing the RNA stability assay in the *Y. pseudotuberculosis* wild type and the *csrA*-deficient strains, it was further investigated whether the degradation of the *lcrF*

transcript plays a role in the CsrA-mediated positive regulation. Taking into account the known YopD-mediated influence on *lcrF* transcript stability, the Δ*yopD* mutant (YP91) as well as the Δ*csrA*Δ*yopD* double mutant (YP145) strains were also included in the experiment. The *Y. pseudotuberculosis* wild type and the three aforementioned mutant strains were grown in LB medium under secretion conditions. Transcription was terminated by addition of rifampicin at a final concentration of 1 mg/ml. Finally, samples were withdrawn at desired time points and *lcrF* mRNA levels were visualized via Northern blotting (Fig. 3.13 A). The decay of *lcrF* transcript for each strain was estimated by quantification of detected signals with the gel analysis tool of the image-processing software ImageJ (Schneider *et al*., 2012). Relative amounts of RNA were calculated and *lcrF* mRNA values are shown as percentages of the time point 0 value (Fig. 3.13 B).

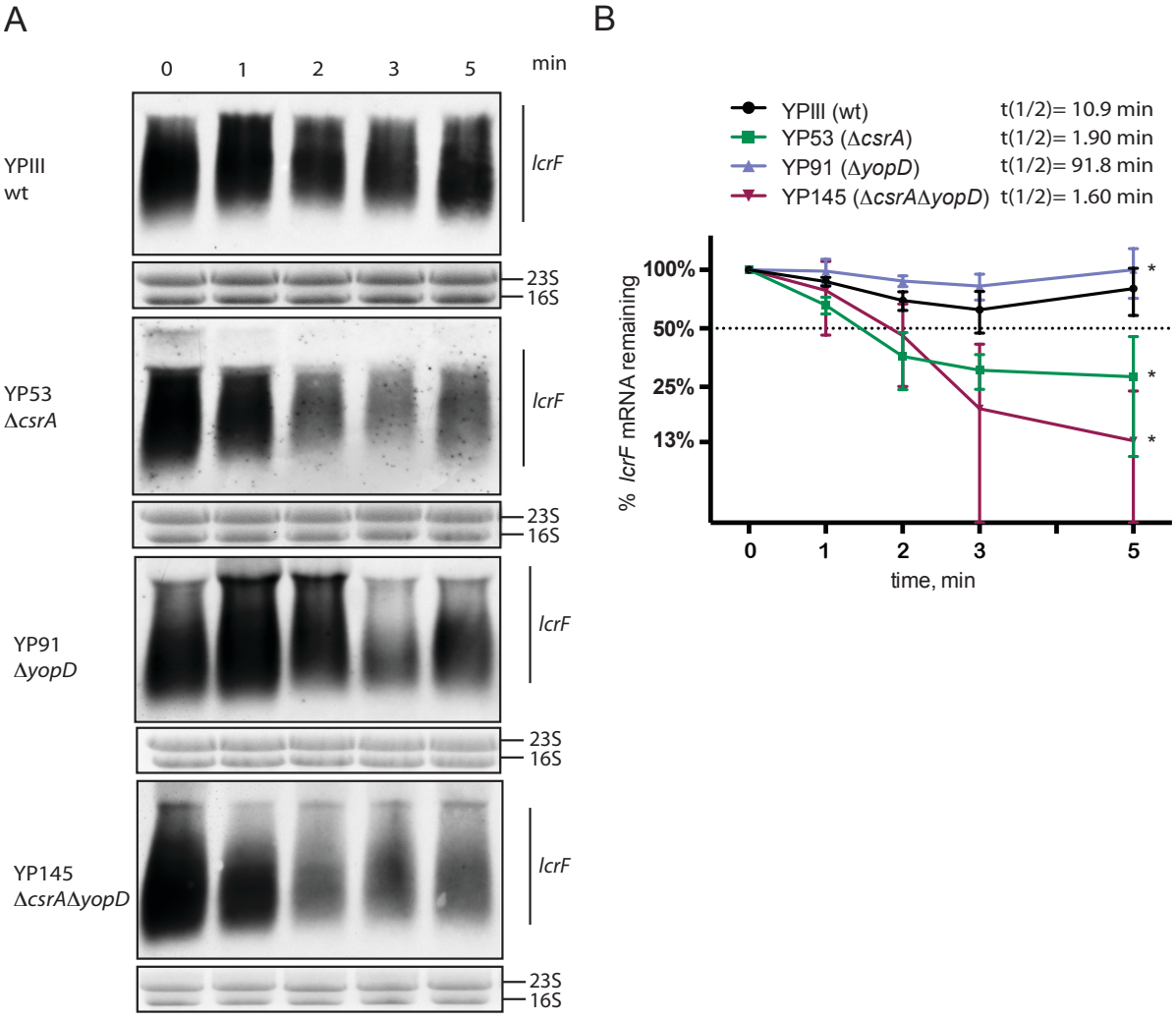

Figure 3.13. CsrA enhances *lcrF* transcript stability under secretion conditions.
A To determine the stability of the *lcrF* transcript in YPIII compared to YP53 (Δ*csrA*), YP91 (Δ*yopD*) and YP145 (Δ*csrA*Δ*yopD*), an RNA stability assay was performed as described in 2.2.3.7. The cells were therefore grown in LB medium (1:50 diluted from overnight cultures, or 1:20 for YP53 and YP145) under secretion conditions. *lcrF* transcript is indicated on the right. **B** Northern blots were documented and densiometrically quantified using the ImageJ software. The graph represents the relative *lcrF* mRNA concentration (y-axis) plotted against the time (x-axis) on a half-logarithmic scale. The half-life of *lcrF* mRNA in the different strains was calculated via the exponential regression. The data represent the mean ± standard deviation of three independent

experiments each performed in duplicates. Data were analyzed by the Student's t-test. Asterisks indicate the results that differed significantly from each other with *($P<0.05$).

The quantitative analysis showed a decreased stability of the *lcrF* transcript in the *csrA* deletion mutant with a half-life of only 1.9 min, compared to the wild type, where the half-life of *lcrF* was about 10.9 min (Fig. 3.13 B). In agreement with the previous results of this work (see 3.1.1), showing the negative effect of YopD on *lcrF* transcript stability, the *lcrF* mRNA decay in the wild type was delayed under secretion conditions, compared to the non-secretion conditions, when YopD was present in the bacterial cytosol (1.64 min; Fig. 3.2 B). Furthermore, the degradation of *lcrF* mRNA was almost completely abolished under secretion permissive conditions in the *yopD*-deficient strain (Fig. 3.13 B). However, even the deletion of *yopD* could not enhance the *lcrF* mRNA stability if CsrA was absent. The half-life of *lcrF* transcript in the Δ*csrA*Δ*yopD* double mutant was only about 1.6 min (Fig. 3.13 B). Hence, CsrA plays a crucial role in stabilization of the *lcrF* transcript under secretion conditions.

3.2.1.2.1 Localization of the CsrA-dependent element within the *lcrF* mRNA

CsrA is able to interact with multiple regions of the *lcrF* transcript (J. Hoßmann, unpublished; Hoßmann, 2017). Both, the *lcrF* 5'-UTR and the putative 3'-UTR were bound by CsrA protein (J. Hoßmann, unpublished). While the 5'-UTR of the polycistronic *yscW-lcrF* transcript was already mapped (Böhme *et al*., 2012), the length of the *lcrF* 3'-UTR is unknown. To find out, which site is essential for CsrA-mediated stabilization of *lcrF* mRNA, it was first necessary to precisely define the 3' end of the *lcrF* transcript. For that, the 3'-RACE (rapid amplification of cDNA ends) approach was applied (Argaman *et al*., 2001). For this analysis, *Y. pseudotuberculosis* wild type strain was grown under secretion conditions and total RNA was isolated, followed by the 3' dephosphorylation. After 3' RNA adapter ligation, the mRNA was reverse transcribed with the 3' reverse primer V941, which is complementary to the 3' RNA adapter. The resulting cDNA was amplified by PCR using the forward gene internal primer VI614 that binds 275 nt upstream of the 3'-UTR start and the 3' reverse primer V941 followed by gel extraction. After that, cloning of the gel extracted 3'-RACE fragments into the pJET1.2/blunt vector (Thermo Scientific) was performed and the 3'-RACE fragments from 33 independent clones were sequenced.

Surprisingly, less than a half of all fragments (15 out of 33 clones) harbored the 3'-UTR sequence (Fig. 3.14 A; Fig. S3). The 3' ends of the majority of 3'-RACE fragments were scattered throughout the *lcrF* coding sequence, most likely representing degradation intermediates (Fig. S3). The large heterogeneity in size of *lcrF* observed on Northern blots (Fig. 3.13) can thus be tentatively explained by rapid processing of *yscW-lcrF* transcript not only from the 5' end (Böhme *et al*., 2012) but also from the 3' end. Analysis of the single major 3'-RACE fragment placed the 3' end at the 22 nt position downstream of the *lcrF* stop codon. In parallel, the secondary structure of the potential *yscW-lcrF* 3'-UTR was systemically analyzed by an RNAfold WebServer (Lorenz *et al*., 2011). A typical Rho-independent terminator structure composed of a stable stem loop followed by the U-rich region (von Hippel, 1998) appeared only if the *yscW-lcrF* 3'-UTR would include 32 nt downstream of the *yscW-lcrF* stop codon (Fig. 3.14 B). Although, the 3'-RACE result

could not confirm that the *yscW-lcrF* transcript ends at the computationally predicted terminator signal, it is consistent with the Northern blot results indicating rapid degradation of *yscW-lcrF* mRNA (Fig. 3.13).

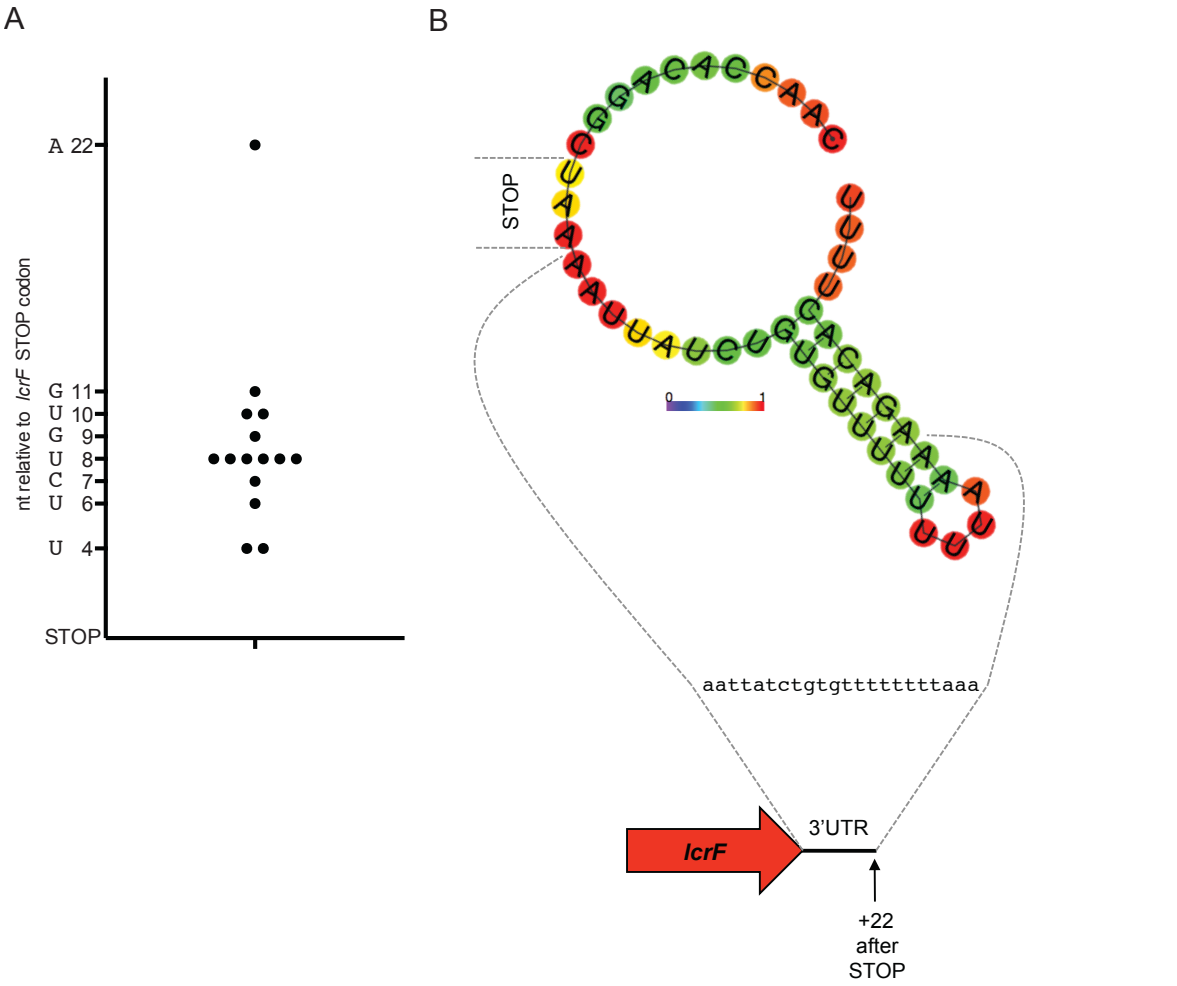

Figure 3.14. Determination of the *lcrF* 3'-UTR length using 3'-RACE.
A The graph represents the varying length of the *lcrF* 3'-UTR (black dots) estimated using the 3'-RACE. The terminal nucleotide as well as its position relative to the *lcrF* STOP codon is given on the y-axis. **B** Schematic representation of the *lcrF* 3'-UTR minimum free energy structure as predicted by RNAfold WebServer (Lorenz *et al*., 2011). The color code shows the base-pair probabilities. The *lcrF* STOP codon and the region of the *lcrF* 3'-UTR detected by 3'-RACE is marked with dashed lines.

To further localize the CsrA-dependent element in the *lcrF* mRNA, the stability of three different transcripts including either the complete *lcrF* mRNA (pMP1), or the *lcrF* mRNA lacking the 3'-UTR (pMP2), or the *lcrF* 5'-UTR with the first 75 nucleotides of the *lcrF* coding sequence (pKB14) was analyzed in the wild type strain (YP179 for pMP1 and pMP2, and YPIII for pKB14) and the *csrA*-deficient strain (YP280 for pMP1 and pMP2, and YP53 for pKB14) (Fig. 3.15). The effect of CsrA on stabilization of the complete *lcrF* mRNA and the *lcrF* mRNA without the 3'-UTR, ectopically expressed from P_{BAD} promoter, was explored in *Y. pseudotuberculosis* Δ*lcrF* background ("wt": Δ*lcrF* YP179; "Δ*csrA*": Δ*csrA*Δ*lcrF* YP280) to exclude the measurement of genomic *yscW-lcrF* transcript. To find out whether the *lcrF* 5'-UTR is required for CsrA-mediated stabilization

of the *lcrF* transcript, pKB14 carrying the complete *lcrF* 5'-UTR and the first 75 nucleotides of the *lcrF* coding sequence fused to *lacZ* gene was introduced into both YPIII (wild type) and YP53 (Δ*csrA*). Cultures were grown under type III secretion inducing. Thereafter, transcription was terminated with rifampicin (final concentration – 1 mg/ml) and samples were collected at indicated time points and the levels of the *lcrF* or *lcrF'-'lacZ* transcripts were assessed (Fig. 3.15 B, C, D). The relative amounts of the *lcrF* or *lcrF'-'lacZ* mRNA are expressed at percentages of the value at the time point 0 minute (Fig. 3.15 B, C, D).

As represented in Fig. 3.15 B the half-life of ectopically expressed whole length *lcrF* transcript (pMP1) was about 5 minutes in the "wild type" (YP179) strain. In comparison, *lcrF* mRNA was significantly destabilized in "Δ*csrA*" (YP280) mutant strain with the half-life of only 2.5 minutes (Fig. 3.15 B). This is in agreement with the data of this work, demonstrating the extended *lcrF* transcript stability under secretion conditions in presence of CsrA (Fig. 3.13). Furthermore, these results indicate that CsrA affects the *lcrF* transcript stability independently of the presence of the *yscW* mRNA.

Similar to the whole length *lcrF* transcript, the *lcrF* mRNA lacking the 3'-UTR (pMP2) was prone to rapid degradation in the absence of CsrA (Fig. 3.15 C). The stabilizing effect of CsrA on the 3'-UTR-less *lcrF* transcript was even more pronounced compared to the complete *lcrF* mRNA. However, this 3'-region of the *lcrF* transcript alone does not seem to be involved in the CsrA-mediated stabilization of the *lcrF* mRNA. Interestingly, the Δ3'-UTR *lcrF* transcript was stabilized in the "wild type" (YP179) throughout the entire examination time with the half-life of 21 minutes compared to the complete *lcrF* transcript (Fig. 3.15 B), suggesting the presence of an RNase target sequence in the *lcrF* 3'-UTR that promotes *lcrF* mRNA degradation. This is consistent with results of the *lcrF* 3'-RACE experiment, demonstrating a rapid decay of the *lcrF* mRNA from the 3' end (Fig. 3.14).

Comparative analysis of the *lcrF* 5'-UTR stability in the wild type (YPIII) and *csrA*-deficient (YP53) strains revealed no CsrA-dependency of this region. In particular, the half-life of the *lcrF* 5'-UTR in both strains was about 3.5 minutes (Fig. 3.15 D).

Taken together, CsrA positively affects stability of the *lcrF* mRNA under Yop secretion conditions. Since the 5'-UTR of *lcrF* was not stabilized by CsrA, and degradation of the Δ3'-UTR *lcrF* transcript was still CsrA-dependent, the region required for CsrA-mediated control of *lcrF* transcript stability is most likely located inside the *lcrF* coding sequence. Furthermore, it is possible that the CsrA-mediated extension of the *lcrF* half-life occurs indirectly via additional factors.

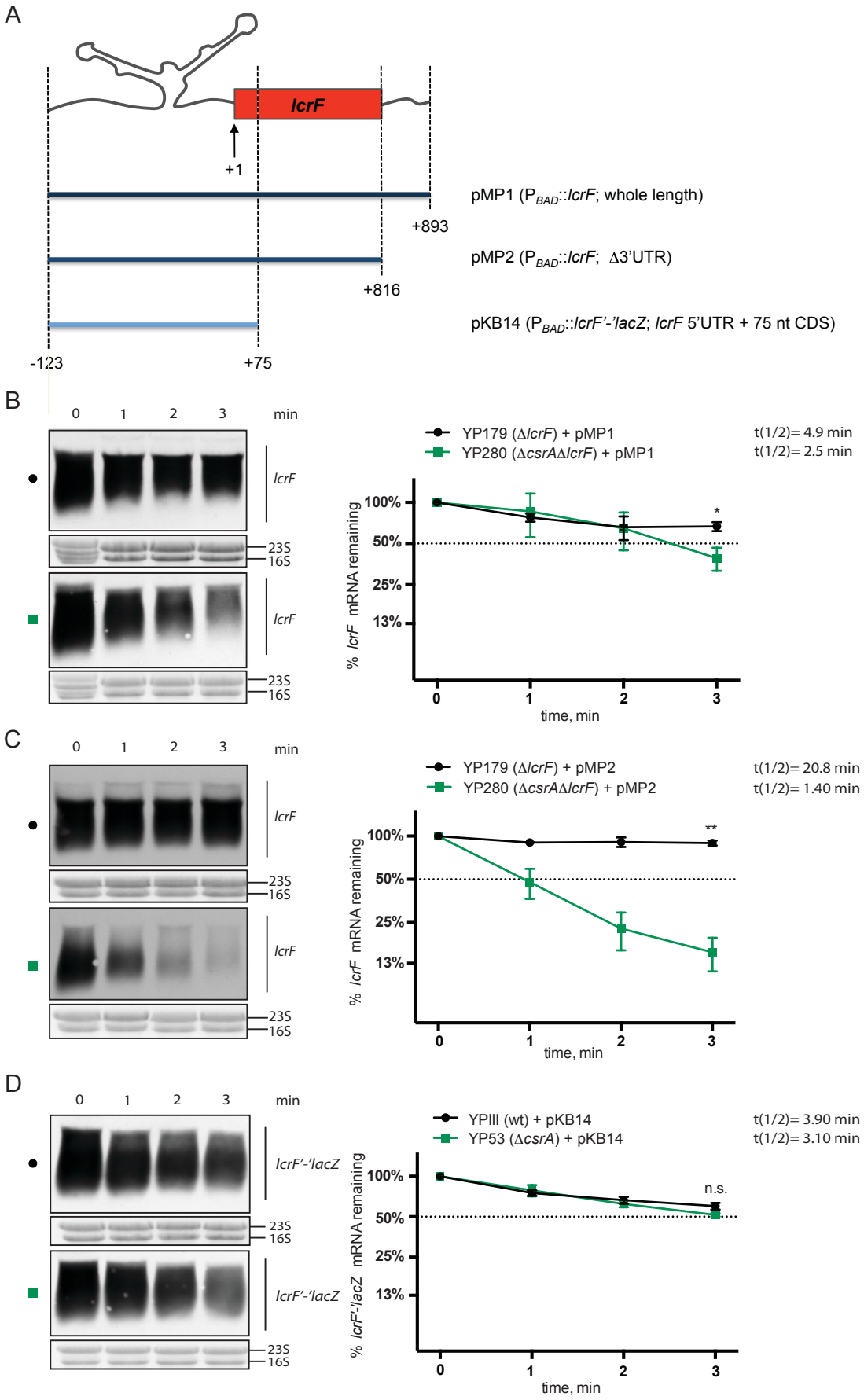

Figure 3.15. CsrA affects *lcrF* transcript stability either via interaction with the *lcrF* CDS or indirectly.

A Schematic representation of plasmid constructions harboring the wild type *lcrF* mRNA (pMP1), the mRNA carrying the 3'-UTR deletion (pMP2), as well as the mRNA harboring the *lcrF* 5'-UTR and the first 75 nt fused to *lacZ* (pKB14). The numbers indicate the nucleotide position relative to the *lcrF* start codon. **B-E** To estimate the stability of various *lcrF* transcript fragments in the wild type (YP179 for pMP1 and pMP2, or YPIII for pKB14) compared to Δ*csrA* strain (YP280 for pMP1 and pMP2, or YP53 for pKB14), an RNA stability assay was performed. The cultures transformed with one of the pBAD::*lcrF* expression plasmids (pMP1 (**B**), pMP2 (**C**), and pKB14 (**D**)) were grown in LB_{BD} medium (1:50 diluted from overnight cultures for YPIII, or 1:20 for YP53) under secretion conditions. Thereafter RNA stability assay was performed as described in 2.2.3.7. The graphs represent the relative *lcrF* mRNA (**B** and **C**) or *lcrF'-'lacZ* mRNA (**D**) concentration (y-axis) plotted against the time (x-axis) on a half-logarithmic scale. The data represent the mean ± standard deviation of three independent experiments. Data were analyzed by the Student's t-test. Asterisks indicate the results that differed significantly from each other with *($P<0.05$), **($P<0.01$), n.s. ($P>0.05$).

3.2.1.2.2 CsrA indirectly controls *lcrF* transcript stability via regulation of the major degradosome components

Previously, Park et al. (2015) demonstrated that CsrA is involved in the degradation process of the *pnp* transcript in *E. coli*. Thus, it was intriguing to investigate, whether CsrA might increase the *lcrF* transcript stability by negative regulation of the major degradosome components, RNase E and PNPase. Therefore, the levels of *rne* and *pnp* transcripts in *Y. pseudotuberculosis* wild type strain (YPIII) and Δ*csrA* mutant strain (YP53) grown under secretion conditions were assessed by northern blot analysis. Complementation was tested by introducing a $csrA^+$ plasmid (pKB60) into YP53. Additionally, YPIII and YP53 were transformed with the empty vector pHSG576 (pV) to exclude unspecific plasmid backbone effects. Strains were grown under secretion conditions and total RNA was isolated, followed by Northern blotting with an *rne* or *pnp* specific probe (Fig. 3.16 A, B). In comparison to YPIII, the amount of both *rne* and *pnp* transcripts was significantly elevated in the Δ*csrA* mutant strain (YP53). Moreover, the influence of *csrA* deletion on *rne* and *pnp* mRNA levels was restored to the wild type by expression of *csrA in trans* (Fig. 3.16 A, B). This data support the hypothesis that CsrA-mediated stabilization of the *lcrF* transcript is accomplished via repression of RNase E and PNPase.

In order to further evaluate the effect of CsrA on *rne* and *pnp* expression considering the already documented positive YopD influence, the Δ*yopD* mutant (YP91) as well as the Δ*csrA*Δ*yopD* double mutant (YP145) strains were also included in the analysis. For this purpose, total mRNA was isolated from strains grown under conditions not permissive for Yop secretion. The yield of *rne* and *pnp* mRNAs in these strains was investigated by Northern blot using *rne* and *pnp* specific probes (Fig. 3.16 C, D).

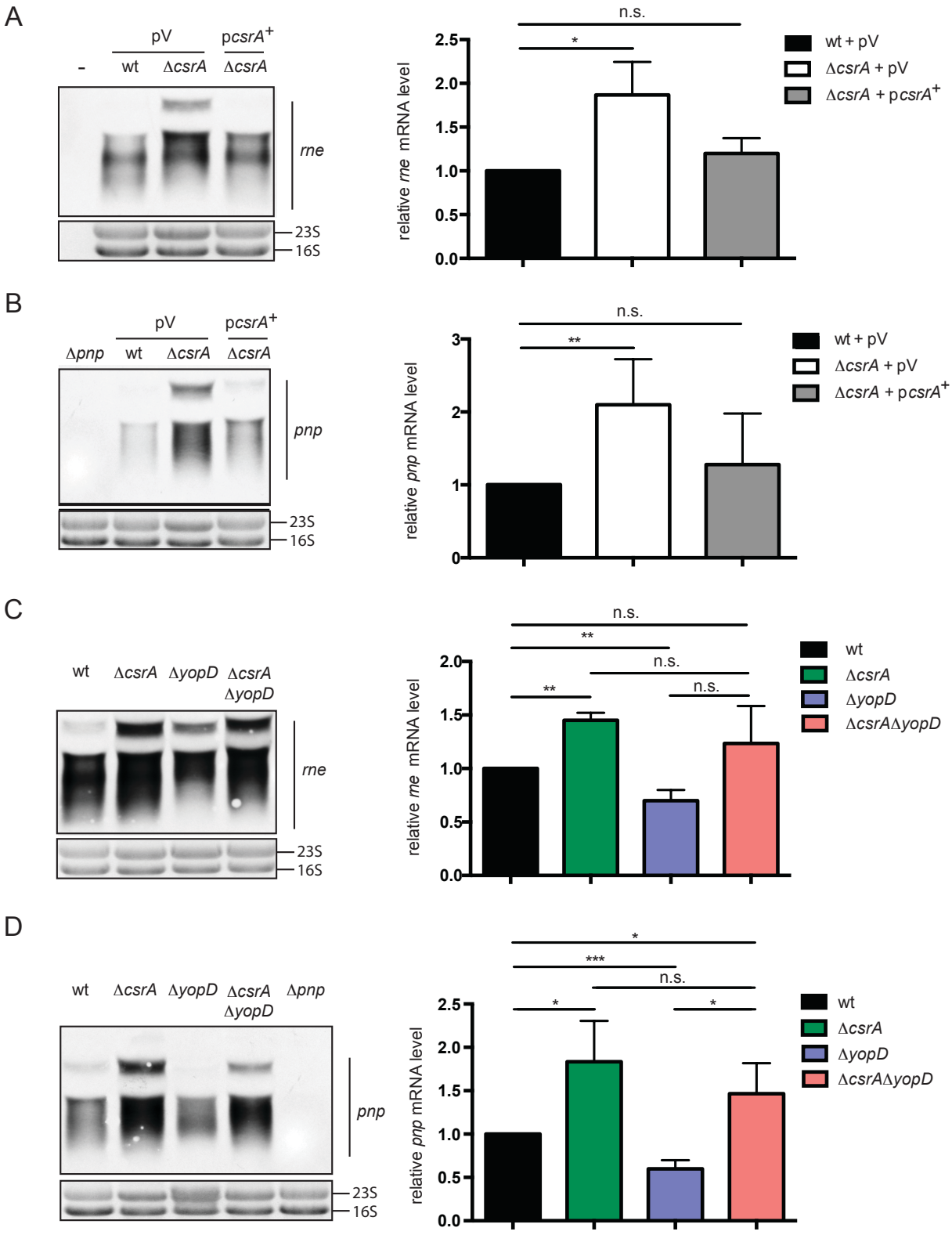

Figure 3.16. CsrA controls the *lcrF* transcript stability via regulation of the major degradosome components.
Strains YPIII and YP53 carrying the empty vector pHSG576 (pV) or the *csrA*$^+$ plasmid (pKB60) were cultured under secretion conditions (**A**,**B**). YPIII, YP53, YP91, and YP145 were grown under non-secretion conditions (**C**,**D**). Thereafter, *rne* and *pnp* transcript levels were analyzed via Northern blot (see 2.2.3.5 – 2.2.3.6). *rne* (**A**,**C**) and *pnp* transcripts (**B**,**D**) are indicated on the right. The *pnp* mutant strain YP138 was used as negative control (**B**,**D**). Quantification of the band intensities was carried out with the image-processing program ImageJ. The intensities of the

loading controls were estimated, and the one of the wild type strain (wt + pV in **A**,**B** and wt in **C**,**D**) was taken as a reference value equal to one. Afterwards, the intensities of the loading controls of the other samples were normalized to this reference value. Next, relative transcript levels were calculated as a normalized mRNA/normalized loading control ratio. The data represent the mean ± standard deviation of three independent experiments. Data were analyzed by the Student's t-test. Asterisks indicate the results that differed significantly from each other with *($P<0.05$), **($P<0.01$), ***($P<0.001$), n.s. ($P>0.05$).

Northern blot analysis revealed significantly higher amounts of *rne* and *pnp* transcripts in the *csrA*-deficient strain (Fig. 3.16 C,D). Consistent with the previous data, the *yopD*-deficient strain synthesized less *rne* and *pnp* mRNAs than the wild type strain (Fig. 3.16 C,D). The loss of both *csrA* and *yopD* in YP145 (Δ*csrA*Δ*yopD*) led to an intermediate amount of *rne* transcript with respect to YP53 and YP91, confirming a contrary mode of action of CsrA and YopD on RNase E synthesis (Fig. 3.16 C right panel). The *pnp* transcript level in the Δ*csrA*Δ*yopD* double mutant strain was comparably high to those of the *csrA*-deficient strain and significantly elevated compared to YP91 (Δ*yopD*) (Fig. 3.16 D right panel). This indicates that the *csrA* deletion is sufficient to enhance PNPase synthesis even in the absence of *yopD*.

To clarify whether CsrA influences the expression of RNase E and PNPase via a direct interaction with their transcripts, the ability of CsrA to bind the 5'-UTRs of *rne* and *pnp* was determined with REMSA (Fig. 3.17). For this purpose, 2 nM of the *in vitro* synthetized and biotinylated "*rne* up" and *pnp* transcripts carrying one (see Fig. 3.5 A) or two GGA motifs (see Fig. 3.6 A), respectively, were incubated with increasing concentration of C-terminally His-tagged CsrA protein for 30 min at 4 °C (Fig. 3.17). Since CsrA requires the presence of at least one GGA motif in the transcript to target it, only the "*rne* up" fragment of the *rne* 5'-UTR was used for analysis (see Fig. 3.5 A).

Neither of the tested transcripts was bound by the CsrA protein (Fig. 3.17). Thus, it is likely that CsrA exerts its inhibitory effect on RNase E and PNPase synthesis indirectly. For PNPase, it is also possible that CsrA requires a prior *pnp* mRNA processing to interact with the GGA motifs located in the 5'-UTR of the *pnp* transcript as reported by Park *et al*., 2015.

In conclusion, these data show that CsrA might enhance the *lcrF* transcript stability via an indirect repression of the degradosome components RNase E and PNPase.

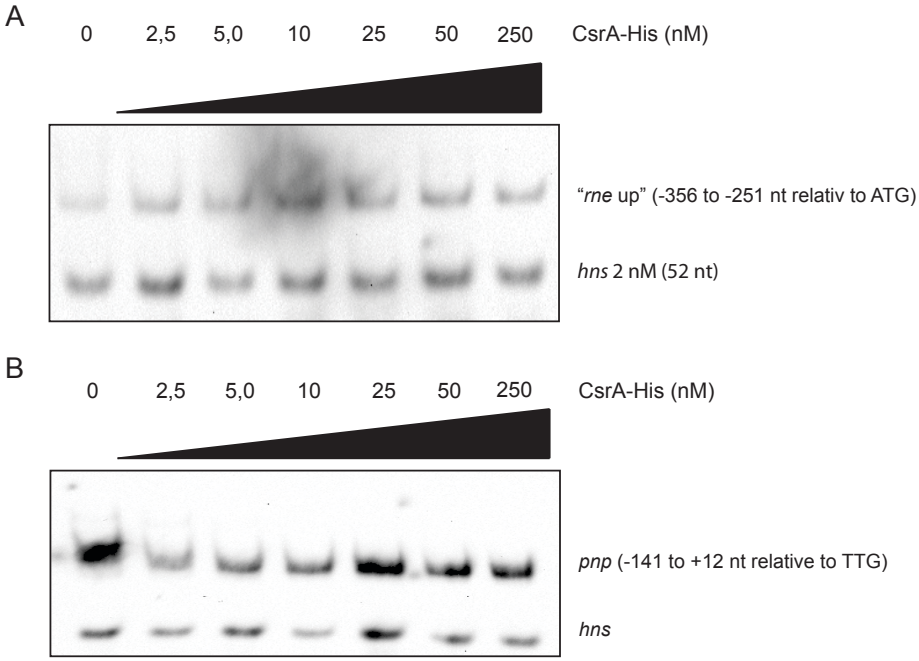

Figure 3.17. CsrA does not interact directly with the 5'-UTRs of *rne* and *pnp* mRNAs.
Binding of CsrA to the *pnp* (**A**) and *rne* (**B**) leader transcripts was analyzed by RNA-EMSAs. Fragments of the *pnp* (see Fig. 3.6 A) and *rne* 5'-UTRs (see Fig. 3.5 A: "*rne up*") as well as the *hns* control fragment were *in vitro* transcribed, followed by labeling with biotin. 2 nM of the resulting *pnp* and *rne* 5'-UTRs as well as the *hns* control fragment were incubated with increasing concentrations of CsrA, separated on a native 7 % TBE-PAA gel, and transferred onto a nitrocellulose membrane. Thereafter, the biotin-labeled RNAs were visualized.

3.2.2 Transcriptome analysis of *Y. pseudotuberculosis* under secretion conditions via RNA-Seq

Depletion of calcium from the growth medium at 37 °C is a well-known signal that induces a so-called low calcium response (LCR) in pathogenic yersiniae. LCR is characterized by restricted growth, enhanced expression and synthesis of the virulence plasmid-encoded genes and massive secretion of Yop effectors (Higuchi *et al*., 1959; Fowler *et al*., 2009). However, the molecular mechanism underlying the development of an LCR in pathogenic yersiniae is still poorly understood. The above results of this work emphasized a crucial effect of the global regulator CsrA and the moonlighting protein YopD in the control of the major virulence activator LcrF under conditions non-permissive ($+Ca^{2+}$) and permissive ($-Ca^{2+}$) for Yop secretion (see 3.1; 3.2.1). In order to explore the impact of the Ca^{2+} depletion signal on gene expression as well as to get deeper insight into the regulatory role of CsrA and YopD in LCR at a global scale, strand-specific RNA sequencing (RNA-Seq) was performed.

3.2.2.1 Immediate alterations in *Y. pseudotuberculosis* transcriptome in response to secretion conditions

First, the immediate gene expression changes in response to the Ca^{2+} depletion signal were analyzed. For this purpose, *Y. pseudotuberculosis* wild type strain YPIII was grown for 2 hours at 25 °C. Thereafter, Ca^{2+} was depleted from the growth medium (secretion conditions) or not (non-secretion conditions) and the cultures were shifted to 37 °C for

further 10 min (Fig. 3.18 A). Based on the results of a qRT-PCR (Fig. S4), 10 min after the shift to 37 °C was assumed to be an optimal time point for visualization of an immediate gene expression response to the Ca^{2+} depletion signal. A similar time point was chosen for investigation of the direct stressor-mediated transcriptomic changes in *Salmonella* Typhimurium (Kröger *et al*., 2013). Finally, the YPIII strains grown under the two different conditions were compared with regard to alterations in gene expression (Fig. 3.18 A). To do so, high quality RNA pools (Fig. S5) obtained from two culture types (YPIII $+Ca^{2+}$ and YPIII $–Ca^{2+}$) were depleted for bacterial ribosomal RNA (rRNA) to increase the informative bacterial transcript coverage. For examination of sequencing accuracy and platform performance, commercially available ERCC (external RNA controls consortia) spike-in control mixes encompassing a 10^6-fold concentration range were employed. Strand-specific cDNA libraries were obtained using the commercial NEBNext® Multiplex Small RNA Library Prep Set for Illumina Kit and sequenced. The strand-specific Illumina-based deep sequencing generated ~2.6 million and ~59,000 uniquely mapped reads for the *Y. pseudotuberculosis* chromosome and virulence plasmid, respectively, (Table S1) offering an appropriate coverage for robust transcriptome profiling. Application of stringent criteria revealed linearity between the read density and RNA input over the entire detection span of around 13 log_2-units of concentration (Fig. S6 A). This is suitable for consistent quantification and comparison of transcript abundance over a wide dynamic range (Haas *et al*., 2012; Ching *et al*., 2014). Additionally, the linear fit demonstrates highly accurate fold change estimates (Fig. S6 B). Moreover, strong correlation between the replicates from the same biological sample group (all $+Ca^{2+}$; all $-Ca^{2+}$) with a Pearson coefficient of $r > 0.958$ was observed (Fig. S7 A). Thus, high quality data were obtained enabling reliable transcript quantification and global expression profile analysis and comparison.

The global gene expression profiles (GGEPs) of the two different conditions were only slightly distinct (Fig. 3.18 B, C). The replicate YPIII $–Ca^{2+}$ I was distant to both sample groups, most likely representing an outlier. However, more replicates are essential to confirm this.

Although most genes were similarly expressed, 12 genes were detected that were significantly downregulated under secretion conditions with log_2-fold change (FC) < -1 (adjusted p-value < 0.05) (Table 3.1) using the differential expression analysis package DESeq 2 (Love *et al*., 2014). Five of them are hypothetical proteins with an unknown function. Remarkably, expression of two genes encoding for tRNAs, tRNA-Met and tRNA-Gln, was decreased in $–Ca^{2+}$ samples compared to $+Ca^{2+}$ samples.

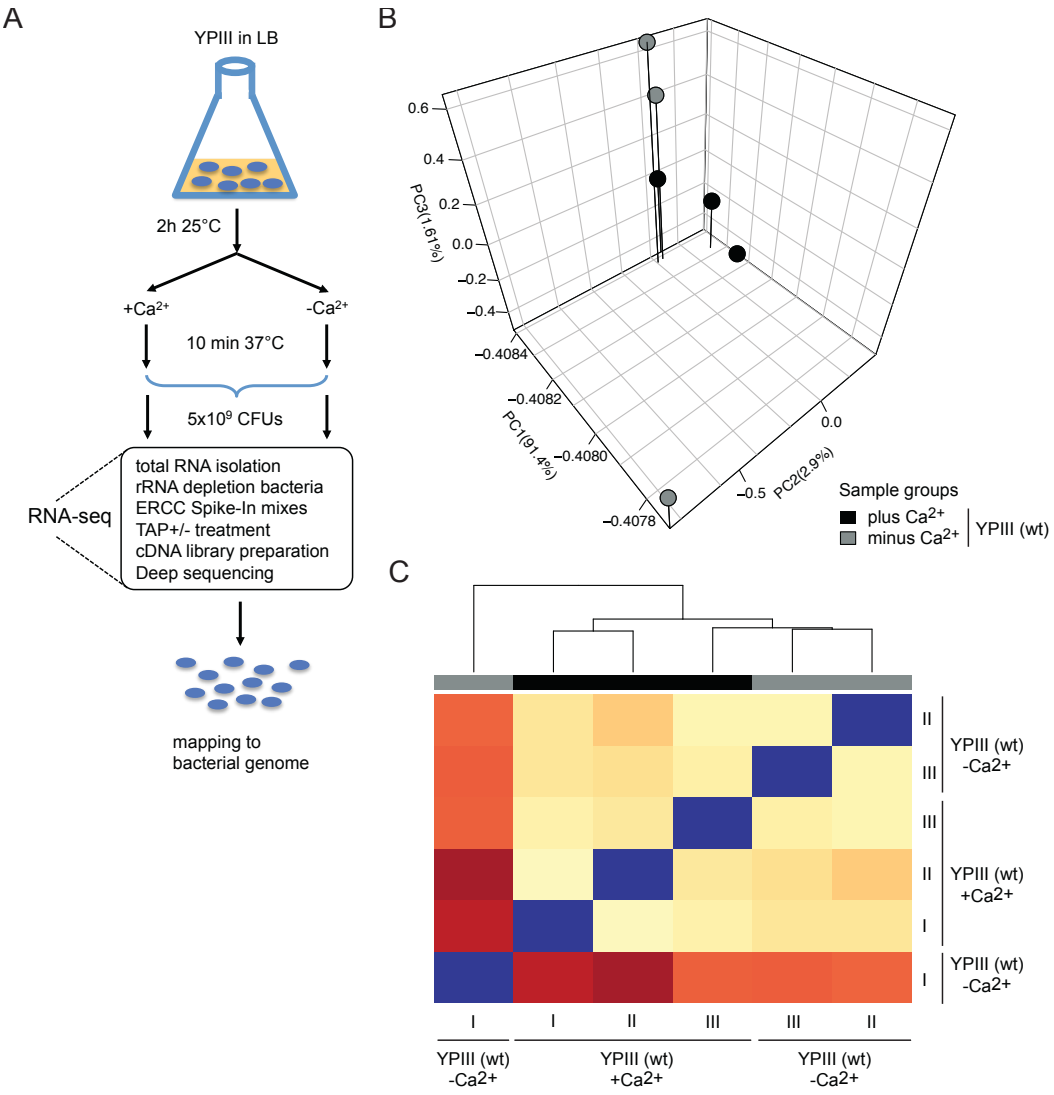

Figure 3.18. The *Y. pseudotuberculosis* global gene expression profile 10 min after Ca^{2+} depletion.
A Workflow for evaluation of the *Y. pseudotuberculosis* transcriptome. The *Y. pseudotuberculosis* wild type strain YPIII was cultivated in LB_{BD} at 25 °C for two hours. Thereafter, depletion of Ca^{2+} was either performed or not and the cultures were shifted to 37 °C for additional 10 min, followed by isolation of total RNA using a water-saturated phenol-based extraction protocol. Next, total RNA was purified from the contaminating DNA and depletion of ribosomal RNA was carried out. After addition of ERCC spike in control mixes, aimed to examine the platform performance, complementary DNA (cDNA) libraries were generated and submitted to strand specific Illumina-based deep sequencing. Thereafter, the obtained reads were demultiplexed and the quality of the sequences was estimated. The adaptor sequences were trimmed from the sequence reads *in silico*. For assessment of the platform-performance control parameters, the remaining reads were mapped to the ERCC spike-in controls. Finally, the reads were mapped to the *Y. pseudotuberculosis* YPIII genome and subjected to differential expression analysis for sequencing data (DESeq2). **B** Three-dimensional principle component analysis of the replicates. **C** Euclidian sample-to-sample distances calculated for the single replicates.

The remaining differentially expressed genes belong to the group of the small non-coding anti-sense (as) and trans RNAs (Table 3.1).

Table 3.1. Classification of genes altered in their expression 10 min after Ca^{2+} depletion.

Locus	Gene Symbol	log2 fold change	DESeq2 normalized counts						adjusted p-value	Description
			YPIII +Ca 1	YPIII +Ca 2	YPIII +Ca 3	YPIII -Ca 1	YPIII -Ca 2	YPIII -Ca 3		
YPK_R0028	tRNA-Met	-1,41							0,001	tRNA Met
Ysr271		-1,28							0,005	Ysr271; Class: asRNA
Ysr187_NU		-1,16							0,008	Ysr187_NU; Class: transRNA
Ysr281		-1,15							0,003	Ysr281; Class: asRNA
Ysr204_NU		-1,15							0,044	Ysr204_NU; Class: transRNA
YPK_2034		-1,14							0,012	hypothetical protein
YPK_3993		-1,12							0,011	hypothetical protein
YPK_3785		-1,09							0,007	hypothetical protein
YPK_2397		-1,04							0,015	hypothetical protein
YPK_R0031	tRNA-Gln	-1,04							0,046	tRNA Gln
YPK_2646		-1,03							0,045	hypothetical protein
Ysr45_KO_Ysr180_BE_sR013_YA	GcvB	-1,03							0,001	Ysr45_KO_Ysr180_BE_sR013_YA; Class: transRNA

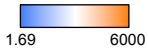

3.2.2.2 Transcriptomic profile of *Y. pseudotuberculosis* under secretion conditions

Next, the gene expression profile of *Y. pseudotuberculosis* under standard secretion/non-secretion conditions was assessed. Of special interest here was to investigate the contribution of CsrA and YopD to the low calcium response. Thus, *Y. pseudotuberculosis* wild type (YPIII), Δ*csrA* (YP53), Δ*yopD* (YP91), and Δ*csrA*Δ*yopD* (YP145) strains were compared with regard to alterations in gene expression. Since YopD was reported to regulate CsrA expression (Steinmann, 2013; Hoßmann, 2017) and CsrA exerts a global influence on the *Yersinia* transcriptome (Heroven *et al*., 2012), a Δ*csrA*Δ*yopD* strain was employed in the analysis to explore pure CsrA and pure YopD effects. The abovementioned *Y. pseudotuberculosis* strains were grown for 2 hours at 25 °C. Thereafter, for each strain depletion of Ca^{2+} was either performed (secretion conditions) or not (non-secretion conditions) and the cultures were shifted to 37 °C for 4 hours. Isolation and processing of total RNA, followed by the strand-specific Illumina-based deep sequencing was performed as described above (see 3.2.2.1).

Of around 6.8 million reads obtained from the cDNA libraries, ~2.4 million and ~630,000 were uniquely mapped to the *Y. pseudotuberculosis* chromosome and virulence plasmid, respectively (Table S2). This provides sufficient coverage for an accurate transcriptome profiling. The dynamic range of the sequencing run was assessed to be around 15 log_2-units concentration and the analysis of the fold change estimates demonstrated high platform accuracy, suitable for consistent quantification and comparison of transcript abundance over a wide dynamic range (Fig. S6 B). Moreover, a strong correlation between the replicates from the same biological sample group with a Pearson coefficient of r >0.9 was observed (Fig. S7 B). Since high quality data were acquired, reliable transcript quantification and global expression profile analysis and comparison were performed.

Comparison of GGEPs of the eight groups revealed the presence of two major clusters: (I) wild type (YPIII) and Δ*yopD* (YP91) strains under both conditions and (II) *csrA*-deficient strains (YP53, YP145) under both conditions (Fig. 3.19 A, middle panel; Fig. 3.19 B).

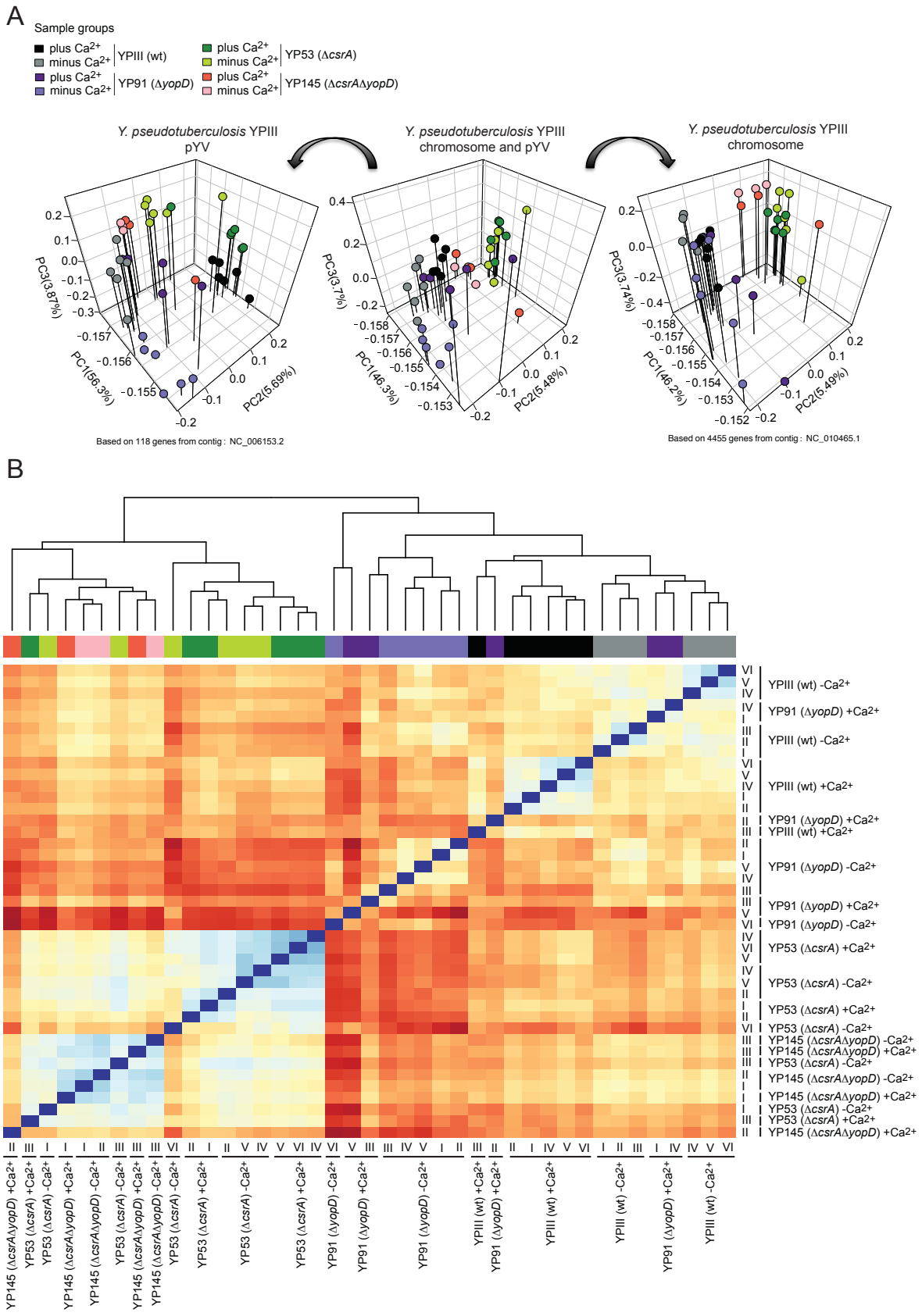

Figure 3.19. The *Y. pseudotuberculosis* global gene expression profile four hours after Ca^{2+} depletion.

Strains YPIII (wild type), YP53 (Δ*csrA*), YP91 (Δ*yopD*), and YP145 (Δ*csrA*Δ*yopD*) were cultivated at 25 °C for two hours. Thereafter, for each strain the type III secretion was either induced or not, followed by further incubation at 37 °C. The total RNA was extracted using a

water-saturated phenol-based isolation protocol. After purification of the total RNA from the contaminating DNA, depletion of ribosomal RNA was conducted. Next, ERCC spike in control mixes, enabling estimation of the platform performance, were added followed by complementary DNA (cDNA) libraries generation. After strand specific Illumina-based deep sequencing of the cDNA libraries, the obtained reads were demultiplexed and the quality of the sequences was estimated. The adaptor sequences were then trimmed from the sequence reads *in silico*. For assessment of the platform-performance control parameters, the remaining reads were mapped to the ERCC spike-in controls. Subsequently, the reads were mapped to the *Y. pseudotuberculosis* YPIII genome and submitted to differential expression analysis for sequencing data (DESeq2). **A** Three-dimensional principle component analysis of the replicates. **B** Euclidian sample-to-sample distances calculated for the single replicates.

This clustering tendency was even more pronounced when expression profiles of only chromosomally-encoded genes were compared (Fig. 3.19 A, right panel), confirming the well-known global impact of CsrA on the *Yersinia* transcriptome (Heroven *et al*., 2012). Moreover, under non-secretion conditions the Δ*csrA* strain did not cluster separately from those under secretion conditions and from the Δ*csrA*Δ*yopD* strain under both conditions (Fig. 3.19 B). Additionally, the Δ*csrA*Δ*yopD* strain expression profile of the virulence plasmid-encoded genes remained almost unchanged under secretion conditions compared to that under non-secretion conditions (Fig. 3.19, left panel). Together, this most probably reflects the hierarchically dominant role of CsrA in LCR induction, which supports other results of this work. It demonstrates the crucial role of CsrA and not YopD for the induction of LcrF synthesis upon Ca^{2+} depletion (see 3.2.1.). CsrA-mediated activation of LcrF synthesis in turn results in an enhanced transcription of the virulence plasmid-associated genes.

Since *yopD* deletion leads to upregulation of *lcrF* expression even under non-secretion conditions, the expression profiles based on virulence plasmid-encoded genes of YP91 $+Ca^{2+}$ as well as of YP91 $-Ca^{2+}$ sample groups were close to those of the YPIII $-Ca^{2+}$ group (Fig. 3.19 A, left panel).

Together, these results indicate, that the majority of genes altered in their expression in an LCR-dependent manner is located on the virulence plasmid. Furthermore, in consistency with the previous results of this work (see 3.2.1), CsrA is indispensible for the LCR-mediated reprogramming of the *Y. pseudotuberculosis* transcriptome.

Aimed to gain further insight into the LCR-triggered alterations in *Y. pseudotuberculosis* gene expression and to assess the role of CsrA and YopD in LCR, the differential expression analysis package DESeq2 was employed (Love *et al*., 2014).

First, the genomic distribution of the uniquely mapped reads between the chromosome and the virulence plasmid (pYV) was estimated for each strain under the respective condition (Fig. 3.20).

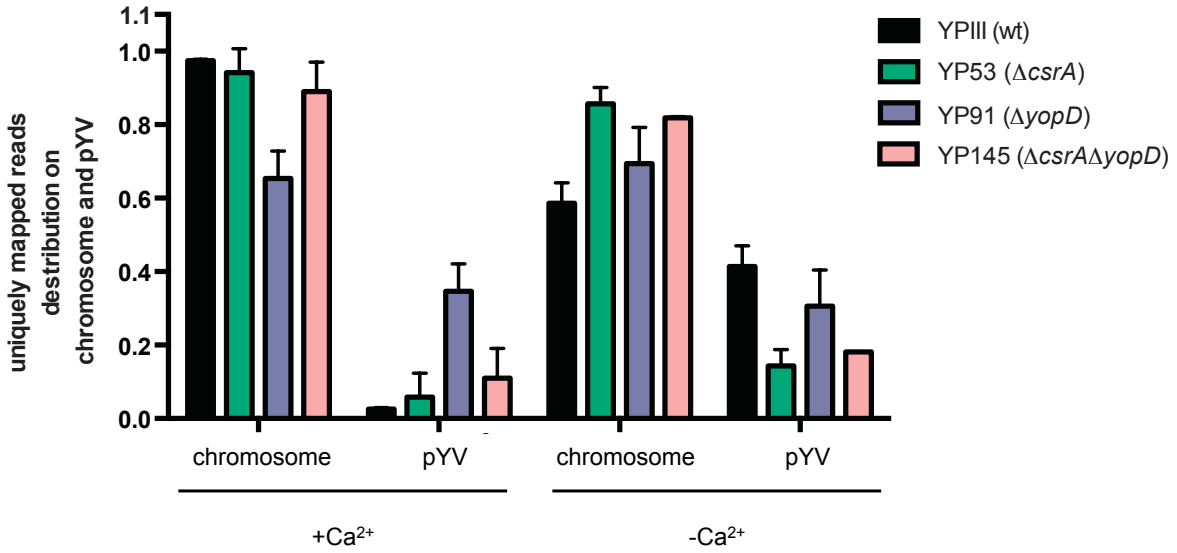

Figure 3.20. Distribution of the uniquely mapped reads.
The relative number of uniquely mapped reads on the chromosome and the virulence plasmid was quantified for each strain under each condition.

As expected, in the wild type strain grown under non-secretion conditions (YPIII $+Ca^{2+}$) almost 100 % of the uniquely mapped reads belong to the chromosomally-encoded genes (Fig. 3.20). A similar uniquely mapped reads distribution was observed for *csrA*- and *csrAyopD*- deficient strains cultivated in presence of Ca^{2+} (YP53 $+Ca^{2+}$ and YP145 $+Ca^{2+}$). In the wild type, the relative number of reads uniquely mapped to the virulence plasmid increased dramatically upon depletion of Ca^{2+} (YPIII $–Ca^{2+}$). Contrary, the chromosome/pYV uniquely mapped reads equilibrium in both Δ*csrA* strains under secretion conditions remained unchanged (Fig. 3.20). This data further confirms the fundamental role of CsrA in LCR-mediated transcriptomic rearrangements. As expected, the distribution of uniquely mapped reads in the Δ*yopD* strain grown under conditions not permissive for Yop secretion (YP91 $+Ca^{2+}$) reflects those of the YPIII $–Ca^{2+}$ and is not affected by LCR (YP91 $–Ca^{2+}$).

Together, these results indicate that the deletion of *csrA* or *yopD* results in two different "Ca^{2+}-blind" phenotypes. Strains deficient for *csrA* lose the ability to reprogram their transcriptomic profile in response to a low calcium signal towards an enhanced expression of virulence plasmid-encoded genes, whereas activation of the pYV-encoded genes in the *yopD*-deficient strain already occurs in the presence of Ca^{2+}.

In order to visualize the changes in the GGEPs with respect to their genomic localization (chromosome or pYV) as well as the type of alterations (induction/repression) dependent on Ca^{2+}-, and/or CsrA-, and/or YopD- presence, a quantitative analysis of the differentially expressed genes was performed in fourteen relevant strain/condition combinations indicated in Fig. 3.21 (absolute numbers).

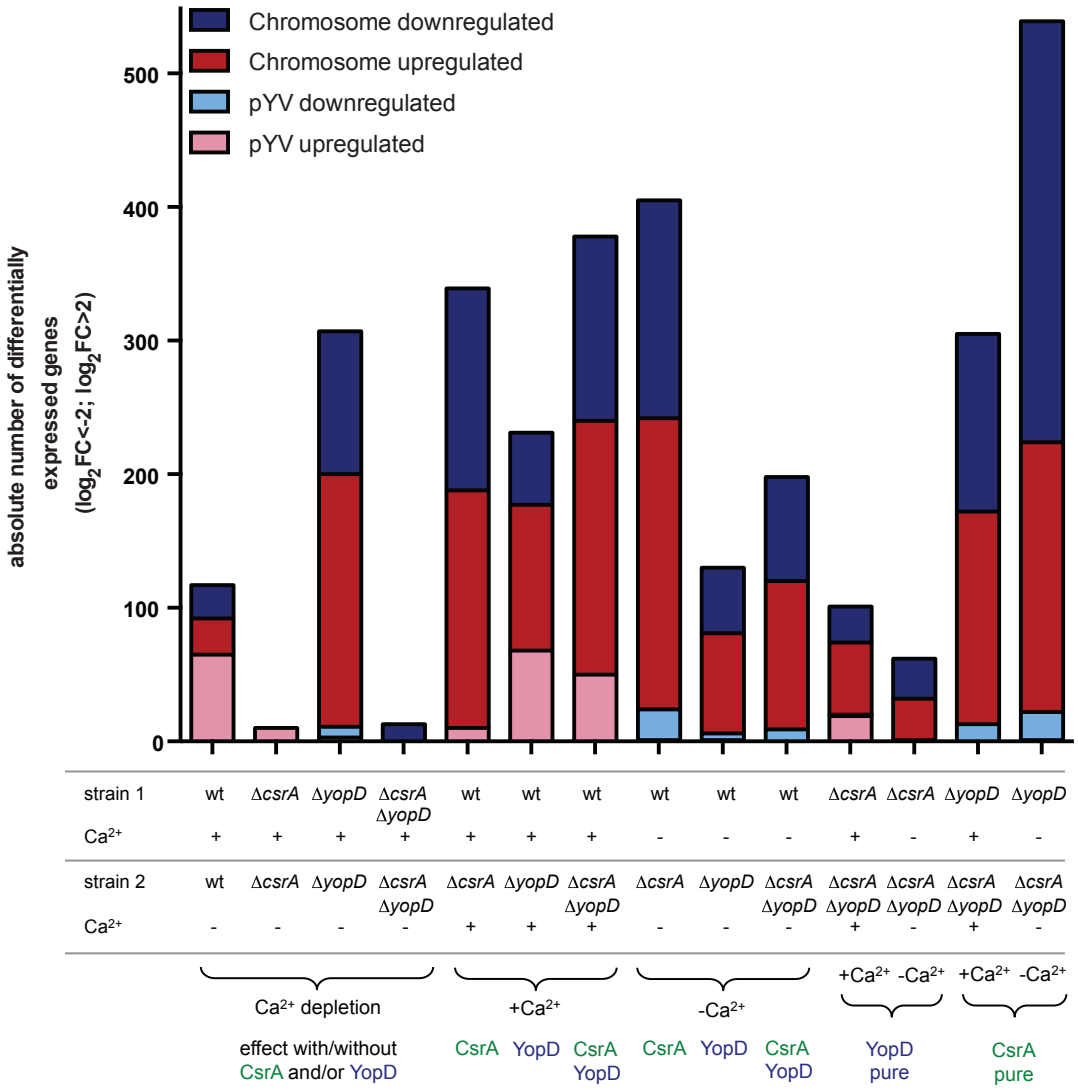

Figure 3.21. Quantitative analysis of genes differentially expressed in LCR- and/or CsrA- and/or YopD-dependent manner.
Bar plot of the differentially expressed genes with cut off: log_2 FC < -2, log_2 FC > 2 and adjusted p-value < 0.05. Each bar represents comparison of two strains (strain 1 *vs*. strain 2, each cultured either with (+) or without (-) Ca^{2+}) indicated in the table below the graph.

For evaluation of the data, genes with log_2FC < -2 were defined as significantly downregulated and with log_2FC > 2 as significantly activated (adjusted p-value < 0.05). The first four columns from the left represent the LCR-mediated alterations in the GGEPs of the *Y. pseudotuberculosis* wild type, Δ*csrA*, Δ*yopD* and Δ*csrA*Δ*yopD* strains. The following six columns show the effect of CsrA, YopD or of both regulatory proteins on the GGEPs under conditions either non-permissive or permissive for Yop secretion. The influence of YopD in the *csrA*-deficient background as well as of CsrA in the *yopD*-deficient background under non-secretion and secretion conditions is demonstrated in the last four columns (Fig. 3.21).

As shown in the Fig. 3.21, more than 50 % of the genes differentially expressed in the wild type strain upon depletion of Ca^{2+} are virulence plasmid-encoded (first column from the left). All of those genes were induced compared to non-secretion conditions. Interestingly, around 50 % of the chromosomally-encoded genes were downregulated under secretion-

permissive conditions. This is consistent with the mapping statistics data, demonstrating a decreased number of the reads uniquely-mapped to the chromosome under Ca^{2+} depletion conditions (Fig. 3.20). Almost no transcriptomic alterations were observed when comparing the Δ*csrA* strains (YP53 and YP145) under non-secretion and secretion conditions, confirming the indispensible role of CsrA in LCR-mediated gene expression profile reprogramming (Fig. 3.21 second and fourth column from the left).

In contrast to the wild type, approx. 98 % of all genes differentially expressed in Δ*yopD* strain in response to the depletion of Ca^{2+} were encoded on the chromosome. Of those genes, around 70% were upregulated (Fig. 3.21 third column from the left). Thus, although no obvious LCR-mediated changes in the uniquely-mapped reads distribution were shown in the *yopD*-deficient strain (Fig. 3.20), the expression of the chromosomally-encoded genes is massively affected. In agreement with previous results showing that LCR-mediated elevated expression of the pYV-encoded genes occurs in the absence of YopD already under non-secretion conditions (Fig. 3.19 A; Fig. 3.20), it is reasonable that almost no virulence plasmid-encoded genes were differentially expressed in the Δ*yopD* background in response to the low Ca^{2+} signal (Fig. 3.21 third column from the left).

Since YopD was shown to positively affect CsrA synthesis (Hoßmann, 2017; Steinmann, 2013), it was important to evaluate the CsrA-independent effect of YopD under both non-secretion (Δ*csrA* $+Ca^{2+}$ vs. Δ*csrA*Δ*yopD* $+Ca^{2+}$; Fig. 3.21 fourth column from the right) and secretion conditions (Δ*csrA* $-Ca^{2+}$ vs. Δ*csrA*Δ*yopD* $-Ca^{2+}$; Fig. 3.21 third column from the right). Consistent with the previous data from our lab showing the CsrA-independent global influence of YopD on *Y. pseudotuberculosis* transcriptome (Steinmann, 2013), some significant YopD-mediated and CsrA-independent alterations in the GGEPs under conditions non-permissive and permissive for Yop secretion were detected (Fig. 3.21 fourth and third column from the right, respectively). In fact, the virulence plasmid-encoded genes were upregulated in *yopD*-deficient strain under conditions non-permissive for Yop secretion, independent from the presence of CsrA. However, the absolute number of the differentially expressed YopD-dependent genes was lower when *csrA* was missing (Fig. 3.21; with CsrA: sixth column from the left, without CsrA: fourth column from the right). Under secretion conditions, only chromosomally-encoded genes were altered in their expression by YopD in a CsrA-independent manner (Fig. 3.21; third bar from the right). In the $csrA^{+}$ background, in turn, some virulence plasmid-encoded genes were also affected (downregulated) by YopD (Fig. 3.21; sixth column from the right). Similarly to $+Ca^{2+}$ conditions, the absolute number of the chromosomally-encoded genes influenced by YopD upon Ca^{2+} depletion was higher in the presence of CsrA. Together, these results indicate the regulatory connection between YopD and CsrA, whereby YopD might control expression of the targeted genes via CsrA.

Next, the global effect of CsrA on gene expression reprogramming in presence and absence of Ca^{2+} was assessed (Fig. 3.21; $+Ca^{2+}$: fifth column from the left, $-Ca^{2+}$: seventh column from the right). Under non-secretion conditions, only 3% of the genes altered in their expression in a CsrA-dependent manner were virulence plasmid-encoded (Fig. 3.21 fifth column from the left). Remarkably, all of them were activated in the *csrA*-deficient

strain compared to the wild type. This might reflect the negative effect of CsrA on the transcription of the major virulence activator LcrF under conditions non-permissive for Yop secretion described in the present work (see 3.1.2). Interestingly, the inhibitory effect of CsrA on expression of the virulence plasmid-encoded genes in presence of Ca^{2+} was less pronounced than that of YopD, where approximately 30 % of the differentially expressed genes were activated virulence plasmid-encoded genes compared to the wild type (Fig. 3.21 fifth and sixth bars from the left, respectively). This observation is consistent with the proposed hierarchy regarding the influence of both regulatory proteins on LcrF synthesis, in which YopD acts upstream of CsrA. In the absence of CsrA and YopD, the entire virulence plasmid-encoded genes altered in their expression (~13% of total) were also activated (Fig. 3.21 seventh bar from the left). In contrast to the non-secretion conditions, all virulence plasmid-encoded genes (~7% of total) were downregulated in response to the low Ca^{2+} signal when CsrA was missing (Fig. 3.21 seventh and fifth bars from the right), confirming the positive influence of CsrA on LcrF synthesis demonstrated in the current study (see 3.2.1).

Regarding the positive effect of YopD on CsrA synthesis, it was reasonable to assess the YopD-independent influence of CsrA on GGEP alterations under both non-secretion and secretion conditions (Fig. 3.21 second and first bar from the right, respectively). Interestingly, no apparent difference in GGEP rearrangements between Δ*yopD* +Ca^{2+} vs. Δ*csrA*Δ*yopD* +Ca^{2+} (second bar from the right) and Δ*yopD* -Ca^{2+} vs. Δ*csrA*Δ*yopD* -Ca^{2+} (first bar from the right) was detected. In particular, similar to the CsrA-dependent GGEP changes in the *yopD*$^{+}$ background under secretion conditions (Fig. 3.21 seventh bar from the right), absence of CsrA in Δ*yopD* background led to downregulation of the pYV-encoded genes independently of the low Ca^{2+} signal. Consistent with previous data, this observation further highlights that deletion of *yopD* results in the Ca^{2+} blind phenotype of *Y. pseudotuberculosis* with respect to the LCR-independent manner of pYV-encoded gene activation.

The following investigation concentrated on genes that were differentially expressed in the *Y. pseudotuberculosis* wild type strain in response to the low Ca^{2+} signal in order to gain a global overview of the LCR-mediated transcriptional rearrangements.

First, it was essential to classify the LCR-dependent genes with respect to their functional categories according to the KEGG database. For this purpose, genes significantly altered in their expression ($\log_2FC < -2$, $\log_2FC > 2$, adjusted p-value < 0.05) in the wild type strain grown under secretion conditions compared to non-secretion conditions (YPIII +Ca^{2+} *vs.* YPIII -Ca^{2+}) were analyzed (Fig. 3.22).

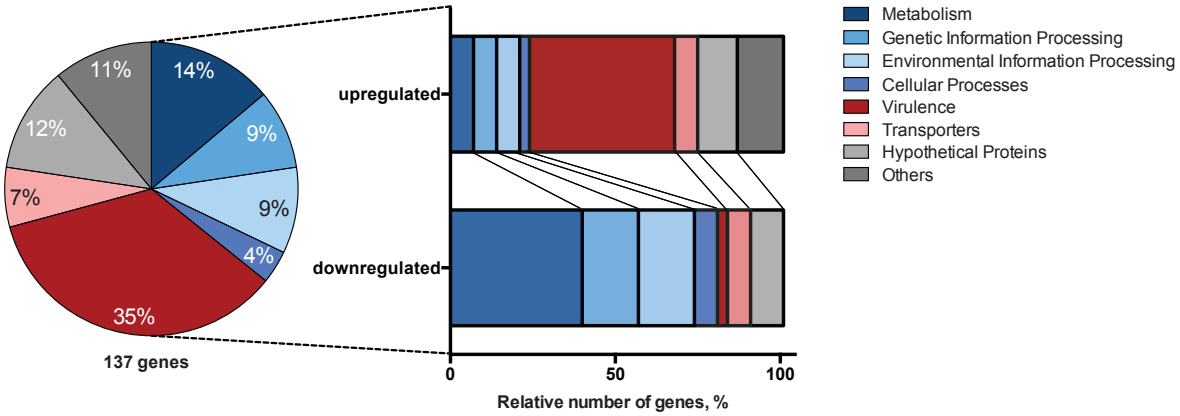

Figure 3.22. Global influence of the low calcium signal on the gene expression profile of *Y. pseudotuberculosis*.
Differentially expressed genes between the wild type strain $+Ca^{2+}$ and the wild type strain $–Ca^{2+}$. Genes with overall $log_2FC > 2$ were clustered into different categories according to the KEGG database. The pie-chart diagram represents the percentages of differentially expressed gene clusters (left panel). The stacked bar diagram demonstrates up-/downregulated gene clusters (right panel). Gene categories are indicated on the right.

As shown in Fig. 3.22, in total 137 genes were altered in their expression by calcium limitation (see Table S3). KEGG Orthology based classification revealed that the Ca^{2+} depletion-dependent genes belong to all functional categories. Remarkably, the group of the virulence genes was shown to be prevalent, covering 35 % of the entire differentially expressed gene pool (Fig. 3.22 left panel). Consistent with previous data of this work (Fig. 3.21 first column from the left), all virulence genes encoded on the pYV were upregulated in response to the low Ca^{2+} signal (Fig. 3.22 right panel, Table S3). Additionally, five chromosomally-encoded genes belonging to the virulence group ("Human diseases" in KEGG classification) were differentially expressed upon Ca^{2+} limitation (Table S3). Of those genes, three were upregulated under secretion conditions (*pla2*, *ompF* and *fliC*) and two downregulated (*psaA* and *degP*). In general, the LCR-mediated increase in gene expression mainly occurred for genes contributing to bacterial virulence (44 %), whereas the majority of genes belonging to other categories such as metabolism, genetic and environmental processing, as well as cellular processes were downregulated upon Ca^{2+} depletion (Fig. 3.22 right panel). Decreased expression levels of these genes could explain a growth arrest seen for *Yersinia* under secretion conditions, which is an obvious LCR consequence.

Lastly, the involvement of CsrA and YopD in the regulation of LCR-dependent genes in the *Y. pseudotuberculosis* wild type strain was explored. To do so, alterations in the expression of 137 Ca^{2+}-dependent genes in the fourteen strain/condition combinations as described above (Fig. 3.21) were compared using DESeq2 analysis (Fig. 3.23). The 137 genes were divided into two groups with respect to their genomic localization (chromosome/virulence plasmid) and sorted according to their log_2FC in the DESeq2 analysis of YPIII $+Ca^{2+}$ *vs*. YPIII $-Ca^{2+}$ (Fig. 3.23).

Based on the similarities in the alterations of the LCR-dependent virulence plasmid-encoded gene expression levels revealed from the direct comparison, the fourteen gene expression profiles were divided into two major clusters: group I and group II (Fig. 3.23).

Additionally, two small groups (III and IV) with similar pYV-encoded gene expression pattern changes were detected (Fig. 3.23).

All members of the group I resemble the respective LCR-mediated alterations in the wild type strain. In particular, deletion of *yopD* or both *yopD* and *csrA* leads to dramatic activation of the indicated pYV-encoded genes under conditions non-permissive for Yop secretion compared to the wild type strain (Fig. 3.23; YPIII $+Ca^{2+}$ *vs*. YP91 $+Ca^{2+}$ and YPIII $+Ca^{2+}$ *vs*. YP145 $+Ca^{2+}$, respectively).

However, deletion of *yopD* in the Δ*csrA* background resulted in less prominent activation of the LCR-controlled pYV-encoded genes under $+Ca^{2+}$ conditions (Fig. 3.23; YP53 $+Ca^{2+}$ *vs*. YP145 $+Ca^{2+}$). Most likely, this occurs due to the upregulation of the major virulence activator LcrF in the absence of *csrA* leading to an increased expression of the pYV-encoded genes (Fig. 3.23; YPIII $+Ca^{2+}$ *vs*. YP53 $+Ca^{2+}$). Likewise, the LCR-mediated changes in the expression pattern of the pYV-encoded genes in the Δ*csrA* background were comparable to those caused by *yopD* deletion in Δ*csrA* background under non-secretion conditions (Fig. 3.23; YP53 $+Ca^{2+}$ *vs*. YP53 $-Ca^{2+}$ and YP53 $+Ca^{2+}$ *vs*. YP145 $+Ca^{2+}$, respectively). Consistent with the results of this work (see 3.1), these data indicate that under conditions non-permissive for Yop secretion, both CsrA and YopD prevent the unnecessary synthesis of the pYV-encoded virulence determinants by repression of LcrF.

In contrast to group I, expression of the LCR-dependent pYV-encoded genes was generally downregulated in group II. Interestingly, a common feature of the four DESeq2-based profiles constituting group II is the comparison of the wild type strain to the Δ*csrA* strain under secretion conditions (Fig. 3.23; YPIII $-Ca^{2+} \approx$ YP91 $+Ca^{2+} \approx$ YP91 $-Ca^{2+}$ *vs*. YP53 $-Ca^{2+} \approx$ YP145 $-Ca^{2+}$). Thus, the observed alterations most likely reflect an essential role of CsrA in LCR-mediated activation of those genes through LcrF, convincingly supporting the discoveries of the present work (see 3.2.1).

The minor group III comprises two gene expression profiles where the wild type under secretion conditions and the *yopD*-deficient strain under non-secretion conditions were compared to the Δ*yopD* strain upon Ca^{2+} limitation (Fig. 3.23; YPIII $-Ca^{2+}$ *vs*. YP91 $-Ca^{2+}$ and YP91 $+Ca^{2+}$ *vs*. YP91 $-Ca^{2+}$). In this way, the effect of YopD on the LCR-dependent transcriptomic changes was determined. Unexpectedly, downregulation of genes encoding for T3SS components such as *yscF*, *yscC*, *yscD*, *yscG*, *yscE*, *yscL*, *yscH* and *yscI* were detected (Fig. 3.23). This result indicates that, although YopD represents a negative regulator of the pYV-encoded genes via repression of the virulence activator LcrF, it seems to be essential for the synthesis of the T3SS components.

The last group IV represents the expression patterns in which the pYV-genes were not affected (Fig. 3.23; YP53 $-Ca^{2+}$ *vs*. YP145 $-Ca^{2+}$ and YP145 $+Ca^{2+}$ *vs*. YP145 $-Ca^{2+}$). This additionally supports the abovementioned "Ca^{2+} blind" phenotype of the Δ*csrA* strains (see Fig. 3.20, Fig. 3.21).

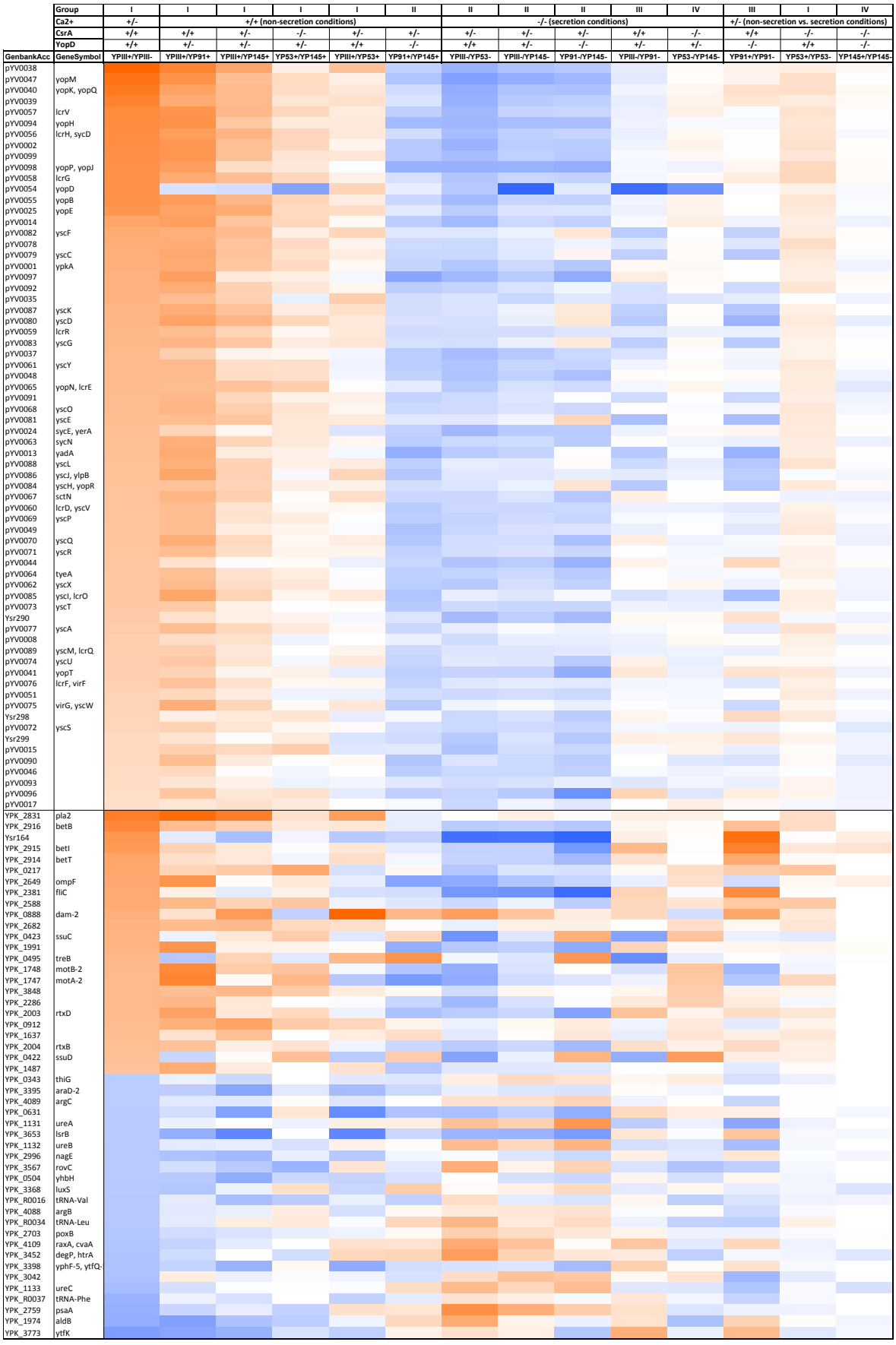

Figure 3.23. The *Y. pseudotuberculosis* transcriptional response to the low calcium signal.

Heat map of the 137 LCR-dependent genes ($log_2FC > 2$; adjusted p-value < 0.05). The respective log_2FC of each gene compared to the indicated strains grown either with or without Ca^{2+} (non-secretion or secretion conditions, respectively).

No obvious clustering was observed for the LCR-dependent chromosomally-encoded genes (Fig. 3.23 lower panel). Nevertheless, the gene encoding for the porin OmpF was identified as a promising candidate for the LCR signal sensing and/or transmission. Firstly, the *ompF* gene was activated in response to Ca^{2+} depletion. Moreover, under $+Ca^{2+}$ conditions its expression was repressed by YopD. Additionally, CsrA enhanced OmpF synthesis under Ca^{2+} depletion conditions. Together, these data propose that the porin OmpF might be the missing link in the YopD- and CsrA-controlled regulatory pathway aimed to activate the expression of the pYV-encoded genes in response to the low calcium signal.

Additionally, expression of the small ncRNA Ysr164, which has previously been described to be CRP-dependent (Nuss *et al*., 2015), was strongly upregulated in response to the low calcium signal. However, this effect seems to be CRP-independent since no LCR-mediated differences in *crp* expression were detected (data not shown). Interestingly, the LCR-mediated upregulation of Ysr164 expression was even more pronounced in the absence of YopD. CsrA, in turn, activates the Ysr164 expression under secretion conditions (Fig. 3.23).

In conclusion, the RNA-seq data gave a global overview of LCR-mediated alterations in the *Y. pseudotuberculosis* transcriptome and confirmed the crucial regulatory role of CsrA and YopD in the LCR-dependent activation of the pYV-encoded genes.

3.2.2.3 Investigation of the CsrA interactome under secretion conditions using CLIP-Seq

The results of this work highlighted the indispensible role of the global regulator CsrA for activation of the pYV-encoded virulence factors in response to the low calcium signal. In order to investigate the target landscape of CsrA upon Ca^{2+} depletion conditions, an approach merging *in vivo* UV-crosslinking with RNA deep sequencing (CLIP-seq) was employed (Fig. 3.24). For this purpose, the *csrA*-deficient strain YP53 carrying the 3xFLAG-tagged CsrA expression vector (pJH35) was grown under conditions permissive for Yop secretion. One half of this culture was irradiated with UV light (+XL) whereas the other half remained untreated (-XL) and served as a negative control. After cell lysis, the CsrA-RNA complexes were immunoprecipitated on beads with a monoclonal anti-FLAG antibody followed by multiple stringent washes. During the next steps, the complexes were treated with RNase, dephosphorylated, and the RNA 5' ends were radioactive labeled. Thereafter, the CsrA-RNA complexes were eluted, separated by denaturating SDS-PAGE and transferred to a membrane. Finally, the complexes from both crosslinked and control samples were isolated from the membrane and treated with proteinase to obtain the RNA fragments saved from digestion by CsrA binding for Illumina-based deep sequencing.

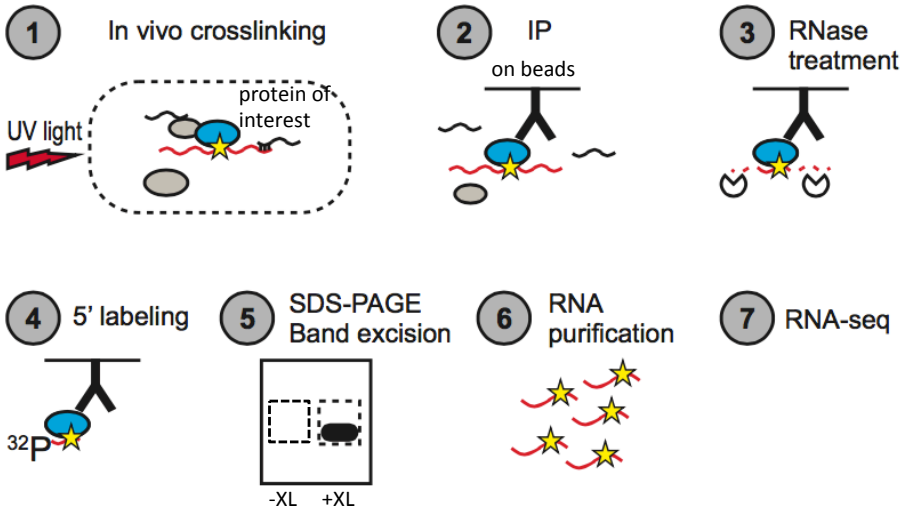

Figure 3.24. Workflow of the CLIP-seq protocol.
UV: ultraviolet; -XL: not crosslinked sample; +XL: crosslinked sample. This figure is adapted from Holmqvist *et al*., 2016[13].

Using the sophisticated peak calling algorithm (Holmqvist *et al*., 2016) for evaluation of the CLIP-seq data, 107 significant (adjusted p-value < 0.1) CsrA peaks were identified (Table 3.2). The number of detected CsrA peaks in *Y. pseudotuberculosis* was approx. four times less than in *Salmonella* (Holmqvist *et al*., 2016). However, this might be explained by specific growth conditions applied for this particular experiment (Ca^{2+} depletion conditions). According to the RNA-seq results of the present work, the low calcium signal leads to reprogramming of the *Y. pseudotuberculosis* transcriptome towards increased expression of the pYV-encoded genes (see 3.2.2.2). Thus, the expression of numerous chromosomally-encoded genes is downregulated under conditions permissive for Yop secretion compared to the standard growth conditions, decreasing the amount of potential CsrA targets. Indeed, 67 % of the CsrA peaks detected in this study mapped to the virulence plasmid of *Y. pseudotuberculosis* (Table 3.2). Remarkably, almost all of the CsrA peaks located on the virulence plasmid correlated with CsrA-mediated regulation according to the transcriptomic analysis performed in the present work (Table 3.2 first column from the right, $\log_2 FC > 1$, adjusted p-value < 0.05). The main part of those peaks was associated with genes encoding for the T3SS components. Surprisingly, a direct interaction between CsrA and the *yopD* transcript was detected. Together, these data indicate that CsrA might influence expression of the pYV-encoded genes not only indirectly via LcrF, but also through direct binding. It would be of great interest to explore the role of CsrA-mediated direct regulation on YopD synthesis.

In conclusion, implication of the CLIP-seq approach allowed investigation of the CsrA interactome under secretion conditions. CsrA targets located on the virulence plasmid were confirmed to be CsrA-dependent by transcriptomic analysis. However, the experimental set-up should be optimized in order to identify further functional CsrA sites on the *Y. pseudotuberculosis* chromosome.

[13] Holmqvist *et al*., 2016 is licensed under the terms of the Creative Commons Attribution-NonCommercial-NoDerivs 4.0.

Table 3.2. Classification of pYV-encoded CsrA-targets under Ca^{2+} depletion conditions.

peak id	peak strand	feature type	feature locus tag	feature name	alignments final unique hits										base Mean	log2FoldChange	adjusted p-value	feature product	log2FoldChange in RNA-seq YPIII minus vs YP53 minus	
					1 +XL	2 +XL	3 +XL	4 +XL	5 +XL	1 -XL	2 -XL	3 -XL	4 -XL	5 -XL						
1	-	gene	pYV0001	ypkA											11,2	5,6	7,62E-05	ypkA; targeted effector protein kinase	-2,20	
4	-	gene													116,9	2,8	5,17E-05		-2,20	
8	-	gene													22,0	6,7	6,06E-06		-2,20	
9	-	gene													87,1	6,5	1,69E-08		-2,20	
10	-	gene													33,8	3,0	2,83E-04		-2,20	
11	-	gene													4,5	5,2	2,59E-02		-2,20	
13	-	gene	pYV0002	pYV0002											13,6	5,4	1,40E-04	hypothetical protein	-3,17	
14	-	gene													107,5	7,1	1,06E-13		-3,17	
15	-	gene													12,0	4,8	3,74E-03		-3,17	
16	+	gene	pYV0008	pYV0008											11,3	4,8	1,39E-03	transposase remnant	-1,18	
19	+	gene	pYV0025	yopE											13,4	2,5	3,16E-02	outer membrane virulence protein	-1,93	
20	+	gene													41,0	5,4	4,34E-07		-1,93	
21	+	gene													47,2	5,9	1,87E-05		-1,93	
22	+	gene													25,2	5,8	1,69E-08		-1,93	
24	-	gene	pYV0032	sopA											15,4	5,0	3,14E-05	plasmid-partitioning protein SopA	-1,14	
25	-	gene													18,2	2,6	3,83E-02		-1,14	
26	-	gene	pYV0037	pYV0037											706,5	2,1	2,01E-02	NA	-2,66	
29	-	intergenic	NA	NA											13,5	4,9	1,53E-02	pYV0038(pseudogene) - pYV0039(transposase)	-3,18	-3,25 *
30	-	gene	pYV0040	yopK/ yopQ											45,6	4,6	1,12E-04	yop targeting protein yopK, yopQ	-3,44	
32	-	intergenic	NA	NA											15,2	4,1	1,36E-04	pYV0040(yopK:yopQ) - pYV0041(yopT)	-3,44	-1,53 *
34	-	gene	pYV0047	yopM											8,0	3,8	1,43E-02	yopM; targeted effector protein	-4,12	
35	-	gene	pYV0054	yopD											20,6	5,6	3,95E-05	yopD; Yop negative regulation/targeting component	-2,10	
36	-	gene													124,9	5,2	1,35E-08		-2,10	
37	-	gene													20,4	5,1	1,37E-04		-2,10	
38	-	gene													56,6	6,0	1,94E-08		-2,10	
40	-	gene	pYV0055	yopB											32,7	5,0	3,13E-07	yopB; Yop targeting protein	-2,76	
40	-	gene	pYV0056	lcrH/ sycD											32,7	5,0	3,13E-07	lcrH, sycD; low calcium response protein H	-2,69	
41	-	gene													7,4	5,4	2,52E-02		-2,69	
42	-	gene													15,4	4,9	3,82E-03		-2,69	
44	-	gene	pYV0057	lcrV											17,6	6,4	7,45E-05	lcrV; V antigen, antihost protein/regulator	-2,92	
46	-	gene	pYV0060	lcrD/ yscV											5,8	5,7	5,06E-03	lcrD, yscV; membrane-bound Yop protein	-1,32	
47	-	gene	pYV0064	tyeA											12,3	4,5	5,44E-04	tyeA; Yop secretion and targeting protein	-1,55	
47	-	gene	pYV0065	yopN/ lcrE											12,3	4,5	5,44E-04	yopN, lcrE; membrane-bound Yop targeting protein	-1,99	
48	-	gene													13,9	4,6	2,62E-03		-1,99	
49	-	gene													12,2	4,0	1,24E-03		-1,99	
50	-	gene													8,0	4,5	3,67E-02		-1,99	
52	+	gene	pYV0067	sctN											15,7	3,4	5,06E-03	type III secretion system ATPase	-1,36	
53	+	gene													11,7	5,7	2,44E-03		-1,36	
55	+	gene													27,0	4,7	5,44E-04		-1,36	
56	+	gene													262,5	4,9	5,07E-10		-1,36	
57	+	gene													82,9	1,3	9,00E-02		-1,36	
58	+	gene													17,6	6,1	3,79E-04		-1,36	
59	+	gene	pYV0068	yscO											20,3	4,7	4,23E-03	yscO; type III secretion protein	-1,17	
65	+	gene	pYV0074	yscU											106,2	3,9	1,62E-06	yscU; type III secretion protein	-0,46	
66	+	intergenic	NA	NA											12,0	2,7	4,92E-02	pYV0077(yscA) - pYV0078(hypothetical protein)	-0,29	-1,28 *
67	+	gene	pYV0078	pYV0078											11,8	5,8	2,28E-04	hypothetical protein	-1,28	
70	+	gene	pYV0079	yscC											51,9	2,8	1,21E-02	yscC; type III secretion protein	-1,39	
71	+	gene													10,3	3,1	9,99E-02		-1,39	
72	+	gene													10,1	5,9	1,17E-02		-1,39	
74	+	gene	pYV0080	yscD											28,8	5,5	2,49E-07	yscD; type III secretion protein	-0,95	
76	+	gene													74,2	6,6	1,06E-13		-0,95	
77	+	gene													24,6	6,1	2,08E-06		-0,95	
79	+	gene	pYV0083	yscG											8,1	4,4	3,92E-03	yscG; type III secretion protein	-1,01	
80	+	gene													29,3	6,6	4,44E-08		-1,01	
80	+	gene	pYV0084	yscH/ yopR											29,3	6,6	4,44E-08	yscH, yopR, lcrP; type III secretion protein	-0,68	
84	+	gene	pYV0088	yscL											7,7	4,9	2,08E-02	type III secretion system protein	-0,22	
86	+	gene	pYV0091	pYV0091											12,1	4,3	4,34E-03	transposase	-1,24	
87	-	gene	pYV0094	yopH											39,0	6,8	4,73E-09	yopH; protein-tyrosine phosphatase Yop effector	-2,96	
88	-	gene													23,7	4,9	1,24E-05		-2,96	
89	-	gene													7,1	5,4	2,91E-03		-2,96	
94	+	intergenic	NA	NA											17,6	3,6	4,10E-04	pYV0096(IS630: family) - pYV0097(hypothetical protein)	-1,48	-2,89 *
95	-	gene	pYV0098	yopP/ yopJ											22,4	5,6	8,05E-07	yopP, yopJ; targeted effector protein	-3,23	
96	-	gene													61,4	5,9	1,83E-07		-3,23	

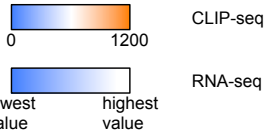

3.3 Regulation of later-stage virulence factors upon contact with the host cells

Contact between the pathogen and the mammalian host cell represents an essential environmental signal that further triggers the expression of the *ysc-yop* T3SS and promotes an active secretion and translocation of Yop effector proteins (Rosqvist *et al*., 1994; Pettersson *et al*., 1996). However, the molecular mechanism underlying this host cell contact-dependent induction of the T3SS and its effectors is poorly understood. Although, the sensors of host cell contact signal are still unknown, previous works suggested the involvement of lipoproteins and two component systems in cell contact sensing (Snyder *et al*., 1995; Miyadai *et al*., 2004; Opitz, 2013; Pimenova, 2014; Shimizu *et al*., 2016; Nisco *et al*., 2018). Moreover, the important role of the T3S translocation pore in sensing of the host cell contact was reported (Veenendaal *et al*., 2007; Armentrout & Rietsch, 2016). Preliminary results demonstrated an induction of the major virulence activator LcrF in response to host cell contact. Additionally, evidence suggests that *Y. pseudotuberculosis* requires the CsrA protein to enhance the expression of the *ysc-yop* T3SS upon contact with host cells (Opitz, 2013). Hence, it was intriguing to obtain deeper insight into the complex regulatory network responsible for the host cell contact signal sensing and transmission, resulting in induction of the T3SS in *Y. pseudotuberculosis*.

3.3.1 Host cell contact-dependent activation of LcrF synthesis is crucial to trigger the expression of the virulence plasmid-encoded genes

First, it was essential to verify whether the host cell contact-mediated induction of the adhesin *yadA* and the *ysc-yop* T3SS occurs via activation of LcrF synthesis. Thus, *lcrF* expression in presence or absence of epithelial host cells was investigated and compared to those of the LcrF-dependent adhesin *yadA*. Therefore, the P_{yscW}::*yscW-lcrF'-luxCDABE* (pWO42; Fig. 3.25 A) and the P_{yadA}::*yadA'-luxCDABE* (pWO41; Fig. 3.25 B) reporter gene fusions were introduced into the *Y. pseudotuberculosis* wild type strain (YPIII) and the bacteria were grown in LB medium at 25 °C overnight. Next, the cultures were incubated either with HEp-2 cells or as a control with PBS at 25 °C for 2.5 hours. To assess the kinetic of *yscW-lcrF* and *yadA* expression, the luciferase activity was documented every 10 min (Fig. 3.25 A, B, left panels). Although the expression of both P_{yscW}::*yscW-lcrF'-luxCDABE* and P_{yadA}::*yadA'-luxCDABE* reporter fusions was significantly increased in the presence of the host cells, the induction of *yadA* was delayed compared to *lcrF* (Fig. 3.25 A, B, left panels).

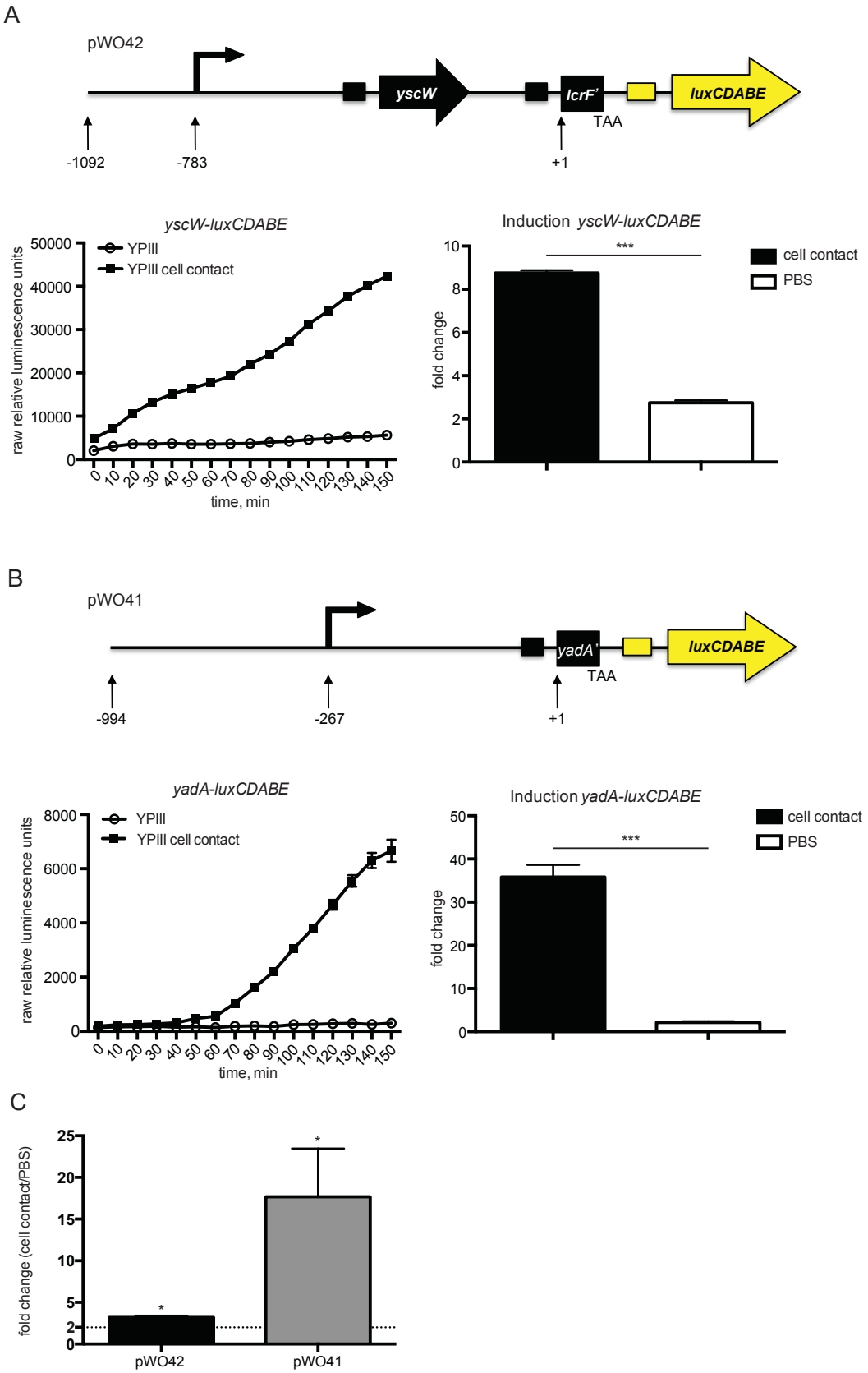

Figure 3.25. Contact with the host cell activates *lcrF* synthesis in a temperature-independent manner.

Schematic overview of the *yscW-lcrF'-luxCDABE* (**A** upper panel) and *yadA'-luxCDABE* (**B** upper panel) transcriptional fusions. The numbers indicate the 5' ends and 3' ends of the *yscW* upstream region fragments fused to the *luxCDABE* operon with respect to the translational start site of the

lcrF or *yadA* gene. *Y. pseudotuberculosis* YPIII (wt) carrying *yscW-lcrF'-luxCDABE* (**A** pWO42) or *yadA'-luxCDABE* (**B** pWO41) was used to infect confluent HEp-2 cells or incubated without cells in PBS at 25 °C for 2.5 hours. Bioluminescence was determined every 10 min to monitor kinetics of host cell-dependent *yscW-lcrF'-luxCDABE* (**A** lower left panel) or *yadA-luxCDABE* (**B** lower left panel) induction. The data represent mean ± standard error of three independent experiments. Mean values are displayed as raw data plotted against time [min]. The fold change (end/start) of the data was calculated. Asterisks indicate the results that differed significantly from those in PBS harboring the same plasmid with ***($P<0.001$). **C** The fold change of the same data was normalized to the respective PBS control. The induction was determined as significant, if the value was >2 (two-fold induction, dashed line). The data represent mean ± standard deviation of three independent experiments. Statistical significance was analyzed by the Student's t-test. Asterisks indicate the results that differed significantly from 2 with *($P<0.05$).

Intriguingly, the host cell contact-triggered induction of *lcrF* can be separated into three phases. The first one is an immediate induction, which occurs directly after bacteria contact the host cells. Thereafter, in the time between 30 to 60 min after cell contact signal acquisition, the rate of *lcrF* expression slows down, followed by a second induction approx. 70 min after contact with HEp-2 cells (Fig. 3.25 A left panel). Damping of the *lcrF* expression intensity might indicate the accumulation of YopD in the bacterial cytosol resulting in downregulation of LcrF synthesis. Reactivation, in turn, might correspond to release of YopD, after the T3SS gets assembled. Interestingly, the time point of *yadA* induction almost completely corresponds to the second induction wave of *lcrF* (60-70 min after contact; Fig. 3.25 B left panel). These data strongly suggest a hierarchy in which host cell contact induces YadA and T3SS/Yop synthesis via LcrF.

In the following, host cell contact-mediated induction was defined as cell contact/PBS fold change ratio (Fig. 3.25 C). For evaluation of the data, a fold-change of > 2.0 was classified as a significant induction. Since the overall extend of cell contact-dependent *yadA* induction was higher (about 20-fold) than the one of *lcrF* (about 3-fold) (Fig. 3.25 C), LcrF-dependent expression of *yadA* was employed as readout to monitor the role of several factors described below in sensing and/or transmission of the host cell contact signal.

3.3.1.1 The needle complex of T3SS is not essential for cell contact sensing

In *Shigella flexneri* and *Pseudomonas aeruginosa* the T3SS needle tip complex and the translocation pore, respectively, were found to sense the host cell contact signal (Veenendaal *et al*., 2007; Armentrout & Rietsch, 2016). Contrary, previous data from our group demonstrated no effect of YopD on cell contact-dependent induction of *yadA* expression in *Y. pseudotuberculosis*, suggesting no involvement of the translocon in cell contact sensing (Opitz, 2013). Thus, it was important to clarify the role of the T3SS translocator (YopB/YopD) in sensing of the host cell contact. To do so, the *Y. pseudotuberculosis* Δ*yopB* (YPIII pIB604) strain was analyzed for its ability to affect cell contact- and LcrF-dependent expression of the *yadA* gene in comparison to the parental strain (YPIII pIB102) (Fig. 3.26). Additionally, the *yscS*-deficient strain was included in this experiment in order to find out whether a functional T3SS is essential for cell contact sensing. To exclude the unspecific effects originating from the parental wild type strains genetic background, cell contact-mediated *yadA* expression was analyzed in

both wild type strains (YPIII pIB1 and YPIII pIB102) and both Δ*yscS* variants (YP101 or YPIII pIB68).

The expression of *yadA* in the absence of YopB was still significantly induced in a cell contact-dependent manner, but, less pronounced than in the corresponding wild type (Fig. 3.26). This indicates that both YopB and YopD modulate, but are not responsible for cell contact sensing. Since *yadA* expression was significantly upregulated in both *yscS* mutant strains upon contact with HEp-2 cells, the functional T3SS seems not to be essential for sensing of the host cell contact signal (Fig. 3.26). However, the induction level was lower compared to each parental strain. Thus, similar to the translocon components, the functional T3SS most likely either positively affects *yadA* expression independently from host cell contact or modulates the cell contact-dependent response of *Y. pseudotuberculosis*.

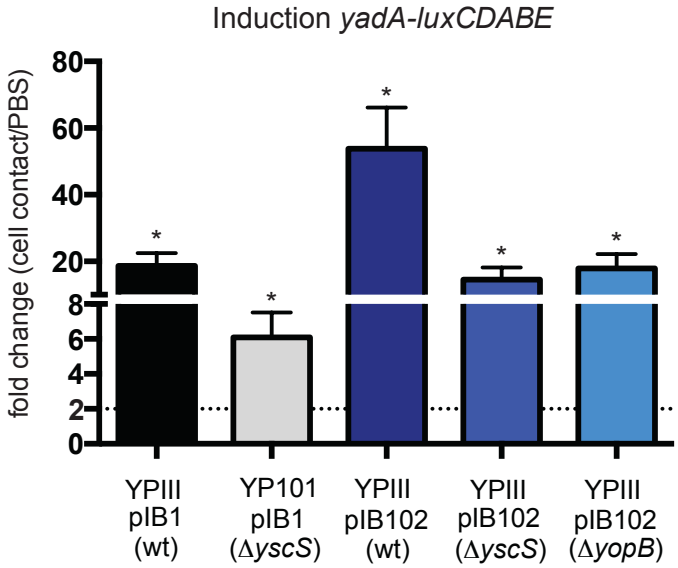

Figure 3.26. The functional T3SS is not essential for cell contact sensing.
Y. pseudotuberculosis YPIII pIB1 (wt), YP101 pIB1 (Δ*yscS*), YPIII pIB102 (wt), YPIII pIB102 (Δ*yscS*; YPIII pIB68), and YPIII pIB102 (Δ*yopB*; YPIII pIB604) strains carrying *yadA'-luxCDABE* were used to infect confluent HEp-2 cells or were incubated without cells in PBS at 25 °C for 2.5 hours. Bioluminescence was determined every 10 min to monitor kinetics of host cell-dependent *yadA-luxCDABE* induction. The fold change (end/start) of the data was calculated and normalized to the respective PBS control. The induction was classified as significant, if the value was >2 (two-fold induction, dashed line). The data represent mean ± standard deviation of three independent experiments. Statistical significance was analyzed by the Student's t-test. Asterisks indicate the results that differed significantly from 2 with *($P<0.05$).

3.3.1.2 Chromosomally-encoded factors are responsible for cell contact-dependent induction of *lcrF*

Next, it was interesting to unravel whether some other virulence plasmid-encoded factors might compromise the ability of *Y. pseudotuberculosis* to sense and respond to the host cell contact signal. For this purpose, cell contact-dependent expression of the P_{yadA}::*yadA'-luxCDABE* reporter fusion (pWO41) was assessed in the *Y. pseudotuberculosis* virulence plasmid-cured strain YP12 (pYV^-) and the virulence plasmid-cured strain harboring a chromosomally integrated *yscW-lcrF* (YP155) operon for *lcrF* complementation

(Fig. 3.27). As a negative control, *yadA* expression was also estimated in the *lcrF*-deficient strain (YP66).

As shown in Fig. 3.27, no significant induction of *yadA* expression upon contact with the host cells was detectable in the virulence plasmid cured strain (YP12) and in the strain lacking *lcrF* (YP66). However, absence of the other virulence plasmid encoded genes in presence of LcrF (YP155) did not alter *yadA* response to the host cell contact signal (Fig. 3.27). This result further confirms that LcrF is absolutely required for cell contact-mediated activation of *yadA* expression. Furthermore, these data suggest that chromosomally- and not the virulence plasmid-encoded factors play a crucial role in host cell contact signal acquisition and transmission, leading to induction of *lcrF* expression. To confirm this hypothesis, influence of several chromosomally-encoded factors on cell contact-mediated and LcrF-dependent induction of *yadA* expression was investigated.

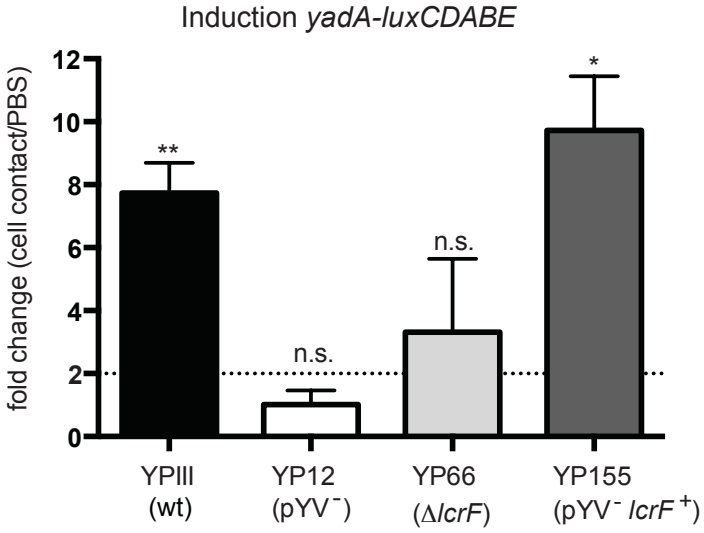

Figure 3.27. Chromosomally-encoded factors are responsible for cell contact-dependent *lcrF* induction.
Y. pseudotuberculosis YPIII (wt), YP12 (pYV^{-}), and YP155 (pYV^{-} *lcrF*$^{+}$) strains carrying *yadA'-luxCDABE* were used to infect confluent HEp-2 cells or were incubated without cells in PBS at 25 °C for 2.5 hours. Bioluminescence was determined every 10 min to monitor kinetics of host cell-dependent *yadA-luxCDABE* induction. The fold change (end/start) of the data was calculated and normalized to the respective PBS control. The induction was determined as significant, if the value were >2 (two-fold induction, dashed line). The data represent mean ± standard deviation of three independent experiments. Statistical significance was analyzed by the Student's t-test. Asterisks indicate the results that differed significantly from 2 with *(P<0.05), **(P<0.01), ***(P<0.001), n.s. (P>0.05).

Since *Yersinia* adhesins such as invasin, Ail and YadA were reported to mediate binding to the host cells (invasin, Ail, YadA) and to facilitate delivery of cytotoxic Yop effectors (Ail, YadA), the involvement of these adhesins in sensing of the host cell contact signal was assessed (Mikula *et al*., 2013; Tsang *et al*., 2013). According to preliminary data from our group, *Y. pseudotuberculosis* strains either deficient for only *yadA*, or for both *yadA* and *invA*, or lacking four invasins (Δ*invA/invB/invC/invD*) were able to induce the *yadA* expression upon contact with HEp-2 cells (Opitz, 2013). However, a possible simultaneous effect of the deletion of all these adhesins on the host cell contact-mediated induction of

yadA expression was not explored. Therefore, strain lacking *invABCD*, *ail* and *yadA* (YP250) was analyzed for its ability to abolish cell contact response (Fig. 3.28).

Unexpectedly, the cell contact assay revealed no difference between the enhanced *yadA* expression in the adhesin mutant strain (YP250) and the wild type strain (YPIII) (Fig. 3.28). Thus, even a deletion of six *Yersinia* adhesins was not able to prevent cell contact-dependent induction of *yadA* expression. This in turn indicates that the tested adhesins are not implicated in the host cell contact signal sensing and/or transmission. However, it cannot be excluded that other *Yersinia* adhesins which were not analyzed in this work (YadB, YadC, Pla) are involved in cell contact sensing (Mikula *et al*., 2013).

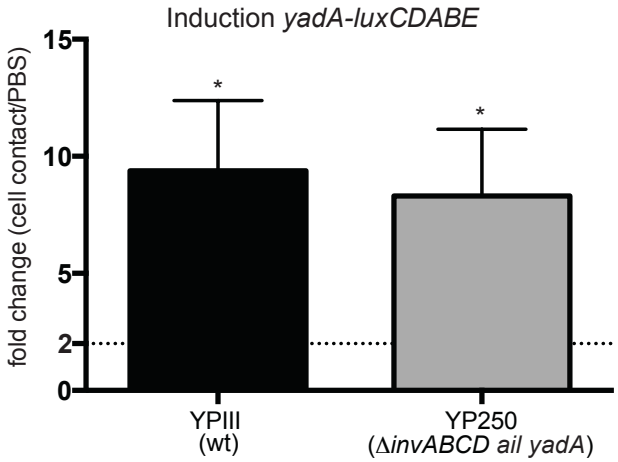

Figure 3.28. Influence of adhesins on cell contact-dependent *yadA* induction.
Y. pseudotuberculosis YPIII (wt), and YP250 (Δ*invABCD ail yadA*) strains carrying *yadA'-luxCDABE* were used to infect confluent HEp-2 cells or were incubated without cells in PBS at 25 °C for 2.5 hours. Bioluminescence was determined every 10 min to monitor kinetics of host cell-dependent *yadA-luxCDABE* induction. The fold change (end/start) of the data was calculated and normalized to the respective PBS control. The induction was classified as significant, if the value were >2 (two-fold induction, dashed line). The data represent mean ± standard deviation of three independent experiments. Statistical significance was analyzed by the Student's t-test. Asterisks indicate the results that differed significantly from 2 with *($P<0.05$).

3.3.1.3 Role of extracytoplasmatic stress-response systems in cell contact sensing

Two-component signal transduction systems (TCS) of bacteria collectively known as extracytoplasmatic/envelope stress responses (ESRs) represent sophisticated and ubiquitous devices for perceiving and rapid adaptation to environmental changes (Rowley *et al*., 2006). Interestingly, microarray analysis performed for the investigation of factors responsible for sensing of the host cell contact signal identified several calcium-dependent ESRs: CpxA/R/CpxP, the PspABCD operon, BasRS, OmpR/EnvZ, RstAB and RcsBC (Opitz, 2013). However, analysis of *Y. pseudotuberculosis* strains deficient for *cpxA*/*R*/*cpxP*, the *pspABCD* operon, and *basRS* revealed no alterations in cell contact-dependent induction of *yadA* expression (Pimenova, 2014). Nevertheless, preliminary results suggest the involvement of Rsc and OmpR/EnvZ ESRs in cell contact sensing (Pimenova, 2014). Additionally, data of this work demonstrated the important role of RcsB in CsrA-mediated regulation of *lcrF* transcription (see 3.1.2.2). Considering a possible

contribution of the Rsc system to cell contact response, it was intriguing to assess if the surface lipoprotein RcsF, which mediates the perception of numerous signals activating the Rcs phosphorelay, might act as a direct sensor of the host cell contact signal (Gervais & Drapeau, 1992; Huang *et al*., 2006). To confirm this hypothesis, strains YP310 (Δ*rcsBC*), strain YP323 (Δ*rcsF*), and YP300 (Δ*ompR/envZ*) were tested in their ability to affect the LcrF-dependent induction of *yadA* expression upon contact with HEp-2 cells (Fig. 3.29).

Although induction of *yadA* expression in *rcsBC*-deficient strain (YP310) was lower than in the wild type (YPIII), deletion of genes encoding for the Rcs sensor histidine kinase (RcsC) and the Rcs response regulator (RcsB) did not abolish the effect of the host cell contact signal (Fig. 3.29 A). In agreement with this result, *yadA* induction upon contact with HEp-2 cells was also not affected in the Δ*rcsF* strain (Fig. 3.29 B). Together, the Rcs phosphorelay does not seem to be crucial for sensing and transmission of the host cell contact signal.

In contrast, cell contact-dependent induction of *yadA* expression was strongly impaired in the Δ*ompR/envZ* mutant strain (Fig. 3.29 C) making the OmpR/EnvZ ESR a potential candidate for cell contact sensing. However, it is unclear how OmpR/EnvZ system controls the cell contact response.

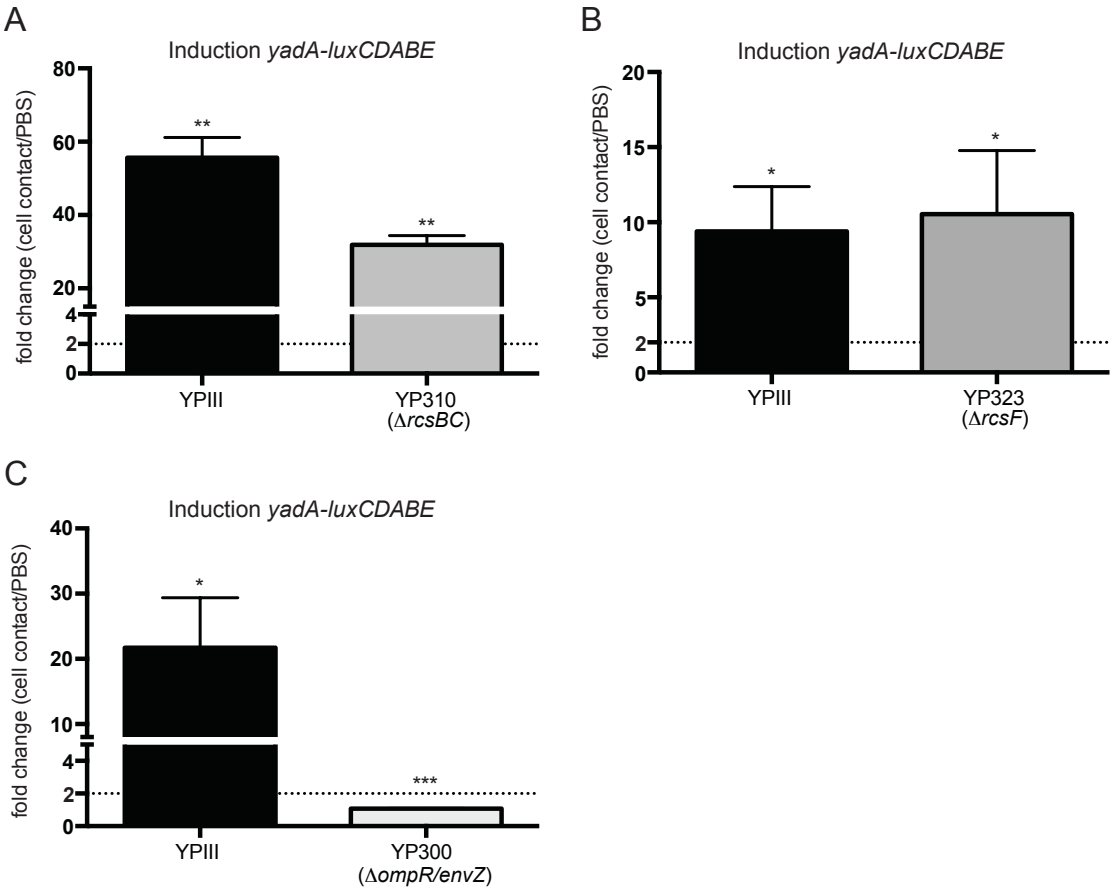

Figure 3.29. Role of extracytoplasmatic stress-response systems in cell contact sensing.
Y. pseudotuberculosis YPIII (wt), YP310 (**A** Δ*rcsBC*), YP323 (**B** Δ*rcsF*), and YP300 (**C** Δ*ompR/envZ*) strains carrying *yadA'-luxCDABE* were used to infect confluent HEp-2 cells or were incubated without cells in PBS at 25 °C for 2.5 hours. Bioluminescence was determined every 10 min to monitor kinetics of host cell-dependent *yadA-luxCDABE* induction. The fold change

(end/start) of the data was calculated and normalized to the respective PBS control. The induction was classified as significant, if the value was >2 (two-fold induction, dashed line). The data represent mean ± standard deviation of three independent experiments. Statistical significance was analyzed by the Student's t-test. Asterisks indicate the results that differed significantly from 2 with *(P<0.05), **(P<0.01), ***(P<0.001).

Of special interest was to find out whether the suppressive effect of the *ompR*/*envZ* deletion on cell contact-dependent induction of virulence plasmid encoded genes can be reproduced *in vitro*. Although depletion of calcium from the growth medium is widely applied to mimic the host cell contact signal, previous data strongly suggest that sensing and/or regulatory pathways resulting in activation of LcrF synthesis differ between these two signals (Pimenova, 2014). Thus, the Δ*rcsBC* strain (YP310) was also investigated regarding its ability to affect Ca^{2+} depletion signal sensing and/or transmission (Fig. 3.30).

First, the impact of these mutations on Ca^{2+} depletion-mediated release of Yops was tested by performing Yop secretion assays (Fig. 3.30 A). To do so, *Y. pseudotuberculosis* wild type strain (YPIII), *ompR*/*envZ*-deficient strain (YP300) and Δ*rcsBC* mutant (YP310) were cultivated under conditions non-permissive ($+Ca^{2+}$) and permissive ($-Ca^{2+}$) for Yop secretion. Released Yops in the corresponding bacterial cultures were precipitated and analyzed on a Coomassie stained polyacrylamide gel.

In agreement with the cell contact assay results, secretion of Yops in the *rcsBC*-deficient strain was still Ca^{2+}-dependent and the amount of released Yops was similar to those observed for the wild type strain (Fig. 3.30 A). Strikingly, although deletion of *ompR*/*envZ* abolished the induction of *yadA* expression upon contact with HEp-2 cells, Yop secretion under permissive conditions was even stronger in the Δ*ompR*/*envZ* mutant culture than in the wild type culture (Fig. 3.30 A). This indicates a different nature of the host cell contact- and Ca^{2+} depletion-dependent induction.

Since both, induction of *yadA* expression upon cell contact and secretion of Yops under Ca^{2+} depletion conditions, is impossible in the absence of the major virulence activator LcrF, it was also important to investigate the effect of OmpR/EnvZ and RcsBC on induction of LcrF synthesis upon depletion of Ca^{2+}. For this purpose, *lcrF* transcript and LcrF protein levels in Δ*ompR*/*envZ* and Δ*rcsBC* mutant strains grown under conditions non-permissive and permissive for Yop secretion were assessed by Northern and Western blotting, respectively, and compared to the wild type strain (Fig. 3.30 B). Regarding the data in this work showing the crucial role of CsrA for secretion-dependent induction of LcrF synthesis, *csrA* transcript and CsrA protein levels as well as the levels of *csrB* and *csrC* RNAs were also determined (Fig. 3.30 B).

A

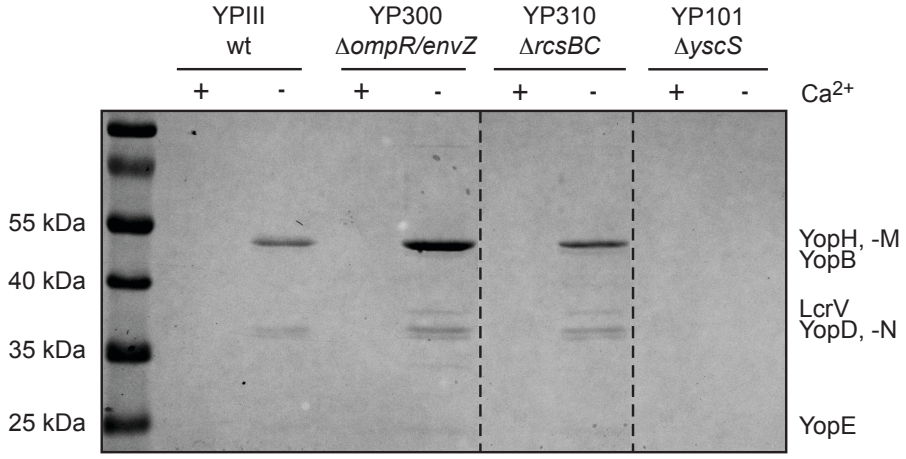

B

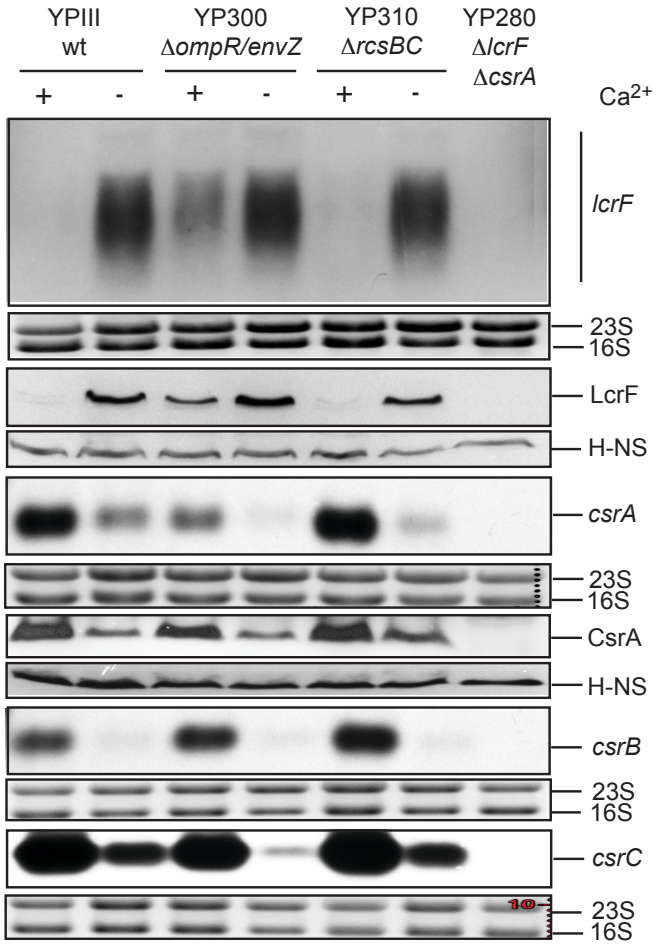

Figure 3.30. OmpR/EnvZ represses LcrF expression but has no effect on its secretion-dependent induction, while RcsBC does not affect LcrF synthesis upon secretion.
A-B *Y. pseudotuberculosis* YPIII (wt), YP300 (Δ*ompR/envZ*), and YP310 (Δ*rcsBC*) strains were grown in LB_{BD} (1:50 diluted from overnight cultures) for two hours at 25 °C. Thereafter, Ca^{2+} depletion was induced (-) by adding 20 mM NaOx and 20 mM $MgCl_2$ or not (+). Subsequently cultures were shifted to 37 °C for four hours. **A** Proteins in the supernatant were precipitated with TCA. Thereafter, samples were prepared for SDS-PAGE and visualized by Coomassie staining. **B** For Northern blot analysis, performed to determine the *lcrF, csrA, csrB,* and *csrC* transcript

levels, total RNA of the same cultures was isolated, separated by 1.2 % MOPS agarose gel electrophoresis, and transferred onto a nylon membrane. The mRNAs of interest were specifically detected by the specific Dig-labeled DNA probe. *lcrF, csrA, csrB,* and *csrC* transcripts are indicated on the right. 23S and 16S rRNA was visualized with ethidium bromide as loading control. The *lcrF csrA* mutant strain YP280 was used as negative control. Furthermore, whole cell extracts of equal cell densities (OD_{600}=1) were prepared for Tricine-SDS-PAGE and transferred onto an Immobilon membrane. LcrF and CsrA proteins were detected by immunoblotting with a polyclonal α-LcrF and α-CsrA antibody, respectively (loading control: α-H-NS). The *lcrF csrA* double-mutant strain YP280 was used as negative control.

Consistent with the previous results, when Ca^{2+} was depleted, the amounts of *lcrF* transcript and protein increased in the wild type strain compared to under non-permissive conditions (Fig. 3.30 B). Similar to YPIII, Ca^{2+} depletion-dependent induction of LcrF synthesis was observable in the Δ*rcsBC* mutant strain (YP310). In fact, both, the wild type and the Δ*rcsBC*-deficient strains, produced very low amounts of *lcrF* transcript and, consequently, LcrF protein under non-secretion conditions and activated *lcrF* expression only after depletion of Ca^{2+}. In contrast, in the absence of *ompR*/*envZ* (YP300) *lcrF* transcript and LcrF protein were clearly detectable already under non-permissive conditions, but less intense compared to the expression levels under permissive conditions in all three strains (Fig. 3.30 B). Under secretion conditions, the LcrF protein level was slightly higher than in the wild type strain and the Δ*rcsBC* mutant strain. This might explain the increased secretion of Yops from YP300 compared to the wild type strain and the Δ*rcsBC* mutant strain (Fig. 3.30 A). Thus, although the Δ*ompR*/*envZ* mutant showed elevated LcrF synthesis upon Yop secretion, due to the enhanced *lcrF* expression under non-secretion conditions the induction was not as prominent as for YPIII and YP310 (Fig. 3.30 B). This indicated that OmpR/EnvZ is a negative regulator of *lcrF* expression under both non-permissive and permissive conditions. Consequently, deletion of *ompR*/*envZ* might lead to a higher overall basal expression level of *lcrF* upon contact with the host cells (see Fig. S8). This, in turn, most likely results in an earlier increase of the LcrF-dependent *yadA* expression in Δ*ompR*/*envZ* mutant strain upon host cell contact compared to the wild type strain reducing the induction of *yadA* expression (Fig. 3.29 C).

CsrA synthesis was also affected by deletion of *ompR*/*envZ*. Northern blot analysis revealed significantly reduced *csrA* transcript amounts in YP300 compared to YPIII and YP310 under both, secretion and non-secretion conditions (Fig. 3.30 B). Moreover, under non-secretion conditions, significantly less *csrA* transcript and somewhat less CsrA protein was produced in the absence of OmpR/EnvZ. Hence, it is possible that OmpR/EnvZ may exert the negative effect on *lcrF* expression under non-secretion conditions via positive regulation of CsrA synthesis.

As shown in Fig. 3.30 B *csrB* expression was almost un-affected by *ompR*/*envZ* deletion, while *csrC* levels were considerably impaired compared to the YPIII and YP310. In particular, under conditions permissive for Yop secretion, significantly lower amounts of *csrC* were detectable in the absence of OmpR/EnvZ. Consequently, less CsrA protein can be sequestered by *csrC*. Considering the nearly similar levels of CsrA protein in the wild type and the *ompR*/*envZ*-deficient strain under secretion conditions (Fig. 3.30 B) it becomes evident that more “free” CsrA is available in the absence OmpR/EnvZ. Since the

results of this work demonstrate that CsrA promotes *lcrF* translation initiation upon secretion (see 3.2.1.1), this may explain an elevated LcrF protein synthesis in Δ*ompR*/*envZ* mutant strain under secretion conditions.

3.3.1.4 CsrA is indispensible for cell contact-dependent induction of *lcrF*

Present work emphasizes that the CsrA protein is absolutely essential for the Ca^{2+} depletion-dependent induction of LcrF synthesis (see 3.2.1.1). Moreover, in enteropathogenic *E. coli* (EPEC) CsrA was reported to be involved in the cell contact-mediated remodeling of gene expression (Katsowich *et al*., 2017). Hence, it was intriguing to investigate the role of CsrA in cell contact-dependent induction of *lcrF* expression. For this purpose strains YPIII (wild type) and YP53 (Δ*csrA*) were investigated for their ability to induce the expression of the P_{yscW}::*yscW-lcrF'-luxCDABE* (pWO42; Fig. 3.25 A) and the P_{yadA}::*yadA'-luxCDABE* (pWO41; Fig. 3.25 B) reporter gene fusions in response to the host cell contact signal (Fig. 3.31). Complementation was tested by introducing a $csrA^+$ plasmid (pKB60) into the *csrA*-deficient strain. The empty vector pHSG576 (pV) was transformed in the wild type strain and the *csrA*-deficient strain to exclude unspecific effects by the plasmid backbone.

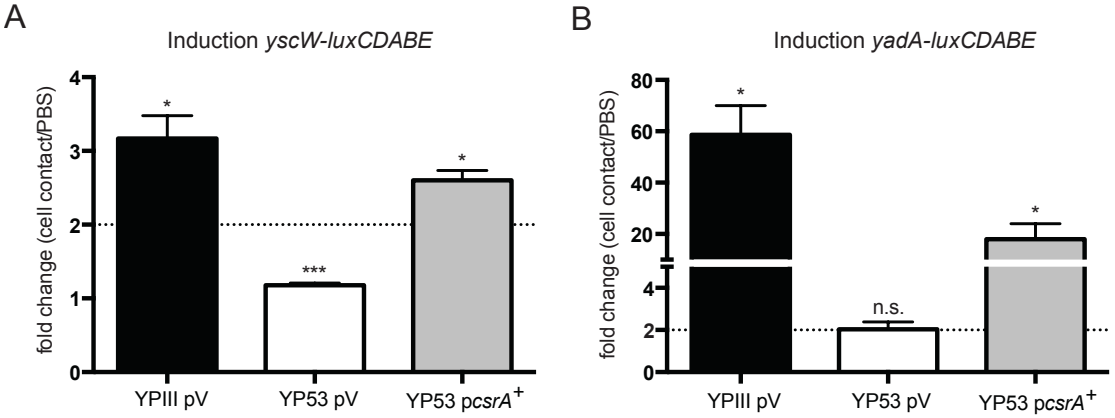

Figure 3.31. CsrA is indispensible for cell contact-dependent *lcrF* induction.
Y. pseudotuberculosis YPIII (wt), and YP53 (Δ*csrA*) strains carrying *yscW-lcrF'-luxCDABE* (**A**) or *yadA'-luxCDABE* (**B**) and the empty vector pHSG576 (pV) or the *csrA*+ plasmid (pKB60) were used to infect confluent HEp-2 cells or were incubated without cells in PBS at 25 °C for 2.5 hours. Bioluminescence was determined every 10 min to monitor kinetics of host cell-dependent *yadA-luxCDABE* induction. The fold change (end/start) of the data was calculated and normalized to the respective PBS control. The induction was determined as significant, if the value was >2 (two-fold induction, dashed line). The data represent mean ± standard deviation of three independent experiments. Statistical significance was analyzed by the Student's t-test. Asterisks indicate the results that differed significantly from 2 with *(P<0.05), **(P<0.01), ***(P<0.001), n.s. (P>0.05).

No cell contact-dependent induction of *lcrF* expression was observed in the *csrA* mutant strain YP53 compared to the wild type YPIII (Fig. 3.31 A). Ectopical expression of *csrA* in YP53 restored the cell contact-mediated *lcrF* induction to a statistically significant value. The positive effect of CsrA on *lcrF* expression in response to the host cell contact signal was directly reflected by the induction level of the LcrF-controlled *yadA* expression (Fig. 3.31 B). Together, this indicates that CsrA is indispensible for triggering LcrF synthesis upon contact with host cells.

3.3.1.5 CsrA is essential for *lcrF* translation upon host cell contact

Next, it was important to unravel how CsrA interferes with the host cell contact-signaling pathway aimed to induce the expression of the late virulence determinants via LcrF. Regarding the previous data presented in this work that demonstrate the positive effect of CsrA on *lcrF* translation initiation under secretion conditions (see 3.2.1.1), it was explored whether the same molecular mechanism enables CsrA-mediated induction of *lcrF* expression in response to host cell contact. To address this question, induction of the P_{yadA}::*yadA'-luxCDABE* (pWO41; Fig. 3.25 B) reporter gene fusion in response to host cell contact was estimated in the *Y. pseudotuberculosis* wild type, the Δ*csrA* mutant, a strain harboring an *lcrF* variant a nucleotide substitutions leading to a stabilization of the *lcrF* thermoloop structure (repressed *lcrF* variant: UU-28/-27CC; see Fig. 3.12 A), and a strain which harbors an *lcrF* variant with a constantly opened thermoloop (derepressed *lcrF* variant: GUU-30/-28AAA; see Fig. 3.12 A), as well as in the derepressed mutant lacking *csrA* (Fig. 3.32 A). In order to complement the *csrA* deletion, pKB60 (p*csrA*$^+$) was transformed in all Δ*csrA* strains. In YP90, *csrA* was overexpressed from pKB60 to test the tightness of the "closed" *lcrF* thermoloop structure in presence of higher CsrA amounts. The empty vector pHSG576 (pV) was introduced separately to exclude effects originated from the plasmid backbone.

Consistent with previous results, cell contact- and LcrF-dependent induction of *yadA* expression was only possible if CsrA was present (Fig. 3.32 A). The "opened" *lcrF* thermoloop structure in YP284 was not sufficient to activate *yadA* expression in response to the host cell contact signal. However, overexpression of *csrA* in the derepressed Δ*csrA* mutant resulted in significant induction of *yadA* expression. This data strongly supports the positive effect of CsrA on *lcrF* translation initiation discovered in this work. Moreover, CsrA-mediated activation of *lcrF* expression seems to occur via stimulation of *lcrF* translation initiation under both cell contact and Ca^{2+} depletion conditions.

To verify this hypothesis, expression of the P_{yadA}::*yadA'-luxCDABE* (pWO41; Fig. 3.25 B) reporter gene fusion was analyzed under secretion conditions in relation to non-secretion condition in the strains YPIII pV, YP53 pV, YP53 p*csrA*$^+$, YP90 pV, YP90 p*csrA*$^+$, YP95 pV, YP95 p*csrA*$^+$, YP284 pV, and YP284 p*csrA*$^+$ (Fig. 3.32 B). As shown in Fig. 3.32 B, the induction of *yadA* expression was blocked in strains deficient for *csrA* (YP53 pV, YP284 pV) as well as in the repressed *lcrF* variant (YP90 pV, YP90 p*csrA*$^+$). Similar to the cell contact conditions, overexpression of *csrA* restored induction of *yadA* expression upon Ca^{2+} depletion.

A

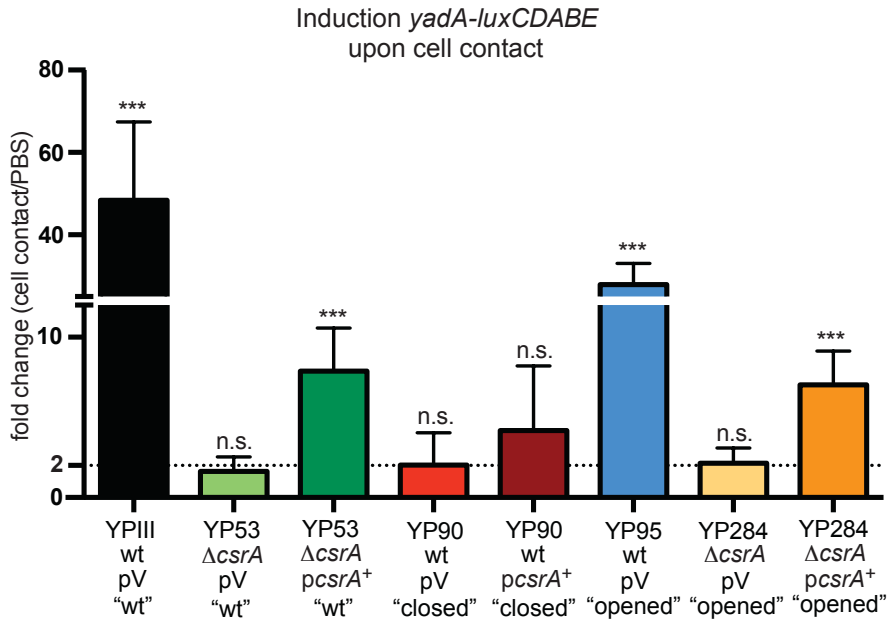

B

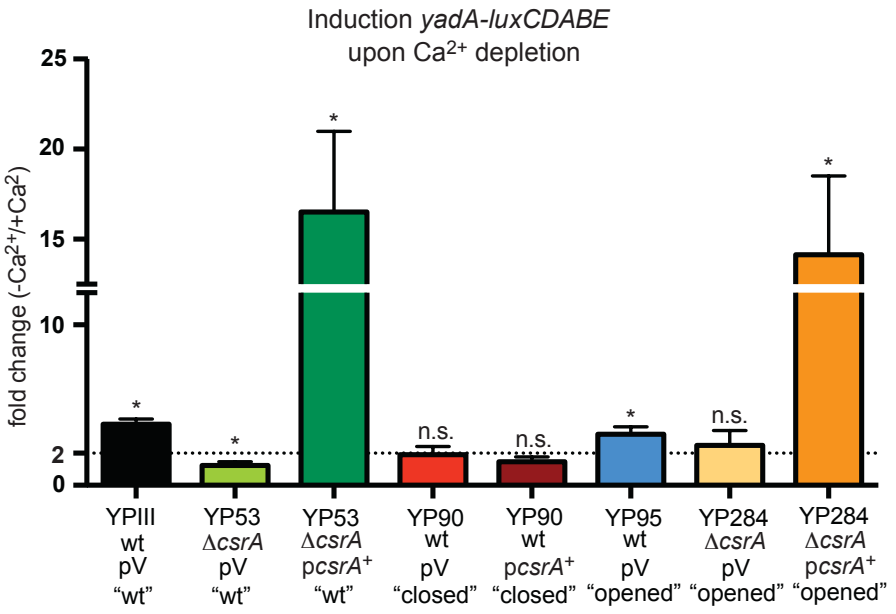

Figure 3.32. CsrA is essential for *lcrF* translation initiation upon host cell contact and under secretion conditions.

Y. pseudotuberculosis YPIII (wt), YP53 (Δ*csrA*), YP90 ("closed" thermoloop), YP95 ("opened" thermoloop), and YP284 (Δ*csrA* "opened" thermoloop) strains carrying *yadA'-luxCDABE* and the empty vector pHSG576 (pV) or the *csrA*+ plasmid (pKB60) were used to infect confluent HEp-2 cells or were incubated without cells in PBS at 25 °C for 2.5 hours (**A**) or were grown under +/- Ca^{2+} conditions in LB_{BD} (**B**). **A** Bioluminescence was determined every 10 min to monitor kinetics of host cell-dependent *yadA-luxCDABE* induction. The fold change (end/start) of the data was calculated and normalized to the respective PBS control. The induction was classified as significant, if the value was >2 (two-fold induction, dashed line). **B** The overnight cultures of the same strains were inoculated in LB_{BD} medium 1:50 (wt) or 1:20 (Δ*csrA*) and grown for two hours at 25 °C. Thereafter, Ca^{2+} depletion was induced by adding 20 mM NaOx and 20 mM $MgCl_2$ or not, and the cultures were further incubated for 4 hours at 37 °C. Subsequently, luciferase activity

was measured. The relative induction of each reporter gene fusion was calculated as luciferase activity under secretion conditions (-Ca^{2+}) normalized to those under non-secretion conditions (+Ca^{2+}) and is indicated on the left. **A-B** The relative induction >2 was determined as a significant induction. The data represent mean ± standard deviation of three independent experiments. Statistical significance was analyzed by the Student's t-test. Asterisks indicate the results that differed significantly from 2 with *($P<0.05$), ***($P<0.001$), n.s. ($P>0.05$).

Together, these data demonstrate that CsrA is absolutely required for cell contact- and Ca^{2+} depletion-dependent induction of LcrF synthesis. Furthermore, the CsrA-mediated induction of *lcrF* expression most likely occurs through stimulation of *lcrF* translation initiation under both conditions (cell contact/-Ca^{2+}).

4 Discussion

Pathogenic *Yersiniae* require several virulence factors for successful establishment of an infection. Expression of certain virulence determinants occurs in dependence on the particular phase of the infection process and is precisely coordinated by diverse regulatory molecules (Atkinson & Williams, 2016). In particular during the ongoing infection phase, enteropathogenic *Yersinia* species are challenged by the host immune system. To overcome phagocytosis and prevent untimely clearance, *Yersinia* employs a powerful arsenal of virulence factors. Among these is the sophisticated T3SS nanomachine, with the corresponding subverting Yop effector proteins, as well as the YadA adhesin, which acts as a docking system for the T3SS-mediated injection of Yops (Visser *et al*., 1995; Cornelis *et al*., 1998; Galindo *et al*., 2011). However, unrestrained synthesis of the aforementioned virulence determinants can minimize survival chances of *Yersinia* inside the host due to the high-energy costs of their production and their strong immunogenicity (Schiano & Lathem, 2012). Therefore, appropriate expression of these pYV-encoded "anti-host" factors is strictly controlled (Portaliou *et al*., 2016).

An exclusive activator of *yadA* and *ysc-yop* gene transcription is the major virulence regulator LcrF (Cornelis *et al*., 1998). Intriguingly, *Y. pseudotuberculosis* strains either deficient for, or constitutively expressing the *lcrF* gene were completely avirulent or attenuated in their virulence, respectively (Böhme *et al*., 2012). This fact emphasizes a key role for the AraC-like transcriptional activator LcrF in the regulation of the anti-phagocytic response in *Y. pseudotuberculosis*.

The initial prerequisite for the activation of LcrF synthesis is a constant thermal upshift to temperatures above 30 °C (Bölin *et al*., 1988). Remarkably, host cell contact signal or depletion of Ca^{2+}, mimicking the mammalian host *in vitro*, further trigger *lcrF* expression (Kupferberg & Higuchi, 1958; Rosqvist *et al*., 1994; Pettersson *et al*., 1996). While the temperature-mediated control of LcrF synthesis has been studied extensively (Böhme *et al*., 2012), the regulatory network underlying cell contact- and Ca^{2+} depletion-dependent induction of *lcrF* expression is still unknown. Consequently, this work aimed to explore the molecular mechanisms responsible for precise fine-tuning of LcrF synthesis under non-secretion ($+Ca^{2+}$) and secretion ($-Ca^{2+}$) conditions, as well as upon contact with the host cell.

4.1 *Y. pseudotuberculosis* prevents the overproduction of the late virulence factors under non-secretion conditions

4.1.1 YopD - a negative post-transcriptional regulator of LcrF

During the ongoing infection phase, when *Yersinia* is subjected to mammalian host temperatures, *lcrF* expression is initiated in order to set up the anti-phagocytic defense apparatus. However, under conditions non-permissive for T3S ($+Ca^{2+}$), inappropriate overexpression of the T3SS-associated genes is prevented. Several studies aimed to explore this phenomenon revealed that the components of T3SS, LcrQ and the translocator

YopD in complex with its chaperone LcrH, abolish the expression of their own transcriptional activator, LcrF, at the post-transcriptional level, comprising an inhibitory feedback loop (Pettersson *et al*., 1996; Francis *et al*., 2001; Anderson *et al*., 2002; Steinmann, 2013). Liberation of these factors (LcrQ and YopD) upon secretion dramatically increases the amount of LcrF compared to non-secretion conditions. Similarly, LcrF synthesis in *Yersinia* strains deficient for each of these regulators under non-permissive conditions was comparable to that of wild type *Yersinia* under permissive conditions (Steinmann, 2013).

While components involved in the negative feedback regulation of the *Yersinia* T3SS were already described (Anderson *et al*., 2002; Chen & Anderson, 2011; Steinmann, 2013), the exact molecular mechanism behind it is poorly understood. In other T3SS-encoding pathogens, regulation of AraC/XylS transcriptional activators, coupled to release of negative regulators by secretion, occurs at the post-translational level via the following mechanisms: (i) partner-switching, (ii) interaction with small molecular weight compounds, and (iii) tyrosine phosphorylation (Dasgupta *et al*., 2004; Diaz *et al*., 2011; Golubeva *et al*., 2016; Standish *et al*., 2016; Schulmeyer & Yahr, 2017).

The partner-switching mechanism is based on the presence of a dual function protein that acts both as a chaperone for a secreted protein and as a positive regulator of T3SS gene transcription. In *P. aeruginosa*, this mechanism is responsible for the activation of the AraC-like transcriptional activator ExsA, which shares 56 % homology with LcrF of *Y. enterocolitica* (Allaoui *et a*l., 1995; Dasgupta *et al*., 2006; Vakulskas *et al*., 2009). In the absence of the environmental secretion signal, ExsA is sequestered by the anti-activator ExsD, preventing the transcription of T3SS-associated genes. Under secretion conditions, release of the T3S substrate ExsE liberates its chaperone ExsC, which in turn sequesters the anti-activator ExsD from the activator ExsA. Thus, ExsC derepresses ExsA activity, playing the role of an anti-anti-activator (Rietsch *et al*., 2005; Urbanowski *et al*., 2005).

In *S. enterica* serovar Typhimurium, the DNA-binding activity of HilD, which represents one of several AraC/XylS transcriptional activators of the SPI1 T3SS, is inhibited by long-chain fatty acids that are absorbed by the pathogen during the migration through the intestine (Penheiter *et al*., 1997). Hence, expression of SPI1 genes is only activated when the pathogen reaches the distal ileum where the concentration of these small molecules drops below the critical value required to impair HilD activity (Golubeva *et al*., 2016).

Recently, an additional post-translational mechanism controlling the functionality of AraC/XylS transcriptional activators was discovered. Phosphorylation of the primary activator of the T3SS in *S. flexneri*, VirB, at tyrosine 1000 was shown to suppress the transcription of genes encoding for the T3SS. However, the detailed mechanism underlying this type of regulation remains unclear (Standish *et al*., 2016; Schulmeyer & Yahr, 2017).

Taken together, *Yersinia* seems to be unique in terms of implementing the T3S effector proteins for repression of LcrF synthesis at the translational level rather than at the post-translational level. The present study describes a mode of action of the

Y. pseudotuberculosis translocon component YopD with respect to downregulation of *lcrF* expression under $+Ca^{2+}$ conditions.

Under conditions non-permissive for Yop secretion, YopD was assumed to prevent LcrF synthesis at the post-transcriptional level by negative regulation of LcrF translation initiation and/or reduction of *lcrF* transcript stability. This work showed that YopD has no direct influence on *lcrF* translation initiation (Fig. 3.1). However, YopD was shown to affect the *lcrF* transcript stability, which was significantly increased in the absence of *yopD*, whereas in the wild type strain the *lcrF* transcript was rapidly degraded (Fig. 3.2). This kind of YopD-mediated regulation was also identified in *Y. pestis* (Chen & Anderson, 2011). In particular, the stability of *yopE*, *yopH* and *yscB* transcripts was prolonged in *Y. pestis* Δ*yopD* strain, compared to the wild type strain (Chen & Anderson, 2011). Previous data from our lab suggest that YopD may interfere with the *lcrF* degradation process either via direct binding to the 5'-UTR of *lcrF* mRNA or by positive regulation of the RNA-degrading enzymes RNase E and PNPase (Steinmann, 2013; Hoßmann, 2017).

Cambronne & Schneewind (2002) were able to show that in *Y. enterocolitica* the sequence 5'-AUAAA-3' located in the 5'-UTR of *yop* transcripts is required for YopD binding and for repression of *yop* translation. Similarly, in *Y. pestis*, the AU-rich sequences in the 5'-UTRs of *yopE*, *yopH* and *yscB* were bound by YopD-LcrH complexes (Chen & Anderson, 2011). In agreement with these data, three 5'-AUAAA-3' motifs specific for YopD binding were identified within the sequence of *yscW-lcrF* transcript: in the *yscW* 5'-UTR, in the *yscW* coding sequence, and in the 5'-UTR of *lcrF* (Steinmann, 2013; Hoßmann, 2017). However, an extensive analysis of these 5'-AUAAA-3' consensus sequences with respect to their role in YopD-dependent regulation of LcrF synthesis revealed that deletion of these motifs did not prevent YopD binding and YopD-mediated repression of *lcrF* translation (Steinmann, 2013; Hoßmann, 2017). This indicates that YopD is most likely able to interact with some alternative sequences and/or that certain mRNA secondary structures might be necessary for YopD-mediated regulation of LcrF synthesis. Thus, further analysis is essential to investigate the criteria YopD requires to bind its target-transcript.

Alternatively, YopD was assumed to repress *lcrF* translation by interfering with the RNA degradation machinery. In particular, a positive effect of YopD on the expression of genes encoding the components of the *Yersinia* degradosome, RNase E, PNPase and RhlB was demonstrated (Steinmann, 2013; Hoßmann, 2017). In general, a relevance of the post-transcriptional regulation, based on mRNA degradation, for the expression of the virulence-associated genes was already reported for *Yersinia* and other pathogens (Rosenzweig *et al*., 2005; Ygberg *et al*., 2006; Yang *et al*., 2008; Rosenzweig & Chopra, 2013; Viegas *et al*., 2013; Chen *et al*., 2016; Chao *et al*., 2017). For instance, in *Y. pseudotuberculosis* RNase E was shown to be implicated in regulation of the T3SS and was crucial for survival within macrophage-like cells (Yang *et al*., 2008; Schiano & Lathem, 2012). In *Salmonella*, RNase E is essential for virulence in mice and in *Galleria mellonella* infection models, survival within macrophages, biofilm formation and antibiotic susceptibility (Lee & Groisman, 2010; Viegas *et al*., 2013; Saramago *et al*., 2014; Chao *et al*., 2017). PNPase was shown to modulate the steady-state amounts of T3SS-associated

transcripts, by regulating the rate of secretion in *Y. pseudotuberculosis*. This explains why a *Y. pseudotuberculosis* strain deficient for the *pnp* gene was less virulent in the murine model compared to the wild type strain (Rosenzweig *et al*., 2005; Rosenzweig *et al*., 2007). In *Salmonella*, PNPase reduced the expression of genes from the SPI-1 and SPI-2 pathogenicity islands, affecting both invasion and intracellular growth of the pathogen (Clements *et al*., 2002; Ygberg *et al*., 2006). Deletion of *pnp* in *E. coli* O157:H7 resulted in decreased ability to adhere to epithelial cells and cattle colonic explant tissues (Hu & Zhu, 2015). Similarly, PNPase was shown to control virulence, motility, as well as colonization and adhesion/invasion properties in *Campylobacter jejuni* (Haddad *et al*., 2012). In *Pseudomonas aeruginosa*, PNPase does not only control the T3SS and virulence but also interferes with the Csr/Rsm system, by regulating the stability of the RsmY/RsmZ sRNAs (Chen *et al*., 2016). Another degradosome component, the DEAD-box RNA helicase RhlB, is involved in RNase E- and PNPase-mediated RNA cleavage and was reported to enhance the activity of these two enzymes (Khemici *et al*., 2005; Py *et al*., 1996). In this way, RhlB might also play a role in regulation of the *Yersinia* T3SS. Interestingly, the DEAD-box RNA helicase RhpA, associated with the degradosome of *Helicobacter pylori*, was demonstrated to be crucial for motility and the ability of the major gastric pathogen to colonize in a mouse model (El Mortaji *et al*., 2018). Additionally, RNA helicase DeaD was shown to stimulate translation of the LcrF homolog ExsA and to promote expression of the *P. aeruginosa* T3SS (Intile *et al*., 2015). Taken together, this emphasizes an important role of the degradosome components in virulence regulation of several pathogenic bacteria.

The present study demonstrated an inhibitory effect of RNase E, PNPase and RhlB on *lcrF* expression in *Y. pseudotuberculosis*. Both *lcrF* transcript and LcrF protein levels were increased in stains deficient for each of the degradosome components compared to the wild type (Fig. 3.4). Although, synthesis of the T3SS activator LcrF was elevated in Δ*rne* and Δ*pnp* of *Y. pseudotuberculosis*, deletion of the *rne* and *pnp* genes resulted in a decreased Yop secretion rate (I. Vollmer, unpublished). These data are in good agreement with the published results, demonstrating an impaired secretion of Yops despite of their increased synthesis in *Y. pseudotuberculosis* and *Y. pestis* Δ*pnp* strains (Rosenzweig *et al*., 2005; Rosenzweig *et al*., 2007). Interestingly, PNPase-mediated repression of the T3SS transcriptional activator InvF, which represents a homolog of *Yersinia* LcrF, was also discovered in *Salmonella*. However, in contrast to *Yersinia*, loss of PNPase in *Salmonella* enchances its virulence, increasing the invasion and intracellular growth rate, and promotes an acute infection (Clements *et al*., 2002). Contrary to *Yersinia* and *Salmonella*, in *P. aeruginosa* both, expression of the LcrF homolog, ExsA, and the T3SS-associated genes, were positively affected by PNPase activity (Chen *et al*., 2016). Thus, it seems that PNPase plays different roles in the regulation of T3SS in *Yersinia*, *Salmonella*, and *P. aeruginosa*, which strongly suggests different regulatory traits or mechanisms for PNPase-mediated control.

The results of this work support the hypothesis of a YopD-mediated repression of *lcrF* translation via positive regulation of the RNA-degrading enzymes. However, the precise mechanism of the YopD-mediated positive influence on RNase E and PNPase synthesis is poorly understood. It is known that both RNase E and PNPase autoregulate their own

synthesis by binding to the 5'-UTR of their own transcript to facilitate its degradation. For RNase E, autoregulation represents a key mechanism for maintaining its cytosolic levels and preventing the toxic effect of *rne* overexpression (Mudd & Higgins, 1993; Jain & Belasco, 1995; Sousa *et al*., 2001). Interestingly, RNase E of *E. coli* employs autoregulation to continuously adjust its synthesis to the level of its substrates that appears to be a common behavior among several autoregulated proteins (Craig & Gross, 1991, Comer *et al*., 1996; Sousa *et al*., 2001). The 5'-UTR of the *rne* transcript, responsible for RNase E autoregulation, is phylogenetically conserved and highly structured, consisting of three hairpin structures and three single stranded regions, that are also present in *Y. pseudotuberculosis*. The hairpin 2 and, to a lesser extent, the hairpin 3 structures of the *rne* 5'-UTR were shown to be essential for autoregulation of RNase E synthesis (Diwa *et al*., 2000).

Autoregulation of PNPase expression differs from that of RNase E. Up to date, two models explaining the autoregulation have been proposed. According to the first model, PNPase requires the presence of an additional RNA degrading enzyme, RNase III, to confer autoregulation (Robert-Le Meur & Portier, 1992; Jarrige *et al*., 2001). In fact, a large secondary hairpin structure in the 5'-UTR of the *pnp* transcript is cleaved by RNase III, resulting in a 37-nucleotide-long 5' RNA fragment (RNA37) that still basepairs with the downstream sequence. This cleavage structure both allows *pnp* translation and prevents accelerated degradation by RNase E. However, the remaining 2 nt extension of RNA37 is recognized by PNPase, leading to a 3'-to-5' degradation of the newly generated 5' fragment. After processing, the resulting *pnp* transcript is subject to an undiscovered translation repression mechanism and/or RNase E-mediated and PNPase-independent degradation. Consequently, the purpose aim of PNPase in this autoregulation model is to remove the 5' fragment of the RNase III-cleaved structure (Robert-Le Meur & Portier, 1992; Robert-Le Meur & Portier, 1994; Jarrige *et al*., 2001; Carzaniga *et al*., 2009). According to the second model, PNPase autocontrols its synthesis independently of the RNase III catalytic activity. Intriguingly, this pathway only requires the RNA binding domains KH and S1 but not the phosphorolytic activity of PNPase. Carzaniga and collaborators suggest that the RNase III-independent autoregulation occurs via repression of *pnp* translation, most probably through competition between PNPase and the ribosomal protein S1 for the *pnp* primary transcript (Carzaniga *et al*., 2015). Recently, the small non-coding RNA SraG was shown to control *pnp* expression in *E. coli* in both, RNase III-dependent and independent autoregulatory pathways (Fontaine *et al*., 2016). The SraG-encoding gene is located in the region between *rpsO*, encoding the ribosomal protein S15, and *pnp* coding sequences and is transcribed in the opposite direction to these two genes (Argaman *et al*., 2001). Overexpression of SraG represses *pnp* expression (i) by decreasing the *pnp* transcript stability, and (ii) by preventing the translation initiation of *pnp*. Moreover, Fontaine and collaborators were able to show, that the SraG-mediated post-transcriptional control of *pnp* expression occurs via direct antisense interaction between SraG and *pnp* RNAs (Fontaine *et al*., 2016). However, investigation of SraG function in *Y. pseudotuberculosis* revealed no effect on *pnp* expression (Lu *et al*., 2012).

In this study, a direct interaction between the YopD-LcrH complex and the 5'-UTRs of *rne* and *pnp* transcripts was detected (Fig. 3.5 and Fig. 3.6, respectively). Taking into account a positive influence of YopD on RNase E and PNPase synthesis (Steinmann, 2013; Hoßmann, 2017), it is likely that the direct binding of YopD increases the stability of *rne* and *pnp* transcripts. Indeed, YopD and RNase E share their preference for targeting AU-rich sequences (Diwa *et al*., 2000; Cambronne & Schneewind, 2002). Thus, YopD binding to the 5'-UTRs of *rne* and *pnp* mRNAs might be able to mask at least the RNase E cleavage site, preventing the RNase E-dependent degradation of *rne* and *pnp* transcripts. Remarkably, comparative analysis of RNase E autoregulatory activity under conditions non-permissive and permissive for Yop secretion revealed that the overall expression level of *rne'-'lacZ*, serving as a readout for RNase E autoregulatory activity was higher under secretion conditions (Fig. 3.3). This further confirms that YopD positively affects RNase E synthesis. In fact, liberation of intracellular YopD upon secretion results in reduction of the RNase E level and decreases the internal RNase E / RNase E substrate ratio. Consequently, available RNase E is sequestered by its substrates, rather than by its own 5'-UTR. A similar principle was described in *E. coli*, where RNase E autoregulation was abolished by overexpression of the RNase E substrate due to the elevated RNase E / RNase E substrate ratio (Sousa *et al*., 2001).

Recently, an additional mechanism of YopD-mediated indirect regulation of LcrF synthesis has been discovered. Wang and collaborators were able to demonstrate, that *Yersinia* achieves rapid changes in pYV-encoded gene expression just by increasing/decreasing the plasmid copy number. The common 70-kb virulence plasmid of pathogenic *Yersinia* represents an IncFII-class plasmid, whose replication is initiated by the RepA protein (Nordström, 2006). In fact, once *Yersinia* infects the mammalian host or senses the low calcium signal *in vitro*, the pYV copy number rapidly rises from ~1 to ~3 per chromosomal equivalent (Wang *et al*., 2016). Interestingly, YopD was shown to abolish the secretion-mediated plasmid copy number increase in *Yersinia* (Wang *et al*., 2016). Consistent with these data, analysis of the *Yersinia* transcriptome, carried out in the present study, demonstrated that YopD influences the expression level of *repA* (Fig. S9 A). Taking into account the respective gene dose of pYV-encoded genes (Fig. S9 B), YopD appears to influence *repA* expression indirectly via control of the *repA*-regulators, *copA* and CopB (P. Engling, unpublished).

4.1.2 CsrA - an RNA-binding protein that represses *lcrF* transcription

CsrA (RsmA/E) represents the central component of an extensively studied carbon storage regulatory system (Csr/Rsm). This system is widely distributed among bacteria and is involved in global regulation of numerous essential cellular processes, such as carbon flux, secondary metabolism, biofilm formation, and quorum sensing. Moreover, it becomes evident that the Csr/Rsm system is indispensible for the adaptation to dramatic environmental alterations of numerous bacterial pathogens (Timmermans & Van Melderen, 2010; Heroven *et al*., 2012; Romeo *et al*., 2013; Oliva *et al*., 2015; Vakulskas *et al*., 2015; Kusmierek & Dersch, 2018). For instance, CsrA possesses a pleiotropic effect on *Y. pseudotuberculosis* physiological- and- stress-related processes and renders the

pathogen avirulent in the murine infection model (Heroven *et al*., 2008; Heroven *et al*., 2012; Nuss *et al*., 2017). Strong reduction of *Y. pseudotuberculosis* virulence in the absence of *csrA* perfectly correlates with an impaired synthesis of the major virulence activator LcrF and, subsequently, with decreased expression of the T3SS-associated genes as well as Yop secretion *in vitro* (Nuss *et al*., 2017).

However, preliminary data of our group suggest that CsrA plays a multi-faceted role in the regulation of the *Yersinia* T3SS, affecting the expression of *lcrF* in a dual manner (Opitz, 2013; Pimenova, 2014). In particular, under conditions non-permissive for Yop secretion, CsrA seems to repress LcrF synthesis at the transcriptional level (Opitz, 2013; Pimenova, 2014). Consistent with the previous observations, global analysis of the *Y. pseudotuberculosis* transcriptome, carried out in the present study, demonstrated an elevated *lcrF* expression level in the absence of *csrA* compared to the wild type strain under non-permissive conditions (Fig. 3.22; for *yscW* $\log_2$FC=1.82, adjusted p-value <0.05; for *lcrF* $\log_2$FC=1.08, adjusted p-value <0.05). Moreover, complementation of the *Y. pseudotuberculosis csrA*-deficient strain with a *csrA*$^+$ plasmid, performed in this work, further confirmed the negative effect of CsrA on *lcrF* transcription under non-secretion conditions (Fig. 3.7). Interestingly, it was demonstrated that the luciferase activity of a reporter fusion harboring solely the promoter region of the *yscW-lcrF* operon (-42 to +24 nt with respect to the *yscW-lcrF* transcriptional start site) was still CsrA-dependent (Pimenova, 2014). Indeed, replacement of P_{yscW} by the artificial P_{lac} or P_{tet} promoter eliminated CsrA-dependent transcriptional regulation (Fig. 3.7), indicating that CsrA downregulates *lcrF* transcription via sequences in or close to the P_{yscW} promoter. The CsrA-dependent regulation of LcrF synthesis at the transcriptional level was rather unexpected, as CsrA is generally known to affect its targets at the post-transcriptional level via binding to the mRNA (Schubert *et al*., 2007; Holmqvist *et al*., 2016). Thus, CsrA most likely inhibits *lcrF* transcription indirectly, affecting a so far unidentified transcriptional regulator (Pimenova, 2014). For this, CsrA might positively regulate a transcriptional repressor and/or inhibit a transcriptional activator of LcrF (Fig. 3.8). Hence, it was tempting to discover the missing link in CsrA-mediated regulation of *lcrF* transcription.

Up to date, three direct regulators of *lcrF* transcription have been described (Fig. 3.8). The *Yersinia* modulator A (YmoA) forms a heterocomplex with H-NS and represents a transcriptional repressor of LcrF (Böhme *et al*., 2012). In contrast to the YmoA-H-NS complex, both IscR and RcsB positively affect *lcrF* transcription (Li *et al*., 2014; Miller *et al*., 2014). However, analysis of regions targeted by the aforementioned regulators of *lcrF* transcription, revealed that only the RcsB binding-box is almost perfectly covered by the empirically predicted CsrA-dependent sequence (Fig. 3.8). Consequently, the transcriptional activator RcsB seems to be a predestined candidate for CsrA-mediated repression of *lcrF* transcription.

RcsB is a response regulator of the Rcs phosphorelay system, also assigned as a non-orthodox two-component system, which is widely employed by the family of *Enterobacteriaceae* for sensing, response and adaptation to environmental alterations (Guo & Sun, 2017). The Rcs system consists of three core proteins, the transmembrane sensor kinase RcsC, the transmembrane sensor protein RcsD, that lacks kinase activity, and the

response regulator RcsB. Both, RcsC and RcsB represent the canonical components of bacterial two-component systems (Majdalani & Gottesman, 2005; Clarke, 2010). Apart from the core members, various accessory components of the Rcs system have also been described, such as the auxiliary regulator RcsA and the envelope stress sensing lipoprotein RcsF (McCallum & Whitfield, 1991; Majdalani *et al*., 2005; Konovalova *et al*., 2016). Remarkably, the Rcs system was shown to exhibit a global effect on bacterial gene expression. Predominantly, the environmental stress-related genes as well as genes implemented in the synthesis of essential cell surface-associated structures, such as LPS, flagella, fimbriae, and exopolysaccharides are controlled by the Rcs phosphorelay (Fredericks *et al*., 2006; Carter *et al*., 2012; McMahon *et al*., 2012; Tao *et al*., 2012; Miajlovic *et al*., 2014; Farizano *et al*., 2014; Fang *et al*., 2015). Consequently, this non-canonical two-component system is responsible for remodeling the cell surface and metabolism for successful adaptation to various environments and it contributes to bacterial virulence (Guo & Sun, 2017). For instance, in *E. coli*, RcsB influences expression of LEE (locus for enterocyte effacement)-encoded genes, affecting the transcriptional regulators GrvA and PchA, and is essential for colonization of the mouse intestine (Tobe *et al*., 2005; Lasaro *et al*., 2014). In *Serratia marcescens*, the Rcs phosphorelay controls biogenesis of the outer membrane vesicles (OMVs), involved in the toxin delivery, and synthesis of the pore-forming toxin ShlA, responsible for early activation of autophagy in host cells (Di Venanzio *et al*., 2014; McMahon *et al*., 2012). In *S. enterica* serovar Typhimurium, Rcs phosphorelay must be strictly repressed during the early stages of infection, while it has to be active at stages when the pathogen undergoes intracellular growth (Arricau *et al*., 1998; Detweiler *et al*., 2003; Domínguez-Bernal *et al*., 2004; Mouslim *et al*., 2004; Bulmer *et al*., 2012). A similar scenario is conceivable for *Y. pseudotuberculosis*, where disadvantageous overproduction of LcrF under conditions non-permissive for T3S might be blocked by CsrA-mediated repression of the transcriptional activator RcsB.

In the present study it was demonstrated that RcsB expression and activity is significantly elevated in the absence of *csrA* (Fig. 3.9). These results were further supported by the RNA sequencing data, where *rcsB* expression was strongly increased in the *Y. pseudotuberculosis csrA*-deficient strain compared to the wild type strain under non-secretion conditions ($log_2FC=1.38$; adjusted p-value <0.05). Moreover, it was shown that CsrA negatively influences RcsB synthesis by decreasing the *rcsB* transcript stability (Fig. 3.9). Notably, the 5'-UTR of the *rcsB* mRNA contains one GGA motif, which could be targeted by CsrA. This GGA motif overlaps with the SD-sequence located at position -19 to -16 with respect to the translational start site of *rcsB*. Thus, CsrA binding might prevent access of the ribosome and enhance degradation of the *rcsB* transcript. However, only one GGA motif might be insufficient for CsrA-binding. Thus, additional factors could be implicated in the CsrA-dependent destabilization of the *rcsB* mRNA. Since the RcsB functionality was also compromised in the presence of *csrA*, it cannot be excluded that CsrA interferes with the RcsB phosphorylation process, thus preventing RcsB activation. Indeed, the transcriptome data of the present work demonstrated an increased level of *rcsC* expression, responsible for RcsB phosphorylation, in the *csrA*-deficient strain

($log_2FC=1.67$; adjusted p-value <0.05). This observation was also supported by Northern blotting (Fig. S10). Thus, CsrA not only affects RcsB synthesis but might also impair RcsB phosphorylation via negative regulation of the sensor kinase RcsC. Collectively, these data indicate the involvement of RcsB in the CsrA-mediated regulation of *lcrF* transcription.

4.1.3 YopD and CsrA: concerted action of two riboregulators aimed to prevent the detrimental LcrF overproduction

Previous data of our group demonstrated that intracellular YopD, in complex with its chaperone LcrH, positively affects CsrA synthesis at the post-transcriptional level (Steinmann, 2013; Hoßmann, 2017). Thus, YopD can promote CsrA-mediated repression of *lcrF* transcription. Combining these data with results of the present work allowed construction of a complex model describing the regulation of LcrF production under conditions non-permissive for Yop secretion in *Y. pseudotuberculosis* (Fig 4.1). The mammalian host temperature (37 °C) induces LcrF synthesis, leading to expression of the T3SS-associated genes. However, in the absence of the secretion signal (+Ca^{2+} *in vitro* or no host cell contact *in vivo*) the excessive production of T3SS components is prevented through an inhibitory feedback loop. This mechanism is mediated by the YopD-LcrH complex, which decreases *lcrF* transcript stability via direct binding to the *lcrF* 5'-UTR and/or positive regulation of LcrF repressors, such as the components of the degradosome (RNase E, PNPase and RhlB) and the global regulator CsrA. The latter inhibits *lcrF* transcription by negative regulation of the transcriptional activator RcsB, reducing *rcsB* mRNA stability. Additionally, YopD prevents replication of the virulence plasmid. This circuit offers numerous access points to fine-tune the LcrF synthesis.

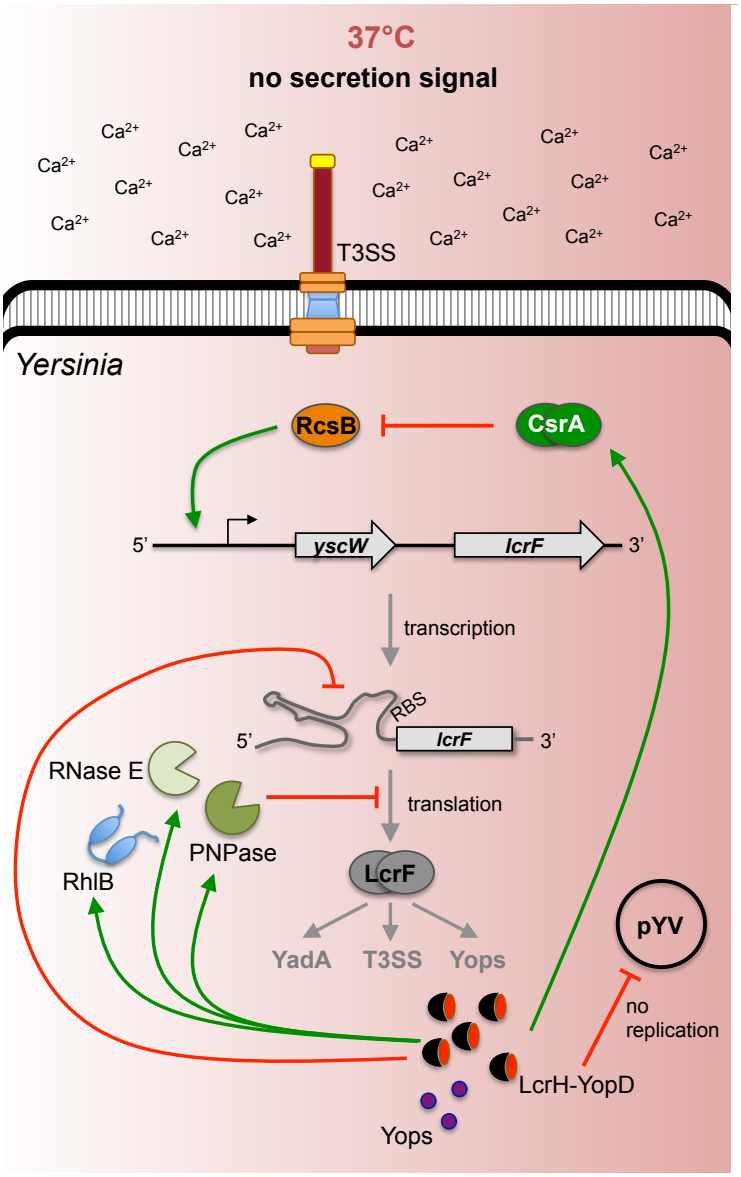

Figure 4.1. Model of the regulatory network involved in the control of LcrF production under conditions non-permissive for Yop secretion.
The figure demonstrates the crucial virulence determinants involved in the regulation of LcrF synthesis under non-secretion conditions. The green arrows and the red T lines indicate positive or negative influence on gene expression and/or protein synthesis, respectively.

4.2 Low Calcium Response: the trigger of *Yersinia* type III secretion

Yersinia possesses the ability to induce massive secretion of Yops at 37 °C in response to low Ca^{2+} concentrations (≤ 80 µM) in the growth medium (Kupferberg & Higuchi, 1958; Lee *et al*., 2001). This phenomenon is also accompanied by severe growth restriction and is referred to as the low calcium response (LCR) (Cornelis *et al*., 1998). Although LCR is widely applied for the activation of T3SS-associated genes in *Yersinia*, the nature of this phenomenon is still not completely resolved. Paradoxically, upon contact with eukaryotic cells *Yersinia* is capable to express and translocate T3SS components even in Ca^{2+}-rich milieu (Kugelmass, 1959; Rosqvist *et al*., 1994; Cornelis & Wolf-Watz, 1997; Cornelis *et al*., 1998). Based on this finding, competition between Ca^{2+} ions and a host cell receptor at the bacterial surface was suggested (Fowler *et al*., 2009). Additionally, insertion of the T3S needle complex into the eukaryotic cell may permit *Yersinia* to estimate the intracellular calcium concentration and trigger the type III pathway (Lee *et al*., 2001). Regarding the growth restriction during the Ca^{2+} limitation, it has been shown that the wild type *Y. pestis* gains sensitivity to Na^{+} ions when the T3SS becomes active, leading to bacteriostasis (Fowler *et al*., 2009). Thus, Ca^{2+}-blind mutants, in which the T3SS is present in the permanent "off-state", are resistant to Na^{+}-mediated toxicity. Vice versa, no LCR-dependent growth defect occurs when Na^{2+} is omitted from the medium (Fowler *et al*., 2009).

Recent data of our group demonstrated the importance of growth at body temperature for the LcrF-dependent activation of the *Yersinia* T3SS *in vitro* (Pimenova, 2014). In fact, *lcrF* expression was only induced when bacteria were grown in Ca^{2+}-deprived medium at 37 °C but not at 25 °C. Additionally, it has been shown that at least one of the possible Ca^{2+}-sensitive elements is located in the 5'-UTR of the *yscW-lcrF* transcript, approximately in the region +28 to +428 nucleotides with respect to the transcriptional site of *yscW* (Pimenova, 2014). Surprisingly, this low calcium-responsive element turned out to be CsrA-dependent, as no induction of *yscW-lcrF* transcription was detected in the absence of *csrA*. Moreover, a direct interaction between CsrA and the 5'-UTR of *yscW* was detected (Hoßmann, 2017). Considered together, these data indicate that CsrA, apart from its repressive role under non-permissive conditions, might positively affect LcrF synthesis during Ca^{2+}-deprivation (Pimenova, 2014). Thus, the present study was aimed to further investigate the role of CsrA in the LCR of *Y. pseudotuberculosis* as well as to clarify the molecular mechanism underlying the CsrA-mediated regulation of LcrF synthesis under secretion conditions.

4.2.1 Role of CsrA for the Low Calcium Response

The present work demonstrated a positive influence of CsrA on the LCR in *Y. pseudotuberculosis*. This is achieved via post-transcriptional regulation of LcrF synthesis (Fig. 3.10). Quantitative analysis of the *lcrF* transcript and the LcrF protein levels under non-secretion *versus* secretion conditions revealed that CsrA is indispensible for increasing the translation efficiency of *lcrF* under Ca^{2+} limitation (Fig. 3.10 B). Two

possible scenarios for CsrA-mediated post-transcriptional regulation of LcrF production were proposed and examined in this study. The first model suggests that CsrA might be involved in stimulation of the *lcrF* translation initiation. An initial indication for this mode of action was obtained by comparing the expression of a translational P_{BAD}::*lcrF'*$_{(-123\ to\ +75\ nt)}$-*'lacZ* reporter gene fusion in the *Y. pseudotuberculosis* wild type and the *csrA*-deficient strain under secretion conditions (Fig. 3.11). Use of this construct allowed uncoupling of the CsrA-mediated transcriptional and post-transcriptional regulation of LcrF synthesis. Reduced expression of P_{BAD}::*lcrF'*$_{(-123\ to\ +75\ nt)}$-*'lacZ* in the absence of *csrA*, which could be restored to the wild type level through complementation with a $csrA^+$ plasmid, indicated a positive effect of CsrA on the *lcrF* translation initiation. Consistently, implementation of the *in vitro* translation approach for the investigation of *lcrF* translation initiation in presence or absence of CsrA provided additional evidence that CsrA stimulates *lcrF* translation (Fig. 3.12 C). Furthermore, CsrA was shown to affect *lcrF* translation independently of the presence of *yopD*. This was not surprising as, according to the results of this study, YopD regulates LcrF synthesis, decreasing the *lcrF* transcript stability but not the *lcrF* translation efficiency (Fig. 3.1). Since the SD sequence of *lcrF* is located inside a stemloop structure, it was intriguing to explore, whether CsrA increases the *lcrF* translation efficiency via stabilization of the stemloop in an "opened" conformation favoring ribosomal access. Indeed, CsrA-dependent elevation of *lcrF* translation was observed even when the complementarity within the SD-containing hairpin II structure was reduced by a nucleotide substitution (GUU-30/-28AAA) in the 'four U' element (Fig. 3.12 A, B). Interestingly, previous data of our group demonstrated a weak interaction between CsrA and the 5'-UTR of *lcrF* (Hoßmann, 2017). Accordingly, although the weak binding of CsrA to the GGA motif in the SD-sequence is sufficient to hold the *lcrF* hairpin II in an "opened" state, it is not strong enough to prevent binding of the ribosome. In this way, CsrA interaction with the SD sequence enhances instead of represses *lcrF* translation. A similar mode of action was observed for the CsrA homolog RsmA in *P. aeruginosa*. Here, binding of RsmA to a GGA motif located 21 nt upstream of the *phz2* (phenazine biosynthetic gene cluster) SD sequence led to destabilization of the stemloop structure and, subsequently, improved ribosome access (Ren *et al*., 2014). In *E. coli*, CsrA was reported to activate the expression of the *moaA* gene at the post-transcriptional level without altering the *moaA* transcript amounts (Patterson-Fortin *et al*., 2013). MoaA is implicated in biosynthesis of the molybdenum cofactor (Moco) that represents a redox center in enzymes of anaerobic metabolism (Mendel, 2013). The untranslated leader region of the *moaA* mRNA represents a Moco-responsive riboswitch and mediates feedback inhibition of the Moco biosynthesis pathway. Binding of CsrA to the 5'-UTR of the *moaA* transcript led to alterations in the *moaA* mRNA structure, preventing the Moco-mediated repression of translation (Patterson-Fortin *et al*., 2013). In the phytopathogen *Xantomonas citri* subsp. *citri*, RsmA was reported to stimulate the expression of the T3SS-encoding genes *hrp*/*hrc* through direct positive regulation of the master regulator HrpG. In this case, interaction between RsmA and the untranslated leader sequence resulted in elevated translation efficiency as well as stabilization of the *hrpG* transcript (Andrade *et al*., 2014). Thus, another possible scenario for CsrA-mediated regulation of LcrF synthesis under secretion conditions is that CsrA contributes to stabilization of the *lcrF* transcript.

The *lcrF* transcript itself seems to be innately highly unstable, which is reflected by smaller-size degradation products in Northern blot assays, irrespective of the presence of *csrA* (Fig. 3.13). This is also in agreement with the results of the primer extension assay performed in our group, showing several abrogation sites within the 5'-UTR of *yscW* (Böhme *et al*., 2012). The pronounced metabolic instability of the *lcrF* mRNA most probably represents an additional regulatory checkpoint, which acts constitutively in order to prevent the detrimental overproduction of the T3SS components. The present work demonstrated that the *yscW-lcrF* mRNA is also actively processed from the 3' end, as more than a half of the 3' ends obtained via 3'-RACE were scattered over the *lcrF* coding sequence. Moreover, deletion of the 3'-UTR resulted in significant prolongation of the *lcrF* transcript half-life from ~5 min for the wild type *lcrF* to ~21 min for the Δ3'-UTR *lcrF* (Fig. 3.15 A, B). According to the results of the 3'-RACE assay, the most frequently cleaved site is located ~8 nt downstream of the *lcrF* stop codon (Fig. 3.14 A; Fig. S3). Computational prediction of the *lcrF* 3'-UTR structure with a RNA fold software (mfold [http://mfold.rna.albany.edu/?q=mfold]) suggested the presence of a typical Rho-independent terminator structure consisting of a stable stemloop at positions 9 to 28 nt downstream of the *lcrF* stop codon and the U-rich sequence (von Hippel, 1998). This implies that the 3'-UTR of *lcrF* would comprise at least 32 nt downstream of the *lcrF* stop codon (Fig. 3.14 B; Fig. S3). However, the longest 3'-RACE fragment placed the 3' end at position 22 nt downstream of the *lcrF* stop codon (Fig. 3.14; Fig. S3). Another option would be, that the termination of *lcrF* transcription occurs in a Rho-dependent manner and, consequently, that the 3'-UTR of *lcrF* contains no Rho-independent terminator structure. Indeed, sequence analysis by ARNold (Naville *et al*., 2011) failed to identify a Rho-independent transcription terminator in the 3'-UTR of *lcrF*. Although this model is a better match compared with the length of the experimentally determined 3'-UTR, the sequence of the *lcrF* 3'-UTR does not match the requirements for Rho-dependent termination. In particular, high-C content, which is not the case for the *lcrF* transcript, is essential for Rho activity (Richardson, 2002; Banerjee *et al*., 2006). Taken together, it is likely that the *lcrF* transcript undergoes Rho-independent termination, and that the 3'-UTR of *lcrF* is recognized and actively targeted by RNases, most probably at a position 8 nt downstream to the *lcrF* stop codon. Thus, the 3'-UTR of the *lcrF* transcript might serve as a regulatory element initiating degradation of the *lcrF* mRNA.

The involvement of 3'-UTRs in the post-transcriptional regulation of gene expression has been widely explored in eukaryotes (St Johnston, 1995; Pesole *et al*., 2001; Wilkie *et al*., 2003; Malka *et al*., 2017). In contrast to eukaryotes, the 3'-UTRs of prokaryotes have traditionally been believed to contain only transcriptional terminator structures. However, during the last few decades, significant progress has been made in understanding the prokaryotic 3'-UTR-mediated post-transcriptional gene regulation (Ren *et al*., 2017). The following mechanisms have been described: (i) targeting of the 3'-UTRs by a ribonuclease initiating the mRNA decay (Maeda & Wachi, 2012; López-Garrido *et al*., 2014; Liu *et al*., 2016; Zhu *et al*., 2016), (ii) regulation via the 3'-UTR-derived regulatory sRNAs (Chao *et al*., 2012; Kim *et al*., 2014; Miyakoshi *et al*., 2015; Chao & Vogel, 2016; Peng *et al*., 2016), (iii) targeting of the 3'-UTRs by regulatory sRNAs (Opdyke *et al*.,

2004; Silvaggi *et al*., 2005), and (iv) basepairing interaction of 3'-UTRs with 5'-UTRs, affecting translation initiation (Balaban & Novick, 1995; Felden *et al*., 2011; Thisted *et al*., 1995; Ruiz de los Mozos *et al*., 2013).

Similar to the 3'-UTR-mediated regulation of *lcrF* in *Y. pseudotuberculosis*, the 3'-UTR of *aceA* in *Corynebacterium glutamicum* was shown to negatively affect the expression of its own gene, encoding for the isocitratelyase, catalyzing the cleavage of isocitrate to succinate and glyoxylate. Analysis of the 63 nt long *aceA* 3'-UTR revealed the presence of a single stranded AU-rich sequence, suggested to serve as a cleavage target for RNase E/G (Maeda & Wachi, 2012). Another example of 3'-UTR-mediated autoregulation was described in *S. enterica*. The 310 nt long 3'-UTR of the *hilD* transcript, which encodes a transcriptional regulator of SPI-1, decreases the HilD synthesis by serving as a target for the degradosome-associated proteins, RNase E and PNPase (López-Garrido *et al*., 2014). In contrast to the 3'-UTRs of *lcrF*, *aceA* and *hilD*, harboring a Rho-independent transcription terminator (Maeda & Wachi, 2012; López-Garrido *et al*., 2014), the 3'-UTR of *hmsT*, encoding a diguanylate cyclase essential for biofilm formation in *Y. pestis*, possess a Rho-dependent terminator (Kirillina *et al*., 2004; Zhu *et al*., 2016). Further analysis revealed, that PNPase is implicated in the 3'-UTR-mediated repression of *hmsT* expression. Remarkably, it has been demonstrated that the PNPase-mediated turnover of *slrA* mRNA in *Bacillus subtilis* requires a Rho-dependent terminator lacking any specific regulatory structure (Liu *et al*., 2016; Zhu *et al*., 2016). The 3'-UTRs of *aceA* and *hilD*, in turn, contain a specific single stranded AU-rich region, which might be targeted by an endonuclease, initiating transcript decay (Maeda & Wachi, 2012; López-Garrido *et al*., 2014). Thus, the involvement of specific RNases in the 3'-UTR-mediated degradation depends on the topology of the 3'-UTR. Although, the 3'-UTR of *lcrF* in *Y. pseudotuberculosis* explored in the present work is AU-rich, the longest AU-stretch is sequestered in a stemloop as predicted by the RNA fold software (mfold [http://mfold.rna.albany.edu/?q=mfold]). This makes it inaccessible for RNase E, which targets only single-stranded RNA (Laalami *et al*., 2014; Redko *et al*., 2003). Nevertheless, it is possible that the stemloop structure can be destabilized in the presence of additional factors, enabling its recognition and cleavage by an endonuclease. For instance, preliminary data of our group demonstrated that YopD is able to bind to the 3'-UTR of the *lcrF* transcript (J. Hoßmann, unpublished). This interaction might lead to conformational changes, preventing the formation of the double-stranded structure in the 3'-UTR of the *lcrF* transcript and, consequently, the endonuclease-mediated initiation of *lcrF* mRNA degradation. Thus, the 3'-UTR of *lcrF* might also be involved in YopD-mediated repression of LcrF synthesis. Additionally, RhlB, shown to downregulate *lcrF* expression (Fig. 3.4), might unwind the RNA duplex in the 3'-UTR, promoting degradation of the *lcrF* mRNA (Holmqvist & Vogel, 2018). Furthermore, other factors implicated in sensing and/or transmission of the low calcium signal might either destabilize the stemloop under non-permissive conditions, or protect *lcrF* from the 3'-UTR-mediated degradation by stabilizing the double-stranded structure in the presence of the triggering signal. Alternatively, processing of the stemloop structure in the 3'-UTR of *lcrF* can occur in an

RNase III-dependent manner, followed by PNPase-mediated decay, as described for the *pnp* transcript (Carzaniga *et al*., 2009; Nicholson, 2014).

This work demonstrated a reduced stability of the *lcrF* mRNA in the *csrA*-deficient strain compared to the wild type and *yopD*-deficient strains, grown under conditions permissive for Yop secretion (Fig. 3.13). Interestingly, deletion of *yopD*, known to destabilize the *lcrF* transcript, did not protect the *lcrF* mRNA from rapid degradation when *csrA* was also absent. These results emphasize the critical role for CsrA in the prolongation of *lcrF* transcript stability. Up to now, CsrA-mediated stabilization of a targeted transcript was quite unusual and was manifested only in *X. citri* subsp. *citri* (Andrade *et al*., 2014; described above) and in *E. coli* (Wei *et al*., 2001; Yakhnin *et al*., 2013). In *E. coli*, binding of CsrA to two motifs located in the 5'-UTR of the *flhDC* mRNA prohibited RNase E-mediated decay of the *flhDC* transcript (Wei *et al*., 2001; Yakhnin *et al*., 2013). Previous results from our group demonstrated that CsrA is able to interact with the 5'- and the 3'-UTRs of the *lcrF* transcript, suggesting a direct protective effect against the degradation process (Hoßmann, 2017; J. Hoßmann, unpublished data). However, extensive search for the CsrA-responsive element performed in this study provided no evidence that CsrA stabilizes the *lcrF* transcript through binding to the 5'- or the 3'-UTR as well as to the coding sequence of *lcrF* mRNA (Fig. 3.15; Table 3.2). The 5'-UTR of *yscW*, reported to interact with CsrA (J. Hoßmann, unpublished data), was also not responsible for the CsrA-mediated stabilization of the *lcrF* mRNA (data not shown). Thus, it is likely that CsrA rather affects *lcrF* transcript stability indirectly. For instance, CsrA might interfere with the major degradosome components, which were already shown to downregulate LcrF synthesis, by decreasing the *lcrF* degradation rate (Fig. 3.4).

Indeed, the results obtained in this study demonstrated a negative influence of CsrA on the degradosome components RNase E and PNPase (Fig. 3.16). Recent data from our group indicated that expression of *rhlB* is also downregulated by CsrA (Hoßmann, 2017). Deletion of *csrA* led to a significant increase of the *pnp* transcript level even in the absence of *yopD*. A similar tendency was observed for the *rne* transcript, although it was less prominent than for the *pnp* transcript (Fig. 3.16). Thus, under conditions permissive for type three secretion, CsrA is able to extend the *lcrF* transcript half-life, most probably through the negative regulation of the major degradosome components RNase E, PNPase as well as RhlB. Notably, CsrA seems to downregulate RNase E and PNPase synthesis indirectly, as no interaction between the CsrA protein and the *rne* and *pnp* transcripts was detected (Fig. 3.17).

Up to date, CsrA-mediated regulation was detected for none of the degradosome components except for PNPase (Park *et al*., 2015). In fact, CsrA participates in the negative autoregulation of *pnp* expression in *E. coli*. An absolutely essential prerequisite for CsrA-dependent downregulation of PNPase synthesis is the RNase III- and PNPase-mediated processing of the *pnp* leader RNA, resulting in liberation of CsrA-binding sites, otherwise sequestered in a secondary structure (Carzaniga *et al*., 2009). Since one of the CsrA-targeted sites overlaps the SD sequence, bound CsrA dramatically affects *pnp* translation (Park *et al*., 2015). Consequently, a similar situation is possible for the CsrA-mediated regulation of *pnp* expression in *Y. pseudotuberculosis*. This would explain the

absence of binding between CsrA and the native *pnp* untranslated leader transcript, demonstrated in the present work (Fig. 3.17). However, the 5'-UTR of the *Y. pseudotuberculosis pnp* transcript differs from that of *E. coli*. In contrast to *E. coli* (SD: AAGGA at position -12 to -8 nt relative to the translational start), the SD sequence of *Y. pseudotuberculosis pnp* does not contain a GGA motif (Fig. 3.6; SD: AAGGG at position -12 to -8 nt relative to the translational start). Thus, further investigations are necessary to address whether PNPase synthesis in *Y. pseudotuberculosis* is also controlled via negative autoregulation or whether CsrA is able to interact with the GGA motif of the processed *pnp* 5'-UTR, repressing translation.

4.2.2 Calcium limitation – a global signal

Examination of the immediate (10 min after induction) alterations of the *Y. pseudotuberculosis* transcriptome in response to the low calcium signal revealed a decreased expression of two genes encoding for tRNAs, tRNA-Met and tRNA-Gln, in -Ca^{2+} samples compared to +Ca^{2+} samples (Table 3.1). Preliminary data of our group suggested that the codon frequencies vary among the virulence plasmid- and the chromosomally- encoded genes (M. Volk & M. Kusmierek, unpublished). In particular, several Leu and Lys codons are more abundant on the virulence plasmid but not the Met codon, which is more frequent for the chromosomally-encoded genes. Interestingly, in eukaryotes changes in the tRNA expression level leading to rearrangements of the global tRNA pool represent one of the mechanisms to fine-tune gene expression at the post-transcriptional level (Orioli, 2017). Additionally, a positive correlation between the codon frequencies and the concentration of tRNAs with corresponding anticodons was observed in prokaryotes and several unicellular eukaryotes (Ikemura, 1985; Kanaya *et al*., 1999; Quax *et al*., 2015). Thus, downregulation of the tRNA-Met expression might reflect a start of gene expression reprogramming towards the virulence plasmid genes.

Genes belonging to the class of the small non-coding anti-sense (as) and trans RNAs were also differentially expressed 10 min after Ca^{2+} depletion (Table 3.1). Of special interest is the GcvB transRNA already described to directly abolish the expression of the response regulator PhoP from the PhoP/PhoQ two component system (TCS) in *E. coli* (Coornaert *et al*., 2013). This TCS belongs to the central regulatory system that is activated at low magnesium concentrations or in presence of antimicrobial peptides. The PhoP/PhoQ system controls dozens of genes involved in crucial cellular functions such as cell envelope composition maintenance, acid resistance, magnesium homeostasis and bacterial virulence (Zwir *et al*., 2005; Vadyvaloo *et al*., 2015). However, since in *Y. pseudotuberculosis* YPIII PhoP is not functional (Grabenstein *et al*., 2004), GcvB-mediated negative regulation of the PhoP/PhoQ TCS cannot contribute to low calcium signal sensing. Nevertheless, GcvB was shown to target more then 20 different mRNAs and to inhibit the expression of numerous genes involved in amino acid transport and metabolism (Urbanowski *et al*., 2000; Sharma *et al*., 2007). Thus, GcvB represents a promising factor for establishment of the LCR in *Y. pseudotuberculosis*. Further investigations of the immediate alterations of the *Y. pseudotuberculosis* transcriptome in response to the low calcium signal will provide new insights into the nature of the LCR phenomenon.

Global transcriptome profiling of the *Y. pseudotuberculosis* wild type strain in response to the low calcium signal (four hours after induction) in comparison to non-permissive conditions revealed a strong upregulation primarily of the virulence plasmid-encoded genes (Fig. 3.22, Table S3). Accordingly, expression of *lcrF* and of the LcrF-dependent, T3SS-associated genes was found to be significantly increased in the absence of Ca^{2+}. In parallel, almost half of the chromosomally-encoded genes were downregulated in response to Ca^{2+}depletion (Fig. 3.21, Table S3). Especially, the expression of metabolic genes was negatively affected under secretion conditions, most likely leading to the observed growth arrest. These data further confirm the previously discovered typical characteristics of the LCR in *Y. pseudotuberculosis*: (i) elevated expression of the pYV-encoded genes and (ii) growth restriction (Cornelis *et al*., 1998).

Apart from the T3SS-associated genes, three ncRNAs (Ysr290, Ysr298 and Ysr299), encoded on the virulence plasmid, were found to be induced in response to the low Ca^{2+} signal (Fig. 3.23, Table S3). Ysr290 is transcribed from the opposite strand of the 5'-UTR of pYV0044 gene, encoding for a hypothetical protein. This leads to the assumption that this asRNA is involved in the regulation of pYV0044 expression. Both, Ysr290 and pYV0044 are upregulated under secretion conditions. However, their possible role in the LCR of *Y. pseudotuberculosis* needs to be clarified. Of special interest are the non-coding asRNAs Ysr298 and Ysr299. Ysr298 overlaps the last 171 nt of the *yscW* coding sequence as well as the 5'-UTR of *lcrF*. Thus, acting *in cis*, Ysr298 might be involved in the complex regulation of LcrF synthesis via a so far unknown mechanism. Most likely, Ysr298 affects *lcrF* expression positively, as this asRNA is also upregulated under secretion conditions. Ysr299 is located within the *virC* operon, in particular, in the intergenic region between *yscA* and the downstream-situated pYV0078 gene, both encoding small the hypothetical proteins. The *virC* operon consists of the T3S-associated genes (*yscA-L*) and it is LcrF-dependent (Cornelis *et al*., 1998). Consequently, Ysr299 might be directly implicated in controlling the aforementioned T3S-associated genes. This would be in agreement with the recent suggestion about a fine-tuned regulation of the *ysc-yop* gene expression via the pYV-encoded asRNAs (Nuss *et al*., 2015; Nuss *et al*., 2017). Indeed, an unstable ncRNA Ysr141-SC, encoded upstream of the *yopH* gene was already shown to increase the synthesis of several T3SS-associated effector proteins as well as of the major virulence activator LcrF in *Y. pestis* (Schiano *et al*., 2014).

The role of small ncRNAs in regulation of bacterial virulence has previously been described in several pathogens (Quereda & Cossart, 2017). In *L. monocytogenes*, flagellum biosynthesis is controlled by a long asRNA (anti0677). This asRNA overlaps with three genes of the *fli* operon and negatively affects the expression of the sense transcript, preventing the synthesis of the flagellum export apparatus at mammalian host temperature (Sesto *et al*., 2013; Toledo-Arana *et al*., 2009). Additionally, the *trans*-acting small ncRNA Rli27 was shown to promote the translation of the *L. monocytogenes* LPXTG surface protein Lmo0514, which is essential for bacterial survival in the blood and for virulence in mice. In fact, binding of Rli27 to the 5'-UTR of *lmo0514* results in liberation of the SD sequence, which is normally inaccessible for the ribosome, and enhances synthesis of Lmo0514 in the intracellular environment (Quereda *et al*., 2014; Quereda *et al*., 2016). In

S. Typhimurium, a small ncRNA IsrM, encoded in a different pathogenicity island of *Salmonella*, was demonstrated to activate the expression of several SPI-1-encoded T3SS genes. In particular, acting *in trans*, IsrM is able to inhibit translation of HilE, which sequesters the global transcriptional activator of SPI-1 genes, HilD. IsrM binding to the 5'-UTR of *hilE* masks the RBS and prevents translation, resulting in HilD release and, consequently, activation of SPI-1 gene expression (Galán, 2001; Gong *et al*., 2011). A PhoP-dependent small ncRNA PinT represents an additional example of the ncRNA-mediated virulence control in *S.* Typhimurium. PinT expression is highly activated during infection. This small ncRNA simultaneously affects SPI-1 and SPI-2 effectors, influencing the transition from the invasion process to intracellular replication. Moreover, PinT binding represses the synthesis of the CRP protein, which regulates activation of SPI-2 via an undiscovered mechanism (Westermann *et al*., 2016). In case of *V. cholerae*, several small ncRNAs contributing to virulence have been identified. Qrr 1-5 small ncRNAs control colonization and escape from the host by interfering with the ToxR virulence cascade and regulating the expression of the T6SS (Skorupski & Taylor, 1999; Rutherford *et al*., 2011; Shao & Bassler, 2012; Shao & Bassler, 2014). A ToxT-dependent ncRNA TarB is induced during *V. cholerae* infection and is involved in the regulation of chemotaxis and intestinal colonization (Davies *et al*., 2012). Also in the Gram-positive pathogen *Staphylococcus aureus* a *cis*-asRNA, $SprA1_{as}$, was shown to inhibit the expression of the human cytolytic peptide SprA1, preventing its translation *in trans* (Sayed *et al*., 2012). These examples highlight that ncRNAs represent important regulators of bacterial virulence.

Transcriptome analysis revealed that the low Ca^{2+} signal, in addition to pYV-encoded genes, also influences the expression of the chromosomally-encoded virulence-associated loci. Among these, *pla2* ($log_2FC=4.4$; adjusted p-value <0.05) and *ompF* ($log_2FC=2.9$; adjusted p-value <0.05) were found to be upregulated. The *pla2* locus encodes for the plasminogen activator Pla, an adhesin possessing a proteolytic activity (Sodeinde *et al*., 1992). In *Y. pestis*, Pla was shown to play a crucial role for rapid dissemination of the pathogen through interaction with a C-type lectin receptors of macrophages and dendritic cells (Zhang *et al*., 2008). However, it has to be clarified, whether *Y. pseudotuberculosis* is able to apply a similar strategy for spreading in the mammalian host. Recently, the porin OmpF was described to be essential for the virulence of avian pathogenic *E. coli* (APEC). In particular, *ompF* deletion significantly reduced the adhesion, invasion, colonization and proliferation properties of APEC (Hejair *et al*., 2017). Interestingly, according to the RNA sequencing data of this study, the *ompF* expression is negatively affected by YopD under non-permissive conditions and positively influenced by CsrA under permissive conditions. Thus, it is possible that OmpF is involved in the CsrA-YopD-mediated LCR regulation, probably acting as a sensor of the low Ca^{2+} signal. Expression of the two additional chromosomally-encoded virulence-associated genes *psaA* ($log_2FC=-3.1$; adjusted p-value <0.05) and *rovC* ($log_2FC=-2.1$; adjusted p-value <0.05) was downregulated under secretion conditions. The pH6 antigen adhesin PsaA is important for establishment of *Y. pestis* infection and colonization (Huang & Lindler, 2004; Torres-Escobar *et al*., 2010). Downregulation of the *psaA* locus under secretion conditions observed in the present work

is consistent with the data demonstrating that PsaA is essential for adherence but is not implicated in the delivery of Yops (Huang & Lindler, 2004). The *rovC* gene encodes for a novel regulator of *Yersinia* virulence and is specific for *Y. pseudotuberculosis* (Seekircher, 2014; Knittel, 2015). Up to date, RovC represents the single known transcriptional activator of the T6SS-4 in *Y. pseudotuberculosis* (Knittel, 2015; V. Knittel, unpublished). Thus, decreased expression of *rovC* and, subsequently, of the T6SS-associated genes under type three secretion conditions might improve the energetic fitness of the pathogen, which is impaired by an enhanced synthesis of the Ysc-Yop proteins.

Interestingly, the *bet* regulon, involved in osmoprotection, was strongly upregulated under secretion conditions. It encodes the regulator BetI, as well as three structural components choline porter BetT, choline dehydrogenase BetA and betaine aldehyde dehydrogenase BetB (Lamark *et al*., 1996). Induction of these genes indicates that *Yersinia* undergo osmotic stress under permissive conditions, most probably through an extremely high level of secreted Yops in the growth medium.

Notably, elevation of the pYV-encoded gene expression, comparable to the LCR-dependent increase, was observed in the Δ*yopD* strain compared to the wild type strain even without Ca^{2+} limitation (Fig. 3.23). This is in strong agreement with the previous studies, demonstrating a repressive effect of YopD on the pYV-encoded genes, in particular via downregulation of the major virulence activator LcrF (Chen & Anderson, 2011; Steinmann, 2013). Moreover, *csrA* deletion also positively affected the expression of pYV-associated genes under non-permissive conditions, although to a lower extend than the *yopD* deletion did (Fig. 3.23). An increased level of the *yscW* mRNA confirms a negative effect of CsrA on the *yscW-lcrF* expression at the level of transcription explored in the present work (Fig. 3.7).

Under secretion conditions, in turn, CsrA was shown to be indispensible for induction of the LCR-dependent genes (Fig. 3.23). This is in agreement with the data of this work, demonstrating the crucial role of CsrA for the LCR-mediated induction of LcrF synthesis (see 3.2.1) and, consequently, for expression of the LcrF-dependent genes. Although the *csrA* expression level was only slightly reduced in response to the low Ca^{2+} signal, most probably through secretion of its positive regulator YopD, the level of the *CsrC* regulatory RNA decreased dramatically ($log_2FC=-1.6$; adjusted p-value <0.05). Thus, under secretion conditions, higher amounts of free CsrA are available, which might be essential for appropriate control of *lcrF* expression. Interestingly, *csrA* deletion in the Δ*yopD* background led to decreased expression of *repA* under secretion conditions ($log_2FC=-1.3$; adjusted p-value <0.05). Thus, CsrA might also interfere with the pYV copy number regulation. Preliminary data of our group support this hypothesis (P. Engling, unpublished).

Interestingly, *rcsB* expression under Ca^{2+} limitation in the wild type strain was only slightly reduced compared to the wild type strain grown under conditions non-permissive for secretion (data not shown), suggesting that CsrA might also repress *lcrF* transcription under Ca^{2+} depletion conditions. However, the present work demonstrated that the LcrF-mediated LCR, as well as response to the host cell contact signal occurs irrespective of

rcsB deletion (Fig. 3.29). Additionally, analysis of synthesis and secretion of the LcrF-dependent T3SS components in the wild type and the *rscB*-deficient strain under Ca^{2+} limitation revealed the inducing effect of RcsB only in presence of Zn^{2+} ions, known to stimulate the Rcs phosphorelay (Hagiwara *et al*., 2003; Li *et al*., 2014). Controversially, a mutation leading to a permanently dephosphorylated and, consequently, inactive RcsB state resulted in a significant decrease of *lcrF* expression under secretion conditions even in the absence of Zn^{2+} (Li *et al*., 2014). Together, these results lead to the assumption that under conditions permissive for the type three secretion (-Ca^{2+} or host cell contact) RcsB-dependent activation of the *lcrF* transcription is advantageous, but most likely dispensable for induction of *lcrF* expression in *Y. pseudotuberculosis*. Regarding the repressive effect of CsrA on RcsB, it is possible that under permissive conditions, an unknown factor prevents CsrA-mediated destabilization of the *rcsB* transcript.

Analysis of the CsrA interactome under Ca^{2+} limitation demonstrated that the majority of CsrA targets was encoded on the virulence plasmid and is associated with the T3SS (Table 3.2). Moreover, RNA sequencing revealed that all of these targets were CsrA-dependent (Table 3.2). These data indicate that apart from the indirect activation of the T3SS-associated genes through the major virulence activator LcrF, CsrA might also influence their expression via direct interaction. The most intriguing finding was that CsrA interacted with the *yopD* transcript. This indicates that CsrA affects *yopD* expression. Taking into account the previous results from our group, demonstrating a positive effect of YopD on CsrA synthesis (Steinmann, 2013; Hoßmann, 2017), it is likely that these riboregulators influence the expression of each other via a positive feedback loop. However, the LcrF-independent effect of CsrA on YopD synthesis needs to be explored.

Surprisingly, under permissive conditions YopD seems to positively affect the expression of the T3S apparatus-associated genes (Fig. 3.23). Preliminary data of our group suggest YopD to be involved in reprogramming of the *Yersinia* translation pattern towards production of the T3SS components (M. Volk, unpublished). In *Y. enterocolitica*, YopD has been shown to interact with 30S ribosome particles. Contrary to the theory proposed in this work, this interaction led to repression of translation (Kopaskie *et al*., 2013). Consequently, the mechanism of YopD-mediated regulation of translation in *Y. pseudotuberculosis* seems to differ from that in *Y. enterocolitica*.

Taken together, these results illustrate that calcium limitation acts globally by attenuating the proliferation properties of *Y. pseudotuberculosis* for almost exclusive expression of T3SS-associated genes. Moreover, a crucial role of CsrA and YopD riboregulators in establishment of the LCR in *Y. pseudotuberculosis* was shown.

4.2.3 Low calcium signal and CsrA: key players in a complex model of LcrF regulation

The effort to unravel the Ca^{2+}-dependent regulation of LcrF production revealed a complex regulatory network comprising several factors (Fig. 4.2). The mammalian host temperature (37 °C) together with the low Ca^{2+} signal induce LcrF synthesis and trigger production and secretion of the T3SS-associated components. Under these conditions, the YopD-LcrH-

mediated inhibitory feedback loop is interrupted by translocation of YopD. This results in increased *lcrF* transcript stability. However, an appropriate LcrF level can only be attained in presence of the global regulator CsrA. This riboregulator positively affects LcrF synthesis at the post-transcriptional level via two different mechanisms. Firstly, CsrA enhances *lcrF* transcript stability, most likely by negative regulation of RNase E, PNPase and RhlB (Hoßmann, 2017). Additionally, CsrA promotes translation initiation of *lcrF* by stabilization of the opened stemloop conformation. Furthermore, CsrA seems to positively affect replication of the virulence plasmid, increasing the total amount of *lcrF*. This circuit offers numerous access points for fine-tuning LcrF synthesis.

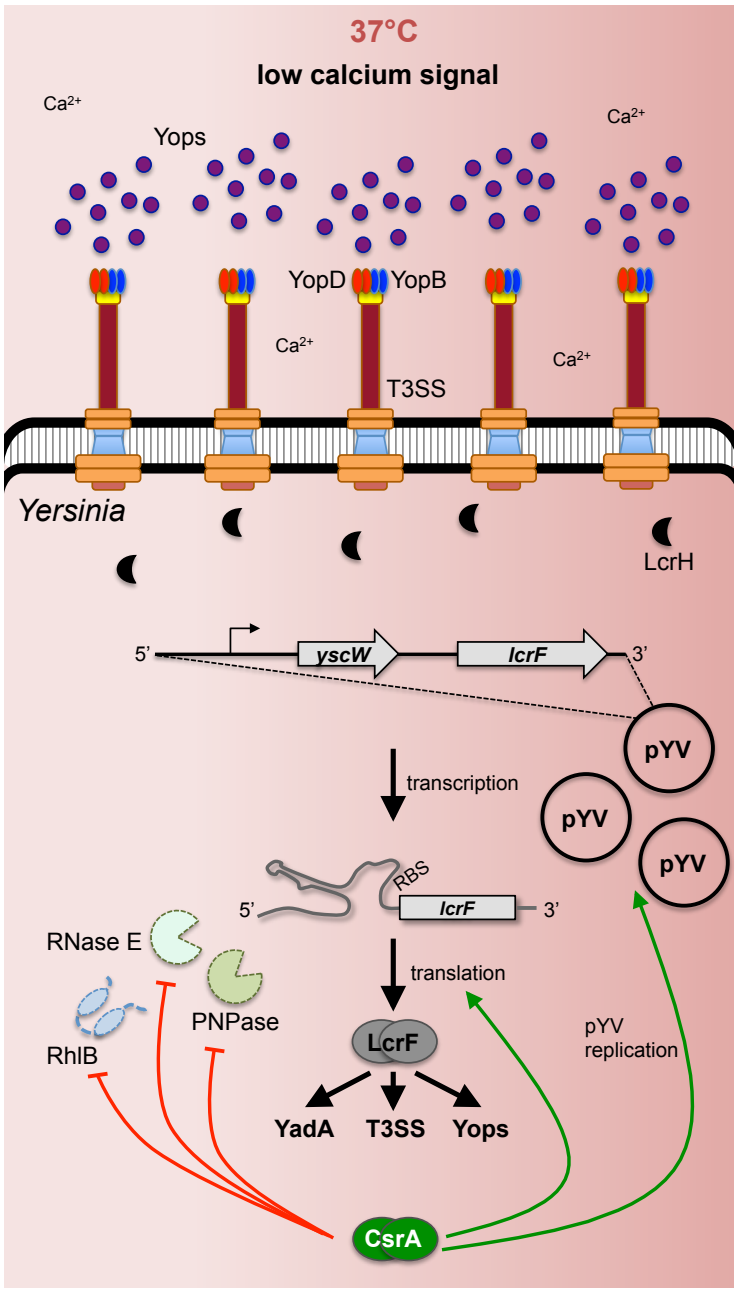

Figure 4.2. Model of the regulatory network involved in the control of LcrF production under conditions permissive for Yop secretion.
The figure demonstrates the crucial virulence determinants involved in LcrF regulation under secretion conditions. The green arrows and the red T lines indicate positive and negative influence, respectively, on gene expression and/or protein synthesis.

4.3 Host cell contact-dependent activation of the late virulence genes

Several environmental and host cues, such as temperature (Hoe & Goguen, 1993; Böhme *et al*., 2012), hormones (Hughes *et al*., 2009; Moreira *et al*., 2016), sugars (Nakanishi *et al*., 2006; Pacheco *et al*., 2012), cationic antimicrobial peptides (Bader *et al*., 2005), fatty acids (Huang *et al*., 2008; Hung *et al*., 2013; Golubeva *et al*., 2016), iron (Ellermeier & Slauch, 2008; Weinberg, 2009) and bile salts (Gotoh *et al*., 2010; Li *et al*., 2016; Letchumanan *et al*., 2017) were shown to play a role in regulation of T3SS synthesis and function in numerous pathogens (Nisco *et al*., 2018). Contact between a pathogen and its host cell has also been postulated to trigger the expression of the T3SS-associated genes. For instance, cell contact-mediated activation of the T3SS has been reported in EHEC (Shimizu *et al*., 2016) and EPEC (Katsowich *et al*., 2017). In EHEC, the outer membrane protein NlpE and the Cpx TCS were suggested to control the expression of T3SS-associated genes via a surface sensing mechanism (Shimizu *et al*., 2016). In EPEC, the T3SS itself seems to sense the host cell contact (Katsowich *et al*., 2017). Similarly to EPEC, the T3SS needle tip complex and the translocation pore were described to sense the host cell contact in *S. flexneri* and *P. aeruginosa*, respectively (Veenendaal *et al*., 2007; Armentrout & Rietsch, 2016). Preliminary data from our group led to the hypothesis that the synthesis of the *Y. pseudotuberculosis* T3SS may also be activated through contact with host cells (Opitz, 2013; Pimenova, 2014). However, a detailed mechanism as well as the factors involved in this type of T3SS activation are poorly understood and require further studies.

4.3.1 LcrF links cell-contact signal with expression of the late virulence genes

The present work clearly demonstrated that cell contact-dependent induction of the late virulence gene *yadA* in *Y. pseudotuberculosis* occurs via activation of *lcrF* expression (Fig. 3.25). Interestingly, LcrF is the only virulence plasmid-encoded factor required for the cell contact-mediated activation of *yadA*-expression (Fig. 3.27). This indicates an important difference in the mechanism of the cell contact-dependent induction of the T3SS-associated genes between the pathogens. In EPEC (Katsowich *et al*., 2017), *S. flexneri* (Veenendaal *et al*., 2007) and *P. aeruginosa* (Armentrout & Rietsch, 2016) the T3SS components are involved in sensing of the host cell contact signal, whereas in *Y. pseudotuberculosis*, even an unfunctional T3SS (Δ*yscS*) did not prevent cell contact-mediated induction of *yadA*-expression (Fig. 3.26). Although, deletion of the translocon components (Δ*yopB*, Δ*yopD*) did not abolish the cell contact response, it was slightly decreased compared to the wild type (Fig. 3.26). Thus, the components of the *Y. pseudotuberculosis* T3SS might be involved in modulation of the host cell contact-mediated response.

In order to identify the factors required for sensing of the host cell contact signal, several chromosomally-encoded surface structures were analyzed in this study. *Yersinia* adhesins (invasin, Ail and YadA) are crucial factors establishing contact with the host cells.

Additionally, Ail and YadA were shown to accelerate delivery of cytotoxic Yop effectors (Mikula *et al*., 2013; Tsang *et al*., 2013). However, simultaneous deletion of *invABCD*, *ail* and *yadA* did not affect cell contact-dependent activation of *yadA* expression (Fig. 3.28). Nevertheless, it is possible that other *Yersinia* adhesins (YadBC, Pla, PsaA) might be involved in cell contact sensing. With respect to the transcriptomic data from this work, Pla2, whose expression was significantly upregulated under secretion conditions (Fig. 3.23), seems to provide a potent candidate for sensing of the T3SS activating signal.

Assuming physical contact with the host cell results in envelope stress. The envelope/extracytoplasmatic stress response systems (ESRS) were also suggested to be promising candidates for sensing of the host cell contact signal (Laloux & Collet, 2017). Several ESRS include the two component signal transduction systems (TCS), which represent a predominant device for bacteria to sense and respond to several environmental stimuli (Tiwari *et al*., 2017). Thus, they were also suggested to be promising factors required for sensing of the host cell contact signal. However, up to date only two TCSs were shown to be directly involved in cell contact sensing. In *Neisseria meningitidis*, the TCS NMA0797 (PhoQ, MisS) / NMA0798 (PhoP/MisR) was shown to be regulated by host cell contact and proposed to sense this environmental signal (Jamet *et al*., 2009). In EHEC, the Cpx pathway was demonstrated to be involved in the NlpE lipoprotein-mediated surface sensing mechanism (Shimizu *et al*., 2016). In *Y. pseudotuberculosis*, preliminary data from our group indicated the involvement of Rcs and OmpR/EnvZ ESRS in cell contact sensing (Opitz, 2013; Pimenova, 2014). The present work demonstrated that deletion of genes encoding for the sensor kinase *rcsC*, the response regulator *rcsB* as well as the outer membrane lipoprotein *rcsF*, did not abrogate cell contact-dependent activation of *yadA* expression in *Y. pseudotuberculosis* (Fig. 3.29). This indicates that the Rcs system is not for sensing and/or transmission of the host cell contact signal, leading to LcrF-dependent *yadA* induction. In contrast, the *ompR*/*envZ* deficient strain was strongly impaired in cell contact-mediated induction of *yadA* expression (Fig. 3.29). Remarkably, investigation of the role of OmpR/EnvZ in sensing of the *in vitro* T3SS activating stimulus (Ca^{2+} limitation) revealed a negative effect of this TCS on LcrF synthesis under both, non-secretion and secretion conditions (Fig. 3.30). Nevertheless, Ca^{2+} depletion-dependent induction of LcrF production was still observed in the absence of OmpR/EnvZ, illustrating a difference between the mechanisms of cell contact- and Ca^{2+} limitation-mediated activation of LcrF synthesis (Fig. 3.30). In the presence of Ca^{2+}, OmpR/EnvZ seems to downregulate *lcrF* expression via positive influence on CsrA synthesis (Fig. 3.30). Under Ca^{2+} limitation, this TCS might negatively act on LcrF synthesis by upregulation of the *csrC* level (Fig. 3.30). This results in a decreased amount of free CsrA, insufficient for appropriate *lcrF* translation. Taken together, compromised induction of *yadA* expression in the absence of OmpR/EnvZ might be explained primarily by elevated LcrF and, consequently, YadA levels. Subsequently, the *ompR*/*envZ* null mutant represents a "cell contact blind" phenotype, where no *yadA* induction can be detected upon contact with the host cells. Recently, a repressive effect of OmpR on YadA synthesis in *Y. enterocolitica* via direct binding to the *yadA* promoter has been described (Nieckarz *et al*., 2016). This finding supports the hypothesis of the present work concerning the elevated *yadA*

expression in the absence of OmpR, and demonstrates that OmpR is able to also regulate *yadA* expression in an LcrF-independent manner. The host cell contact signal might serve as a "switch-off" signal for the OmpR/EnvZ activity, leading to induction of the late virulence genes. Moreover, proteomic analysis revealed that OmpR affects synthesis of 120 proteins, a third of which are implicated in uptake and/or transport. Thus OmpR/EnvZ might also contribute to the host cell contact sensing, altering the surface structures that might be involved in direct recognition of the host cell contact signal. In particular, an increased amount of active (phosphorylated) OmpR (OmpR-P) represses synthesis of the major outer membrane porin OmpF (Cai & Inouye, 2002). According to the data of the present work, OmpF might be essential for the LCR in *Y. pseudotuberculosis* (Fig. 3.23). Consequently, the OmpR-mediated downregulation of *ompF* expression might negatively affect the LCR and, probably, also the response to the host cell contact. These results indicate that the OmpR/EnvZ TCS plays an important role in the complex regulation of cell contact-mediated expression of the late virulence genes. For instance, restricting LcrF production in the absence of the host cell contact, OmpR/EnvZ might prevent an uncontrolled expression of the *ysc-yop* genes, improving *Yersinia* virulence. Indeed, the *Y. pseudotuberculosis* 32777 strain lacking *ompR* was shown to be less virulent in the BALB/c mouse infection model compared to the wild type (Flamez *et al*., 2008). Moreover, OmpR was previously described to promote acid resistance of *Y. pseudotuberculosis* YPIII through activation of urease expression (Hu *et al*., 2009). OmpR was also reported to directly interact with the promoter of the thermo-regulated T6SS-4, which is important for *Yersinia* acid survival (Zhang *et al*., 2013). Interestingly, in *Y. enterocolitica* O:9, OmpR regulates motility, initiating the expression of the master flagellar operon *flhDC* (Raczkowska *et al*., 2011). Additionally, OmpR was demonstrated to negatively affect the *Y. enterocolitica* O:9 invasin expression and to alter the serum resistance of this pathogen (Brzostek *et al*., 2007; Skorek *et al*., 2013). Similar to *Y. pseudotuberculosis*, the OmpR/EnvZ system was also shown to control the virulence of *E. coli* in the *Drosophila melanogaster* infection model. The authors propose that OmpR/EnvZ-mediated alleviation of *E. coli* virulence most likely demonstrates a strategy to attain a persistent infection (Pukklay *et al*., 2013). In *Acinetobacter baumannii*, perturbation of the OmpR/EnvZ TCS results in attenuation of virulence in an invertebrate infection system (Tipton & Rather, 2017). In contrast to *Y. pseudotuberculosis*, HrpG, the response regulator of the OmpR family in the plant pathogen *Xanthomonas*, induces expression of the AraC-like transcriptional activator of T3SS, HrpX (Wengelnik *et al*., 1996; Andrade *et al*., 2014). This indicates a large spectrum of the OmpR/EnvZ activities that vary in different pathogens.

4.3.2 CsrA and host cell contact-mediated LcrF synthesis

Similar to its role in the *Y. pseudotuberculosis* LCR, CsrA was found to be absolutely essential for the cell contact-dependent induction of LcrF synthesis. Deletion of *csrA* in *Y. pseudotuberculosis* resulted in a cell contact-blind phenotype, unable to induce *lcrF* and, consequently, *yadA* expression in response to the host cell contact signal (Fig. 3.31). Analogous to *Y. pseudotuberculosis*, the CsrA homolog, RsmA, was shown to activate the

LcrF homolog, ExsA, in *P. aeruginosa* via an unknown mechanism (Brencic & Lory, 2009; Intile *et al*., 2014). In EPEC/EHEC, CsrA was also demonstrated to control the T3SS synthesis through direct activation of *escD* and *LEE4* genes, encoding the T3SS translocators. However, multicopy expression of *csrA* resulted in transcriptional repression of several LEE operons via the regulators GrlA and Ler (Bhatt *et al*., 2009). Recently, CsrA was shown to interact with the T3SS effector-binding chaperone CesT, which is unique in EPEC/EHEC, in order to control cell contact-dependent expression of T3SS effectors (Katsowich *et al*., 2017).

This work demonstrated for the first time that CsrA positively affects cell contact-dependent activation of the late virulence genes promoting *lcrF* translation. CsrA was shown to stabilize the SD-containing hairpin II structure located in the 5'-UTR of the *lcrF* transcript in an "opened" conformation supporting the ribosomal access. In this way, CsrA increases LcrF-mediated *yadA*-induction in response to host cell contact and the low calcium signal (Fig. 3.32). However, it cannot be excluded that CsrA also positively affects the *lcrF* transcript stability during contact with the host cells, as it does under Ca^{2+} limitation (see 3.2.1.2). These results demonstrate that both, Ca^{2+} depletion and the host cell contact signal require the presence of CsrA in order to induce LcrF synthesis. Since *lcrF* expression during the host cell contact is already activated at moderate temperatures, CsrA might also contribute to abrogate the negative regulation of LcrF synthesis at the transcriptional level (Fig. 4.3). Moreover, CsrA might participate in transmission of the host cell contact signal from an unknown cell contact sensor (Fig. 4.3).

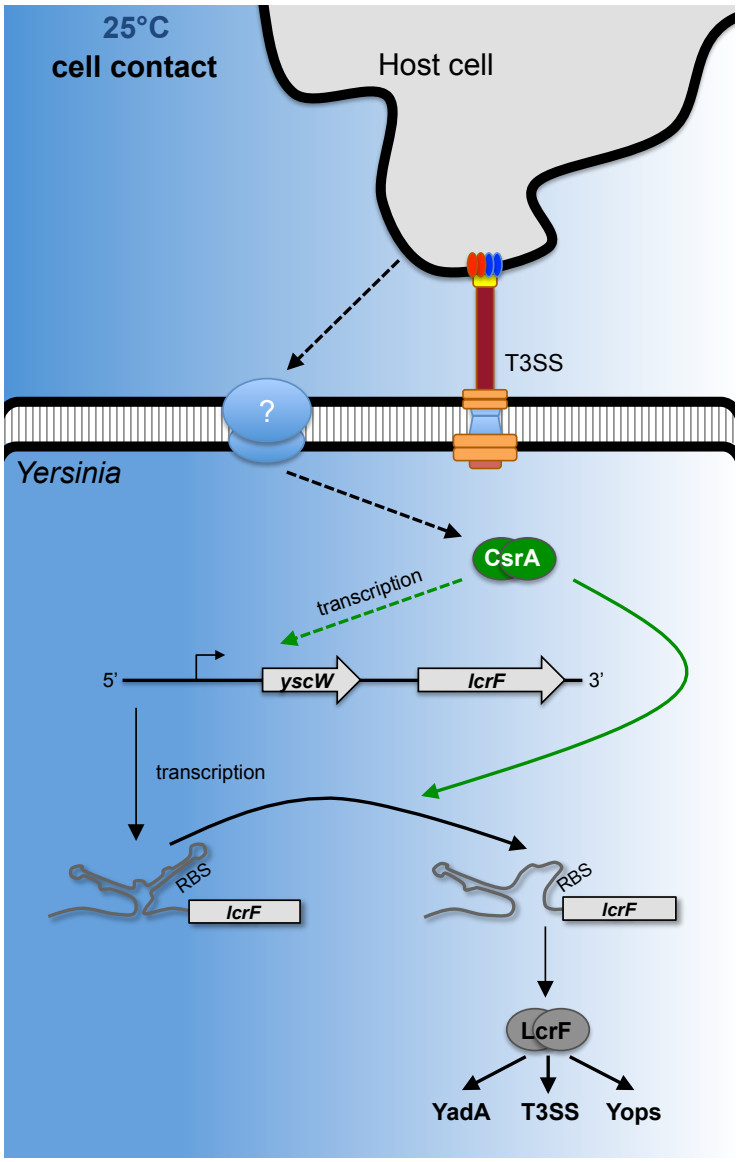

Figure 4.3. Model of the CsrA role in the control of LcrF production upon contact with the host cell.
The figure demonstrates the CsrA mode of action involved in activation of LcrF synthesis upon host cell contact. The green arrow indicates positive influence on gene expression and/or protein synthesis. The green dashed arrow demonstrates a possible positive effect of CsrA on *lcrF* transcription under these conditions.

5 Outlook

To further investigate the detailed mechanism of YopD- and CsrA-mediated regulation of degradosome components, implicated in control of LcrF synthesis (RNase E, PNPase and RhlB), the effect of YopD and CsrA on stability and translation initiation of the corresponding transcripts should be determined. Cocrystallization of YopD with the 5'-UTRs of *rne* and *pnp* transcripts would provide essential information about YopD-*rne* and YopD-*pnp* interactions. This work indicated that the negative effect of CsrA on *rne* and *pnp* expression is indirect. Future experiments will be directed the CsrA-dependent factor/factors (i.e., CsrA-repressed activators, or CsrA-activated repressors of *rne* and *pnp* expression) enabling regulation of RNase E and PNPase synthesis. It will be also interesting to assess, whether processing of the *pnp* 5'-UTR is required for CsrA-mediated regulation.

The present work demonstrated that CsrA inhibits *lcrF* transcription via negative regulation of RcsB under non-secretion conditions. To determine a direct interaction of CsrA with the *rcsB* transcript, RNA EMSA studies need to be performed. Moreover, a possible role of CsrA in regulation of *rcsB* translation initiation should be addressed, by employing the *in vitro* translation assay. Since phosphorylated RcsB (RcsB-P) is required for activation of *lcrF* transcription, the role of CsrA in regulation of the sensor kinase RcsC needs to be clarified. Additionally, it is important to investigate the CsrA-RcsB interactions under secretion conditions.

CsrA was found to increase the *lcrF* transcript stability under secretion conditions indirectly. Whether this influence is mediated only by CsrA-dependent negative regulation of the LcrF-repressors RNase E and PNPase needs to be clarified. For this, RNA stability assays should be performed comparing the half-life of *lcrF* in the wild type, the Δ*csrA* strain and the Δ*csrA*Δ*rne*, Δ*csrA*Δ*pnp*, Δ*rne*Δ*pnp* double mutant strains as well as the Δ*csrA*Δ*rne*Δ*pnp* triple mutant strain. Since the *rne* deletion is lethal, the dominant negative RNase E version should be implemented for construction of the aforementioned mutants. These RNA stability assays could elucidate the possible hierarchy of CsrA, RNase E and PNPase in regulation of the *lcrF* mRNA degradation rate. Moreover, the role of the *lcrF* 3'-UTR in destabilization of the *lcrF* transcript should be further explored.

The global transcriptome profiling revealed several pYV-encoded small regulatory ncRNAs. Their role in the LCR of *Y. pseudotuberculosis* needs to be determined. Proteomic analysis in ncRNA deletion or overexpression strains will help to investigate the roles of these ncRNAs in regulation of the LCR. Moreover, the outer membrane porin, OmpF, could be a sensor of the low calcium signal. To further address whether OmpF is responsible for sensing of Ca^{2+} limitation, an *ompF*-deficient strain needs to be constructed and analyzed for its ability to induce the LCR under secretion conditions. Exploration of the immediate response of *Y. pseudotuberculosis* to the low calcium signal turned out to be challenging and requires further improvement.

The present work indicated that YopD acts positively on the expression of genes encoding the T3SS- machinery under secretion conditions. Ribosome profiling in the wild type and

Δ*yopD* strains will address, whether YopD might shift the *Yersinia* translation towards synthesis of the T3SS components upon secretion. Additionally, analysis of the YopD interactome via CLIP-seq will provide information about the YopD-specific sequence, which is still controversial.

Investigation of the CsrA interactome under permissive conditions revealed that CsrA is able to directly interact with several T3SS-associated transcripts. Among those was the *yopD* transcript. RNA EMSA as well as analysis of RNA and protein levels in the *lcrF*- and the *csrAlcrF*-deficient strains will elucidate the role of CsrA in regulation of YopD synthesis.

Finally, CsrA was shown to be indispensible for cell contact-dependent induction of *lcrF* expression, as it promotes the translation initiation of *lcrF*. However, it will be interesting to investigate whether CsrA might also affect the *lcrF* transcript stability upon host cell contact. Most important is to find out how the host cell contact is sensed as well as how *Yersinia* does overcome the temperature-mediated blockage of *lcrF* expression (at 25 °C) at the transcriptional level when host cells are present. The present study indicated that the TCS OmpR/EnvZ is involved in sensing and/or transmission of the host cell contact signal. Nevertheless, further experiments are essential to address a precise mechanism of OmpR/EnvZ-mediated regulation of *lcrF* expression upon contact with host cells. To determine whether OmpR affects *lcrF* expression by binding to the *yscW-lcrF* promoter region, EMSA have to be performed. Furthermore, cell contact dependency of *ompR/envZ* expression could be assessed via qRT-PCR. Moreover, cell contact-mediated regulation of OmpR/EnvZ system at the post-translational level should be assessed. Lastly, it will be interesting to address the involvement of the OmpR/EnvZ-dependent protein OmpF in cell contact-mediated activation of *lcrF* expression.

6 Summary

The virulence strategy of pathogenic *Yersinia* relies on a sophisticated antiphagocytic program, which is encoded on the *Yersinia* virulence plasmid, pYV. It consists of the adhesion factor YadA and the Ysc-Yop type III secretion system (T3SS). This program enables translocation of bacterial effector proteins directly into the host cell, thus subverting the host immune defense. However, inappropriate synthesis of the T3SS components can dramatically impair bacterial growth rate and fitness. Moreover, high immunogenicity of the macromolecular syringe can cause early elimination of the pathogen by the host immune system. Consequently, expression of the T3SS-associated genes must be tightly controlled. To do so, *Yersinia* have evolved a complex regulatory network aimed at fine-tuning expression of the late virulence genes in response to environmental and host signals. The most important environmental cues triggering synthesis of these virulence factors are temperature and host cell contact. Transcription of genes encoding for the antiphagocytic program is activated by the AraC-like transcriptional regulator LcrF. Consequently, synthesis of this major virulence activator is also strictly controlled. LcrF production occurs only at host temperatures (37 °C), preventing expression of *yadA* and *ysc-yop* genes outside the host environment. Host cell contact (*in vivo*) or low calcium signals (*in vitro*) further trigger *lcrF* expression and result in massive synthesis of antiphagocytic virulence factors.

In the present study, multilayered regulatory cascades adjusting the *lcrF* expression were investigated. In the absence of cell contact or secretion signal, *lcrF* expression is downregulated via a negative feedback loop. Under these conditions, the translocon component YopD, in complex with its chaperone LcrH, accumulates inside the pathogen and prevents LcrF synthesis at the post-transcriptional level. The present work demonstrated that YopD exerts a negative effect on the *lcrF* transcript stability. Moreover, YopD was shown to exert a positive influence on the components of the *Yersinia* degradosome, RNase E and PNPase, via direct interaction with the 5'-UTRs of their mRNAs. RNase E, PNPase and RhlB, in turn, were found to downregulate LcrF synthesis. Additionally, YopD was demonstrated to reduce the pYV copy number, thus decreasing the initial *lcrF* amount.

Furthermore, this work unraveled the mechanism of CsrA-mediated transcriptional repression of LcrF synthesis under non-secretion conditions. The global post-transcriptional regulator CsrA was shown to negatively influence the transcriptional activator of LcrF, RcsB. In fact, CsrA was found to reduce the *rcsB* transcript stability, which decreases *lcrF* transcription. Since YopD has previously been shown to positively affect CsrA synthesis, this regulatory Yop might exert its negative influence on LcrF not only via positive regulation of the degradosome components, but also through upregulation of CsrA.

The present work demonstrates that calcium limitation represents a global signal that induces large-scale rearrangements in the *Yersinia* transcriptome mainly towards expression of the pYV-encoded virulence factors. The low calcium signal induces secretion of Yops, including the post-transcriptional regulator YopD, which increases the

pYV copy number and abolishes feedback inhibition of LcrF synthesis. Moreover, in this study it was discovered why CsrA is indispensible for *lcrF* translation under secretion conditions and upon contact with the host cell. CsrA was shown to positively influence *lcrF* translation initiation. Binding of CsrA to the 5'-UTR of the *lcrF* mRNA results in capturing of the second stemloop structure in an "opened" conformation. This makes the *lcrF* SD sequence more accessible for ribosome promoting translation. A similar mode of action was demonstrated for CsrA-promoted positive regulation of LcrF synthesis upon contact with host cells. The present work demonstrates that the *lcrF* transcript is extremely unstable and actively processed, not only from the 5'-UTR, but also from the 3'-UTR. CsrA was found to increase the *lcrF* transcript stability. Data of this study suggest that CsrA stabilizes *lcrF* mRNA indirectly, via negative regulation of *lcrF* mRNA-degrading RNases such as, RNase E and PNPase. Interestingly, this work indicated that apart from its role in upregulation of LcrF synthesis at the post-transcriptional level, CsrA elevates the LcrF amount by increasing the pYV copy number.

The present work further showed that LcrF is the only pYV-encoded factor required for the cell contact-dependent induction of *yadA* expression. Apart from CsrA, the OmpR/EnvZ two-component system, as well as the outer membrane porin OmpF have been suggested as promising chromosomally-encoded factors that might be involved in sensing and/or transmission of the host cell contact signal to LcrF synthesis.

In conclusion, in this study multiple regulatory traits controlling LcrF synthesis have been identified. The post-transcriptional regulators CsrA and YopD were shown to play a key role in the complex regulation of *lcrF* expression. Furthermore, several additional factors, such as the RNA degradosome, pYV copy number and ESRS, were shown to be implicated in the CsrA- and YopD-mediated control of *lcrF* expression. This multilayered regulation allows a finely-tuned and tightly controlled synthesis of the major virulence activator.

References

Achtman, M., Morelli, G., Zhu, P., Wirth, T., Diehl, I., Kusecek, B., … Keim, P. (2004). Microevolution and history of the plague bacillus, *Yersinia pestis*. *Proceedings of the National Academy of Sciences*, *101*(51), 17837–17842. https://doi.org/10.1073/pnas.0408026101

Achtman, M., Zurth, K., Morelli, G., Torrea, G., Guiyoule, A., & Carniel, E. (1999). *Yersinia pestis*, the cause of plague, is a recently emerged clone of *Yersinia pseudotuberculosis*. *Proceedings of the National Academy of Sciences of the United States of America*, *96*(24), 14043–8. Retrieved from http://www.pubmedcentral.nih.gov/articlerender.fcgi?artid=24187&tool=pmcentrez&rendertype=abstract

Ackermann, N., Tiller, M., Anding, G., Roggenkamp, A., & Heesemann, J. (2008). Contribution of trimeric autotransporter C-terminal domains of oligomeric coiled-coil adhesin (Oca) family members YadA, UspA1, EibA, and Hia to translocation of the YadA passenger domain and virulence of *Yersinia enterocolitica*. *Journal of Bacteriology*, *190*(14), 5031–43. https://doi.org/10.1128/JB.00161-08

Adkins, I., Köberle, M., Gröbner, S., Bohn, E., Autenrieth, I. B., & Borgmann, S. (2007). *Yersinia* outer proteins E, H, P, and T differentially target the cytoskeleton and inhibit phagocytic capacity of dendritic cells. *International Journal of Medical Microbiology*, *297*(4), 235–244. https://doi.org/10.1016/j.ijmm.2007.02.005

Aepfelbacher, M., Roppenser, B., Hentschke, M., & Ruckdeschel, K. (2011). Activity modulation of the bacterial Rho GAP YopE: An inspiration for the investigation of mammalian Rho GAPs. *European Journal of Cell Biology*, *90*(11), 951–954. https://doi.org/10.1016/j.ejcb.2010.12.004

Aepfelbacher, M., Trasak, C., & Ruckdeschel, K. (2007). Effector functions of pathogenic *Yersinia* species. *Thrombosis and Haemostasis*, *98*(3), 521–9. Retrieved from http://www.ncbi.nlm.nih.gov/pubmed/17849040

Agrain, C., Sorg, I., Paroz, C., & Cornelis, G. R. (2005). Secretion of YscP from *Yersinia enterocolitica* is essential to control the length of the injectisome needle but not to change the type III secretion substrate specificity. *Molecular Microbiology*, *57*(5), 1415–1427. https://doi.org/10.1111/j.1365-2958.2005.04758.x

Aiba, H. (2007). Mechanism of RNA silencing by Hfq-binding small RNAs. *Current Opinion in Microbiology*, *10*(2), 134–139. https://doi.org/10.1016/j.mib.2007.03.010

Aït-Bara, S., & Carpousis, A. J. (2015). RNA degradosomes in bacteria and chloroplasts: classification, distribution and evolution of RNase E homologs. *Molecular Microbiology*, *97*(6), 1021–135. https://doi.org/10.1111/mmi.13095

Akeda, Y., & Galán, J. E. (2005). Chaperone release and unfolding of substrates in type III secretion. *Nature*, *437*(7060), 911–915. https://doi.org/10.1038/nature03992

Akopyan, K., Edgren, T., Wang-Edgren, H., Rosqvist, R., Fahlgren, A., Wolf-Watz, H., & Fallman, M. (2011). Translocation of surface-localized effectors in type III secretion. *Proceedings of the National Academy of Sciences of the United States of America*, *108*(4), 1639–44. https://doi.org/10.1073/pnas.1013888108

Allaoui, A., Scheen, R., Lambert de Rouvroit, C., & Cornelis, G. R. (1995). VirG, a *Yersinia enterocolitica* lipoprotein involved in Ca^{2+} dependency, is related to *exsB* of *Pseudomonas aeruginosa*. *Journal of Bacteriology*, *177*(15), 4230–7. Retrieved from http://www.ncbi.nlm.nih.gov/pubmed/7635810

Altegoer, F., Rensing, S. A., & Bange, G. (2016). Structural basis for the CsrA-dependent modulation of translation initiation by an ancient regulatory protein. *Proceedings of the National Academy of Sciences*, *113*(36), 10168–10173. https://doi.org/10.1073/pnas.1602425113

Anderson, D. M., Ramamurthi, K. S., Tam, C., & Schneewind, O. (2002). YopD and LcrH regulate

expression of *Yersinia enterocolitica* YopQ by a posttranscriptional mechanism and bind to *yopQ* RNA. *Journal of Bacteriology*, *184*(5), 1287–95. Retrieved from http://www.ncbi.nlm.nih.gov/pubmed/11844757

Andersson, K., Magnusson, K. E., Majeed, M., Stendahl, O., & Fällman, M. (1999). *Yersinia pseudotuberculosis*-induced calcium signaling in neutrophils is blocked by the virulence effector YopH. *Infection and Immunity*, *67*(5), 2567–74. Retrieved from http://www.ncbi.nlm.nih.gov/pubmed/10225922

Andrade, M. O., Farah, C. S., Wang, N., Pascarella, S., & Tsuno, K. (2014). The Post-transcriptional Regulator *rsmA*/*csrA* Activates T3SS by Stabilizing the 5′ UTR of *hrpG*, the Master Regulator of *hrp*/*hrc* Genes, in *Xanthomonas*. *PLoS Pathogens*, *10*(2), e1003945. https://doi.org/10.1371/journal.ppat.1003945

Argaman, L., Hershberg, R., Vogel, J., Bejerano, G., Wagner, E. G. H., Margalit, H., & Altuvia, S. (2001). Novel small RNA-encoding genes in the intergenic regions of *Escherichia coli*. *Current Biology*, *11*(12), 941–950. https://doi.org/10.1016/S0960-9822(01)00270-6

Armentrout, E. I., & Rietsch, A. (2016). The Type III Secretion Translocation Pore Senses Host Cell Contact. *PLoS Pathogens*, *12*(3). https://doi.org/10.1371/journal.ppat.1005530

Arricau, N., Hermant, D., Waxin, H., Ecobichon, C., Duffey, P. S., & Popoff, M. Y. (1998). The RcsB-RcsC regulatory system of *Salmonella typhi* differentially modulates the expression of invasion proteins, flagellin and Vi antigen in response to osmolarity. *Molecular Microbiology*, *29*(3), 835–850. https://doi.org/10.1046/j.1365-2958.1998.00976.x

Atkinson, S., & Williams, P. (2016). *Yersinia* virulence factors - a sophisticated arsenal for combating host defences. *F1000Research*, *5*. https://doi.org/10.12688/f1000research.8466.1

Autenrieth, I. B., Kempf, V., Sprinz, T., Preger, S., & Schnell, A. (1996). Defense mechanisms in Peyer's patches and mesenteric lymph nodes against *Yersinia enterocolitica* involve integrins and cytokines. *Infection and Immunity*, *64*(4), 1357–68. Retrieved from http://www.ncbi.nlm.nih.gov/pubmed/8606101

Avican, K., Fahlgren, A., Huss, M., Heroven, A. K., Beckstette, M., Dersch, P., & Fällman, M. (2015). Reprogramming of *Yersinia* from Virulent to Persistent Mode Revealed by Complex In Vivo RNA-seq Analysis. *PLOS Pathogens*, *11*(1), e1004600. https://doi.org/10.1371/journal.ppat.1004600

Bader, M. W., Sanowar, S., Daley, M. E., Schneider, A. R., Cho, U., Xu, W., … Miller, S. I. (2005). Recognition of Antimicrobial Peptides by a Bacterial Sensor Kinase. *Cell*, *122*(3), 461–472. https://doi.org/10.1016/J.CELL.2005.05.030

Baker, C. S., Morozov, I., Suzuki, K., Romeo, T., & Babitzke, P. (2002). CsrA regulates glycogen biosynthesis by preventing translation of *glgC* in *Escherichia coli*. *Molecular Microbiology*, *44*(6), 1599–610. Retrieved from http://www.ncbi.nlm.nih.gov/pubmed/12067347

Balaban, N., & Novick, R. P. (1995). Translation of RNAIII, the *Staphylococcus aureus agr* regulatory RNA molecule, can be activated by a 3'-end deletion. *FEMS Microbiology Letters*, *133*(1–2), 155–61. Retrieved from http://www.ncbi.nlm.nih.gov/pubmed/8566701

Banerjee, S., Chalissery, J., Bandey, I., & Sen, R. (2006). Rho-dependent transcription termination: more questions than answers. *Journal of Microbiology (Seoul, Korea)*, *44*(1), 11–22. Retrieved from http://www.ncbi.nlm.nih.gov/pubmed/16554712

Barnes, P. D., Bergman, M. A., Mecsas, J., & Isberg, R. R. (2006). *Yersinia pseudotuberculosis* disseminates directly from a replicating bacterial pool in the intestine. *The Journal of Experimental Medicine*, *203*(6), 1591–1601. https://doi.org/10.1084/jem.20060905

Beckert, B., & Masquida, B. (2011). Synthesis of RNA by In Vitro Transcription. In *Methods in molecular biology (Clifton, N.J.)* (Vol. 703, pp. 29–41). https://doi.org/10.1007/978-1-59745-248-9_3

Benabdillah, R., Jaime Mota, L., Lützelschwab, S., Demoinet, E., & Cornelis, G. R. (2004). Identification of a nuclear targeting signal in YopM from *Yersinia* spp. *Microbial Pathogenesis*, *36*(5), 247–261. https://doi.org/10.1016/j.micpath.2003.12.006

Bergman, T., Erickson, K., Galyov, E., Persson, C., & Wolf-Watz, H. (1994). The *lcrB* (*yscN*/*U*) gene cluster of *Yersinia pseudotuberculosis* is involved in Yop secretion and shows high homology to the *spa* gene clusters of *Shigella flexneri* and *Salmonella typhimurium*. *Journal of Bacteriology*, *176*(9), 2619–26. Retrieved from http://www.ncbi.nlm.nih.gov/pubmed/8169210

Bhatt, S., Edwards, A. N., Nguyen, H. T. T., Merlin, D., Romeo, T., & Kalman, D. (2009). The RNA Binding Protein CsrA Is a Pleiotropic Regulator of the Locus of Enterocyte Effacement Pathogenicity Island of Enteropathogenic *Escherichia coli*. *Infection and Immunity*, *77*(9), 3552–3568. https://doi.org/10.1128/IAI.00418-09

Bhunia, A. (2008). *Yersinia enterocolitica* and *Yersinia pestis*. In *Foodborne Microbial Pathogens* (pp. 227–240). New York, NY: Springer New York. https://doi.org/10.1007/978-0-387-74537-4_13

Biedzka-Sarek, M., Venho, R., & Skurnik, M. (2005). Role of YadA, Ail, and Lipopolysaccharide in Serum Resistance of *Yersinia enterocolitica* Serotype O:3. *Infection and Immunity*, *73*(4), 2232–44. https://doi.org/10.1128/IAI.73.4.2232-2244.2005

Black, D. S., Marie-Cardine, A., Schraven, B., & Bliska, J. B. (2000). The *Yersinia* tyrosine phosphatase YopH targets a novel adhesion-regulated signalling complex in macrophages. *Cellular Microbiology*, *2*(5), 401–14. Retrieved from http://www.ncbi.nlm.nih.gov/pubmed/11207596

Black, D. S., Montagna, L. G., Zitsmann, S., & Bliska, J. B. (1998). Identification of an amino-terminal substrate-binding domain in the *Yersinia* tyrosine phosphatase that is required for efficient recognition of focal adhesion targets. *Molecular Microbiology*, *29*(5), 1263–74. Retrieved from http://www.ncbi.nlm.nih.gov/pubmed/9767593

Blaylock, B., Berube, B. J., & Schneewind, O. (2010). YopR impacts type III needle polymerization in *Yersinia* species. *Molecular Microbiology*, *75*(1), 221–229. https://doi.org/10.1111/j.1365-2958.2009.06988.x

Blaylock, B., Riordan, K. E., Missiakas, D. M., & Schneewind, O. (2006). Characterization of the *Yersinia enterocolitica* Type III Secretion ATPase YscN and Its Regulator, YscL. *Journal of Bacteriology*, *188*(10), 3525–3534. https://doi.org/10.1128/JB.188.10.3525-3534.2006

Bliska, J. B., Ryndak, M. B., & Grabenstein, J. P. (2006). Type III Secretion Systems in *Yersinia pestis* and *Yersinia pseudotuberculosis*. In *Bacterial Genomes and Infectious Diseases* (pp. 213–226). Totowa, NJ: Humana Press. https://doi.org/10.1007/978-1-59745-152-9_12

Bliska, J. B., Wang, X., Viboud, G. I., & Brodsky, I. E. (2013). Modulation of innate immune responses by *Yersinia* type III secretion system translocators and effectors. *Cellular Microbiology*, *15*(10), 1622–31. https://doi.org/10.1111/cmi.12164

Bogdanovich, T., Carniel, E., Fukushima, H., & Skurnik, M. (2003). Use of O-antigen gene cluster-specific PCRs for the identification and O-genotyping of *Yersinia pseudotuberculosis* and *Yersinia pestis*. *Journal of Clinical Microbiology*, *41*(11), 5103–12. Retrieved from http://www.ncbi.nlm.nih.gov/pubmed/14605146

Böhme, K., Steinmann, R., Kortmann, J., Seekircher, S., Heroven, A. K., Berger, E., … Dersch, P. (2012). Concerted actions of a thermo-labile regulator and a unique intergenic RNA thermosensor control *Yersinia* virulence. *PLoS Pathogens*, *8*(2), e1002518. https://doi.org/10.1371/journal.ppat.1002518

Bölin, I., Forsberg, A., Norlander, L., Skurnik, M., & Wolf-Watz, H. (1988). Identification and mapping of the temperature-inducible, plasmid-encoded proteins of *Yersinia* spp. *Infection and Immunity*, *56*(2), 343–8. Retrieved from http://www.ncbi.nlm.nih.gov/pubmed/3338844

Bölin, I., Norlander, L., & Wolf-Watz, H. (1982). Temperature-inducible outer membrane protein of *Yersinia*

pseudotuberculosis and *Yersinia enterocolitica* is associated with the virulence plasmid. *Infection and Immunity*, *37*(2), 506–12. Retrieved from http://www.ncbi.nlm.nih.gov/pubmed/6749681

Bottone, E. J. (1997). *Yersinia enterocolitica*: the charisma continues. *Clinical Microbiology Reviews*, *10*(2), 257–76. Retrieved from http://www.ncbi.nlm.nih.gov/pubmed/9105754

Bottone, E. J. (1999). *Yersinia enterocolitica*: overview and epidemiologic correlates. *Microbes and Infection*, *1*(4), 323–33. Retrieved from http://www.ncbi.nlm.nih.gov/pubmed/10602666

Bradford, M. M. (1976). A rapid and sensitive method for the quantitation of microgram quantities of protein utilizing the principle of protein-dye binding. *Analytical Biochemistry*, *72*, 248–54. Retrieved from http://www.ncbi.nlm.nih.gov/pubmed/942051

Brencic, A., & Lory, S. (2009). Determination of the regulon and identification of novel mRNA targets of *Pseudomonas aeruginosa* RsmA. *Molecular Microbiology*, *72*(3), 612–32. https://doi.org/10.1111/j.1365-2958.2009.06670.x

Bröms, J. E., Forslund, A. L., Forsberg, Å., & Francis, M. S. (2003). Dissection of homologous translocon operons reveals a distinct role for YopD in type III secretion by *Yersinia pseudotuberculosis*. *Microbiology*, *149*(9), 2615–2626.

Broz, P., Mueller, C. A., Müller, S. A., Philippsen, A., Sorg, I., Engel, A., & Cornelis, G. R. (2007). Function and molecular architecture of the *Yersinia* injectisome tip complex. *Molecular Microbiology*, *65*(5), 1311–1320. https://doi.org/10.1111/j.1365-2958.2007.05871.x

Brubaker, R. R. (1991). Factors Promoting Acute and Chronic Diseases Caused by *Yersiniae*. *CLINICAL MICROBIOLOGY REVIEWS*, *4*(3), 309–324. Retrieved from https://www.ncbi.nlm.nih.gov/pmc/articles/PMC358201/pdf/cmr00044-0075.pdf

Bruce, H. A., Du, D., Matak-Vinkovic, D., Bandyra, K. J., Broadhurst, R. W., Martin, E., … Luisi, B. F. (2017). Analysis of the natively unstructured RNA/protein-recognition core in the *Escherichia coli* RNA degradosome and its interactions with regulatory RNA/Hfq complexes. *Nucleic Acids Research*. https://doi.org/10.1093/nar/gkx1083

Brutinel, E. D., Vakulskas, C. A., Brady, K. M., & Yahr, T. L. (2008). Characterization of ExsA and of ExsA-dependent promoters required for expression of the *Pseudomonas aeruginosa* type III secretion system. *Molecular Microbiology*, *68*(3), 657–671. https://doi.org/10.1111/j.1365-2958.2008.06179.x

Brzostek, K., Brzostkowska, M., Bukowska, I., Karwicka, E., & Raczkowska, A. (2007). OmpR negatively regulates expression of invasin in *Yersinia enterocolitica*. *Microbiology*, *153*(8), 2416–2425. https://doi.org/10.1099/mic.0.2006/003202-0

Bücker, R., Heroven, A. K., Becker, J., Dersch, P., & Wittmann, C. (2014). The Pyruvate-Tricarboxylic Acid Cycle Node. *Journal of Biological Chemistry*, *289*(43), 30114–30132. https://doi.org/10.1074/jbc.M114.581348

Bulmer, D. M., Kharraz, L., Grant, A. J., Dean, P., Morgan, F. J. E., Karavolos, M. H., … Anjam Khan, C. M. (2012). The Bacterial Cytoskeleton Modulates Motility, Type 3 Secretion, and Colonization in Salmonella. *PLoS Pathogens*, *8*(1), e1002500. https://doi.org/10.1371/journal.ppat.1002500

Burghout, P., van Boxtel, R., Van Gelder, P., Ringler, P., Müller, S. A., Tommassen, J., & Koster, M. (2004). Structure and electrophysiological properties of the YscC secretin from the type III secretion system of *Yersinia enterocolitica*. *Journal of Bacteriology*, *186*(14), 4645–54. https://doi.org/10.1128/JB.186.14.4645-4654.2004

Burkinshaw, B. J., Deng, W., Lameignère, E., Wasney, G. A., Zhu, H., Worrall, L. J., … Strynadka, N. C. J. (2015). Structural analysis of a specialized type III secretion system peptidoglycan-cleaving enzyme. *The Journal of Biological Chemistry*, *290*(16), 10406–17. https://doi.org/10.1074/jbc.M115.639013

Butler, T. (2013). Plague Gives Surprises in the First Decade of the 21st Century in the United States and

Worldwide. *The American Journal of Tropical Medicine and Hygiene*, *89*(4), 788–793. https://doi.org/10.4269/ajtmh.13-0191

Büttner, C. R., Sorg, I., Cornelis, G. R., Heinz, D. W., & Niemann, H. H. (2008). Structure of the *Yersinia enterocolitica* Type III Secretion Translocator Chaperone SycD. *Journal of Molecular Biology*, *375*(4), 997–1012. https://doi.org/10.1016/j.jmb.2007.11.009

Buttner, D. (2012). Protein Export According to Schedule: Architecture, Assembly, and Regulation of Type III Secretion Systems from Plant- and Animal-Pathogenic Bacteria. *Microbiology and Molecular Biology Reviews*, *76*(2), 262–310. https://doi.org/10.1128/MMBR.05017-11

Cai, S. J., & Inouye, M. (2002). EnvZ-OmpR interaction and osmoregulation in *Escherichia coli*. *The Journal of Biological Chemistry*, *277*(27), 24155–61. https://doi.org/10.1074/jbc.M110715200

Callaghan, A. J., Aurikko, J. P., Ilag, L. L., Günter Grossmann, J., Chandran, V., Kühnel, K., … Luisi, B. F. (2004). Studies of the RNA Degradosome-organizing Domain of the *Escherichia coli* Ribonuclease RNase E. *Journal of Molecular Biology*, *340*(5), 965–979. https://doi.org/10.1016/j.jmb.2004.05.046

Callaghan, A. J., Marcaida, M. J., Stead, J. A., McDowall, K. J., Scott, W. G., & Luisi, B. F. (2005). Structure of *Escherichia coli* RNase E catalytic domain and implications for RNA turnover. *Nature*, *437*(7062), 1187–1191. https://doi.org/10.1038/nature04084

Cambronne, E. D., & Schneewind, O. (2002). *Yersinia enterocolitica* type III secretion: *yscM1* and *yscM2* regulate *yop* gene expression by a posttranscriptional mechanism that targets the 5' untranslated region of *yop* mRNA. *Journal of Bacteriology*, *184*(21), 5880–93. Retrieved from http://www.ncbi.nlm.nih.gov/pubmed/12374821

Cambronne, E. D., Sorg, J. A., & Schneewind, O. (2004). Binding of SycH chaperone to YscM1 and YscM2 activates effector yop expression in *Yersinia enterocolitica*. *Journal of Bacteriology*, *186*(3), 829–41. Retrieved from http://www.ncbi.nlm.nih.gov/pubmed/14729710

Carniel, E. (2001). The *Yersinia* high-pathogenicity island: an iron-uptake island. *Microbes and Infection*, *3*(7), 561–9. Retrieved from http://www.ncbi.nlm.nih.gov/pubmed/11418330

Carpousis, A. J. (2007). The RNA Degradosome of *Escherichia coli* : An mRNA-Degrading Machine Assembled on RNase E. *Annual Review of Microbiology*, *61*(1), 71–87. https://doi.org/10.1146/annurev.micro.61.080706.093440

Carzaniga, T., Briani, F., Zangrossi, S., Merlino, G., Marchi, P., & Dehò, G. (2009). Autogenous regulation of *Escherichia coli* polynucleotide phosphorylase expression revisited. *Journal of Bacteriology*, *191*(6), 1738–48. https://doi.org/10.1128/JB.01524-08

Carzaniga, T., Dehò, G., & Briani, F. (2015). RNase III-Independent Autogenous Regulation of *Escherichia coli* Polynucleotide Phosphorylase via Translational Repression. *Journal of Bacteriology*, *197*(11), 1931–8. https://doi.org/10.1128/JB.00105-15

Chandran, V., & Luisi, B. F. (2006). Recognition of Enolase in the *Escherichia coli* RNA Degradosome. *Journal of Molecular Biology*, *358*(1), 8–15. https://doi.org/10.1016/j.jmb.2006.02.012

Chandran, V., Poljak, L., Vanzo, N. F., Leroy, A., Miguel, R. N., Fernandez-Recio, J., … Luisi, B. F. (2007). Recognition and Cooperation Between the ATP-dependent RNA Helicase RhlB and Ribonuclease RNase E. *Journal of Molecular Biology*, *367*(1), 113–132. https://doi.org/10.1016/j.jmb.2006.12.014

Chao, Y., Li, L., Girodat, D., Förstner, K. U., Said, N., Corcoran, C., … Vogel, J. (2017). In Vivo Cleavage Map Illuminates the Central Role of RNase E in Coding and Non-coding RNA Pathways. *Molecular Cell*, *65*(1), 39–51. https://doi.org/10.1016/j.molcel.2016.11.002

Chao, Y., Papenfort, K., Reinhardt, R., Sharma, C. M., & Vogel, J. (2012). An atlas of Hfq-bound transcripts reveals 3' UTRs as a genomic reservoir of regulatory small RNAs. *The EMBO Journal*, *31*(20), 4005–19. https://doi.org/10.1038/emboj.2012.229

Chao, Y., & Vogel, J. (2016). A 3′ UTR-Derived Small RNA Provides the Regulatory Noncoding Arm of the Inner Membrane Stress Response. *Molecular Cell*, *61*(3), 352–363. https://doi.org/10.1016/J.MOLCEL.2015.12.023

Chen, R., Weng, Y., Zhu, F., Jin, Y., Liu, C., Pan, X., … Wu, W. (2016). Polynucleotide Phosphorylase Regulates Multiple Virulence Factors and the Stabilities of Small RNAs RsmY/Z in *Pseudomonas aeruginosa*. *Frontiers in Microbiology*, *7*, 247. https://doi.org/10.3389/fmicb.2016.00247

Chen, Y., & Anderson, D. M. (2011). Expression hierarchy in the *Yersinia* type III secretion system established through YopD recognition of RNAm mi_7623 966..980. https://doi.org/10.1111/j.1365-2958.2011.07623.x

Ching, T., Huang, S., & Garmire, L. X. (2014). Power analysis and sample size estimation for RNA-Seq differential expression. *RNA (New York, N.Y.)*, *20*(11), 1684–96. https://doi.org/10.1261/rna.046011.114

Chung, L. K., Park, Y. H., Zheng, Y., Brodsky, I. E., Hearing, P., Kastner, D. L., … Bliska, J. B. (2016). The *Yersinia* Virulence Factor YopM Hijacks Host Kinases to Inhibit Type III Effector-Triggered Activation of the Pyrin Inflammasome. *Cell Host & Microbe*, *20*(3), 296–306. https://doi.org/10.1016/j.chom.2016.07.018

Chung, L. K., Philip, N. H., Schmidt, V. A., Koller, A., Strowig, T., Flavell, R. A., … Bliska, J. B. (2014). IQGAP1 Is Important for Activation of Caspase-1 in Macrophages and Is Targeted by *Yersinia pestis* Type III Effector YopM. *MBio*, *5*(4), e01402-14-e01402-14. https://doi.org/10.1128/mBio.01402-14

Clarke, D. J. (2010). The Rcs phosphorelay: more than just a two-component pathway. *Future Microbiology*, *5*(8), 1173–1184. https://doi.org/10.2217/fmb.10.83

Clements, M. O., Eriksson, S., Thompson, A., Lucchini, S., Hinton, J. C. D., Normark, S., & Rhen, M. (2002). Polynucleotide phosphorylase is a global regulator of virulence and persistency in *Salmonella enterica*. *Proceedings of the National Academy of Sciences*, *99*(13), 8784–8789. https://doi.org/10.1073/pnas.132047099

Cliff, M. J., Williams, M. A., Brooke-Smith, J., Barford, D., & Ladbury, J. E. (2005). Molecular Recognition via Coupled Folding and Binding in a TPR Domain. *Journal of Molecular Biology*, *346*(3), 717–732. https://doi.org/10.1016/j.jmb.2004.12.017

Comer, M. M., Dondon, J., Graffe, M., Yarchuk, O., & Springer, M. (1996). Growth Rate-dependent Control, Feedback Regulation and Steady-state mRNA Levels of the Threonyl-tRNA Synthetase Gene of *Escherichia coli*. *Journal of Molecular Biology*, *261*(2), 108–124. https://doi.org/10.1006/jmbi.1996.0445

Coornaert, A., Chiaruttini, C., Springer, M., & Guillier, M. (2013). Post-transcriptional control of the *Escherichia coli* PhoQ-PhoP two-component system by multiple sRNAs involves a novel pairing region of GcvB. *PLoS Genetics*, *9*(1), e1003156. https://doi.org/10.1371/journal.pgen.1003156

Cornelis, G. R. (2002). *Yersinia* type III secretion: send in the effectors. *The Journal of Cell Biology*, *084018*(3), 21–9525. https://doi.org/10.1083/jcb.200205077

Cornelis, G. R., Biot, T., Lambert de Rouvroit, C., Michiels, T., Mulder, B., Sluiters, C., … Vanooteghem, J. C. (1989). The *Yersinia yop* regulon. *Molecular Microbiology*, *3*(10), 1455–9. Retrieved from http://www.ncbi.nlm.nih.gov/pubmed/2693899

Cornelis, G. R., Boland, A., Boyd, A. P., Geuijen, C., Iriarte, M., Neyt, C., … Stainier, I. (1998). The virulence plasmid of *Yersinia*, an antihost genome. *Microbiology and Molecular Biology Reviews : MMBR*, *62*(4), 1315–52. Retrieved from http://www.ncbi.nlm.nih.gov/pubmed/9841674

Cornelis, G. R., Sluiters, C., Delor, I., Geib, D., Kaniga, K., Lambert de Rouvroit, C., … Michiels, T. (1991). *ymoA*, a *Yersinia enterocolitica* chromosomal gene modulating the expression of virulence functions. *Molecular Microbiology*, *5*(5), 1023–34. Retrieved from

http://www.ncbi.nlm.nih.gov/pubmed/1956283

Cornelis, G. R., & Van Gijsegem, F. (2000). Assembly and function of type III secretory systems. *Annual Review of Microbiology*, *54*, 735–74. https://doi.org/10.1146/annurev.micro.54.1.735

Cornelis, G. R., & Wolf-Watz, H. (1997). The *Yersinia Yop* virulon: a bacterial system for subverting eukaryotic cells. *Molecular Microbiology*, *23*(5), 861–7. Retrieved from http://www.ncbi.nlm.nih.gov/pubmed/9076724

Cornelis, G., Sluiters, C., de Rouvroit, C. L., & Michiels, T. (1989). Homology between *virF*, the transcriptional activator of the *Yersinia* virulence regulon, and AraC, the *Escherichia coli* arabinose operon regulator. *Journal of Bacteriology*, *171*(1), 254–62. Retrieved from http://www.ncbi.nlm.nih.gov/pubmed/2644192

Cornelis, G., Vanootegem, J. C., & Sluiters, C. (1987). Transcription of the yop regulon from *Y. enterocolitica* requires trans acting pYV and chromosomal genes. *Microbial Pathogenesis*, *2*(5), 367–79. Retrieved from http://www.ncbi.nlm.nih.gov/pubmed/3507556

Costa, T. R. D., Amer, A. A. A., Fällman, M., Fahlgren, A., & Francis, M. S. (2012). Coiled-coils in the YopD translocator family: A predicted structure unique to the YopD N-terminus contributes to full virulence of *Yersinia pseudotuberculosis*. *Infection, Genetics and Evolution*, *12*(8), 1729–1742. https://doi.org/10.1016/j.meegid.2012.07.016

Costa, T. R. D., Edqvist, P. J., Bröms, J. E., Åhlund, M. K., Forsberg, Å., & Francis, M. S. (2010). YopD Self-assembly and Binding to LcrV Facilitate Type III Secretion Activity by *Yersinia pseudotuberculosis*. *Journal of Biological Chemistry*, *285*(33), 25269–25284. https://doi.org/10.1074/jbc.M110.144311

Costa, T. R. D., Felisberto-Rodrigues, C., Meir, A., Prevost, M. S., Redzej, A., Trokter, M., & Waksman, G. (2015). Secretion systems in Gram-negative bacteria: structural and mechanistic insights. *Nature Reviews Microbiology*, *13*(6), 343–359. https://doi.org/10.1038/nrmicro3456

Craig, E. A., & Gross, C. A. (1991). Is hsp70 the cellular thermometer? *Trends in Biochemical Sciences*, *16*(4), 135–40. Retrieved from http://www.ncbi.nlm.nih.gov/pubmed/1877088

Dach, K., Zovko, J., Hogardt, M., Koch, I., van Erp, K., Heesemann, J., & Hoffmann, R. (2009). Bacterial Toxins Induce Sustained mRNA Expression of the Silencing Transcription Factor *klf2* via Inactivation of RhoA and Rhophilin 1. *Infection and Immunity*, *77*(12), 5583–5592. https://doi.org/10.1128/IAI.00121-09

Dasgupta, N., Ashare, A., Hunninghake, G. W., & Yahr, T. L. (2006). Transcriptional induction of the *Pseudomonas aeruginosa* type III secretion system by low Ca^{2+} and host cell contact proceeds through two distinct signaling pathways. *Infection and Immunity*, *74*(6), 3334–41. https://doi.org/10.1128/IAI.00090-06

Dasgupta, N., Lykken, G. L., Wolfgang, M. C., & Yahr, T. L. (2004). A novel anti-anti-activator mechanism regulates expression of the *Pseudomonas aeruginosa* type III secretion system. *Molecular Microbiology*, *53*(1), 297–308. https://doi.org/10.1111/j.1365-2958.2004.04128.x

Datsenko, K. A., & Wanner, B. L. (2000). One-step inactivation of chromosomal genes in *Escherichia coli* K-12 using PCR products. *Proceedings of the National Academy of Sciences*, *97*(12), 6640–6645. https://doi.org/10.1073/pnas.120163297

Davies, B. W., Bogard, R. W., Young, T. S., & Mekalanos, J. J. (2012). Coordinated regulation of accessory genetic elements produces cyclic di-nucleotides for *V. cholerae* virulence. *Cell*, *149*(2), 358–70. https://doi.org/10.1016/j.cell.2012.01.053

Day, J. B., & Plano, G. V. (2000). The *Yersinia pestis* YscY protein directly binds YscX, a secreted component of the type III secretion machinery. *Journal of Bacteriology*, *182*(7), 1834–43. Retrieved from http://www.ncbi.nlm.nih.gov/pubmed/10714987

De Lay, N., & Gottesman, S. (2011). Role of polynucleotide phosphorylase in sRNA function in *Escherichia coli*. *RNA*, *17*(6), 1172–1189. https://doi.org/10.1261/rna.2531211

Denecker, G., Tötemeyer, S., Mota, L. J., Troisfontaines, P., Lambermont, I., Youta, C., … Cornelis, G. R. (2002). Effect of low- and high-virulence *Yersinia enterocolitica* strains on the inflammatory response of human umbilical vein endothelial cells. *Infection and Immunity*, *70*(7), 3510–20. Retrieved from http://www.ncbi.nlm.nih.gov/pubmed/12065490

Deng, W., Marshall, N. C., Rowland, J. L., McCoy, J. M., Worrall, L. J., Santos, A. S., … Finlay, B. B. (2017). Assembly, structure, function and regulation of type III secretion systems. *Nature Reviews Microbiology*, *15*(6). https://doi.org/10.1038/nrmicro.2017.20

Dersch, P., & Isberg, R. R. (1999). A region of the *Yersinia pseudotuberculosis* invasin protein enhances integrin-mediated uptake into mammalian cells and promotes self- association. *Embo J*, *18*(5), 1199–1213. https://doi.org/10.1093/emboj/18.5.1199

Detweiler, C. S., Monack, D. M., Brodsky, I. E., Mathew, H., & Falkow, S. (2003). *virK*, *somA* and *rcsC* are important for systemic *Salmonella enterica* serovar Typhimurium infection and cationic peptide resistance. *Molecular Microbiology*, *48*(2), 385–400. Retrieved from http://www.ncbi.nlm.nih.gov/pubmed/12675799

Deutscher, M. P., & Li, Z. (2001). Exoribonucleases and their multiple roles in RNA metabolism. *Progress in Nucleic Acid Research and Molecular Biology*, *66*, 67–105. Retrieved from http://www.ncbi.nlm.nih.gov/pubmed/11051762

Dewoody, R. S., Merritt, P. M., & Marketon, M. M. (2013). Regulation of the *Yersinia* type III secretion system: traffic control. *Frontiers in Cellular and Infection Microbiology*, *3*, 4. https://doi.org/10.3389/fcimb.2013.00004

Di Venanzio, G., Stepanenko, T. M., & García Véscovi, E. (2014). Serratia marcescens ShlA Pore-Forming Toxin Is Responsible for Early Induction of Autophagy in Host Cells and Is Transcriptionally Regulated by RcsB. *Infection and Immunity*, *82*(9), 3542–3554. https://doi.org/10.1128/IAI.01682-14

Diaz, M. R., King, J. M., & Yahr, T. L. (2011). Intrinsic and Extrinsic Regulation of Type III Secretion Gene Expression in *Pseudomonas Aeruginosa*. *Frontiers in Microbiology*, *2*, 89. https://doi.org/10.3389/fmicb.2011.00089

Diepold, A., Amstutz, M., Abel, S., Sorg, I., Jenal, U., & Cornelis, G. R. (2010). Deciphering the assembly of the *Yersinia* type III secretion injectisome. *The EMBO Journal*, *29*(11), 1928–40. https://doi.org/10.1038/emboj.2010.84

Diepold, A., Wiesand, U., Amstutz, M., & Cornelis, G. R. (2012). Assembly of the *Yersinia* injectisome: the missing pieces. *Molecular Microbiology*, *85*(5), 878–892. https://doi.org/10.1111/j.1365-2958.2012.08146.x

Diepold, A., Wiesand, U., & Cornelis, G. R. (2011). The assembly of the export apparatus (YscR,S,T,U,V) of the *Yersinia* type III secretion apparatus occurs independently of other structural components and involves the formation of an YscV oligomer. *Molecular Microbiology*, *82*(2), 502–514. https://doi.org/10.1111/j.1365-2958.2011.07830.x

Diwa, A., Bricker, A. L., Jain, C., & Belasco, J. G. (2000). An evolutionarily conserved RNA stem-loop functions as a sensor that directs feedback regulation of RNase E gene expression. *Genes & Development*, *14*(10), 1249–60. https://doi.org/10.1101/GAD.14.10.1249

Dohlich, K., Zumsteg, A. B., Goosmann, C., & Kolbe, M. (2014). A Substrate-Fusion Protein Is Trapped inside the Type III Secretion System Channel in *Shigella flexneri*. *PLoS Pathogens*, *10*(1), e1003881. https://doi.org/10.1371/journal.ppat.1003881

Domínguez-Bernal, G., Pucciarelli, M. G., Ramos-Morales, F., García-Quintanilla, M., Cano, D. A., Casadesús, J., & García-del Portillo, F. (2004). Repression of the RcsC-YojN-RcsB phosphorelay by

the IgaA protein is a requisite for *Salmonella* virulence. *Molecular Microbiology*, *53*(5), 1437–1449. https://doi.org/10.1111/j.1365-2958.2004.04213.x

Dubey, A. K., Baker, C. S., Romeo, T., & Babitzke, P. (2005). RNA sequence and secondary structure participate in high-affinity CsrA-RNA interaction. *RNA (New York, N.Y.)*, *11*(10), 1579–87. https://doi.org/10.1261/rna.2990205

Dubey, A. K., Baker, C. S., Suzuki, K., Jones, A. D., Pandit, P., Romeo, T., & Babitzke, P. (2003). CsrA regulates translation of the *Escherichia coli* carbon starvation gene, *cstA*, by blocking ribosome access to the *cstA* transcript. *Journal of Bacteriology*, *185*(15), 4450–60. Retrieved from http://www.ncbi.nlm.nih.gov/pubmed/12867454

Dugar, G., Svensson, S. L., Bischler, T., Wäldchen, S., Reinhardt, R., Sauer, M., & Sharma, C. M. (2016). The CsrA-FliW network controls polar localization of the dual-function flagellin mRNA in *Campylobacter jejuni*. *Nature Communications*, *7*, 11667. https://doi.org/10.1038/ncomms11667

Duss, O., Michel, E., Diarra dit Konté, N., Schubert, M., & Allain, F. H.-T. (2014). Molecular basis for the wide range of affinity found in Csr/Rsm protein–RNA recognition. *Nucleic Acids Research*, *42*(8), 5332–5346. https://doi.org/10.1093/nar/gku141

Edgren, T., Forsberg, Å., Rosqvist, R., & Wolf-Watz, H. (2012). Type III Secretion in *Yersinia*: Injectisome or Not? *PLoS Pathogens*, *8*(5), e1002669. https://doi.org/10.1371/journal.ppat.1002669

Eitel, J., & Dersch, P. (2002). The YadA protein of *Yersinia pseudotuberculosis* mediates high-efficiency uptake into human cells under environmental conditions in which invasin is repressed. *Infection and Immunity*, *70*(9), 4880–91. Retrieved from http://www.ncbi.nlm.nih.gov/pubmed/12183532

Eitel, J., Heise, T., Thiesen, U., & Dersch, P. (2004). Cell invasion and IL-8 production pathways initiated by YadA of *Yersinia pseudotuberculosis* require common signalling molecules (FAK, c-Src, Ras) and distinct cell factors. *Cellular Microbiology*, *7*(1), 63–77. https://doi.org/10.1111/j.1462-5822.2004.00434.x

El Mortaji, L., Aubert, S., Galtier, E., Schmitt, C., Anger, K., Redko, Y., … De Reuse, H. (2018). The Sole DEAD-Box RNA Helicase of the Gastric Pathogen *Helicobacter pylori* Is Essential for Colonization. *MBio*, *9*(2), e02071-17. https://doi.org/10.1128/mBio.02071-17

Ellermeier, J. R., & Slauch, J. M. (2008). Fur regulates expression of the *Salmonella* pathogenicity island 1 type III secretion system through HilD. *Journal of Bacteriology*, *190*(2), 476–86. https://doi.org/10.1128/JB.00926-07

Erhardt, M., & Dersch, P. (2015). Regulatory principles governing *Salmonella* and *Yersinia* virulence. *Frontiers in Microbiology*. https://doi.org/10.3389/fmicb.2015.00949

Erhardt, M., Namba, K., & Hughes, K. T. (2010). Bacterial Nanomachines: The Flagellum and Type III Injectisome. *Cold Spring Harbor Perspectives in Biology*, *2*(11), a000299–a000299. https://doi.org/10.1101/cshperspect.a000299

Erhardt, M., Singer, H. M., Wee, D. H., Keener, J. P., & Hughes, K. T. (2011). An infrequent molecular ruler controls flagellar hook length in *Salmonella enterica*. *The EMBO Journal*, *30*(14), 2948–2961. https://doi.org/10.1038/emboj.2011.185

Esquerré, T., Bouvier, M., Turlan, C., Carpousis, A. J., Girbal, L., & Cocaign-Bousquet, M. (2016). The Csr system regulates genome-wide mRNA stability and transcription and thus gene expression in Escherichia coli. *Scientific Reports*, *6*(1), 25057. https://doi.org/10.1038/srep25057

Evdokimov, A. G., Tropea, J. E., Routzahn, K. M., & Waugh, D. S. (2009). Crystal structure of the *Yersinia pestis* GTPase activator YopE. *Protein Science*, *11*(2), 401–408. https://doi.org/10.1110/ps.34102

Fahlgren, A., Avican, K., Westermark, L., Nordfelth, R., & Fällman, M. (2014). Colonization of cecum is important for development of persistent infection by *Yersinia pseudotuberculosis*. *Infection and*

Immunity, *82*(8), 3471–82. https://doi.org/10.1128/IAI.01793-14

Fang, N., Yang, H., Fang, H., Liu, L., Zhang, Y., Wang, L., … Yang, R. (2015). RcsAB is a major repressor of *Yersinia* biofilm development through directly acting on *hmsCDE*, *hmsT* and *hmsHFRS*. *Scientific Reports*, *5*(1), 9566. https://doi.org/10.1038/srep09566

Farizano, J. V., Torres, M. A., Pescaretti, M. d. l. M., & Delgado, M. A. (2014). The RcsCDB regulatory system plays a crucial role in the protection of *Salmonella enterica* serovar Typhimurium against oxidative stress. *Microbiology*, *160*(Pt_10), 2190–2199. https://doi.org/10.1099/mic.0.081133-0

Felden, B., Vandenesch, F., Bouloc, P., & Romby, P. (2011). The Staphylococcus aureus RNome and Its Commitment to Virulence. *PLoS Pathogens*, *7*(3), e1002006. https://doi.org/10.1371/journal.ppat.1002006

Flamez, C., Ricard, I., Arafah, S., Simonet, M., & Marceau, M. (2008). Phenotypic analysis of *Yersinia pseudotuberculosis* 32777 response regulator mutants: New insights into two-component system regulon plasticity in bacteria. *International Journal of Medical Microbiology*, *298*(3–4), 193–207. https://doi.org/10.1016/j.ijmm.2007.05.005

Fleischhacker, A. S., Stubna, A., Hsueh, K.-L., Guo, Y., Teter, S. J., Rose, J. C., … Kiley, P. J. (2012). Characterization of the [2Fe-2S] Cluster of *Escherichia coli* Transcription Factor IscR. *Biochemistry*, *51*(22), 4453–4462. https://doi.org/10.1021/bi3003204

Flügel, A., Schulze-Koops, H., Heesemann, J., Kühn, K., Sorokin, L., Burkhardt, H., … Emmrich, F. (1994). Interaction of enteropathogenic *Yersinia enterocolitica* with complex basement membranes and the extracellular matrix proteins collagen type IV, laminin-1 and -2, and nidogen/entactin. *The Journal of Biological Chemistry*, *269*(47), 29732–8. Retrieved from http://www.ncbi.nlm.nih.gov/pubmed/7961965

Fogelson, S. B., Yau, W., & Rissi, D. R. (2015). Disseminated *Yersinia pseudotuberculosis* infection in a paca (*Cuniculus paca*). *Journal of Zoo and Wildlife Medicine*, *46*(1), 130–134. https://doi.org/10.1638/2014-0150R.1

Fontaine, F., Gasiorowski, E., Gracia, C., Ballouche, M., Caillet, J., Marchais, A., & Hajnsdorf, E. (2016). The small RNA SraG participates in PNPase homeostasis. *RNA (New York, N.Y.)*, *22*(10), 1560–73. https://doi.org/10.1261/rna.055236.115

Fowler, J. M., Wulff, C. R., Straley, S. C., & Brubaker, R. R. (2009). Growth of calcium-blind mutants of *Yersinia pestis* at 37 degrees C in permissive Ca^{2+}-deficient environments. *Microbiology (Reading, England)*, *155*(Pt 8), 2509–21. https://doi.org/10.1099/mic.0.028852-0

Francis, M. S., Aili, M., Wiklund, M. L., & Wolf-Watz, H. (2000). A study of the YopD-lcrH interaction from *Yersinia pseudotuberculosis* reveals a role for hydrophobic residues within the amphipathic domain of YopD. *Molecular Microbiology*, *38*(1), 85–102. Retrieved from http://www.ncbi.nlm.nih.gov/pubmed/11029692

Francis, M. S., Lloyd, S. A., & Wolf-Watz, H. (2001). The type III secretion chaperone LcrH co-operates with YopD to establish a negative, regulatory loop for control of Yop synthesis in *Yersinia pseudotuberculosis*. *Molecular Microbiology*, *42*(4), 1075–93. Retrieved from http://www.ncbi.nlm.nih.gov/pubmed/11737648

Frandölich, K., Wisser, J., Schmüser, H., Fehlberg, U., Neubauer, H., Grunow, R., … Speck, S. (2003). Epizootiologic and ecologic investigations of european brown hares (*Lepus europaeus*) in selected populations from Schleswig-Holstein, Germany. *Journal of Wildlife Diseases*, *39*(4), 751–761. https://doi.org/10.7589/0090-3558-39.4.751

Fredericks, C. E., Shibata, S., Aizawa, S.-I., Reimann, S. A., & Wolfe, A. J. (2006). Acetyl phosphate-sensitive regulation of flagellar biogenesis and capsular biosynthesis depends on the Rcs phosphorelay. *Molecular Microbiology*, *61*(3), 734–747. https://doi.org/10.1111/j.1365-2958.2006.05260.x

Fukumoto, Y., Hiraoka, M., Takano, T., Hori, C., Tsuchida, S., Kikawa, Y., & Sudo, M. (1995). Acute tubulointerstitial nephritis in association with *Yersinia pseudotuberculosis* infection. *Pediatric Nephrology*, *9*(1), 78–80. https://doi.org/10.1007/BF00858979

Fukushima, H. (2003). Molecular Epidemiology of *Yersinia pseudotuberculosis*. In *The Genus Yersinia* (Vol. 529, pp. 357–358). Boston: Kluwer Academic Publishers. https://doi.org/10.1007/0-306-48416-1_70

Fukushima, H., Tsubokura, M., Otsuki, K., Kawaoka, Y., Nishio, R., Moriki, S., … Karino, K. (1985). Epidemiological study of *Yersinia enterocolitica* and *Yersinia pseudotuberculosis* infections in Shimane Prefecture, Japan. *Zentralblatt Fur Bakteriologie, Mikrobiologie Und Hygiene. 1. Abt. Originale B, Hygiene*, *180*(5–6), 515–27. Retrieved from http://www.ncbi.nlm.nih.gov/pubmed/3895776

Galán, J. E. (2001). *Salmonella* Interactions with Host Cells: Type III Secretion at Work. *Annual Review of Cell and Developmental Biology*, *17*(1), 53–86. https://doi.org/10.1146/annurev.cellbio.17.1.53

Galindo, C. L., Rosenzweig, J. A., Kirtley, M. L., & Chopra, A. K. (2011). Pathogenesis of Y. enterocolitica and Y. pseudotuberculosis in Human Yersiniosis. *Journal of Pathogens*, *2011*, 182051. https://doi.org/10.4061/2011/182051

Galyov, E. E., Håkansson, S., Forsberg, Å., & Wolf-Watz, H. (1993). A secreted protein kinase of *Yersinia pseudotuberculosis* is an indispensable virulence determinant. *Nature*, *361*(6414), 730–732. https://doi.org/10.1038/361730a0

Gauthier, A., Puente, J. L., & Finlay, B. B. (2003). Secretin of the enteropathogenic *Escherichia coli* type III secretion system requires components of the type III apparatus for assembly and localization. *Infection and Immunity*, *71*(6), 3310–9. Retrieved from http://www.ncbi.nlm.nih.gov/pubmed/12761113

Gay, P., Le Coq, D., Steinmetz, M., Berkelman, T., & Kado, C. I. (1985). Positive selection procedure for entrapment of insertion sequence elements in gram-negative bacteria. *Journal of Bacteriology*, *164*(2), 918–21. Retrieved from http://www.ncbi.nlm.nih.gov/pubmed/2997137

Gemski, P., Lazere, J. R., Casey, T., & Wohlhieter, J. A. (1980). Presence of a virulence-associated plasmid in *Yersinia pseudotuberculosis*. *Infection and Immunity*, *28*(3), 1044–7. Retrieved from http://www.ncbi.nlm.nih.gov/pubmed/6249747

Gervais, F. G., & Drapeau, G. R. (1992). Identification, cloning, and characterization of *rcsF*, a new regulator gene for exopolysaccharide synthesis that suppresses the division mutation *ftsZ84* in *Escherichia coli* K-12. *Journal of Bacteriology*, *174*(24), 8016–22. Retrieved from http://www.ncbi.nlm.nih.gov/pubmed/1459951

Girschick, H. J., Guilherme, L., Inman, R. D., Latsch, K., Rihl, M., Sherer, Y., … Doria, A. (2008). Bacterial triggers and autoimmune rheumatic diseases. *Clinical and Experimental Rheumatology*, *26*(1 Suppl 48), S12-7. Retrieved from http://www.ncbi.nlm.nih.gov/pubmed/18570749

Golubeva, Y. A., Ellermeier, J. R., Cott Chubiz, J. E., & Slauch, J. M. (2016). Intestinal Long-Chain Fatty Acids Act as a Direct Signal To Modulate Expression of the *Salmonella* Pathogenicity Island 1 Type III Secretion System. *MBio*, *7*(1), e02170-15. https://doi.org/10.1128/mBio.02170-15

Gong, H., Vu, G.-P., Bai, Y., Chan, E., Wu, R., Yang, E., … Lu, S. (2011). A *Salmonella* small non-coding RNA facilitates bacterial invasion and intracellular replication by modulating the expression of virulence factors. *PLoS Pathogens*, *7*(9), e1002120. https://doi.org/10.1371/journal.ppat.1002120

Gonzalez Chavez, R., Alvarez, A. F., Romeo, T., & Georgellis, D. (2010). The Physiological Stimulus for the BarA Sensor Kinase. *Journal of Bacteriology*, *192*(7), 2009–2012. https://doi.org/10.1128/JB.01685-09

Górna, M. W., Carpousis, A. J., & Luisi, B. F. (2012). From conformational chaos to robust regulation: the structure and function of the multi-enzyme RNA degradosome. *Quarterly Reviews of Biophysics*, *45*(02), 105–145. https://doi.org/10.1017/S003358351100014X

Gotoh, K., Kodama, T., Hiyoshi, H., Izutsu, K., Park, K.-S., Dryselius, R., … Iida, T. (2010). Bile Acid-Induced Virulence Gene Expression of *Vibrio parahaemolyticus* Reveals a Novel Therapeutic Potential for Bile Acid Sequestrants. *PLoS ONE*, *5*(10), e13365. https://doi.org/10.1371/journal.pone.0013365

Goure, J., Broz, P., Attree, O., Cornelis, G. R., & Attree, I. (2005). Protective Anti-V Antibodies Inhibit *Pseudomonas* and *Yersinia* Translocon Assembly within Host Membranes. *The Journal of Infectious Diseases*, *192*(2), 218–225. https://doi.org/10.1086/430932

Grabenstein, J. P., Marceau, M., Pujol, C., Simonet, M., & Bliska, J. B. (2004). The Response Regulator PhoP of *Yersinia pseudotuberculosis* Is Important for Replication in Macrophages and for Virulence. *Infection and Immunity*, *72*(9), 4973–4984. https://doi.org/10.1128/IAI.72.9.4973-4984.2004

Grassl, G. A., Bohn, E., Müller, Y., Bühler, O. T., & Autenrieth, I. B. (2003). Interaction of *Yersinia enterocolitica* with epithelial cells: invasin beyond invasion. *International Journal of Medical Microbiology*, *293*(1), 41–54. https://doi.org/10.1078/1438-4221-00243

Groves, E., Dart, A. E., Covarelli, V., & Caron, E. (2008). Molecular mechanisms of phagocytic uptake in mammalian cells. *Cellular and Molecular Life Sciences*, *65*(13), 1957–1976. https://doi.org/10.1007/s00018-008-7578-4

Grutzkau, A., Hanski, C., Hahn, H., & Riecken, E. O. (1990). Involvement of M cells in the bacterial invasion of Peyer's patches: a common mechanism shared by *Yersinia enterocolitica* and other enteroinvasive bacteria. *Gut*, *31*(9), 1011–1015. https://doi.org/10.1136/gut.31.9.1011

Guarneros, G., & Portier, C. (1990). Different specificities of ribonuclease II and polynucleotide phosphorylase in 3'mRNA decay. *Biochimie*, *72*(11), 771–7. Retrieved from http://www.ncbi.nlm.nih.gov/pubmed/2085542

Guinet, F., Carniel, E., & Leclercq, A. (2011). Transfusion-Transmitted *Yersinia enterocolitica* Sepsis. *Clinical Infectious Diseases*, *53*(6), 583–591. https://doi.org/10.1093/cid/cir452

Guiyoule, A., Gerbaud, G., Buchrieser, C., Galimand, M., Rahalison, L., Chanteau, S., … Carniel, E. (2001). Transferable plasmid-mediated resistance to streptomycin in a clinical isolate of *Yersinia pestis*. *Emerging Infectious Diseases*, *7*(1), 43–8. https://doi.org/10.3201/eid0701.700043

Guo, X.-P., & Sun, Y.-C. (2017). New Insights into the Non-orthodox Two Component Rcs Phosphorelay System. *Frontiers in Microbiology*, *8*, 2014. https://doi.org/10.3389/fmicb.2017.02014

Gutierrez, P., Li, Y., Osborne, M. J., Pomerantseva, E., Liu, Q., & Gehring, K. (2005). Solution Structure of the Carbon Storage Regulator Protein CsrA from *Escherichia coli*. *Journal of Bacteriology*, *187*(10), 3496–3501. https://doi.org/10.1128/JB.187.10.3496-3501.2005

Haas, B. J., Chin, M., Nusbaum, C., Birren, B. W., & Livny, J. (2012). How deep is deep enough for RNA-Seq profiling of bacterial transcriptomes? *BMC Genomics*, *13*(1), 734. https://doi.org/10.1186/1471-2164-13-734

Haddad, N., Tresse, O., Rivoal, K., Chevret, D., Nonglaton, Q., Burns, C. M., … Cappelier, J. M. (2012). Polynucleotide phosphorylase has an impact on cell biology of *Campylobacter jejuni*. *Frontiers in Cellular and Infection Microbiology*, *2*, 30. https://doi.org/10.3389/fcimb.2012.00030

Hagiwara, D., Sugiura, M., Oshima, T., Mori, H., Aiba, H., Yamashino, T., & Mizuno, T. (2003). Genome-wide analyses revealing a signaling network of the RcsC-YojN-RcsB phosphorelay system in *Escherichia coli*. *Journal of Bacteriology*, *185*(19), 5735–46. Retrieved from http://www.pubmedcentral.nih.gov/articlerender.fcgi?artid=193970&tool=pmcentrez&rendertype=abstract

Håkansson, S., Galyov, E. E., Rosqvist, R., & Wolf-Watz, H. (1996). The *Yersinia* YpkA Ser/Thr kinase is translocated and subsequently targeted to the inner surface of the HeLa cell plasma membrane. *Molecular Microbiology*, *20*(3), 593–603. Retrieved from http://www.ncbi.nlm.nih.gov/pubmed/8736538

Håkansson, S., Schesser, K., Persson, C., Galyov, E. E., Rosqvist, R., Homblé, F., & Wolf-Watz, H. (1996). The YopB protein of *Yersinia pseudotuberculosis* is essential for the translocation of Yop effector proteins across the target cell plasma membrane and displays a contact-dependent membrane disrupting activity. *The EMBO Journal*, *15*(21), 5812–23. Retrieved from http://www.ncbi.nlm.nih.gov/pubmed/8918459

Hamburger, Z. A., Brown, M. S., Isberg, R. R., & Bjorkman, P. J. (1999). Crystal structure of invasin: a bacterial integrin-binding protein. *Science (New York, N.Y.)*, *286*(5438), 291–5. Retrieved from http://www.ncbi.nlm.nih.gov/pubmed/10514372

Han, Y. W., & Miller, V. L. (1997). Reevaluation of the virulence phenotype of the *inv yadA* double mutants of *Yersinia pseudotuberculosis*. *Infection and Immunity*, *65*(1), 327–30. Retrieved from http://www.ncbi.nlm.nih.gov/pubmed/8975933

Hannu, T., Mattila, L., Nuorti, J. P., Ruutu, P., Mikkola, J., Siitonen, A., & Leirisalo-Repo, M. (2003). Reactive arthritis after an outbreak of *Yersinia pseudotuberculosis* serotype O:3 infection. *Ann Rheum Dis*, *62*, 866–869. Retrieved from https://pdfs.semanticscholar.org/ab72/5ced61d203eea9feaee4cf27630f3f161605.pdf

Hargreaves, C. E., Grasso, M., Hampe, C. S., Stenkova, A., Atkinson, S., Joshua, G. W. P., … Banga, J. P. (2013). *Yersinia enterocolitica* Provides the Link between Thyroid-Stimulating Antibodies and Their Germline Counterparts in Graves' Disease. *The Journal of Immunology*, *190*(11), 5373–5381. https://doi.org/10.4049/jimmunol.1203412

Harmon, D. E., Murphy, J. L., Davis, A. J., & Mecsas, J. (2013). A mutant with aberrant extracellular LcrV-YscF interactions fails to form pores and translocate Yop effector proteins but retains the ability to trigger Yop secretion in response to host cell contact. *Journal of Bacteriology*, *195*(10), 2244–54. https://doi.org/10.1128/JB.02011-12

Hawgood, B. J. (2008). Alexandre Yersin (1863–1943): discoverer of the plague bacillus, explorer and agronomist. *Journal of Medical Biography*, *16*(3), 167–172. https://doi.org/10.1258/jmb.2007.007017

Heesemann, J., Gross, U., & Grüter, L. (1987). Genetic manipulation of virulence of *Yersinia enterocolitica*. *Contributions to Microbiology and Immunology*, *9*, 312–6. Retrieved from http://www.ncbi.nlm.nih.gov/pubmed/2822353

Heise, T., & Dersch, P. (2006). Identification of a domain in *Yersinia* virulence factor YadA that is crucial for extracellular matrix-specific cell adhesion and uptake. *Proceedings of the National Academy of Sciences*, *103*(9), 3375–3380. https://doi.org/10.1073/pnas.0507749103

Hejair, H. M. A., Zhu, Y., Ma, J., Zhang, Y., Pan, Z., Zhang, W., & Yao, H. (2017). Functional role of *ompF* and *ompC* porins in pathogenesis of avian pathogenic Escherichia coli. *Microbial Pathogenesis*, *107*, 29–37. https://doi.org/10.1016/j.micpath.2017.02.033

Henderson, I. R., Navarro-Garcia, F., Desvaux, M., Fernandez, R. C., & Ala'Aldeen, D. (2004). Type V Protein Secretion Pathway: the Autotransporter Story. *Microbiology and Molecular Biology Reviews*, *68*(4), 692–744. https://doi.org/10.1128/MMBR.68.4.692-744.2004

Heroven, A. K., Böhme, K., & Dersch, P. (2012). The Csr/Rsm system of *Yersinia* and related pathogens: a post-transcriptional strategy for managing virulence. *RNA Biology*, *9*(4), 379–91. https://doi.org/10.4161/rna.19333

Heroven, A. K., Böhme, K., Rohde, M., & Dersch, P. (2008). A Csr-type regulatory system, including small non-coding RNAs, regulates the global virulence regulator RovA of *Yersinia pseudotuberculosis* through RovM. *Molecular Microbiology*, *68*(5), 1179–95. https://doi.org/10.1111/j.1365-2958.2008.06218.x

Heroven, A. K., & Dersch, P. (2006). RovM, a novel LysR-type regulator of the virulence activator gene *rovA*, controls cell invasion, virulence and motility of *Yersinia pseudotuberculosis*. *Molecular Microbiology*, *62*(5), 1469–1483. https://doi.org/10.1111/j.1365-2958.2006.05458.x

Heroven, A. K., & Dersch, P. (2014). Coregulation of host-adapted metabolism and virulence by pathogenic yersiniae. *Frontiers in Cellular and Infection Microbiology*, *4*. https://doi.org/10.3389/fcimb.2014.00146

Higuchi, K., Kupferberg, L. L., & Smith, J. L. (1959). Studies on the nutrition and physiology of *Pasteurella pestis*. III. Effects of calcium ions on the growth of virulent and avirulent strains of *Pasteurella pestis*. *Journal of Bacteriology*, *77*(3), 317–21. Retrieved from http://www.ncbi.nlm.nih.gov/pubmed/13641190

Hinnebusch, B. J., Chouikha, I., & Sun, Y.-C. (2016). Ecological Opportunity, Evolution, and the Emergence of Flea-Borne Plague. *Infection and Immunity*, *84*(7), 1932–40. https://doi.org/10.1128/IAI.00188-16

Hoe, N. P., & Goguen, J. D. (1993). Temperature sensing in *Yersinia pestis*: translation of the LcrF activator protein is thermally regulated. *Journal of Bacteriology*, *175*(24), 7901–9. Retrieved from http://www.ncbi.nlm.nih.gov/pubmed/7504666

Hoffman, J. M., Sullivan, S., Wu, E., Wilson, E., & Erickson, D. L. (2017). Differential impact of lipopolysaccharide defects caused by loss of RfaH in *Yersinia pseudotuberculosis* and *Yersinia pestis*. https://doi.org/10.1038/s41598-017-11334-6

Hoiczyk, E., Roggenkamp, A., Reichenbecher, M., Lupas, A., & Heesemann, J. (2000). Structure and sequence analysis of *Yersinia* YadA and *Moraxella* UspAs reveal a novel class of adhesins. *The EMBO Journal*, *19*(22), 5989–99. https://doi.org/10.1093/emboj/19.22.5989

Holmqvist, E., & Vogel, J. (2018). RNA-binding proteins in bacteria. *Nature Reviews Microbiology*, 1. https://doi.org/10.1038/s41579-018-0049-5

Holmqvist, E., Wright, P. R., Li, L., Bischler, T., Barquist, L., Reinhardt, R., … Vogel, J. (2016). Global RNA recognition patterns of post-transcriptional regulators Hfq and CsrA revealed by UV crosslinking *in vivo*. *The EMBO Journal*, *35*(9), 991–1011. https://doi.org/10.15252/embj.201593360

Holmstrom, A., Olsson, J., Cherepanov, P., Maier, E., Nordfelth, R., Pettersson, J., … Forsberg, A. (2001). LcrV is a channel size-determining component of the Yop effector translocon of *Yersinia*. *Molecular Microbiology*, *39*(3), 620–632. https://doi.org/10.1046/j.1365-2958.2001.02259.x

Horinouchi, T., Nozu, K., Hamahira, K., Inaguma, Y., Abe, J., Nakajima, H., … Iijima, K. (2015). *Yersinia pseudotuberculosis* infection in Kawasaki disease and its clinical characteristics. *BMC Pediatrics*, *15*, 177. https://doi.org/10.1186/s12887-015-0497-2

Hoßmann, J. (2017). RNA-based control of the expression of the type III secretion system of *Yersinia pseudotuberculosis*.

Hu, J., & Zhu, M.-J. (2015). Defects in polynucleotide phosphorylase impairs virulence in *Escherichia coli* O157:H7. *Frontiers in Microbiology*, *6*, 806. https://doi.org/10.3389/fmicb.2015.00806

Hu, Y., Lu, P., Wang, Y., Ding, L., Atkinson, S., & Chen, S. (2009). OmpR positively regulates urease expression to enhance acid survival of *Yersinia pseudotuberculosis*. *Microbiology*. https://doi.org/10.1099/mic.0.028381-0

Huang, X.-Z., & Lindler, L. E. (2004). The pH 6 antigen is an antiphagocytic factor produced by *Yersinia pestis* independent of *Yersinia* outer proteins and capsule antigen. *Infection and Immunity*, *72*(12), 7212–9. https://doi.org/10.1128/IAI.72.12.7212-7219.2004

Huang, Y.-H., Ferrières, L., & Clarke, D. J. (2006). The role of the Rcs phosphorelay in Enterobacteriaceae. *Research in Microbiology*, *157*(3), 206–212. https://doi.org/10.1016/j.resmic.2005.11.005

Huang, Y., Suyemoto, M., Garner, C. D., Cicconi, K. M., & Altier, C. (2008). Formate acts as a diffusible signal to induce *Salmonella* invasion. *Journal of Bacteriology*, *190*(12), 4233–41. https://doi.org/10.1128/JB.00205-08

Hughes, D. T., Clarke, M. B., Yamamoto, K., Rasko, D. A., & Sperandio, V. (2009). The QseC Adrenergic Signaling Cascade in Enterohemorrhagic *E. coli* (EHEC). *PLoS Pathogens*, *5*(8), e1000553. https://doi.org/10.1371/journal.ppat.1000553

Hui, M. P., Foley, P. L., & Belasco, J. G. (2014). Messenger RNA Degradation in Bacterial Cells. *Annual Review of Genetics*, *48*(1), 537–559. https://doi.org/10.1146/annurev-genet-120213-092340

Hung, C.-C., Garner, C. D., Slauch, J. M., Dwyer, Z. W., Lawhon, S. D., Frye, J. G., … Altier, C. (2013). The intestinal fatty acid propionate inhibits *Salmonella* invasion through the post-translational control of HilD. *Molecular Microbiology*, *87*(5), 1045–1060. https://doi.org/10.1111/mmi.12149

Ikemura, T. (1985). Codon usage and tRNA content in unicellular and multicellular organisms. *Molecular Biology and Evolution*, *2*(1), 13–34. https://doi.org/10.1093/oxfordjournals.molbev.a040335

Imataki, O., Uemura, M., Matsumoto, K., & Ishibashi, N. (2014). *Yersinia pseudotuberculosis* enterocolitis mimicking enteropathic γδ T-cell lymphoma with abnormal clonality. *BMC Infectious Diseases*, *14*(1), 42. https://doi.org/10.1186/1471-2334-14-42

Intile, P. J., Balzer, G. J., Wolfgang, M. C., & Yahr, T. L. (2015). The RNA Helicase DeaD Stimulates ExsA Translation To Promote Expression of the *Pseudomonas aeruginosa* Type III Secretion System. *Journal of Bacteriology*, *197*(16), 2664–74. https://doi.org/10.1128/JB.00231-15

Intile, P. J., Diaz, M. R., Urbanowski, M. L., Wolfgang, M. C., & Yahr, T. L. (2014). The AlgZR two-component system recalibrates the RsmAYZ posttranscriptional regulatory system to inhibit expression of the *Pseudomonas aeruginosa* type III secretion system. *Journal of Bacteriology*, *196*(2), 357–66. https://doi.org/10.1128/JB.01199-13

Iriarte, M., & Cornelis, G. R. (1998). YopT, a new *Yersinia* Yop effector protein, affects the cytoskeleton of host cells. *Molecular Microbiology*, *29*(3), 915–29. Retrieved from http://www.ncbi.nlm.nih.gov/pubmed/9723929

Isberg, R. R. (1990). Pathways for the penetration of enteroinvasive *Yersinia* into mammalian cells. *Molecular Biology & Medicine*, *7*(1), 73–82. Retrieved from http://www.ncbi.nlm.nih.gov/pubmed/2182969

Izoré, T., Job, V., & Dessen, A. (2011). Biogenesis, regulation, and targeting of the type III secretion system. *Structure (London, England : 1993)*, *19*(5), 603–12. https://doi.org/10.1016/j.str.2011.03.015

Jackson, M. W., & Plano, G. V. (2000). Interactions between type III secretion apparatus components from *Yersinia pestis* detected using the yeast two-hybrid system. *FEMS Microbiology Letters*, *186*(1), 85–90. Retrieved from http://www.ncbi.nlm.nih.gov/pubmed/10779717

Jackson, M. W., Silva-Herzog, E., & Plano, G. V. (2004). The ATP-dependent ClpXP and Lon proteases regulate expression of the *Yersinia pestis* type III secretion system via regulated proteolysis of YmoA, a small histone-like protein. *Molecular Microbiology*, *54*(5), 1364–1378. https://doi.org/10.1111/j.1365-2958.2004.04353.x

Jain, C., & Belasco, J. G. (1995). Autoregulation of RNase E synthesis in *Escherichia coli*. *Nucleic Acids Symposium Series*, (33), 85–8. Retrieved from http://www.ncbi.nlm.nih.gov/pubmed/8643409

Jalava, K., Hakkinen, M., Valkonen, M., Nakari, U.-M., Palo, T., Hallanvuo, S., … Nuorti, P. (2006). An Outbreak of Gastrointestinal Illness and Erythema Nodosum from Grated Carrots Contaminated with *Yersinia pseudotuberculosis*. *The Journal of Infectious Diseases*, *194*, 1209–16. Retrieved from https://pdfs.semanticscholar.org/93aa/282aa53b0dc4a8d7610d07a35de78b796aef.pdf

Jalava, K., Hallanvuo, S., Nakari, U.-M., Ruutu, P., Kela, E., Heinäsmäki, T., … Nuorti, J. P. (2004). Multiple outbreaks of *Yersinia pseudotuberculosis* infections in Finland. *Journal of Clinical Microbiology*, *42*(6), 2789–91. https://doi.org/10.1128/JCM.42.6.2789-2791.2004

Jamet, A., Rousseau, C., Benoiˆ, J.-B., Monfort, B., Frapy, E., Nassif, X., & Martin, P. (2009). A two-

component system is required for colonization of host cells by meningococcus, *23*, 17. https://doi.org/10.1099/mic.0.027755-0

Jang, M. H., Kweon, M.-N., Iwatani, K., Yamamoto, M., Terahara, K., Sasakawa, C., … Kiyono, H. (2004). Intestinal villous M cells: An antigen entry site in the mucosal epithelium. *Proceedings of the National Academy of Sciences*, *101*(16), 6110–6115. https://doi.org/10.1073/pnas.0400969101

Jarrige, A. C., Mathy, N., & Portier, C. (2001). PNPase autocontrols its expression by degrading a double-stranded structure in the *pnp* mRNA leader. *The EMBO Journal*, *20*(23), 6845–55. https://doi.org/10.1093/emboj/20.23.6845

Jorgensen, M. G., Thomason, M. K., Havelund, J., Valentin-Hansen, P., & Storz, G. (2013). Dual function of the McaS small RNA in controlling biofilm formation. *Genes & Development*, *27*(10), 1132–1145. https://doi.org/10.1101/gad.214734.113

Journet, L., Agrain, C., Broz, P., & Cornelis, G. R. (2003). The Needle Length of Bacterial Injectisomes Is Determined by a Molecular Ruler. *Science*, *302*(5651), 1757–1760. https://doi.org/10.1126/science.1091422

Kamińska, S., & Sadkowska-Todys, M. (2016). Yersiniosis in Poland in 2014. *Przeglad Epidemiologiczny*, *70*(3), 367–374. Retrieved from http://www.ncbi.nlm.nih.gov/pubmed/27869401

Kanaya, S., Yamada, Y., Kudo, Y., & Ikemura, T. (1999). Studies of codon usage and tRNA genes of 18 unicellular organisms and quantification of *Bacillus subtilis* tRNAs: gene expression level and species-specific diversity of codon usage based on multivariate analysis. *Gene*, *238*(1), 143–155. https://doi.org/10.1016/S0378-1119(99)00225-5

Katsowich, N., Elbaz, N., Pal, R. R., Mills, E., Kobi, S., Kahan, T., & Rosenshine, I. (2017). Host cell attachment elicits posttranscriptional regulation in infecting enteropathogenic bacteria. *Science*, *355*(6326), 735–739. https://doi.org/10.1126/science.aah4886

Kendall, M. M. (2017). Extra! Extracellular Effector Delivery into Host Cells via the Type 3 Secretion System. *MBio*, *8*(3). https://doi.org/10.1128/mBio.00594-17

Kenyon, J. J., Cunneen, M. M., & Reeves, P. R. (2017). Genetics and evolution of *Yersinia pseudotuberculosis* O-specific polysaccharides: A novel pattern of O-antigen diversity. *FEMS Microbiology Reviews*. https://doi.org/10.1093/femsre/fux002

Khemici, V., Poljak, L., Luisi, B. F., & Carpousis, A. J. (2008). The RNase E of *Escherichia coli* is a membrane-binding protein. *Molecular Microbiology*, *70*(4), 799–813. https://doi.org/10.1111/j.1365-2958.2008.06454.x

Khemici, V., Poljak, L., Toesca, I., & Carpousis, A. J. (2005). Evidence in vivo that the DEAD-box RNA helicase RhlB facilitates the degradation of ribosome-free mRNA by RNase E. *Proceedings of the National Academy of Sciences*, *102*(19), 6913–6918. https://doi.org/10.1073/pnas.0501129102

Kim, H. M., Shin, J.-H., Cho, Y.-B., & Roe, J.-H. (2014). Inverse regulation of Fe- and Ni-containing SOD genes by a Fur family regulator Nur through small RNA processed from 3'UTR of the *sodF* mRNA. *Nucleic Acids Research*, *42*(3), 2003–14. https://doi.org/10.1093/nar/gkt1071

Kimbrough, T. G., & Miller, S. I. (2000). Contribution of *Salmonella typhimurium* type III secretion components to needle complex formation. *Proceedings of the National Academy of Sciences of the United States of America*, *97*(20), 11008–13. https://doi.org/10.1073/pnas.200209497

King, J. M., Schesser Bartra, S., Plano, G., & Yahr, T. L. (2013). ExsA and LcrF recognize similar consensus binding sites, but differences in their oligomeric state influence interactions with promoter DNA. *Journal of Bacteriology*, *195*(24), 5639–50. https://doi.org/10.1128/JB.00990-13

Kirillina, O., Fetherston, J. D., Bobrov, A. G., Abney, J., & Perry, R. D. (2004). HmsP, a putative phosphodiesterase, and HmsT, a putative diguanylate cyclase, control Hms-dependent biofilm

formation in *Yersinia pestis*. *Molecular Microbiology*, *54*(1), 75–88. https://doi.org/10.1111/j.1365-2958.2004.04253.x

Knittel, V. (2015). Function and regulation of RovC – a new virulence factor in *Yersinia pseudotuberculosis*.

Köberle, M., Göppel, D., Grandl, T., Gaentzsch, P., Manncke, B., Berchtold, S., … Bohn, E. (2012). *Yersinia enterocolitica* YopT and *Clostridium difficile* Toxin B Induce Expression of GILZ in Epithelial Cells. *PLoS ONE*, *7*(7), e40730. https://doi.org/10.1371/journal.pone.0040730

Konovalova, A., Mitchell, A. M., & Silhavy, T. J. (2016). A lipoprotein/β-barrel complex monitors lipopolysaccharide integrity transducing information across the outer membrane. *ELife*, *5*, e15276. https://doi.org/10.7554/eLife.15276

Koo, J. W., Park, S. N., Choi, S. M., Chang, C. H., Cho, C. R., Paik, I. K., & Chung, C. Y. (1996). Acute renal failure associated with *Yersinia pseudotuberculosis* infection in children. *Pediatric Nephrology*, *10*(5), 582–586. https://doi.org/10.1007/s004670050165

Koornhof, H. J., Smego, R. a, & Nicol, M. (1999). Yersiniosis. II: The pathogenesis of *Yersinia* infections. *European Journal of Clinical Microbiology & Infectious Diseases : Official Publication of the European Society of Clinical Microbiology*, *18*(2), 87–112. Retrieved from http://www.ncbi.nlm.nih.gov/pubmed/10219574

Kopaskie, K. S., Ligtenberg, K. G., & Schneewind, O. (2013). Translational Regulation of *Yersinia enterocolitica* mRNA Encoding a Type III Secretion Substrate. *Journal of Biological Chemistry*, *288*(49), 35478–35488. https://doi.org/10.1074/jbc.M113.504811

Koslover, D. J., Callaghan, A. J., Marcaida, M. J., Garman, E. F., Martick, M., Scott, W. G., & Luisi, B. F. (2008). The crystal structure of the *Escherichia coli* RNase E apoprotein and a mechanism for RNA degradation. *Structure (London, England : 1993)*, *16*(8), 1238–44. https://doi.org/10.1016/j.str.2008.04.017

Koster, M., Bitter, W., de Cock, H., Allaoui, A., Cornelis, G. R., & Tommassen, J. (1997). The outer membrane component, YscC, of the Yop secretion machinery of *Yersinia enterocolitica* forms a ring-shaped multimeric complex. *Molecular Microbiology*, *26*(4), 789–97. Retrieved from http://www.ncbi.nlm.nih.gov/pubmed/9427408

Kowal, J., Chami, M., Ringler, P., Müller, S. A., Kudryashev, M., Castaño-Díez, D., … Engel, A. (2013). Structure of the dodecameric *Yersinia enterocolitica* secretin YscC and its trypsin-resistant core. *Structure (London, England : 1993)*, *21*(12), 2152–61. https://doi.org/10.1016/j.str.2013.09.012

Kröger, C., Colgan, A., Srikumar, S., Händler, K., Sivasankaran, S. K., Hammarlöf, D. L., … Hinton, J. C. D. (2013). An Infection-Relevant Transcriptomic Compendium for *Salmonella enterica* Serovar Typhimurium. *Cell Host & Microbe*, *14*(6), 683–695. https://doi.org/10.1016/J.CHOM.2013.11.010

Kudryashev, M., Stenta, M., Schmelz, S., Amstutz, M., Wiesand, U., Castaño-Díez, D., … Stahlberg, H. (2013). In situ structural analysis of the *Yersinia enterocolitica* injectisome. *ELife*, *2*, e00792. https://doi.org/10.7554/eLife.00792

Kulkarni, P. R., Cui, X., Williams, J. W., Stevens, A. M., & Kulkarni, R. V. (2006). Prediction of CsrA-regulating small RNAs in bacteria and their experimental verification in *Vibrio fischeri*. *Nucleic Acids Research*, *34*(11), 3361–3369. https://doi.org/10.1093/nar/gkl439

Kupferberg, L. L., & Higuchi, K. (1958). Role of calcium ions in the stimulation of growth of virulent strains of *Pasteurella pestis*. *Journal of Bacteriology*, *76*(1), 120–1. Retrieved from http://www.ncbi.nlm.nih.gov/pubmed/13563403

Kusmierek, M., & Dersch, P. (2018). Regulation of host–pathogen interactions via the post-transcriptional Csr/Rsm system. *Current Opinion in Microbiology*, *41*, 58–67. https://doi.org/10.1016/j.mib.2017.11.022

Laalami, S., Zig, L., & Putzer, H. (2014). Initiation of mRNA decay in bacteria. *Cellular and Molecular Life Sciences : CMLS*, *71*(10), 1799–828. https://doi.org/10.1007/s00018-013-1472-4

Laemmli, U. K. (1970). Cleavage of Structural Proteins during the Assembly of the Head of Bacteriophage T4. *Nature*, *227*(5259), 680–685. https://doi.org/10.1038/227680a0

Laloux, G., & Collet, J.-F. (2017). Major Tom to Ground Control: How Lipoproteins Communicate Extracytoplasmic Stress to the Decision Center of the Cell. *Journal of Bacteriology*, *199*(21), JB.00216-17. https://doi.org/10.1128/JB.00216-17

Lamark, T., Røkenes, T. P., McDougall, J., & Strøm, A. R. (1996). The complex *bet* promoters of *Escherichia coli*: regulation by oxygen (ArcA), choline (BetI), and osmotic stress. *Journal of Bacteriology*, *178*(6), 1655–62. Retrieved from http://www.ncbi.nlm.nih.gov/pubmed/8626294

Lamboy, J. A., Kim, H., Lee, K. S., Ha, T., & Komives, E. A. (2011). Visualization of the nanospring dynamics of the IkappaBalpha ankyrin repeat domain in real time. *Proceedings of the National Academy of Sciences of the United States of America*, *108*(25), 10178–83. https://doi.org/10.1073/pnas.1102226108

Lambris, J. D., Ricklin, D., & Geisbrecht, B. V. (2008). Complement evasion by human pathogens. *Nature Reviews Microbiology*, *6*(2), 132–142. https://doi.org/10.1038/nrmicro1824

Langford, E. V. (1972). *Pasteurella pseudotuberculosis* infections in Western Canada. *The Canadian Veterinary Journal = La Revue Veterinaire Canadienne*, *13*(4), 85–7. Retrieved from http://www.ncbi.nlm.nih.gov/pubmed/5025378

Lapouge, K., Perozzo, R., Iwaszkiewicz, J., Bertelli, C., Zoete, V., Michielin, O., … Haas, D. (2013). RNA pentaloop structures as effective targets of regulators belonging to the RsmA/CsrA protein family. *RNA Biology*, *10*(6), 1030–1041. https://doi.org/10.4161/rna.24771

Lasaro, M., Liu, Z., Bishar, R., Kelly, K., Chattopadhyay, S., Paul, S., … Goulian, M. (2014). *Escherichia coli* Isolate for Studying Colonization of the Mouse Intestine and Its Application to Two-Component Signaling Knockouts. *Journal of Bacteriology*, *196*(9), 1723–1732. https://doi.org/10.1128/JB.01296-13

Lee, E.-J., & Groisman, E. A. (2010). An antisense RNA that governs the expression kinetics of a multifunctional virulence gene. *Molecular Microbiology*, *76*(4), 1020–1033. https://doi.org/10.1111/j.1365-2958.2010.07161.x

Lee, V. T., Anderson, D. M., & Schneewind, O. (1998). Targeting of *Yersinia* Yop proteins into the cytosol of HeLa cells: one-step translocation of YopE across bacterial and eukaryotic membranes is dependent on SycE chaperone. *Molecular Microbiology*, *28*(3), 593–601. Retrieved from http://www.ncbi.nlm.nih.gov/pubmed/9632261

Lee, V. T., Mazmanian, S. K., & Schneewind, O. (2001). A program of *Yersinia enterocolitica* type III secretion reactions is activated by specific signals. *Journal of Bacteriology*, *183*(17), 4970–8. Retrieved from http://www.ncbi.nlm.nih.gov/pubmed/11489848

Leo, J. C., Grin, I., & Linke, D. (2012). Type V secretion: mechanism(s) of autotransport through the bacterial outer membrane. *Philosophical Transactions of the Royal Society of London. Series B, Biological Sciences*, *367*(1592), 1088–101. https://doi.org/10.1098/rstb.2011.0208

Letchumanan, V., Chan, K. G., Khan, T. M., Bukhari, S. I., Mutalib, N. S. A., Goh, B. H., & Lee, L. H. (2017). Bile sensing: The activation of *Vibrio parahaemolyticus* virulence. *Frontiers in Microbiology*. https://doi.org/10.3389/fmicb.2017.00728

Letzelter, M., Sorg, I., Mota, L. J., Meyer, S., Stalder, J., Feldman, M., … Cornelis, G. R. (2006). The discovery of SycO highlights a new function for type III secretion effector chaperones. *The EMBO Journal*, *25*(13), 3223–33. https://doi.org/10.1038/sj.emboj.7601202

Li, L., Yan, H., Feng, L., Li, Y., Lu, P., Hu, Y., & Chen, S. (2014). LcrQ blocks the role of LcrF in regulating the Ysc-Yop type III secretion genes in *Yersinia pseudotuberculosis*. *PloS One*, *9*(3), e92243. https://doi.org/10.1371/journal.pone.0092243

Li, P., Rivera-Cancel, G., Kinch, L. N., Salomon, D., Tomchick, D. R., Grishin, N. V, & Orth, K. (2016). Bile salt receptor complex activates a pathogenic type III secretion system. *ELife*, *5*. https://doi.org/10.7554/eLife.15718

Li, Y., Hu, Y., Francis, M. S., & Chen, S. (2014). RcsB positively regulates the *Yersinia* Ysc-Yop type III secretion system by activating expression of the master transcriptional regulator LcrF. *Environmental Microbiology*. https://doi.org/10.1111/1462-2920.12556

Linke, D., Riess, T., Autenrieth, I. B., Lupas, A., & Kempf, V. A. J. (2006). Trimeric autotransporter adhesins: variable structure, common function. *Trends in Microbiology*, *14*(6), 264–270. https://doi.org/10.1016/j.tim.2006.04.005

Liou, G.-G., Chang, H.-Y., Lin, C.-S., & Lin-Chao, S. (2002). DEAD Box RhlB RNA Helicase Physically Associates with Exoribonuclease PNPase to Degrade Double-stranded RNA Independent of the Degradosome-assembling Region of RNase E. *Journal of Biological Chemistry*, *277*(43), 41157–41162. https://doi.org/10.1074/jbc.M206618200

Liu, B., Kearns, D. B., & Bechhofer, D. H. (2016). Expression of multiple *Bacillus subtilis* genes is controlled by decay of *slrA* mRNA from Rho-dependent 3′ ends. *Nucleic Acids Research*, *44*(7), 3364–3372. https://doi.org/10.1093/nar/gkw069

Ljungberg, P., Valtonen, M., Harjola, V. P., Kaukoranta-Tolvanen, S. S., & Vaara, M. (1995). Report of four cases of *Yersinia pseudotuberculosis* septicemia and a literature review. *European Journal of Clinical Microbiology & Infectious Diseases : Official Publication of the European Society of Clinical Microbiology*, *14*(9), 804–10. Retrieved from http://www.ncbi.nlm.nih.gov/pubmed/8536731

López-Garrido, J., Puerta-Fernández, E., & Casadesús, J. (2014). A eukaryotic-like 3' untranslated region in *Salmonella enterica hilD* mRNA. *Nucleic Acids Research*, *42*(9), 5894–906. https://doi.org/10.1093/nar/gku222

Lorenz, R., Bernhart, S. H., Höner Zu Siederdissen, C., Tafer, H., Flamm, C., Stadler, P. F., & Hofacker, I. L. (2011). ViennaRNA Package 2.0. *Algorithms for Molecular Biology : AMB*, *6*, 26. https://doi.org/10.1186/1748-7188-6-26

Love, M. I., Huber, W., & Anders, S. (2014). Moderated estimation of fold change and dispersion for RNA-seq data with DESeq2. *Genome Biology*, *15*(12), 550. https://doi.org/10.1186/s13059-014-0550-8

Lu, P., Zhang, Y., Li, L., Hu, Y., Huang, L., Li, Y., … Chen, S. (2012). Small non-coding RNA SraG regulates the operon YPK_1206-1205 in *Yersinia pseudotuberculosis*. *FEMS Microbiology Letters*, *331*(1), 37–43. https://doi.org/10.1111/j.1574-6968.2012.02548.x

Mabbott, N. A., Donaldson, D. S., Ohno, H., Williams, I. R., & Mahajan, A. (2013). Microfold (M) cells: important immunosurveillance posts in the intestinal epithelium. *Mucosal Immunology*, *6*(4), 666–77. https://doi.org/10.1038/mi.2013.30

Madrid, C., Balsalobre, C., García, J., & Juárez, A. (2007). The novel Hha/YmoA family of nucleoid-associated proteins: use of structural mimicry to modulate the activity of the H-NS family of proteins. *Molecular Microbiology*, *63*(1), 7–14. https://doi.org/10.1111/j.1365-2958.2006.05497.x

Maeda, T., & Wachi, M. (2012a). 3′ Untranslated Region-Dependent Degradation of the *aceA* mRNA, Encoding the Glyoxylate Cycle Enzyme Isocitrate Lyase, by RNase E/G in Corynebacterium glutamicum. *Applied and Environmental Microbiology*, *78*(24), 8753–8761. https://doi.org/10.1128/AEM.02304-12

Maeda, T., & Wachi, M. (2012b). 3′ Untranslated Region-Dependent Degradation of the *aceA* mRNA, Encoding the Glyoxylate Cycle Enzyme Isocitrate Lyase, by RNase E/G in Corynebacterium

glutamicum. *Applied and Environmental Microbiology*, *78*(24), 8753–8761. https://doi.org/10.1128/AEM.02304-12

Majdalani, N., & Gottesman, S. (2005). The Rcs Phosphorelay: A Complex Signal Transduction System. *Annual Review of Microbiology*, *59*(1), 379–405. https://doi.org/10.1146/annurev.micro.59.050405.101230

Majdalani, N., Heck, M., Stout, V., & Gottesman, S. (2005). Role of RcsF in signaling to the Rcs phosphorelay pathway in *Escherichia coli*. *Journal of Bacteriology*, *187*(19), 6770–8. https://doi.org/10.1128/JB.187.19.6770-6778.2005

Majdalani, N., Hernandez, D., & Gottesman, S. (2002). Regulation and mode of action of the second small RNA activator of RpoS translation, RprA. *Doi.Org*, *46*(3), 813–826. https://doi.org/10.1046/j.1365-2958.2002.03203.x

Malka, Y., Steiman-Shimony, A., Rosenthal, E., Argaman, L., Cohen-Daniel, L., Arbib, E., … Berger, M. (2017). Post-transcriptional 3′-UTR cleavage of mRNA transcripts generates thousands of stable uncapped autonomous RNA fragments. *Nature Communications*, *8*(1), 2029. https://doi.org/10.1038/s41467-017-02099-7

Marlovits, T. C., Kubori, T., Sukhan, A., Thomas, D. R., Galán, J. E., & Unger, V. M. (2004). Structural Insights into the Assembly of the Type III Secretion Needle Complex. *Science*, *306*(5698), 1040–1042. https://doi.org/10.1126/science.1102610

Marra, A., & Isberg, R. R. (1997). Invasin-dependent and invasin-independent pathways for translocation of *Yersinia pseudotuberculosis* across the Peyer's patch intestinal epithelium. *Infection and Immunity*, *65*(8), 3412–21. Retrieved from http://www.ncbi.nlm.nih.gov/pubmed/9234806

McCallum, K. L., & Whitfield, C. (1991). The *rcsA* gene of *Klebsiella pneumoniae* O1:K20 is involved in expression of the serotype-specific K (capsular) antigen. *Infection and Immunity*, *59*(2), 494–502. Retrieved from http://www.ncbi.nlm.nih.gov/pubmed/1987069

McCoy, M. W., Marré, M. L., Lesser, C. F., & Mecsas, J. (2010). The C-terminal tail of *Yersinia pseudotuberculosis* YopM is critical for interacting with RSK1 and for virulence. *Infection and Immunity*, *78*(6), 2584–98. https://doi.org/10.1128/IAI.00141-10

McMahon, K. J., Castelli, M. E., García Vescovi, E., & Feldman, M. F. (2012). Biogenesis of outer membrane vesicles in *Serratia marcescens* is thermoregulated and can be induced by activation of the Rcs phosphorelay system. *Journal of Bacteriology*, *194*(12), 3241–9. https://doi.org/10.1128/JB.00016-12

McNally, A., Cheasty, T., Fearnley, C., Dalziel, R. W., Paiba, G. A., Manning, G., & Newell, D. G. (2004). Comparison of the biotypes of *Yersinia enterocolitica* isolated from pigs, cattle and sheep at slaughter and from humans with yersiniosis in Great Britain during 1999-2000. *Letters in Applied Microbiology*, *39*(1), 103–108. https://doi.org/10.1111/j.1472-765X.2004.01548.x

McNally, A., Thomson, N. R., Reuter, S., & Wren, B. W. (2016). "Add, stir and reduce": *Yersinia* spp. as model bacteria for pathogen evolution. *Nature Reviews Microbiology*, *14*(3). https://doi.org/10.1038/nrmicro.2015.29

McPhee, J. B., Mena, P., & Bliska, J. B. (2010). Delineation of Regions of the *Yersinia* YopM Protein Required for Interaction with the RSK1 and PRK2 Host Kinases and Their Requirement for Interleukin-10 Production and Virulence. *Infection and Immunity*, *78*(8), 3529–3539. https://doi.org/10.1128/IAI.00269-10

McPhee, J. B., Mena, P., Zhang, Y., & Bliska, J. B. (2012). Interleukin-10 induction is an important virulence function of the *Yersinia pseudotuberculosis* type III effector YopM. *Infection and Immunity*, *80*(7), 2519–27. https://doi.org/10.1128/IAI.06364-11

Mendel, R. R. (2013). The molybdenum cofactor. *The Journal of Biological Chemistry*, *288*(19), 13165–72.

https://doi.org/10.1074/jbc.R113.455311

Mercante, J., Edwards, A. N., Dubey, A. K., Babitzke, P., & Romeo, T. (2009). Molecular Geometry of CsrA (RsmA) Binding to RNA and Its Implications for Regulated Expression. *Journal of Molecular Biology*, *392*(2), 511–528. https://doi.org/10.1016/j.jmb.2009.07.034

Mettert, E. L., & Kiley, P. J. (2014). Coordinate Regulation of the Suf and Isc Fe-S Cluster Biogenesis Pathways by IscR Is Essential for Viability of *Escherichia coli*. *Journal of Bacteriology*, *196*(24), 4315–4323. https://doi.org/10.1128/JB.01975-14

Michiels, T., Vanooteghem, J. C., Lambert de Rouvroit, C., China, B., Gustin, A., Boudry, P., & Cornelis, G. R. (1991). Analysis of virC, an operon involved in the secretion of Yop proteins by Yersinia enterocolitica. *Journal of Bacteriology*, *173*(16), 4994–5009. Retrieved from http://www.ncbi.nlm.nih.gov/pubmed/1860816

Mikula, K. M., Kolodziejczyk, R., & Goldman, A. (2013). *Yersinia* infection tools—characterization of structure and function of adhesins. *Frontiers in Cellular and Infection Microbiology*, *2*, 169. https://doi.org/10.3389/fcimb.2012.00169

Miller, H. K., Kwuan, L., Schwiesow, L., Bernick, D. L., Mettert, E., Ramirez, H. A., … Auerbuch, V. (2014). IscR is essential for *Yersinia pseudotuberculosis* type III secretion and virulence. *PLoS Pathogens*, *10*(6), e1004194. https://doi.org/10.1371/journal.ppat.1004194

Miller, J. H. (1992). A short course in bacterial genetics: a laboratory manual and handbook for *Escherichia coli* and related bacteria. Plainview, N.Y: Cold Spring Harbor Laboratory Press. Retrieved from https://catalyst.library.jhu.edu/catalog/bib_512800

Miyadai, H., Tanaka-Masuda, K., Matsuyama, S., & Tokuda, H. (2004). Effects of lipoprotein overproduction on the induction of DegP (HtrA) involved in quality control in the *Escherichia coli* periplasm. *The Journal of Biological Chemistry*, *279*(38), 39807–13. https://doi.org/10.1074/jbc.M406390200

Miyakoshi, M., Chao, Y., & Vogel, J. (2015). Regulatory small RNAs from the 3′ regions of bacterial mRNAs. *Current Opinion in Microbiology*, *24*, 132–139. https://doi.org/10.1016/j.mib.2015.01.013

Moffitt, J. R., Pandey, S., Boettiger, A. N., Wang, S., & Zhuang, X. (2016). Spatial organization shapes the turnover of a bacterial transcriptome. *ELife*, *5*, e13065. https://doi.org/10.7554/eLife.13065

Molofsky, A. B., & Swanson, M. S. (2003). *Legionella pneumophila* CsrA is a pivotal repressor of transmission traits and activator of replication. *Molecular Microbiology*, *50*(2), 445–61. Retrieved from http://www.ncbi.nlm.nih.gov/pubmed/14617170

Moreira, C. G., Russell, R., Mishra, A. A., Narayanan, S., Ritchie, J. M., Waldor, M. K., … Sperandio, V. (2016). Bacterial Adrenergic Sensors Regulate Virulence of Enteric Pathogens in the Gut. *MBio*, *7*(3). https://doi.org/10.1128/mBio.00826-16

Morin, M., Ropers, D., Letisse, F., Laguerre, S., Portais, J.-C., Cocaign-Bousquet, M., & Enjalbert, B. (2016). The post-transcriptional regulatory system CSR controls the balance of metabolic pools in upper glycolysis of *Escherichia coli*. *Molecular Microbiology*, *100*(4), 686–700. https://doi.org/10.1111/mmi.13343

Morita, T., Maki, K., & Aiba, H. (2005). RNase E-based ribonucleoprotein complexes: mechanical basis of mRNA destabilization mediated by bacterial noncoding RNAs. *Genes & Development*, *19*(18), 2176–2186. https://doi.org/10.1101/gad.1330405

Mota, L. J., Journet, L., Sorg, I., Agrain, C., & Cornelis, G. R. (2005). Bacterial Injectisomes: Needle Length Does Matter. *Science*, *307*(5713), 1278–1278. https://doi.org/10.1126/science.1107679

Mouslim, C., Delgado, M., & Groisman, E. A. (2004). Activation of the RcsC/YojN/RcsB phosphorelay system attenuates *Salmonella* virulence. *Molecular Microbiology*, *54*(2), 386–395. https://doi.org/10.1111/j.1365-2958.2004.04293.x

Mudd, E. A., & Higgins, C. F. (1993). *Escherichia coli* endoribonuclease RNase E: autoregulation of expression and site-specific cleavage of mRNA. *Molecular Microbiology*, *9*(3), 557–68. Retrieved from http://www.ncbi.nlm.nih.gov/pubmed/8412702

Mueller, C. A., Broz, P., & Cornelis, G. R. (2008). The type III secretion system tip complex and translocon. *Molecular Microbiology*, *68*(5), 1085–1095. https://doi.org/10.1111/j.1365-2958.2008.06237.x

Mueller, C. A., Broz, P., Müller, S. A., Ringler, P., Erne-Brand, F., Sorg, I., … Cornelis, G. R. (2005). The V-Antigen of *Yersinia* Forms a Distinct Structure at the Tip of Injectisome Needles. *Science*, *310*(5748), 674–676. https://doi.org/10.1126/science.1118476

Muhldorfer, K., Wibbelt, G., Haensel, J., Riehm, J., & Speck, S. (2010). *Yersinia* species isolated from bats, Germany. *Emerging Infectious Diseases*, *16*(3), 578–80. https://doi.org/10.3201/eid1603.091035

Mühlenkamp, M., Oberhettinger, P., Leo, J. C., Linke, D., & Schütz, M. S. (2015). *Yersinia* adhesin A (YadA) – Beauty & beast. *International Journal of Medical Microbiology*, *305*(2), 252–258. https://doi.org/10.1016/j.ijmm.2014.12.008

Mukherjee, S., Keitany, G., Li, Y., Wang, Y., Ball, H. L., Goldsmith, E. J., & Orth, K. (2006). *Yersinia* YopJ Acetylates and Inhibits Kinase Activation by Blocking Phosphorylation. *Science*, *312*(5777), 1211–1214. https://doi.org/10.1126/science.1126867

Mukherjee, S., Oshiro, R. T., Yakhnin, H., Babitzke, P., & Kearns, D. B. (2016). FliW antagonizes CsrA RNA binding by a noncompetitive allosteric mechanism. *Proceedings of the National Academy of Sciences of the United States of America*, *113*(35), 9870–5. https://doi.org/10.1073/pnas.1602455113

Nagel, G., Lahrz, A., & Dersch, P. (2001). Environmental control of invasin expression in *Yersinia pseudotuberculosis* is mediated by regulation of RovA, a transcriptional activator of the SlyA/Hor family. *Molecular Microbiology*, *41*(6), 1249–69. Retrieved from http://www.ncbi.nlm.nih.gov/pubmed/11580832

Naiel, B., & Raul, R. (1998). Chronic prostatitis due to *Yersinia pseudotuberculosis*. *Journal of Clinical Microbiology*, *36*(3), 856. Retrieved from http://www.ncbi.nlm.nih.gov/pubmed/9508336

Nakanishi, N., Abe, H., Ogura, Y., Hayashi, T., Tashiro, K., Kuhara, S., … Tobe, T. (2006). ppGpp with DksA controls gene expression in the locus of enterocyte effacement (LEE) pathogenicity island of enterohaemorrhagic *Escherichia coli* through activation of two virulence regulatory genes. *Molecular Microbiology*, *61*(1), 194–205. https://doi.org/10.1111/j.1365-2958.2006.05217.x

Navarro, L., Koller, A., Nordfelth, R., Wolf-Watz, H., Taylor, S., & Dixon, J. E. (2007). Identification of a Molecular Target for the *Yersinia* Protein Kinase A. *Molecular Cell*, *26*(4), 465–477. https://doi.org/10.1016/j.molcel.2007.04.025

Naville, M., Ghuillot-Gaudeffroy, A., Marchais, A., & Gautheret, D. (2011). ARNold: A web tool for the prediction of Rho-independent transcription terminators. *RNA Biology*, *8*(1), 11–13. https://doi.org/10.4161/rna.8.1.13346

Nesbit, A. D., Giel, J. L., Rose, J. C., & Kiley, P. J. (2009). Sequence-Specific Binding to a Subset of IscR-Regulated Promoters Does Not Require IscR Fe–S Cluster Ligation. *Journal of Molecular Biology*, *387*(1), 28–41. https://doi.org/10.1016/j.jmb.2009.01.055

Neyt, C., & Cornelis, G. R. (1999). Role of SycD, the chaperone of the *Yersinia* Yop translocators YopB and YopD. *Molecular Microbiology*, *31*(1), 143–156. https://doi.org/10.1046/j.1365-2958.1999.01154.x

Nicholson, A. W. (2014). Ribonuclease III mechanisms of double-stranded RNA cleavage. *Wiley Interdisciplinary Reviews. RNA*, *5*(1), 31–48. https://doi.org/10.1002/wrna.1195

Nieckarz, M., Raczkowska, A., Dębski, J., Kistowski, M., Dadlez, M., Heesemann, J., … Brzostek, K. (2016). Impact of OmpR on the membrane proteome of *Yersinia enterocolitica* in different environments: repression of major adhesin YadA and heme receptor HemR. *Environmental*

Microbiology, *18*(3), 997–1021. https://doi.org/10.1111/1462-2920.13165

Nieto, J. M., Madrid, C., Miquelay, E., Parra, J. L., Rodríguez, S., & Juárez, A. (2002). Evidence for direct protein-protein interaction between members of the enterobacterial Hha/YmoA and H-NS families of proteins. *Journal of Bacteriology*, *184*(3), 629–35. Retrieved from http://www.ncbi.nlm.nih.gov/pubmed/11790731

Nisco, N. J. De, Rivera-Cancel, G., & Orth, K. (2018). The Biochemistry of Sensing: Enteric Pathogens Regulate Type III Secretion in Response to Environmental and Host Cues. *MBio*, *9*(1), e02122-17. https://doi.org/10.1128/MBIO.02122-17

Nordström, K. (2006). Plasmid R1--replication and its control. *Plasmid*, *55*(1), 1–26. https://doi.org/10.1016/j.plasmid.2005.07.002

Nuss, A. M., Beckstette, M., Pimenova, M., Schmühl, C., Opitz, W., Pisano, F., … Dersch, P. (2017). Tissue dual RNA-seq allows fast discovery of infection-specific functions and riboregulators shaping host-pathogen transcriptomes. *Proceedings of the National Academy of Sciences of the United States of America*, *114*(5). https://doi.org/10.1073/pnas.1613405114

Nuss, A. M., Heroven, A. K., & Dersch, P. (2017). RNA Regulators: Formidable Modulators of *Yersinia* Virulence. *Trends in Microbiology*, *25*(1), 19–34. https://doi.org/10.1016/J.TIM.2016.08.006

Nuss, A. M., Heroven, A. K., Waldmann, B., Reinkensmeier, J., Jarek, M., Beckstette, M., & Dersch, P. (2015). Transcriptomic Profiling of *Yersinia pseudotuberculosis* Reveals Reprogramming of the Crp Regulon by Temperature and Uncovers Crp as a Master Regulator of Small RNAs. *PLOS Genetics*, *11*(3), e1005087. https://doi.org/10.1371/journal.pgen.1005087

O'Neil, D., Glowatz, H., & Schlumpberger, M. (2013). Ribosomal RNA depletion for efficient use of RNA-seq capacity. *Current Protocols in Molecular Biology*, *Chapter 4*, Unit 4.19. https://doi.org/10.1002/0471142727.mb0419s103

Oellerich, M. F., Jacobi, C. A., Freund, S., Niedung, K., Bach, A., Heesemann, J., & Trülzsch, K. (2007). *Yersinia enterocolitica* infection of mice reveals clonal invasion and abscess formation. *Infection and Immunity*, *75*(8), 3802–11. https://doi.org/10.1128/IAI.00419-07

Olsson, J., Edqvist, P. J., Broms, J. E., Forsberg, A., Wolf-Watz, H., & Francis, M. S. (2004). The YopD Translocator of *Yersinia pseudotuberculosis* Is a Multifunctional Protein Comprised of Discrete Domains. *Journal of Bacteriology*, *186*(13), 4110–4123. https://doi.org/10.1128/JB.186.13.4110-4123.2004

Opdyke, J. A., Kang, J.-G., & Storz, G. (2004). GadY, a small-RNA regulator of acid response genes in *Escherichia coli*. *Journal of Bacteriology*, *186*(20), 6698–705. https://doi.org/10.1128/JB.186.20.6698-6705.2004

Opitz, W. S. (2013). Cell contact-dependent virulence gene expression in *Yersinia pseudotuberculosis*.

Orioli, A. (2017). tRNA biology in the omics era: Stress signalling dynamics and cancer progression. *BioEssays*, *39*(3), 1600158. https://doi.org/10.1002/bies.201600158

Pacheco, A. R., Curtis, M. M., Ritchie, J. M., Munera, D., Waldor, M. K., Moreira, C. G., & Sperandio, V. (2012). Fucose sensing regulates bacterial intestinal colonization. *Nature*, *492*(7427), 113–117. https://doi.org/10.1038/nature11623

Pallen, M. J., Dougan, G., & Frankel, G. (1997). Coiled-coil domains in proteins secreted by type III secretion systems. *Molecular Microbiology*, *25*(2), 423–5. Retrieved from http://www.ncbi.nlm.nih.gov/pubmed/9282753

Park, H., Yakhnin, H., Connolly, M., Romeo, T., & Babitzke, P. (2015). CsrA Participates in a PNPase Autoregulatory Mechanism by Selectively Repressing Translation of *pnp* Transcripts That Have Been Previously Processed by RNase III and PNPase. *Journal of Bacteriology*, *197*(24), 3751–9.

https://doi.org/10.1128/JB.00721-15

Park, Y. H., Wood, G., Kastner, D. L., & Chae, J. J. (2016). Pyrin inflammasome activation and RhoA signaling in the autoinflammatory diseases FMF and HIDS. *Nature Immunology*, *17*(8), 914–921. https://doi.org/10.1038/ni.3457

Patterson-Fortin, L. M., Vakulskas, C. A., Yakhnin, H., Babitzke, P., & Romeo, T. (2013). Dual Posttranscriptional Regulation via a Cofactor-Responsive mRNA Leader. *Journal of Molecular Biology*, *425*(19), 3662–3677. https://doi.org/10.1016/j.jmb.2012.12.010

Payne, P. L., & Straley, S. C. (1998). YscO of *Yersinia pestis* is a mobile core component of the Yop secretion system. *Journal of Bacteriology*, *180*(15), 3882–90. Retrieved from http://www.ncbi.nlm.nih.gov/pubmed/9683485

Peng, T., Berghoff, B. A., Oh, J.-I., Weber, L., Schirmer, J., Schwarz, J., … Klug, G. (2016). Regulation of a polyamine transporter by the conserved 3′ UTR-derived sRNA SorX confers resistance to singlet oxygen and organic hydroperoxides in *Rhodobacter sphaeroides*. *RNA Biology*, *13*(10), 988–999. https://doi.org/10.1080/15476286.2016.1212152

Penheiter, K. L., Mathur, N., Giles, D., Fahlen, T., & Jones, B. D. (1997). Non-invasive *Salmonella typhimurium* mutants are avirulent because of an inability to enter and destroy M cells of ileal Peyer's patches. *Molecular Microbiology*, *24*(4), 697–709. Retrieved from http://www.ncbi.nlm.nih.gov/pubmed/9194698

Pepe, J. C., & Miller, V. L. (1993). *Yersinia enterocolitica* invasin: a primary role in the initiation of infection. *Proceedings of the National Academy of Sciences of the United States of America*, *90*(14), 6473–7. Retrieved from http://www.ncbi.nlm.nih.gov/pubmed/8341658

Pepe, J. C., Wachtel, M. R., Wagar, E., & Miller, V. L. (1995). Pathogenesis of defined invasion mutants of *Yersinia enterocolitica* in a BALB/c mouse model of infection. *Infection and Immunity*, *63*(12), 4837–48. Retrieved from http://www.ncbi.nlm.nih.gov/pubmed/7591144

Perham, M., Chen, M., Ma, J., & Wittung-Stafshede, P. (2005). Unfolding of Heptameric Co-chaperonin Protein Follows "Fly Casting" Mechanism: Observation of Transient Nonnative Heptamer. *Journal of the American Chemical Society*, *127*(47), 16402–16403. https://doi.org/10.1021/ja055574o

Perry, R. D., & Fetherston, J. D. (1997). *Yersinia pestis*--etiologic agent of plague. *Clinical Microbiology Reviews*, *10*(1), 35–66. Retrieved from http://www.ncbi.nlm.nih.gov/pubmed/8993858

Perry, R. D., & Fetherston, J. D. (2007). *The genus Yersinia: from genomics to function*. Springer. Retrieved from https://www.ncbi.nlm.nih.gov/nlmcatalog/101319337

Perry, R. D., Harmon, P. A., Bowmer, W. S., & Straley, S. C. (1986). A low-Ca^{2+} response operon encodes the V antigen of *Yersinia pestis*. *Infection and Immunity*, *54*(2), 428–34. Retrieved from http://www.ncbi.nlm.nih.gov/pubmed/3021629

Persson, C., Carballeira, N., Wolf-Watz, H., & Fällman, M. (1997). The PTPase YopH inhibits uptake of *Yersinia*, tyrosine phosphorylation of $p130^{Cas}$ and FAK, and the associated accumulation of these proteins in peripheral focal adhesions. *The EMBO Journal*, *16*(9), 2307–2318. https://doi.org/10.1093/emboj/16.9.2307

Persson, C., Nordfelth, R., Andersson, K., Forsberg, A., Wolf-Watz, H., & Fällman, M. (1999). Localization of the *Yersinia* PTPase to focal complexes is an important virulence mechanism. *Molecular Microbiology*, *33*(4), 828–38. Retrieved from http://www.ncbi.nlm.nih.gov/pubmed/10447891

Pettersson, J., Nordfelth, R., Dubinina, E., Bergman, T., Gustafsson, M., Magnusson, K. E., & Wolf-Watz, H. (1996). Modulation of virulence factor expression by pathogen target cell contact. *Science (New York, N.Y.)*, *273*(5279), 1231–3. Retrieved from http://www.ncbi.nlm.nih.gov/pubmed/8703058

Pfaffl, M. W. (2001). A new mathematical model for relative quantification in real-time RT-PCR. *Nucleic*

Acids Research, *29*(9), e45. Retrieved from http://www.ncbi.nlm.nih.gov/pubmed/11328886

Pha, K., & Navarro, L. (2016). *Yersinia* type III effectors perturb host innate immune responses. *World Journal of Biological Chemistry*, *7*(1), 1–13. https://doi.org/10.4331/wjbc.v7.i1.1

Pimenova, M. (2014). Regulation of the cell contact-dependent expression of the major virulence activator LcrF in *Yersinia pseudotuberculosis*.

Plano, G. V, & Schesser, K. (2013). The *Yersinia pestis* type III secretion system: expression, assembly and role in the evasion of host defenses. *Immunologic Research*, *57*(1–3), 237–45. https://doi.org/10.1007/s12026-013-8454-3

Portaliou, A. G., Tsolis, K. C., Loos, M. S., Zorzini, V., & Economou, A. (2016). Type III Secretion: Building and Operating a Remarkable Nanomachine. *Trends in Biochemical Sciences*. https://doi.org/10.1016/j.tibs.2015.09.005

Portnoyt, D. A., & Falkowt, S. (1981). Virulence-Associated Plasmids from *Yersinia enterocolitica* and *Yersinia pestis*. *JOURNAL OF BACTERIOLOGY*, *148*(3), 877–883. Retrieved from http://jb.asm.org/content/148/3/877.full.pdf

Potts, A. H., Vakulskas, C. A., Pannuri, A., Yakhnin, H., Babitzke, P., & Romeo, T. (2017). Global role of the bacterial post-transcriptional regulator CsrA revealed by integrated transcriptomics. *Nature Communications*, *8*(1), 1596. https://doi.org/10.1038/s41467-017-01613-1

Prehna, G., Ivanov, M. I., Bliska, J. B., & Stebbins, C. E. (2006). *Yersinia* Virulence Depends on Mimicry of Host Rho-Family Nucleotide Dissociation Inhibitors. *Cell*, *126*(5), 869–880. https://doi.org/10.1016/j.cell.2006.06.056

Pukklay, P., Nakanishi, Y., Nitta, M., Yamamoto, K., Ishihama, A., & Shiratsuchi, A. (2013). Involvement of EnvZ–OmpR two-component system in virulence control of *Escherichia coli* in *Drosophila melanogaster*. *Biochemical and Biophysical Research Communications*, *438*(2), 306–311. https://doi.org/10.1016/j.bbrc.2013.07.062

Py, B., Higgins, C. F., Krisch, H. M., & Carpousis, A. J. (1996). A DEAD-box RNA helicase in the *Escherichia coli* RNA degradosome. *Nature*, *381*(6578), 169–172. https://doi.org/10.1038/381169a0

Quax, T. E. F., Claassens, N. J., Söll, D., & van der Oost, J. (2015). Codon Bias as a Means to Fine-Tune Gene Expression. *Molecular Cell*, *59*(2), 149–161. https://doi.org/10.1016/j.molcel.2015.05.035

Quereda, J. J., & Cossart, P. (2017). Regulating Bacterial Virulence with RNA. *Annual Review of Microbiology*, *71*(1), 263–280. https://doi.org/10.1146/annurev-micro-030117-020335

Quereda, J. J., García-del Portillo, F., & Pucciarelli, M. G. (2016). *Listeria monocytogenes* remodels the cell surface in the blood-stage. *Environmental Microbiology Reports*, *8*(5), 641–648. https://doi.org/10.1111/1758-2229.12416

Quereda, J. J., Ortega, Á. D., Pucciarelli, M. G., & García-del Portillo, F. (2014). The Listeria Small RNA Rli27 Regulates a Cell Wall Protein inside Eukaryotic Cells by Targeting a Long 5′-UTR Variant. *PLoS Genetics*, *10*(10), e1004765. https://doi.org/10.1371/journal.pgen.1004765

Raczkowska, A., Skorek, K., Bielecki, J., & Brzostek, K. (2011). OmpR controls *Yersinia enterocolitica* motility by positive regulation of *flhDC* expression. *Antonie van Leeuwenhoek*, *99*(2), 381–94. https://doi.org/10.1007/s10482-010-9503-8

Radics, J., Königsmaier, L., & Marlovits, T. C. (2013). Structure of a pathogenic type 3 secretion system in action. *Nature Structural & Molecular Biology*, *21*(1), 82–87. https://doi.org/10.1038/nsmb.2722

Radomska, K. A., Ordoñez, S. R., Wösten, M. M. S. M., Wagenaar, J. A., & van Putten, J. P. M. (2016). Feedback control of *Campylobacter jejuni* flagellin levels through reciprocal binding of FliW to flagellin and the global regulator CsrA. *Molecular Microbiology*, *102*(2), 207–220.

https://doi.org/10.1111/mmi.13455

Redko, Y., Tock, M. R., Adams, C. J., Kaberdin, V. R., Grasby, J. A., & McDowall, K. J. (2003). Determination of the Catalytic Parameters of the N-terminal Half of *Escherichia coli* Ribonuclease E and the Identification of Critical Functional Groups in RNA Substrates. *Journal of Biological Chemistry*, *278*(45), 44001–44008. https://doi.org/10.1074/jbc.M306760200

Ren, B., Shen, H., Lu, Z. J., Liu, H., & Xu, Y. (2014). The *phzA2-G2* Transcript Exhibits Direct RsmA-Mediated Activation in *Pseudomonas aeruginosa* M18. *PLoS ONE*, *9*(2), e89653. https://doi.org/10.1371/journal.pone.0089653

Ren, G.-X., Guo, X.-P., & Sun, Y.-C. (2017). Regulatory 3' Untranslated Regions of Bacterial mRNAs. *Frontiers in Microbiology*, *8*, 1276. https://doi.org/10.3389/fmicb.2017.01276

Reuter, S., Connor, T. R., Barquist, L., Walker, D., Feltwell, T., Harris, S. R., … Thomson, N. R. (2014). Parallel independent evolution of pathogenicity within the genus *Yersinia*. *Proceedings of the National Academy of Sciences*, *111*(18), 6768–6773. https://doi.org/10.1073/pnas.1317161111

Revell, P. A., & Miller, V. L. (2000). A chromosomally encoded regulator is required for expression of the *Yersinia enterocolitica inv* gene and for virulence. *Molecular Microbiology*, *35*(3), 677–85. Retrieved from http://www.ncbi.nlm.nih.gov/pubmed/10672189

Rhee, S., Martin, R. G., Rosner, J. L., & Davies, D. R. (1998). A novel DNA-binding motif in MarA: the first structure for an AraC family transcriptional activator. *Proceedings of the National Academy of Sciences of the United States of America*, *95*(18), 10413–8. Retrieved from http://www.ncbi.nlm.nih.gov/pubmed/9724717

Richardson, J. P. (2002). Rho-dependent termination and ATPases in transcript termination. *Biochimica et Biophysica Acta (BBA) - Gene Structure and Expression*, *1577*(2), 251–260. https://doi.org/10.1016/S0167-4781(02)00456-6

Rietsch, A., Vallet-Gely, I., Dove, S. L., & Mekalanos, J. J. (2005). ExsE, a secreted regulator of type III secretion genes in *Pseudomonas aeruginosa*. *Proceedings of the National Academy of Sciences*, *102*(22), 8006–8011. https://doi.org/10.1073/pnas.0503005102

Rimpiläinen, M., Forsberg, A., & Wolf-Watz, H. (1992). A novel protein, LcrQ, involved in the low-calcium response of *Yersinia pseudotuberculosis* shows extensive homology to YopH. *Journal of Bacteriology*, *174*(10), 3355–63. Retrieved from http://www.ncbi.nlm.nih.gov/pubmed/1577700

Robert-Le Meur, M., & Portier, C. (1992). *E.coli* polynucleotide phosphorylase expression is autoregulated through an RNase III-dependent mechanism. *The EMBO Journal*, *11*(7), 2633–41. Retrieved from http://www.ncbi.nlm.nih.gov/pubmed/1628624

Robert-Le Meur, M., & Portier, C. (1994). Polynucleotide phosphorylase of *Escherichia coli* induces the degradation of its RNase III processed messenger by preventing its translation. *Nucleic Acids Research*, *22*(3), 397–403. https://doi.org/10.1093/nar/22.3.397

Roggenkamp, A., Neuberger, H. R., Flügel, A., Schmoll, T., & Heesemann, J. (1995). Substitution of two histidine residues in YadA protein of *Yersinia enterocolitica* abrogates collagen binding, cell adherence and mouse virulence. *Molecular Microbiology*, *16*(6), 1207–19. Retrieved from http://www.ncbi.nlm.nih.gov/pubmed/8577254

Roggenkamp, A., Ruckdeschel, K., Leitritz, L., Schmitt, R., & Heesemann, J. (1996). Deletion of amino acids 29 to 81 in adhesion protein YadA of *Yersinia enterocolitica* serotype O:8 results in selective abrogation of adherence to neutrophils. *Infection and Immunity*, *64*(7), 2506–14. Retrieved from http://www.ncbi.nlm.nih.gov/pubmed/8698473

Rohde, J. R., Fox, J. M., & Minnich, S. A. (1994). Thermoregulation in *Yersinia enterocolitica* is coincident with changes in DNA supercoiling. *Molecular Microbiology*, *12*(2), 187–99. Retrieved from http://www.ncbi.nlm.nih.gov/pubmed/8057844

Rohde, J. R., Luan, X. S., Rohde, H., Fox, J. M., & Minnich, S. A. (1999). The *Yersinia enterocolitica* pYV virulence plasmid contains multiple intrinsic DNA bends which melt at 37 degrees C. *Journal of Bacteriology*, *181*(14), 4198–204. Retrieved from http://www.ncbi.nlm.nih.gov/pubmed/10400576

Rolán, H. G., Durand, E. A., & Mecsas, J. (2013). Identifying *Yersinia* YopH-Targeted Signal Transduction Pathways that Impair Neutrophil Responses during *In Vivo* Murine Infection. *Cell Host & Microbe*, *14*(3), 306–317. https://doi.org/10.1016/j.chom.2013.08.013

Romeo, T. (1998). Global regulation by the small RNA-binding protein CsrA and the non-coding RNA molecule *CsrB*. *Molecular Microbiology*, *29*(6), 1321–30. Retrieved from http://www.ncbi.nlm.nih.gov/pubmed/9781871

Romeo, T., Vakulskas, C. A., & Babitzke, P. (2013). Post-transcriptional regulation on a global scale: form and function of Csr/Rsm systems. *Environmental Microbiology*, *15*(2), 313–24. https://doi.org/10.1111/j.1462-2920.2012.02794.x

Roppenser, B., Roder, A., Hentschke, M., Ruckdeschel, K., & Aepfelbacher, M. (2009). *Yersinia enterocolitica* differentially modulates RhoG activity in host cells. *Journal of Cell Science*, *122*(5), 696–705. https://doi.org/10.1242/jcs.040345

Rosenzweig, J. A., & Chopra, A. K. (2013). The exoribonuclease Polynucleotide Phosphorylase influences the virulence and stress responses of yersiniae and many other pathogens. *Frontiers in Cellular and Infection Microbiology*, *3*, 81. https://doi.org/10.3389/fcimb.2013.00081

Rosenzweig, J. A., Chromy, B., Echeverry, A., Yang, J., Adkins, B., Plano, G. V., … Schesser, K. (2007). Polynucleotide phosphorylase independently controls virulence factor expression levels and export in *Yersinia* spp. *FEMS Microbiology Letters*, *270*(2), 255–264. https://doi.org/10.1111/j.1574-6968.2007.00689.x

Rosenzweig, J. A., Weltman, G., Plano, G. V., & Schesser, K. (2005). Modulation of *Yersinia* Type Three Secretion System by the S1 Domain of Polynucleotide Phosphorylase. *Journal of Biological Chemistry*, *280*(1), 156–163. https://doi.org/10.1074/jbc.M405662200

Rosner, B. M., Stark, K., & Werber, D. (2010). Epidemiology of reported *Yersinia enterocolitica* infections in Germany, 2001-2008. *BMC Public Health*, *10*(1), 337. https://doi.org/10.1186/1471-2458-10-337

Rosqvist, R., Magnusson, K. E., & Wolf-Watz, H. (1994). Target cell contact triggers expression and polarized transfer of *Yersinia* YopE cytotoxin into mammalian cells. *The EMBO Journal*, *13*(4), 964–72. Retrieved from http://www.ncbi.nlm.nih.gov/pubmed/8112310

Rosqvist, R., Skurnik, M., & Wolf-Watz, H. (1988). Increased virulence of *Yersinia pseudotuberculosis* by two independent mutations. *Nature*, *334*(6182), 522–525. https://doi.org/10.1038/334522a0

Ross, J. A., & Plano, G. V. (2011). A C-Terminal Region of *Yersinia pestis* YscD Binds the Outer Membrane Secretin YscC. *Journal of Bacteriology*, *193*(9), 2276–2289. https://doi.org/10.1128/JB.01137-10

Rowley, G., Spector, M., Kormanec, J., & Roberts, M. (2006). Pushing the envelope: extracytoplasmic stress responses in bacterial pathogens. *Nature Reviews Microbiology*, *4*(5), 383–394. https://doi.org/10.1038/nrmicro1394

Ruiz de los Mozos, I., Vergara-Irigaray, M., Segura, V., Villanueva, M., Bitarte, N., Saramago, M., … Toledo-Arana, A. (2013). Base Pairing Interaction between 5′- and 3′-UTRs Controls icaR mRNA Translation in *Staphylococcus aureus*. *PLoS Genetics*, *9*(12), e1004001. https://doi.org/10.1371/journal.pgen.1004001

Rutherford, S. T., van Kessel, J. C., Shao, Y., & Bassler, B. L. (2011). AphA and LuxR/HapR reciprocally control quorum sensing in vibrios. *Genes & Development*, *25*(4), 397–408. https://doi.org/10.1101/gad.2015011

Sahr, T., Rusniok, C., Impens, F., Oliva, G., Sismeiro, O., Coppée, J.-Y., & Buchrieser, C. (2017). The

Legionella pneumophila genome evolved to accommodate multiple regulatory mechanisms controlled by the CsrA-system. *PLOS Genetics*, *13*(2), e1006629. https://doi.org/10.1371/journal.pgen.1006629

Saiki, R. K., Gelfand, D. H., Stoffel, S., Scharf, S. J., Higuchi, R., Horn, G. T., … Erlich, H. A. (1988). Primer-directed enzymatic amplification of DNA with a thermostable DNA polymerase. *Science (New York, N.Y.)*, *239*(4839), 487–91. Retrieved from http://www.ncbi.nlm.nih.gov/pubmed/2448875

Sal-Man, N., Deng, W., & Finlay, B. B. (2012). EscI: a crucial component of the type III secretion system forms the inner rod structure in enteropathogenic *Escherichia coli*. *Biochemical Journal*, *442*(1), 119–125. https://doi.org/10.1042/BJ20111620

Sambrook, J., & Russell, D. W. (David W. (2001). *Molecular cloning: a laboratory manual*. Cold Spring Harbor Laboratory Press.

Sansonetti, P. (2002). Host-pathogen interactions: the seduction of molecular cross talk. *Gut*, *50 Suppl 3*(Suppl 3), III2-8. https://doi.org/10.1136/gut.50.suppl_3.iii2

Sansonetti, P. J. (2004). War and peace at mucosal surfaces. *Nature Reviews Immunology*, *4*(12), 953–964. https://doi.org/10.1038/nri1499

Saramago, M., Domingues, S., Viegas, S. C., & Arraiano, C. M. (2014). Biofilm formation and antibiotic resistance in *Salmonella* Typhimurium are affected by different ribonucleases. *Journal of Microbiology and Biotechnology*, *24*(1), 8–12. Retrieved from http://www.ncbi.nlm.nih.gov/pubmed/24150497

Sauvonnet, N., Lambermont, I., van der Bruggen, P., & Cornelis, G. R. (2002). YopH prevents monocyte chemoattractant protein 1 expression in macrophages and T-cell proliferation through inactivation of the phosphatidylinositol 3-kinase pathway. *Molecular Microbiology*, *45*(3), 805–15. Retrieved from http://www.ncbi.nlm.nih.gov/pubmed/12139625

Sayed, N., Jousselin, A., & Felden, B. (2012). A cis-antisense RNA acts in trans in *Staphylococcus aureus* to control translation of a human cytolytic peptide. *Nature Structural & Molecular Biology*, *19*(1), 105–112. https://doi.org/10.1038/nsmb.2193

Schägger, H. (2006). Tricine–SDS-PAGE. *Nature Protocols*, *1*(1), 16–22. https://doi.org/10.1038/nprot.2006.4

Schiano, C. A., Koo, J. T., Schipma, M. J., Caulfield, A. J., Jafari, N., & Lathem, W. W. (2014). Genome-Wide Analysis of Small RNAs Expressed by *Yersinia pestis* Identifies a Regulator of the Yop-Ysc Type III Secretion System. *Journal of Bacteriology*, *196*(9), 1659–1670. https://doi.org/10.1128/JB.01456-13

Schiano, C. A., & Lathem, W. W. (2012). Post-transcriptional regulation of gene expression in *Yersinia* species. *Frontiers in Cellular and Infection Microbiology*, *2*, 129. https://doi.org/10.3389/fcimb.2012.00129

Schleif, R. (2010). AraC protein, regulation of the l-arabinose operon in *Escherichia coli* , and the light switch mechanism of AraC action. *FEMS Microbiology Reviews*, *34*(5), 779–796. https://doi.org/10.1111/j.1574-6976.2010.00226.x

Schneider, C. A., Rasband, W. S., & Eliceiri, K. W. (2012). NIH Image to ImageJ: 25 years of image analysis. *Nature Methods*, *9*(7), 671–5. Retrieved from http://www.ncbi.nlm.nih.gov/pubmed/22930834

Schubert, M., Lapouge, K., Duss, O., Oberstrass, F. C., Jelesarov, I., Haas, D., & Allain, F. H.-T. (2007). Molecular basis of messenger RNA recognition by the specific bacterial repressing clamp RsmA/CsrA. *Nature Structural & Molecular Biology*, *14*(9), 807–813. https://doi.org/10.1038/nsmb1285

Schulmeyer, K. H., & Yahr, T. L. (2017). Post-transcriptional regulation of type III secretion in plant and animal pathogens. *Current Opinion in Microbiology*, *36*, 30–36. https://doi.org/10.1016/j.mib.2017.01.009

Schulze-Koops, H., Burkhardt, H., Heesemann, J., von der Mark, K., & Emmrich, F. (1992). Plasmid-encoded outer membrane protein YadA mediates specific binding of enteropathogenic yersiniae to various types of collagen. *Infection and Immunity*, *60*(6), 2153–9. Retrieved from http://www.ncbi.nlm.nih.gov/pubmed/1587583

Schwartz, C. J., Giel, J. L., Patschkowski, T., Luther, C., Ruzicka, F. J., Beinert, H., & Kiley, P. J. (2001). IscR, an Fe-S cluster-containing transcription factor, represses expression of *Escherichia coli* genes encoding Fe-S cluster assembly proteins. *Proceedings of the National Academy of Sciences*, *98*(26), 14895–14900. https://doi.org/10.1073/pnas.251550898

Schwiesow, L., Lam, H., Dersch, P., & Auerbuch, V. (2015). *Yersinia* Type III Secretion System Master Regulator LcrF. *Journal of Bacteriology*, *198*(4), 604–14. https://doi.org/10.1128/JB.00686-15

Seekircher, S. (2014). Identification of regulatory factors that control the synthesis of the small regulatory RNA CsrC in *Yersinia pseudotuberculosis*.

Sesto, N., Wurtzel, O., Archambaud, C., Sorek, R., & Cossart, P. (2013). The excludon: a new concept in bacterial antisense RNA-mediated gene regulation. *Nature Reviews Microbiology*, *11*(2), 75–82. https://doi.org/10.1038/nrmicro2934

Shao, F., Vacratsis, P. O., Bao, Z., Bowers, K. E., Fierke, C. A., & Dixon, J. E. (2003). Biochemical characterization of the *Yersinia* YopT protease: Cleavage site and recognition elements in Rho GTPases. *Proceedings of the National Academy of Sciences*, *100*(3), 904–909. https://doi.org/10.1073/pnas.252770599

Shao, Y., & Bassler, B. L. (2012). Quorum-sensing non-coding small RNAs use unique pairing regions to differentially control mRNA targets. *Molecular Microbiology*, *83*(3), 599–611. https://doi.org/10.1111/j.1365-2958.2011.07959.x

Shao, Y., & Bassler, B. L. (2014). Quorum regulatory small RNAs repress type VI secretion in *Vibrio cholerae*. *Molecular Microbiology*, *92*(5), 921–930. https://doi.org/10.1111/mmi.12599

Sharma, C. M., Darfeuille, F., Plantinga, T. H., & Vogel, J. (2007). A small RNA regulates multiple ABC transporter mRNAs by targeting C/A-rich elements inside and upstream of ribosome-binding sites. *Genes & Development*, *21*(21), 2804–2817. https://doi.org/10.1101/gad.447207

Shi, Z., Yang, W.-Z., Lin-Chao, S., Chak, K.-F., & Yuan, H. S. (2008). Crystal structure of *Escherichia coli* PNPase: central channel residues are involved in processive RNA degradation. *RNA (New York, N.Y.)*, *14*(11), 2361–71. https://doi.org/10.1261/rna.1244308

Shimizu, T., Ichimura, K., & Noda, M. (2016). The Surface Sensor NlpE of Enterohemorrhagic *Escherichia coli* Contributes to Regulation of the Type III Secretion System and Flagella by the Cpx Response to Adhesion. *Infection and Immunity*, *84*(2), 537–49. https://doi.org/10.1128/IAI.00881-15

Shoemaker, B. A., Portman, J. J., & Wolynes, P. G. (2000). Speeding molecular recognition by using the folding funnel: the fly-casting mechanism. *Proceedings of the National Academy of Sciences of the United States of America*, *97*(16), 8868–73. https://doi.org/10.1073/pnas.160259697

Silvaggi, J. M., Perkins, J. B., & Losick, R. (2005). Small Untranslated RNA Antitoxin in *Bacillus subtilis*. *Journal of Bacteriology*, *187*(19), 6641–6650. https://doi.org/10.1128/JB.187.19.6641-6650.2005

Simon, R., Priefer, U., & Pühler, A. (1983). A Broad Host Range Mobilization System for In Vivo Genetic Engineering: Transposon Mutagenesis in Gram Negative Bacteria. *Bio/Technology*, *1*(9), 784–791. https://doi.org/10.1038/nbt1183-784

Simonet, M., Richard, S., & Berche, P. (1990). Electron microscopic evidence for *in vivo* extracellular localization of *Yersinia pseudotuberculosis* harboring the pYV plasmid. *Infection and Immunity*, *58*(3), 841–5. Retrieved from http://www.ncbi.nlm.nih.gov/pubmed/2307522

Singh, S. K., Boyle, A. L., & Main, E. R. G. (2013). LcrH, a Class II Chaperone from the Type Three

Secretion System, Has a Highly Flexible Native Structure. *Journal of Biological Chemistry*, *288*(6), 4048–4055. https://doi.org/10.1074/jbc.M112.395889

Skorek, K., Raczkowska, A., Dudek, B., Miętka, K., Guz-Regner, K., Pawlak, A., … Brzostek, K. (2013). Regulatory protein OmpR influences the serum resistance of *Yersinia enterocolitica* O:9 by modifying the structure of the outer membrane. *PloS One*, *8*(11), e79525. https://doi.org/10.1371/journal.pone.0079525

Skorupski, K., & Taylor, R. K. (1999). A new level in the *Vibrio cholerae* ToxR virulence cascade: AphA is required for transcriptional activation of the *tcpPH* operon. *Molecular Microbiology*, *31*(3), 763–71. Retrieved from http://www.ncbi.nlm.nih.gov/pubmed/10048021

Skrzypek, E., Cowan, C., & Straley, S. C. (1998). Targeting of the *Yersinia* pestis YopM protein into HeLa cells and intracellular trafficking to the nucleus. *Molecular Microbiology*, *30*(5), 1051–65. Retrieved from http://www.ncbi.nlm.nih.gov/pubmed/9988481

Skurnik, M. (2004). Molecular Genetics, Biochemistry and Biological Role of *Yersinia* Lipopolysaccharide. In *The Genus Yersinia* (pp. 187–197). Boston: Kluwer Academic Publishers. https://doi.org/10.1007/0-306-48416-1_38

Skurnik, M., & Wolf-Watz, H. (1989). Analysis of the *yopA* gene encoding the Yop1 virulence determinants of *Yersinia* spp. *Molecular Microbiology*, *3*(4), 517–29. Retrieved from http://www.ncbi.nlm.nih.gov/pubmed/2761389

Smego, R. a, Frean, J., & Koornhof, H. J. (1999). Yersiniosis I: microbiological and clinicoepidemiological aspects of plague and non-plague *Yersinia* infections. *European Journal of Clinical Microbiology & Infectious Diseases : Official Publication of the European Society of Clinical Microbiology*, *18*(1), 1–15. Retrieved from http://www.ncbi.nlm.nih.gov/pubmed/10192708

Snyder, W. B., Davis, L. J., Danese, P. N., Cosma, C. L., & Silhavy, T. J. (1995). Overproduction of NlpE, a new outer membrane lipoprotein, suppresses the toxicity of periplasmic LacZ by activation of the Cpx signal transduction pathway. *Journal of Bacteriology*, *177*(15), 4216–23. Retrieved from http://www.ncbi.nlm.nih.gov/pubmed/7635808

Sodeinde, O. A., Subrahmanyam, Y. V, Stark, K., Quan, T., Bao, Y., & Goguen, J. D. (1992). A surface protease and the invasive character of plague. *Science (New York, N.Y.)*, *258*(5084), 1004–7. Retrieved from http://www.ncbi.nlm.nih.gov/pubmed/1439793

Songsungthong, W., Higgins, M. C., Rolán, H. G., Murphy, J. L., & Mecsas, J. (2010). ROS-inhibitory activity of YopE is required for full virulence of *Yersinia* in mice. *Cellular Microbiology*, *12*(7), 988–1001. https://doi.org/10.1111/j.1462-5822.2010.01448.x

Sousa, S., Marchand, I., & Dreyfus, M. (2001). Autoregulation allows *Escherichia coli* RNase E to adjust continuously its synthesis to that of its substrates. *Molecular Microbiology*, *42*(3), 867–78. Retrieved from http://www.ncbi.nlm.nih.gov/pubmed/11722748

Sowa, S. W., Gelderman, G., Leistra, A. N., Buvanendiran, A., Lipp, S., Pitaktong, A., … Contreras, L. M. (2017). Integrative FourD omics approach profiles the target network of the carbon storage regulatory system. *Nucleic Acids Research*, *45*(4), 1673–1686. https://doi.org/10.1093/nar/gkx048

Spreter, T., Yip, C. K., Sanowar, S., André, I., Kimbrough, T. G., Vuckovic, M., … Strynadka, N. C. J. (2009). A conserved structural motif mediates formation of the periplasmic rings in the type III secretion system. *Nature Structural & Molecular Biology*, *16*(5), 468–476. https://doi.org/10.1038/nsmb.1603

St Johnston, D. (1995). The intracellular localization of messenger RNAs. *Cell*, *81*(2), 161–70. Retrieved from http://www.ncbi.nlm.nih.gov/pubmed/7736568

Standish, A. J., Teh, M. Y., Tran, E. N. H., Doyle, M. T., Baker, P. J., & Morona, R. (2016). Unprecedented Abundance of Protein Tyrosine Phosphorylation Modulates *Shigella flexneri* Virulence. *Journal of*

Molecular Biology, *428*(20), 4197–4208. https://doi.org/10.1016/j.jmb.2016.06.016

Stebbins, C. E., & Galán, J. E. (2001). Maintenance of an unfolded polypeptide by a cognate chaperone in bacterial type III secretion. *Nature*, *414*(6859), 77–81. https://doi.org/10.1038/35102073

Steinmann, R. (2013). Characterization of temperature-dependent and feedback-controlled expression of the virulence activator LcrF in *Yersinia pseudotuberculosis*.

Steinmann, R., & Dersch, P. (2013). Thermosensing to adjust bacterial virulence in a fluctuating environment. *Future Microbiology*, *8*(1), 85–105. https://doi.org/10.2217/fmb.12.129

Sterzenbach, T., Nguyen, K. T., Nuccio, S.-P., Winter, M. G., Vakulskas, C. A., Clegg, S., … Bäumler, A. J. (2013). A novel CsrA titration mechanism regulates fimbrial gene expression in *Salmonella typhimurium*. *The EMBO Journal*, *32*(21), 2872–2883. https://doi.org/10.1038/emboj.2013.206

Stickney, L. M., Hankins, J. S., Miao, X., & Mackie, G. A. (2005). Function of the conserved S1 and KH domains in polynucleotide phosphorylase. *Journal of Bacteriology*, *187*(21), 7214–21. https://doi.org/10.1128/JB.187.21.7214-7221.2005

Strahl, H., Turlan, C., Khalid, S., Bond, P. J., Kebalo, J.-M., Peyron, P., … Carpousis, A. J. (2015). Membrane Recognition and Dynamics of the RNA Degradosome. *PLOS Genetics*, *11*(2), e1004961. https://doi.org/10.1371/journal.pgen.1004961

Strober, W. (2001). Trypan Blue Exclusion Test of Cell Viability. In *Current Protocols in Immunology* (Vol. Appendix 3, p. Appendix 3B). Hoboken, NJ, USA: John Wiley & Sons, Inc. https://doi.org/10.1002/0471142735.ima03bs21

Studier, F. W., & Moffatt, B. A. (1986). Use of bacteriophage T7 RNA polymerase to direct selective high-level expression of cloned genes. *Journal of Molecular Biology*, *189*(1), 113–30. Retrieved from http://www.ncbi.nlm.nih.gov/pubmed/3537305

Suggs, S. V, Wallace, R. B., Hirose, T., Kawashima, E. H., & Itakura, K. (1981). Use of synthetic oligonucleotides as hybridization probes: isolation of cloned cDNA sequences for human beta 2-microglobulin. *Proceedings of the National Academy of Sciences of the United States of America*, *78*(11), 6613–7. Retrieved from http://www.ncbi.nlm.nih.gov/pubmed/6171820

Sun, P., Tropea, J. E., Austin, B. P., Cherry, S., & Waugh, D. S. (2008). Structural characterization of the *Yersinia pestis* type III secretion system needle protein YscF in complex with its heterodimeric chaperone YscE/YscG. *Journal of Molecular Biology*, *377*(3), 819–30. https://doi.org/10.1016/j.jmb.2007.12.067

Sweet, C. R., Conlon, J., Golenbock, D. T., Goguen, J., & Silverman, N. (2007). YopJ targets TRAF proteins to inhibit TLR-mediated NF-?B, MAPK and IRF3 signal transduction. *Cellular Microbiology*, *9*(11), 2700–2715. https://doi.org/10.1111/j.1462-5822.2007.00990.x

Symmons, M. F., Jones, G. H., & Luisi, B. F. (2000). A duplicated fold is the structural basis for polynucleotide phosphorylase catalytic activity, processivity, and regulation. *Structure (London, England : 1993)*, *8*(11), 1215–26. Retrieved from http://www.ncbi.nlm.nih.gov/pubmed/11080643

Szczesny, P., & Lupas, A. (2008). Domain annotation of trimeric autotransporter adhesins--daTAA. *Bioinformatics (Oxford, England)*, *24*(10), 1251–6. https://doi.org/10.1093/bioinformatics/btn118

Taheri, N., Fahlgren, A., & Fällman, M. (2016). Yersinia pseudotuberculosis Blocks Neutrophil Degranulation. *Infection and Immunity*, *84*(12), 3369–3378. https://doi.org/10.1128/IAI.00760-16

Takeshita, S., Sato, M., Toba, M., Masahashi, W., & Hashimoto-Gotoh, T. (1987). High-copy-number and low-copy-number plasmid vectors for *lacZ* alpha-complementation and chloramphenicol- or kanamycin-resistance selection. *Gene*, *61*(1), 63–74. Retrieved from http://www.ncbi.nlm.nih.gov/pubmed/3327753

Tao, K., Narita, S.-I., & Tokuda, H. (2012). Defective lipoprotein sorting induces *lolA* expression through the Rcs stress response phosphorelay system. *Journal of Bacteriology*, *194*(14), 3643–50. https://doi.org/10.1128/JB.00553-12

Tawk, C., Sharan, M., Eulalio, A., & Vogel, J. (2017). A systematic analysis of the RNA-targeting potential of secreted bacterial effector proteins. *Scientific Reports*, *7*(1), 9328. https://doi.org/10.1038/s41598-017-09527-0

Tejeda-Dominguez, F., Huerta-Cantillo, J., Chavez-Dueñas, L., & Navarro-Garcia, F. (2017). A Novel Mechanism for Protein Delivery by the Type 3 Secretion System for Extracellularly Secreted Proteins. *MBio*, *8*(2), e00184-17. https://doi.org/10.1128/mBio.00184-17

Tengel, T., Sethson, I., & Francis, M. S. (2002). Conformational analysis by CD and NMR spectroscopy of a peptide encompassing the amphipathic domain of YopD from *Yersinia*. *European Journal of Biochemistry*, *269*(15), 3659–68. Retrieved from http://www.ncbi.nlm.nih.gov/pubmed/12153562

Ternhag, A., Törner, A., Svensson, A., Ekdahl, K., & Giesecke, J. (2008). Short- and long-term effects of bacterial gastrointestinal infections. *Emerging Infectious Diseases*, *14*(1), 143–8. https://doi.org/10.3201/eid1401.070524

Tertti, R., Vuento, R., Mikkola, P., Granfors, K., Mäkelä, A. L., & Toivanen, A. (1989). Clinical manifestations of *Yersinia pseudotuberculosis* infection in children. *European Journal of Clinical Microbiology & Infectious Diseases : Official Publication of the European Society of Clinical Microbiology*, *8*(7), 587–91. Retrieved from http://www.ncbi.nlm.nih.gov/pubmed/2506017

Thinwa, J., Segovia, J. A., Bose, S., & Dube, P. H. (2014). Integrin-Mediated First Signal for Inflammasome Activation in Intestinal Epithelial Cells. *The Journal of Immunology*, *193*(3), 1373–1382. https://doi.org/10.4049/jimmunol.1400145

Thisted, T., Sørensen, N. S., & Gerdes, K. (1995). Mechanism of Post-segregational Killing: Secondary Structure Analysis of the Entire Hok mRNA from Plasmid R1 Suggests a Fold-back Structure that Prevents Translation and Antisense RNA Binding. *Journal of Molecular Biology*, *247*(5), 859–873. https://doi.org/10.1006/jmbi.1995.0186

Tipple, M. A., Bland, L. A., Murphy, J. J., Arduino, M. J., Panlilio, A. L., Farmer, J. J., … Grindon, A. J. (n.d.). Sepsis associated with transfusion of red cells contaminated with *Yersinia enterocolitica*. *Transfusion*, *30*(3), 207–13. Retrieved from http://www.ncbi.nlm.nih.gov/pubmed/2315994

Tipton, K. A., & Rather, P. N. (2017). An *ompR-envZ* Two-Component System Ortholog Regulates Phase Variation, Osmotic Tolerance, Motility, and Virulence in *Acinetobacter baumannii* Strain AB5075. *Journal of Bacteriology*, *199*(3). https://doi.org/10.1128/JB.00705-16

Tiwari, S., Jamal, S. B., Hassan, S. S., Carvalho, P. V. S. D., Almeida, S., Barh, D., … Azevedo, V. (2017). Two-Component Signal Transduction Systems of Pathogenic Bacteria As Targets for Antimicrobial Therapy: An Overview. *Frontiers in Microbiology*. https://doi.org/10.3389/fmicb.2017.01878

Tobe, T., Ando, H., Ishikawa, H., Abe, H., Tashiro, K., Hayashi, T., … Sugimoto, N. (2005). Dual regulatory pathways integrating the RcsC-RcsD-RcsB signalling system control enterohaemorrhagic Escherichia coli pathogenicity. *Molecular Microbiology*, *58*(1), 320–333. https://doi.org/10.1111/j.1365-2958.2005.04828.x

Toledo-Arana, A., Dussurget, O., Nikitas, G., Sesto, N., Guet-Revillet, H., Balestrino, D., … Cossart, P. (2009). The *Listeria* transcriptional landscape from saprophytism to virulence. *Nature*, *459*(7249), 950–956. https://doi.org/10.1038/nature08080

Toolan, H. W. (1954). Transplantable human neoplasms maintained in cortisone-treated laboratory animals: H.S. No. 1; H.Ep. No. 1; H.Ep. No. 2; H.Ep. No. 3; and H.Emb.Rh. No. 1. *Cancer Research*, *14*(9), 660–6. Retrieved from http://www.ncbi.nlm.nih.gov/pubmed/13209540

Torres-Escobar, A., JuÃ¡rez-RodrÃ-guez, M. D., & Curtiss III, R. (2010). Biogenesis of *Yersinia pestis* PsaA

in recombinant attenuated *Salmonella* Typhimurium vaccine (RASV) strain. *FEMS Microbiology Letters*, *302*(2), 106–113. https://doi.org/10.1111/j.1574-6968.2009.01827.x

Towbin, H., Staehelin, T., & Gordon, J. (1979). Electrophoretic transfer of proteins from polyacrylamide gels to nitrocellulose sheets: procedure and some applications. *Proceedings of the National Academy of Sciences of the United States of America*, *76*(9), 4350–4. Retrieved from http://www.ncbi.nlm.nih.gov/pubmed/388439

Trülzsch, K., Heesemann, J., & Oellerich, M. F. (2007). Invasion and Dissemination of *Yersinia enterocolitica* in the Mouse Infection Model. In *Advances in experimental medicine and biology* (Vol. 603, pp. 279–285). https://doi.org/10.1007/978-0-387-72124-8_25

Tsai, J. C., Yen, M.-R., Castillo, R., Leyton, D. L., Henderson, I. R., & Saier, M. H. (2010). The Bacterial Intimins and Invasins: A Large and Novel Family of Secreted Proteins. *PLoS ONE*, *5*(12), e14403. https://doi.org/10.1371/journal.pone.0014403

Tsang, T. M., Wiese, J. S., Felek, S., Kronshage, M., & Krukonis, E. S. (2013). Ail Proteins of *Yersinia pestis* and *Y. pseudotuberculosis* Have Different Cell Binding and Invasion Activities. *PLoS ONE*, *8*(12), e83621. https://doi.org/10.1371/journal.pone.0083621

Tseng, Y.-T., Chiou, N.-T., Gogiraju, R., & Lin-Chao, S. (2015). The Protein Interaction of RNA Helicase B (RhlB) and Polynucleotide Phosphorylase (PNPase) Contributes to the Homeostatic Control of Cysteine in Escherichia coli. *The Journal of Biological Chemistry*, *290*(50), 29953–63. https://doi.org/10.1074/jbc.M115.691881

Tuompo, R., Hannu, T., Huovinen, E., Sihvonen, L., Siitonen, A., & Leirisalo-Repo, M. (2017). *Yersinia enterocolitica* biotype 1A: a possible new trigger of reactive arthritis. *Rheumatology International*. https://doi.org/10.1007/s00296-017-3816-0

Uliczka, F., Pisano, F., Kochut, A., Opitz, W., Herbst, K., Stolz, T., & Dersch, P. (2011). Monitoring of gene expression in bacteria during infections using an adaptable set of bioluminescent, fluorescent and colorigenic fusion vectors. *PloS One*, *6*(6), e20425. https://doi.org/10.1371/journal.pone.0020425

Uliczka, F., Pisano, F., Schaake, J., Stolz, T., Rohde, M., Fruth, A., … Dersch, P. (2011). Unique Cell Adhesion and Invasion Properties of *Yersinia enterocolitica* O:3, the Most Frequent Cause of Human Yersiniosis. *PLoS Pathogens*, *7*(7), e1002117. https://doi.org/10.1371/journal.ppat.1002117

Urbanowski, M. L., Lykken, G. L., & Yahr, T. L. (2005). A secreted regulatory protein couples transcription to the secretory activity of the *Pseudomonas aeruginosa* type III secretion system. *Proceedings of the National Academy of Sciences of the United States of America*, *102*(28), 9930–5. https://doi.org/10.1073/pnas.0504405102

Urbanowski, M. L., Stauffer, L. T., & Stauffer, G. V. (2000). The *gcvB* gene encodes a small untranslated RNA involved in expression of the dipeptide and oligopeptide transport systems in *Escherichia coli*. *Molecular Microbiology*, *37*(4), 856–68. Retrieved from http://www.ncbi.nlm.nih.gov/pubmed/10972807

Vadyvaloo, V., Viall, A. K., Jarrett, C. O., Hinz, A. K., Sturdevant, D. E., & Joseph Hinnebusch, B. (2015). Role of the PhoP-PhoQ gene regulatory system in adaptation of *Yersinia pestis* to environmental stress in the flea digestive tract. *Microbiology (Reading, England)*, *161*(6), 1198–1210. https://doi.org/10.1099/mic.0.000082

Vagima, Y., Zauberman, A., Levy, Y., Gur, D., Tidhar, A., Aftalion, M., … Mamroud, E. (2015). Circumventing *Y. pestis* Virulence by Early Recruitment of Neutrophils to the Lungs during Pneumonic Plague. *PLOS Pathogens*, *11*(5), e1004893. https://doi.org/10.1371/journal.ppat.1004893

Vakulskas, C. A., Brady, K. M., & Yahr, T. L. (2009). Mechanism of Transcriptional Activation by *Pseudomonas aeruginosa* ExsA. *Journal of Bacteriology*, *191*(21), 6654–6664. https://doi.org/10.1128/JB.00902-09

Vakulskas, C. A., Potts, A. H., Babitzke, P., Ahmer, B. M. M., & Romeo, T. (2015). Regulation of Bacterial Virulence by Csr (Rsm) Systems. *Microbiology and Molecular Biology Reviews*, *79*(2), 193–224. https://doi.org/10.1128/MMBR.00052-14

van Nues, R. W., Castro-Roa, D., Yuzenkova, Y., & Zenkin, N. (2016). Ribonucleoprotein particles of bacterial small non-coding RNA IsrA (IS61 or McaS) and its interaction with RNA polymerase core may link transcription to mRNA fate. *Nucleic Acids Research*, *44*(6), 2577–92. https://doi.org/10.1093/nar/gkv1302

Veenendaal, A. K. J., Hodgkinson, J. L., Schwarzer, L., Stabat, D., Zenk, S. F., & Blocker, A. J. (2007). The type III secretion system needle tip complex mediates host cell sensing and translocon insertion. *Molecular Microbiology*, *63*(6), 1719–1730. https://doi.org/10.1111/j.1365-2958.2007.05620.x

Viboud, G. I., & Bliska, J. B. (2005). *YERSINIA* OUTER PROTEINS: Role in Modulation of Host Cell Signaling Responses and Pathogenesis. *Annual Review of Microbiology*, *59*(1), 69–89. https://doi.org/10.1146/annurev.micro.59.030804.121320

Viboud, G. I., Mejia, E., & Bliska, J. B. (2006). Comparison of YopE and YopT activities in counteracting host signalling responses to *Yersinia pseudotuberculosis* infection. *Cellular Microbiology*, *8*(9), 1504–1515. https://doi.org/10.1111/j.1462-5822.2006.00729.x

Viegas, S. C., Mil-Homens, D., Fialho, A. M., & Arraiano, C. M. (2013). The virulence of *Salmonella enterica* Serovar Typhimurium in the insect model *Galleria mellonella* is impaired by mutations in RNase E and RNase III. *Applied and Environmental Microbiology*, *79*(19), 6124–33. https://doi.org/10.1128/AEM.02044-13

Visser, L. G., Annema, A., & van Furth, R. (1995). Role of Yops in inhibition of phagocytosis and killing of opsonized *Yersinia enterocolitica* by human granulocytes. *Infection and Immunity*, *63*(7), 2570–5. Retrieved from http://www.ncbi.nlm.nih.gov/pubmed/7790071

von Hippel, P. H. (1998). An integrated model of the transcription complex in elongation, termination, and editing. *Science (New York, N.Y.)*, *281*(5377), 660–5. Retrieved from http://www.ncbi.nlm.nih.gov/pubmed/9685251

Voskressenskaya, E. A., Klimov, V. T., Tseneva, G. Y., Carniel, E., Foulon, J., & Chesnokova, M. V. (2004). Molecular Epidemiological Characterization of *Yersinia pseudotuberculosis* Circulating in Different Geographic Areas of the Russian Federation. In *The Genus Yersinia* (pp. 391–394). Boston: Kluwer Academic Publishers. https://doi.org/10.1007/0-306-48416-1_79

Wagner, S., Königsmaier, L., Lara-Tejero, M., Lefebre, M., Marlovits, T. C., & Galán, J. E. (2010). Organization and coordinated assembly of the type III secretion export apparatus. *Proceedings of the National Academy of Sciences of the United States of America*, *107*(41), 17745–50. https://doi.org/10.1073/pnas.1008053107

Waldminghaus, T., Heidrich, N., Brantl, S., & Narberhaus, F. (2007). FourU: a novel type of RNA thermometer in *Salmonella*. *Molecular Microbiology*, *65*(2), 413–424. https://doi.org/10.1111/j.1365-2958.2007.05794.x

Wang, H., Avican, K., Fahlgren, A., Erttmann, S. F., Nuss, A. M., Dersch, P., … Wolf-Watz, H. (2016). Increased plasmid copy number is essential for *Yersinia* T3SS function and virulence. *Science*, *353*(6298). https://doi.org/10.1126/science.aaf7501

Wei, B. L., Brun-Zinkernagel, A. M., Simecka, J. W., Prüss, B. M., Babitzke, P., & Romeo, T. (2001). Positive regulation of motility and flhDC expression by the RNA-binding protein CsrA of *Escherichia coli*. *Molecular Microbiology*, *40*(1), 245–56. Retrieved from http://www.ncbi.nlm.nih.gov/pubmed/11298291

Weilbacher, T., Suzuki, K., Dubey, A. K., Wang, X., Gudapaty, S., Morozov, I., … Romeo, T. (2003). A novel sRNA component of the carbon storage regulatory system of *Escherichia coli*. *Molecular Microbiology*, *48*(3), 657–70. Retrieved from http://www.ncbi.nlm.nih.gov/pubmed/12694612

Weinberg, E. D. (2009). Iron availability and infection. *Biochimica et Biophysica Acta (BBA) - General Subjects*, *1790*(7), 600–605. https://doi.org/10.1016/j.bbagen.2008.07.002

Wengelnik, K., Van den Ackerveken, G., & Bonas, U. (1996). HrpG, a key hrp regulatory protein of *Xanthomonas campestris* pv. *vesicatoria* is homologous to two-component response regulators. *Molecular Plant-Microbe Interactions : MPMI*, *9*(8), 704–12. Retrieved from http://www.ncbi.nlm.nih.gov/pubmed/8870269

Westermann, A. J., Förstner, K. U., Amman, F., Barquist, L., Chao, Y., Schulte, L. N., … Vogel, J. (2016). Dual RNA-seq unveils noncoding RNA functions in host–pathogen interactions. *Nature*. https://doi.org/10.1038/nature16547

WHO | Plague – Madagascar. (2017). *WHO*. Retrieved from http://www.who.int/csr/don/02-november-2017-plague-madagascar/en/

Wiley, D. J., Nordfeldth, R., Rosenzweig, J., DaFonseca, C. J., Gustin, R., Wolf-Watz, H., & Schesser, K. (2006). The Ser/Thr kinase activity of the *Yersinia* protein kinase A (YpkA) is necessary for full virulence in the mouse, mollifying phagocytes, and disrupting the eukaryotic cytoskeleton. *Microbial Pathogenesis*, *40*(5), 234–243. https://doi.org/10.1016/j.micpath.2006.02.001

Wilkie, G. S., Dickson, K. S., & Gray, N. K. (2003). Regulation of mRNA translation by 5′- and 3′-UTR-binding factors. *Trends in Biochemical Sciences*, *28*(4), 182–188. https://doi.org/10.1016/S0968-0004(03)00051-3

Worrall, J. A., & Luisi, B. F. (2007). Information available at cut rates: structure and mechanism of ribonucleases. *Current Opinion in Structural Biology*, *17*(1), 128–137. https://doi.org/10.1016/j.sbi.2006.12.001

Worrall, J. A. R., Górna, M., Crump, N. T., Phillips, L. G., Tuck, A. C., Price, A. J., … Luisi, B. F. (2008). Reconstitution and Analysis of the Multienzyme *Escherichia coli* RNA Degradosome. *Journal of Molecular Biology*, *382*(4), 870–883. https://doi.org/10.1016/j.jmb.2008.07.059

Worrall, L. J., Hong, C., Vuckovic, M., Deng, W., Bergeron, J. R. C., Majewski, D. D., … Strynadka, N. C. J. (2016). Near-atomic-resolution cryo-EM analysis of the *Salmonella* T3S injectisome basal body. *Nature*, *540*(7634), 597–601. https://doi.org/10.1038/nature20576

Wren, B. W. (2003). The Yersiniae — a model genus to study the rapid evolution of bacterial pathogens. *Nature Reviews Microbiology*, *1*(1), 55–64. https://doi.org/10.1038/nrmicro730

Wulff-Strobel, C. R., Williams, A. W., & Straley, S. C. (2002). LcrQ and SycH function together at the Ysc type III secretion system in *Yersinia pestis* to impose a hierarchy of secretion. *Molecular Microbiology*, *43*(2), 411–23. Retrieved from http://www.ncbi.nlm.nih.gov/pubmed/11985718

Yakhnin, H., Yakhnin, A. V., Baker, C. S., Sineva, E., Berezin, I., Romeo, T., & Babitzke, P. (2011). Complex regulation of the global regulatory gene *csrA*: CsrA-mediated translational repression, transcription from five promoters by Eσ70 and EσS, and indirect transcriptional activation by CsrA. *Molecular Microbiology*, *81*(3), 689–704. https://doi.org/10.1111/j.1365-2958.2011.07723.x

Yakhnin, A. V., Baker, C. S., Vakulskas, C. A., Yakhnin, H., Berezin, I., Romeo, T., & Babitzke, P. (2013). CsrA activates *flhDC* expression by protecting *flhDC* mRNA from RNase E-mediated cleavage. *Molecular Microbiology*, *87*(4), 851–866. https://doi.org/10.1111/mmi.12136

Yang, J., Jain, C., & Schesser, K. (2008). RNase E regulates the *Yersinia* type 3 secretion system. *Journal of Bacteriology*, *190*(10), 3774–8. https://doi.org/10.1128/JB.00147-08

Yang, P.-C., & Mahmood, T. (2012). Western blot: Technique, theory, and trouble shooting. *North American Journal of Medical Sciences*, *4*(9), 429. https://doi.org/10.4103/1947-2714.100998

Yeo, W.-S., Lee, J.-H., Lee, K.-C., & Roe, J.-H. (2006). IscR acts as an activator in response to oxidative stress for the *suf* operon encoding Fe-S assembly proteins. *Molecular Microbiology*, *61*(1), 206–218.

https://doi.org/10.1111/j.1365-2958.2006.05220.x

Ygberg, S. E., Clements, M. O., Rytkonen, A., Thompson, A., Holden, D. W., Hinton, J. C. D., & Rhen, M. (2006). Polynucleotide Phosphorylase Negatively Controls spv Virulence Gene Expression in *Salmonella enterica*. *Infection and Immunity*, *74*(2), 1243–1254. https://doi.org/10.1128/IAI.74.2.1243-1254.2006

Yip, C. K., Kimbrough, T. G., Felise, H. B., Vuckovic, M., Thomas, N. A., Pfuetzner, R. A., … Strynadka, N. C. J. (2005). Structural characterization of the molecular platform for type III secretion system assembly. *Nature*, *435*(7042), 702–707. https://doi.org/10.1038/nature03554

Yother, J., Chamness, T. W., & Goguen, J. D. (1986). Temperature-controlled plasmid regulon associated with low calcium response in *Yersinia pestis*. *Journal of Bacteriology*, *165*(2), 443–7. Retrieved from http://www.ncbi.nlm.nih.gov/pubmed/3944056

Yother, J., & Goguen, J. D. (1985). Isolation and characterization of Ca^{2+}-blind mutants of *Yersinia pestis*. *Journal of Bacteriology*, *164*(2), 704–11. Retrieved from http://www.ncbi.nlm.nih.gov/pubmed/2997127

Young, G. M., Badger, J. L., & Miller, V. L. (2000). Motility is required to initiate host cell invasion by *Yersinia enterocolitica*. *Infection and Immunity*, *68*(7), 4323–6. https://doi.org/10.1128/IAI.68.7.4323-4326.2000

Zhang, S., Park, C. G., Zhang, P., Bartra, S. S., Plano, G. V., Klena, J. D., … Chen, T. (2008). Plasminogen Activator Pla of *Yersinia pestis* Utilizes Murine DEC-205 (CD205) as a Receptor to Promote Dissemination. *Journal of Biological Chemistry*, *283*(46), 31511–31521. https://doi.org/10.1074/jbc.M804646200

Zhang, W., Wang, Y., Song, Y., Wang, T., Xu, S., Peng, Z., … Shen, X. (2013). A type VI secretion system regulated by OmpR in *Yersinia pseudotuberculosis* functions to maintain intracellular pH homeostasis. *Environmental Microbiology*, *15*(2), 557–569. https://doi.org/10.1111/1462-2920.12005

Zhang, Y., Romanov, G., & Bliska, J. B. (2011). Type III Secretion System-Dependent Translocation of Ectopically Expressed Yop Effectors into Macrophages by Intracellular *Yersinia pseudotuberculosis*. *Infection and Immunity*, *79*(11), 4322–4331. https://doi.org/10.1128/IAI.05396-11

Zheng, Y., Lilo, S., Mena, P., & Bliska, J. B. (2012). YopJ-Induced Caspase-1 Activation in *Yersinia*-Infected Macrophages: Independent of Apoptosis, Linked to Necrosis, Dispensable for Innate Host Defense. *PLoS ONE*, *7*(4), e36019. https://doi.org/10.1371/journal.pone.0036019

Zhou, D., & Yang, R. (2009). Molecular Darwinian evolution of virulence in *Yersinia pestis*. *Infection and Immunity*, *77*(6), 2242–50. https://doi.org/10.1128/IAI.01477-08

Zhou, L., Tan, A., & Hershenson, M. B. (2004). *Yersinia* YopJ inhibits pro-inflammatory molecule expression in human bronchial epithelial cells. *Respiratory Physiology & Neurobiology*, *140*(1), 89–97. https://doi.org/10.1016/j.resp.2003.12.003

Zhu, H., Mao, X.-J., Guo, X.-P., & Sun, Y.-C. (2016). The *hmsT* 3′ untranslated region mediates c-di-GMP metabolism and biofilm formation in *Yersinia pestis*. *Molecular Microbiology*, *99*(6), 1167–1178. https://doi.org/10.1111/mmi.13301

Zietz, B. P., & Dunkelberg, H. (2004). The history of the plague and the research on the causative agent *Yersinia pestis*. *International Journal of Hygiene and Environmental Health*, *207*(2), 165–178. https://doi.org/10.1078/1438-4639-00259

Zumbihl, R., Aepfelbacher, M., Andor, A., Jacobi, C. A., Ruckdeschel, K., Rouot, B., & Heesemann, J. (1999). The cytotoxin YopT of *Yersinia enterocolitica* induces modification and cellular redistribution of the small GTP-binding protein RhoA. *The Journal of Biological Chemistry*, *274*(41), 29289–93. Retrieved from http://www.ncbi.nlm.nih.gov/pubmed/10506187

Zwir, I., Shin, D., Kato, A., Nishino, K., Latifi, T., Solomon, F., … Groisman, E. A. (2005). Dissecting the PhoP regulatory network of *Escherichia coli* and *Salmonella enterica*. *Proceedings of the National Academy of Sciences of the United States of America*, *102*(8), 2862–7. https://doi.org/10.1073/pnas.0408238102

Supplementary material

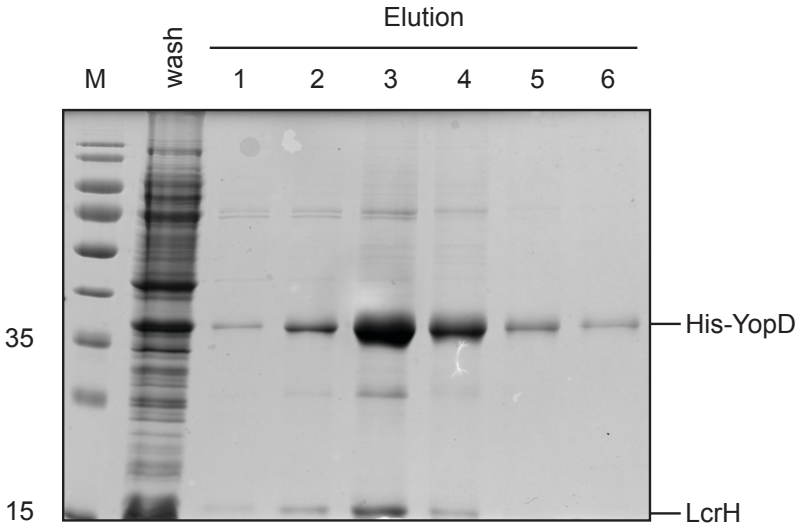

Figure S1. Coomassie blue-stained SDS-PAGE of Ni-NTA affinity chromatography-purified His_6-YopD/LcrH complexes.

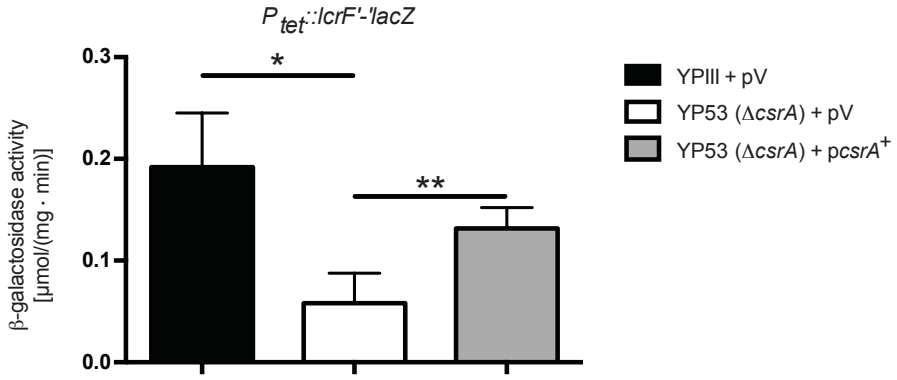

Figure S2. CsrA promotes translation initiation of *lcrF*.
Y. pseudotuberculosis strains YPIII (wt), and YP53 (Δ*csrA*) harboring the translational reporter gene fusion P_{tet}::*lcrF'–'lacZ* (pKB14) and the empty vector pHSG576 (pV) or the *csrA*+ plasmid (pKB60) were grown in LB_{BD} medium (1:50 diluted from overnight cultures for YPIII, or 1:20 for YP53) for two hours at 25°C. Secretion conditions were induced by adding 20 mM NaOx and 20 mM $MgCl_2$. Bacteria were further cultivated for four hours at 37°C. The β-galactosidase activity was determined and is given in µmol · mg^{-1} · min^{-1} for comparison. The data represent the mean ± standard deviation of three independent experiments each performed in duplicates. Data were analyzed by the Student's t-test. Stars indicate the results that differed significantly from each other with *($P<0.05$), **($P<0.01$).

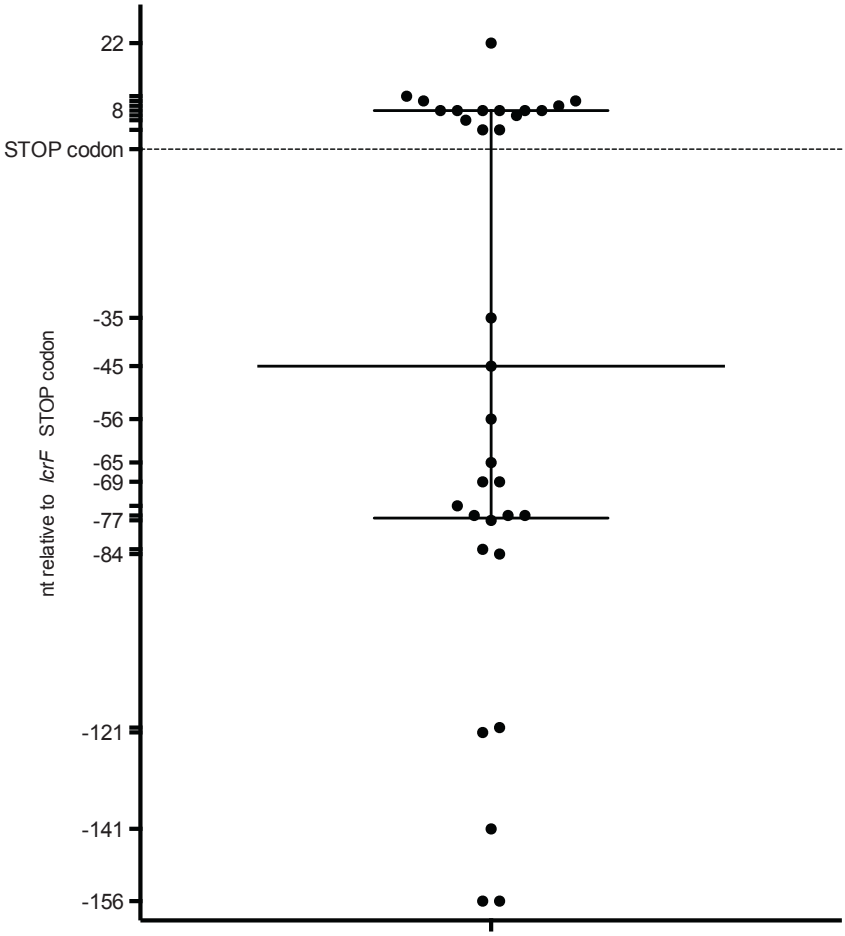

Figure S3. Determination of the *lcrF* 3'-UTR length using 3'-RACE.
A The graph represents the varying length of the *lcrF* 3'-UTR (black dots) estimated via the 3'-RACE (all 33 clones). The terminal nucleotide as well as its position relative to the *lcrF* STOP codon is given on the y-axis.

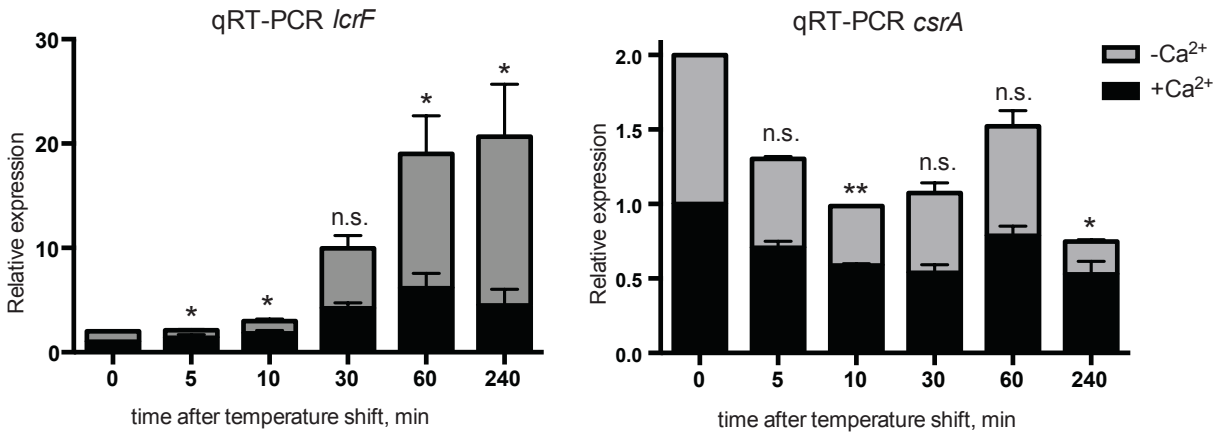

Figure S4. Determination of an optimal time point for detection of immediate LCR-mediated changes in gene expression.
Y. pseudotuberculosis YPIII was grown under at 25°C for 2 hours. Thereafter Ca^{2+} depletion was either performed (secretion conditions) or not (non-secretion conditions) and the cultures were shifted to 37°C. At time points indicated on the graph total RNA was extracted and prepared for analysis of the relative expression level of *lcrF* (left panel) or *csrA* (right panel). The relative expression of each gene was normalized to *sopB* and calculated relative to time point 0 min. The data show the mean ± standard deviation of three independent experiments each performed in duplicates. Data were analyzed by the Student's t-test. Stars indicate the results that differed significantly from each other with *(P<0.05), **(P<0.01), n.s. (P>0.05).

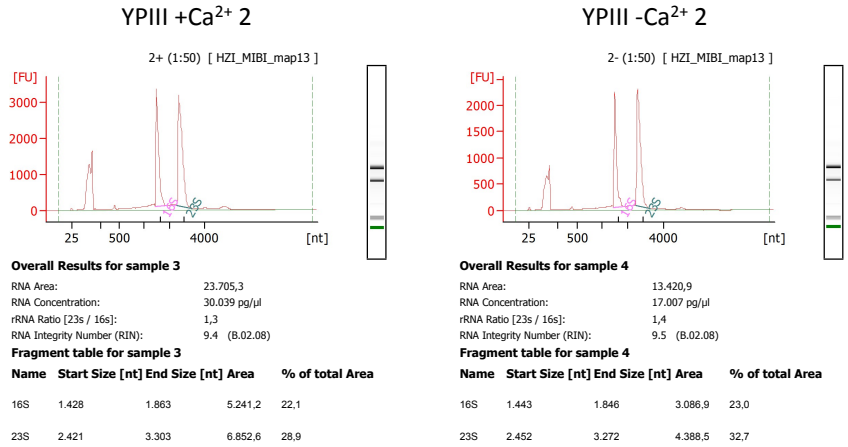

Figure S5. RNA electropherograms of two representative replicates from immediate Ca^{2+} depletion response experiment.
The RIN indicates the quality of the total RNA.

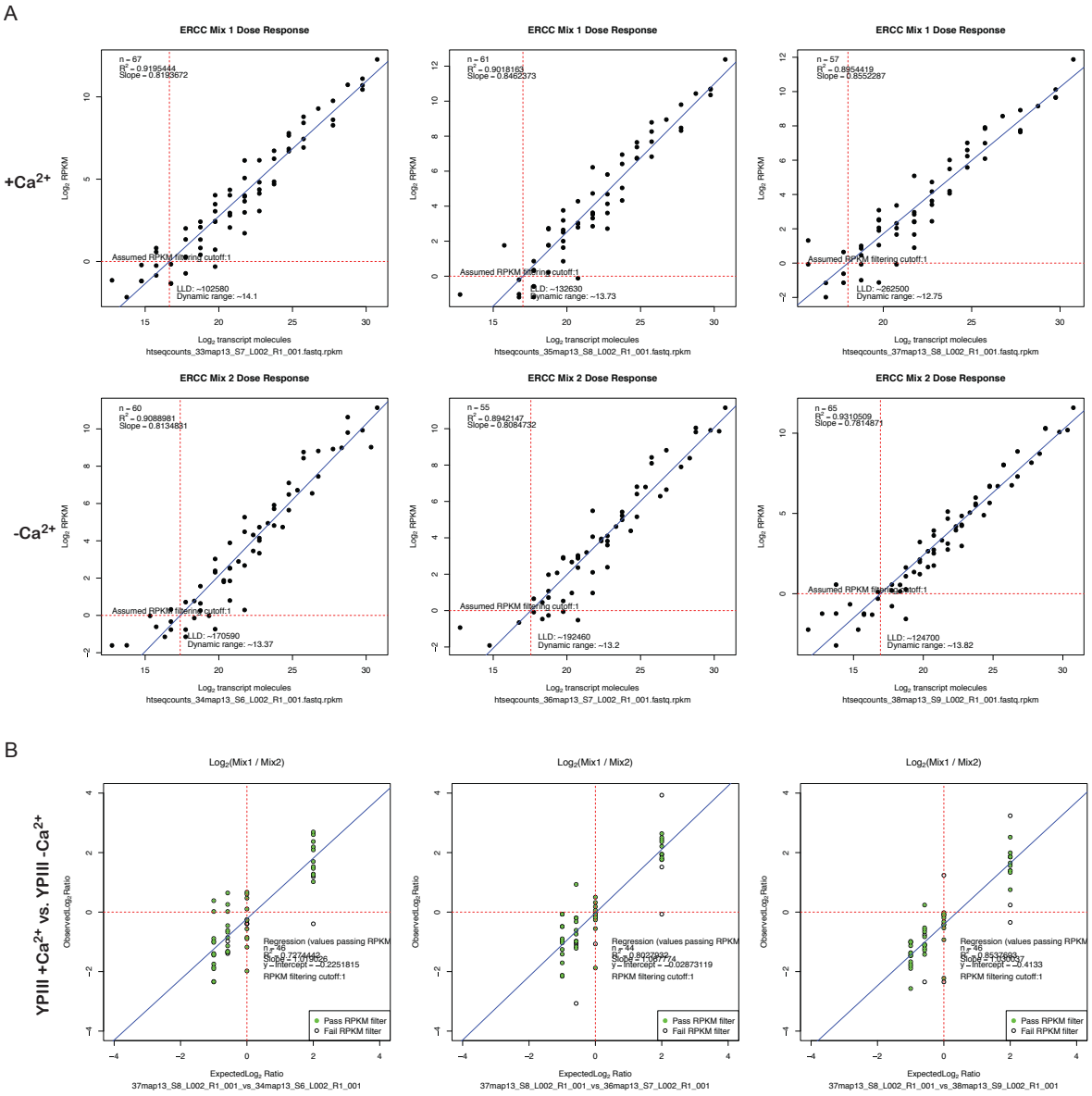

Figure S6. RNA-seq platform performance (representative from immediate Ca^{2+} depletion response experiment).

A Platform dynamic range and lower limit of detection (dose response). Either ERCC ExFold RNA Spike-In Mix 1 or Mix 2 was added to RNA pools obtained from plus Ca^{2+} and plus Ca^{2+} samples. **B** Assessment of platform fold-change responses. ERCC ExFold RNA Spike-In Mix 1 or Mix 2 was added to mouse RNA pools, which were then converted into cDNA libraries and sequenced. The observed fold-change ratios between Mix 1 and Mix 2 should match with the expected ratios, which can be determined by linear regression. Controls with an RPKM $\leq$ 1 (open circles) were removed in either sample and the linear fit illustrates highly accurate fold-change estimates (filled circles).

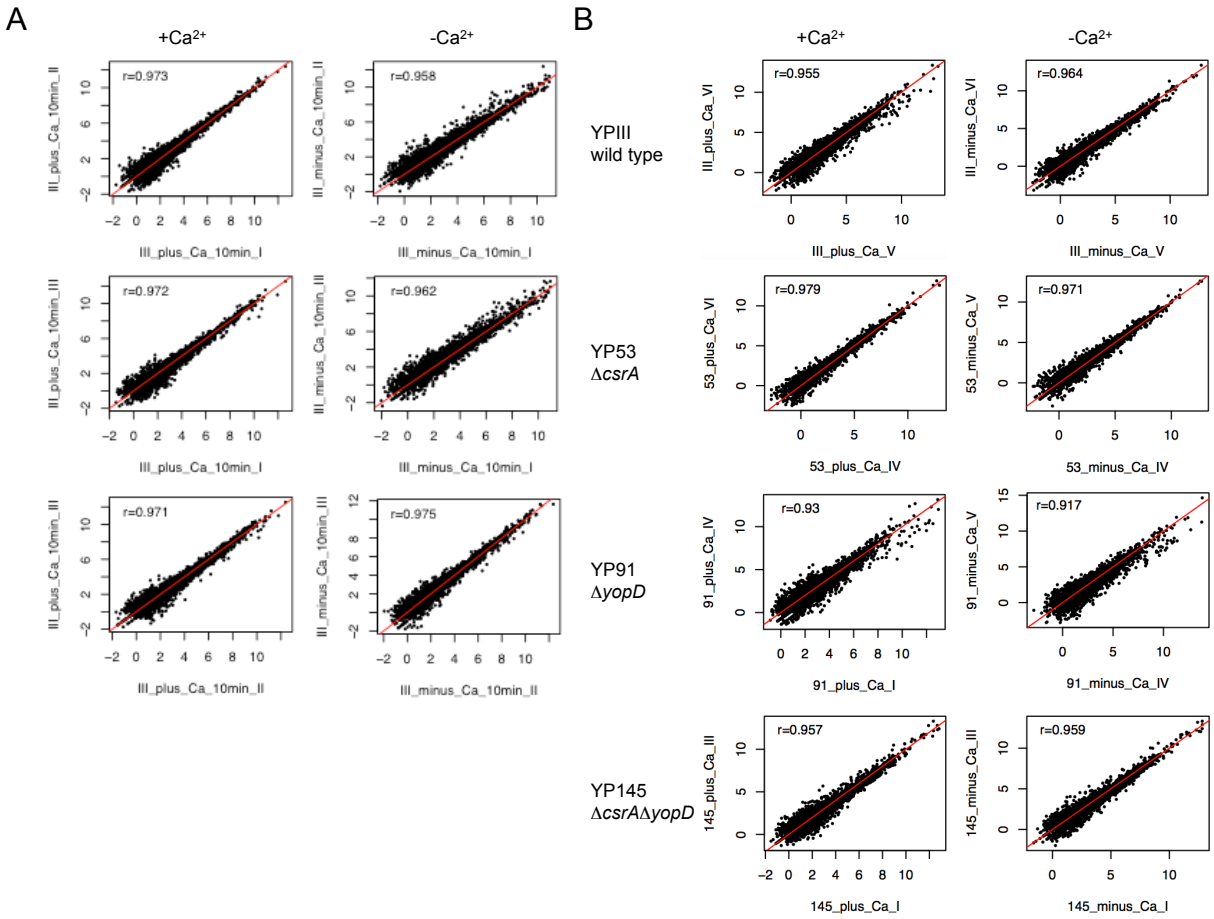

Figure S7. Replicate correlation of RNA-seq data.
RPKM normalized read counts for all detected genes are plotted for the biological replicates representative for immediate LCR (**A**) and for LCR 4 hours after induction (**B**) datasets. The Pearson correlation coefficient (r) is given for each replicate.

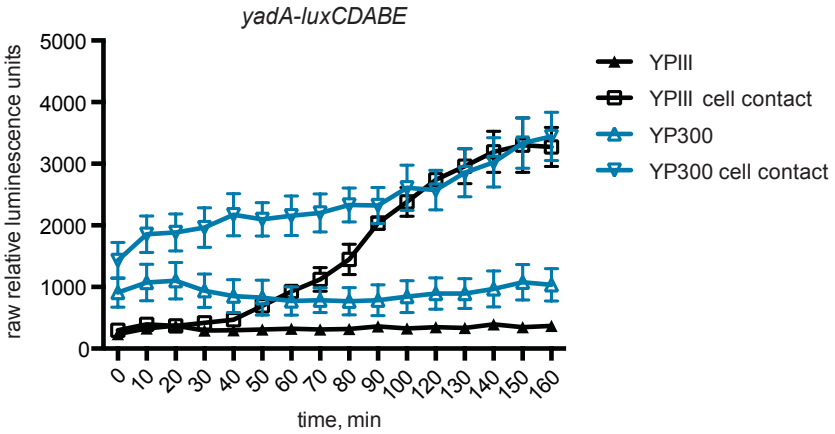

Figure S8. Role of the OmpR/EnvZ TCS in cell contact-dependent *yadA* induction.
A *Y. pseudotuberculosis* YPIII (wt) and YP300 (Δ*ompR/envZ*) strains carrying pWO41 (*yadA-luxCDABE*) were used to infect confluent HEp-2 cells or incubated without cells in PBS at 25 °C for 2.5 hours. Bioluminescent emission was measured every 10 min to monitor kinetics of host cell-dependent *yadA-luxCDABE* induction.

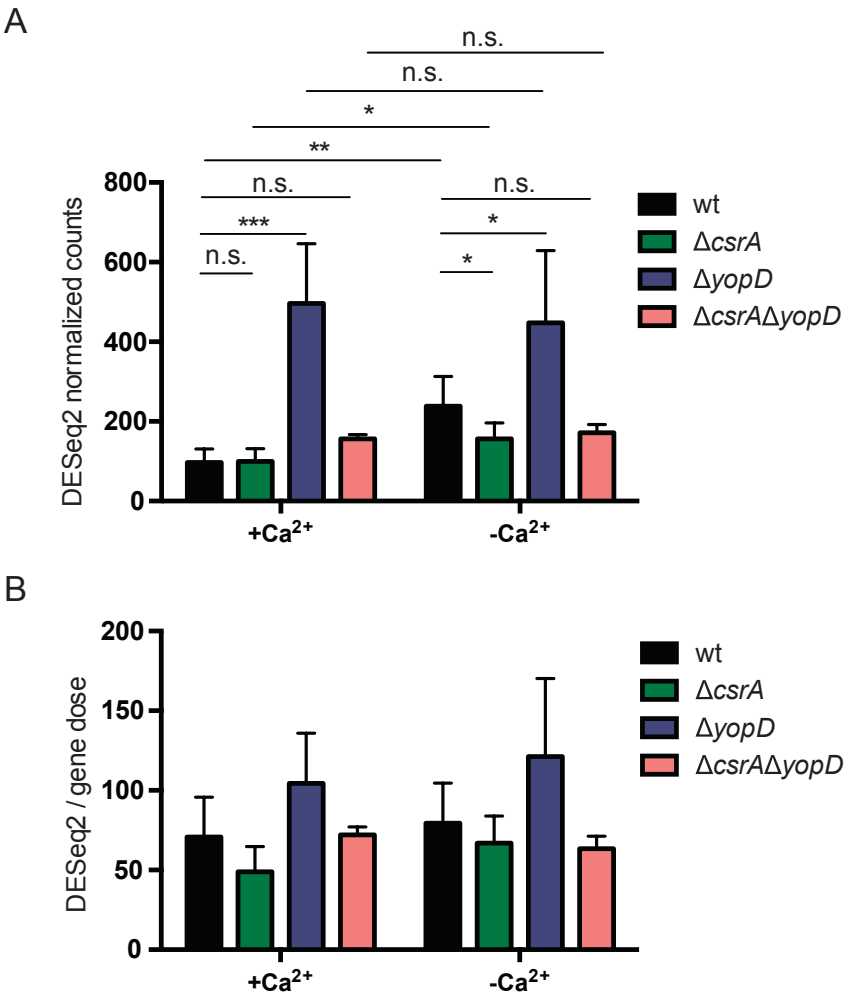

Figure S9. RepA expression in response to the low calcium signal.
A DESeq2 normalized read counts of *repA* mRNA from YPIII, YP53, YP91 and YP145 grown under non-secretion (+Ca^{2+}) and secretion conditions (-Ca^{2+}). **B** DESeq2 normalized read counts of *repA* mRNA relative to the measured gene dose in the respective sample (in cooperation with I. Vollmer). The data represent the mean ± standard deviation of three independent experiments. Data were analyzed by the Student's t-test. Stars indicate the results that differed significantly from each other with *(P<0.05), **(P<0.01), ***(P<0.001), and n.s. (not significant).

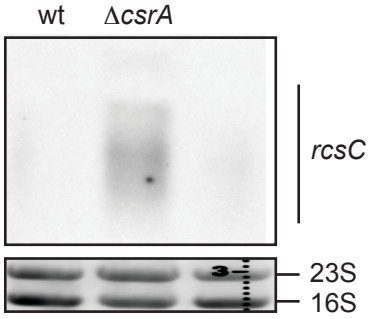

Figure S10. CsrA affects *rcsC* expression.
Y. pseudotuberculosis strains YPIII (wt), and YP53 (Δ*csrA*) were grown in LB_{BD} medium (1:50 diluted from overnight cultures for YPIII, or 1:20 for YP53) for two hours at 25°C, followed by four hours at 37°C. For Northern blot analysis, performed to determine the *rcsC* transcript level, total RNA of the cultures was isolated, separated by 1.2% MOPS agarose gel electrophoresis, and transferred onto a nylon membrane. The mRNA of interest were specifically detected by the specific Dig-labeled DNA probe. *csrC* transcript is indicated on the right. 23S and 16S rRNA was visualized with ethidium bromide as loading control. The Δ*rcsBC* mutant strain YP310 was used as negative control.

Table S1. Mapping statistics for immediate Ca^{2+} response

Sample group	Replicate	Total mapped reads	Total uniquely mapped reads including ERCC	Uniqely mapped to chromosome	Uniquely mapped to pYV	Total uniquely mapped to genes
YPIII plus calcium	1	4676524	2254018	2167295	53573	1907239
	2	4392822	2048259	1973227	45740	1742259
	3	4173929	1976621	1915462	42756	1669254
YPIII minus calcium	1	5990773	3007598	2931157	49530	2677149
	2	3935634	1881393	1828508	37652	1599028
	3	8970361	4665558	4495361	124839	4066497

Table S2. Mapping statistics for Ca^{2+} response after four hours

Sample group	Replicate	Total mapped reads	Total uniquely mapped reads including ERCC	Uniqely mapped to chromosome	Uniquely mapped to pYV	Total uniquely mapped to genes
YPIII plus calcium	1	3196106	504942	460909	12198	450166
	2	3302812	564991	532531	10881	500142
	3	2529716	382184	350126	8432	343734
	4	22792255	6843740	6416007	200093	5980963
	5	13605673	2740935	2589440	73092	2449293
	6	12366378	3215110	3006493	86661	2932063
YPIII minus calcium	1	3395252	841256	484258	308987	744310
	2	5519095	1866868	1169945	626206	1655412
	3	6000433	1697951	1060463	603614	1519845
	4	12336959	4413044	2455311	1849220	3951285
	5	13590428	4903733	2507071	2312152	4448043
	6	34405570	10487998	5381623	4865101	9631019
YP53 plus calcium	1	5761000	1762167	1639855	44631	1552122
	2	3763748	845031	796823	24398	746612
	3	3310705	1227191	961552	226942	1072702
	4	23931469	9106884	8584427	314624	7973222
	5	17088354	5876041	5533970	195147	5150469
	6	27474027	9647489	9122122	320045	8392402
YP53 minus calcium	1	4300739	827213	685759	126383	674890
	2	7334787	1856062	1665472	131379	1611329
	3	6449512	2535870	2218886	284075	2159035
	4	11012177	4374224	3496056	795397	3884624
	5	15226736	6175406	4890125	1137012	5470604
	6	30123123	11219320	9429667	1573231	9710697
YP91 plus calcium	1	8330086	979135	632040	297867	859785
	2	2968133	543669	389799	115622	499319
	3	3346465	860058	494897	310216	762712
	4	11612162	1975486	1110759	794969	1704464
	5	25011133	5964693	3540297	2180517	5245101
YP91 minus calcium	1	5128802	1079376	752366	235409	957107
	2	5121020	1193955	933172	189666	1075299
	3	3138550	426263	219108	169433	384146
	4	13065642	2414083	1601198	676691	2191059
	5	25919936	7523585	5100026	2199919	7042405
	6	14157482	2985223	1712879	1120529	2643348
YP145 plus calcium	1	6820638	1702398	1368545	255329	1500373
	2	4351002	1113247	1090229	18760	992529
	3	4714354	1608195	1320970	245414	1393364
YP145 minus calcium	1	6251587	1627346	1276884	282420	1414690
	2	8130583	2781334	2211384	480613	2397110
	3	5064668	1659613	1318716	299239	1402907

Table S3. Classification of LCR-dependent genes

Locus	Gene name	Log_2FC	Description	
Virulence				
LCR-activated loci				
pYV0047	*yopM*	7,8	YopM, targeted effector protein	virulence factor, pYV
pYV0040	*yopK, yopQ*	7,5	YopK, targeting protein YopK, YopQ	virulence factor, pYV
pYV0057	*lcrV*	6,6	LcrV, V antigen, antihost protein/regulator	virulence factor, pYV
pYV0094	*yopH*	6,5	YopH, protein-tyrosine phosphatase Yop effector	virulence factor, pYV
pYV0056	*lcrH, sycD*	6,5	LcrH, SycD, low calcium response protein H	virulence factor, pYV
pYV0098	*yopP, yopJ*	6,3	YopP, YopJ, targeted effector protein	virulence factor, pYV
pYV0058	*lcrG*	6,3	LcrG, Yop regulator	virulence factor, pYV
pYV0054	*yopD*	6,3	YopD, Yop negative regulation/targeting component	virulence factor, pYV
pYV0055	*yopB*	6,2	YopB, Yop targeting protein	virulence factor, pYV
pYV0025	*yopE*	6,0	outer membrane virulence protein	virulence factor, pYV
pYV0082	*yscF*	4,9	YscF, type III secretion protein	virulence factor, pYV
pYV0079	*yscC*	4,7	YscC, type III secretion protein	virulence factor, pYV
pYV0001	*ypkA*	4,7	YpkA, targeted effector protein kinase	virulence factor, pYV
YPK_2831	*pla2*	4,4	outer membrane protease	virulence factor; outer membrane protease: involved in virulence in many organisms; OmpT; IcsP; SopA; Pla; PgtE; omptin; in *E. coli* OmpT can degrade antimicrobial peptides; in *Yersinia* Pla activates plasminogen during infection; in *S. flexneri* SopA cleaves the autotransporter IcsA
pYV0087	*yscK*	4,4	YscK, type III secretion protein	virulence factor, pYV
pYV0080	*yscD*	4,4	YscD, type III secretion protein	virulence factor, pYV
pYV0059	*lcrR*	4,3	hypothetical protein LcrR	virulence factor, pYV
pYV0083	*yscG*	4,2	YscG, type III secretion protein	virulence factor, pYV
pYV0061	*yscY*	4,1	YscY, type III secretion protein	virulence factor, pYV
pYV0065	*yopN, lcrE*	4,1	YopN, LcrE, membrane-bound Yop targeting protein	virulence factor, pYV
pYV0068	*yscO*	4,0	YscO, type III secretion protein	virulence factor, pYV

pYV0081	*yscE*	4,0	YscE, type III secretion protein	virulence factor, pYV
pYV0024	*sycE, yerA*	3,9	YopE chaperone	virulence factor, pYV
pYV0063	*sycN*	3,9	SycN, type III secretion protein	virulence factor, pYV
pYV0013	*yadA*	3,8	Yersinia adhesin A, YadA	virulence factor, pYV
pYV0088	*yscL*	3,8	type III secretion system protein	virulence factor, pYV
pYV0086	*yscJ, ylpB*	3,7	YscJ, YlpB, type III secretion lipoprotein	virulence factor, pYV
pYV0084	*yscH, yopR*	3,7	YscH, YopR, LcrP, type III secretion protein	virulence factor, pYV
pYV0067	*sctN*	3,6	type III secretion system ATPase	virulence factor, pYV
pYV0060	*lcrD, yscV*	3,6	LcrD, YscV, membrane-bound Yop protein	virulence factor, pYV
pYV0069	*yscP*	3,6	YscP, type III secretion protein	virulence factor, pYV
pYV0070	*yscQ*	3,6	type III secretion system protein	virulence factor, pYV
pYV0071	*yscR*	3,5	type III secretion system protein	virulence factor, pYV
pYV0064	*tyeA*	3,5	TyeA, Yop secretion and targeting protein	virulence factor, pYV
pYV0062	*yscX*	3,5	YscX, type III secretion protein	virulence factor, pYV
pYV0085	*yscI, lcrO*	3,4	YscI, LcrO, type III secretion protein	virulence factor, pYV
pYV0073	*yscT*	3,4	YscT, type III secretion protein	virulence factor, pYV
pYV0077	*yscA*	3,2	YscA, type III secretion protein	virulence factor, pYV
pYV0089	*yscM, lcrQ*	3,1	YscM, LcrQ, type III secretion regulatory	virulence factor, pYV
pYV0074	*yscU*	3,1	YscU, type III secretion protein	virulence factor, pYV
pYV0041	*yopT*	3,1	yop targeted effector YopT	virulence factor, pYV
pYV0076	*lcrF, virF*	3,0	LcrF, VirF, thermoregulatory protein	virulence factor, pYV
YPK_2649	*ompF*	2,9	porin	virulence factor; Drug resistance: beta-Lactam resistance; outer membrane pore protein F
YPK_2381	*fliC*	2,9	flagellin	virulence factor; Infectious diseases: Salmonella infection; Legionellosis
pYV0075	*virG, yscW*	2,9	VirG, YscW, Yop targeting lipoprotein	virulence factor, pYV
pYV0072	*yscS*	2,7	YscS, type III secretion protein	virulence factor, pYV
LCR-repressed loci				
YPK_2759	*psaA*	-3,1	pH 6 antigen	virulence factor
YPK_3452	*degP, htrA*	-2,4	serine endoprotease	virulence factor; Drug resistance: Cationic antimicrobial peptide (CAMP) resistance; serine protease Do

Metabolism

LCR-activated loci

YPK_2831	*pla2*	4,4	outer membrane protease	Metabolism: Enzyme families; Peptidases
YPK_2916	*betB*	4,1	betaine aldehyde dehydrogenase	Amino acid metabolism: Glycine, serine and threonine metabolism; betaine-aldehyde dehydrogenase
YPK_0423	*ssuC*	2,6	binding-protein-dependent transport systems inner membrane component	Energy metabolism: Sulfur metabolism; sulfonate transport system permease protein
YPK_0495	*treB*	2,4	PTS system trehalose (maltose)-specific transporter subunit IIBC	Carbohydrate metabolism: Starch and sucrose metabolism; PTS-Tre-EIIC; PTS system
YPK_3848		2,4	lactaldehyde reductase	Carbohydrate metabolism: Glycolysis/Gluconeogenesis; alcohol dehydrogenase
YPK_1637		2,2	glycosidase PH1107-like protein	Unclassified; Metabolism: Carbohydrate metabolism; 4-O-beta-D-mannosyl-D-glucose phosphorylase
YPK_0422	*ssuD*	2,2	alkanesulfonate monooxygenase	Energy metabolism: Sulfur metabolism; alkanesulfonate monooxygenase

LCR-repressed loci

YPK_1974	*aldB*	-3,2	aldehyde dehydrogenase	Carbohydrate metabolism: Pyruvate metabolism; aldehyde dehydrogenase
YPK_1133	*ureC*	-2,6	urease subunit alpha	Nucleotide metabolism: Purine metabolism; urease subunit alpha; Amino acid metabolism: Arginine biosynthesis; Xenobiotics biodegradation and metabolism: Atrazine degradation
YPK_3042		-2,4	oxidoreductase domain-containing protein	Carbohydrate metabolism: Galactose metabolism; GenBank: Gfo/Idh/MocA family oxidoreductase
YPK_2703	*poxB*	-2,2	pyruvate dehydrogenase	Carbohydrate metabolism: Pyruvate metabolism; pyruvate dehydrogenase (quinone)
YPK_4088	*argB*	-2,2	acetylglutamate kinase	Amino acid metabolism: Arginine biosynthesis; acetylglutamate kinase
YPK_3368	*luxS*	-2,1	S-ribosylhomocysteinase	Amino acid metabolism: Cysteine and methionine metabolism; S-ribosylhomocysteine lyase
YPK_2996	*nagE*	-2,1	PTS system N-	Carbohydrate metabolism:

			acetylglucosamine-specific transporter subunit IIBC	Amino sugar and nucleotide sugar metabolism
YPK_1132	*ureB*	-2,1	urease subunit beta	Nucleotide metabolism: Purine metabolism; urease subunit beta; Amino acid metabolism: Arginine biosynthesis; Xenobiotics biodegradation and metabolism: Atrazine degradation
YPK_1131	*ureA*	-2,0	urease subunit gamma	Nucleotide metabolism: Purine metabolism; urease subunit gamma; Amino acid metabolism: Arginine biosynthesis; Xenobiotics biodegradation and metabolism: Atrazine degradation
YPK_4089	*argC*	-2,0	N-acetyl-gamma-glutamyl-phosphate reductase	Amino acid metabolism: Arginine biosynthesis; N-acetyl-gamma-glutamyl-phosphate reductase
YPK_3395	*araD-2*	-2,0	L-ribulose-5-phosphate 4-epimerase	Carbohydrate metabolism: Pentose and glucuronate interconversions; L-ribulose-5-phosphate 4-epimerase; Ascorbate and aldarate metabolism; L-ribulose-5-phosphate 4-epimerase
YPK_0343	*thiG*	-2,0	thiazole synthase	Metabolism of cofactors and vitamins: Thiamine metabolism; thiazole synthase
Cellular Processes				
LCR-activated loci				
YPK_2381	*fliC*	2,9	flagellin	Cell motility: Flagellar assembly; flagellin
YPK_1748	*motB-2*	2,4	flagellar motor protein MotB	Cell motility: Bacterial chemotaxis; Flagellar assembly
YPK_1747	*motA-2*	2,4	flagellar motor protein MotA	Cell motility: Bacterial chemotaxis; Flagellar assembly
LCR-repressed loci				
YPK_3368	*luxS*	-2,1	S-ribosylhomocysteinase	Cellular community - prokaryotes: Quorum sensing; S-ribosylhomocysteine lyase; Biofilm formation - *Vibrio cholerae*; Biofilm formation - *Escherichia coli*; S-ribosylhomocysteine lyase
YPK_3653	*lsrB*	-2,0	autoinducer AI-2 ABC transporter periplasmic AI-2-binding protein	Cellular community – prokaryotes: Quorum sensing; AI-2 transport system substrate-

				binding protein
Environmental Information Processing				
LCR-activated loci				
YPK_2914	*betT*	3,1	choline transport protein BetT	Membrane transport: Transporters; choline/glycine/proline betaine transport protein
YPK_2649	*ompF*	2,9	porin	Signal transduction: Two-component system; outer membrane pore protein F
YPK_2381	*fliC*	2,9	flagellin	Signal transduction: Two-component system; flagellin
YPK_0423	*ssuC*	2,6	binding-protein-dependent transport systems inner membrane component	Membrane transport: ABC transporters; sulfonate transport system permease protein
YPK_0495	*treB*	2,4	PTS system trehalose (maltose)-specific transporter subunit IIBC	Membrane transport: Phosphotransferase system (PTS)
YPK_1747	*motA-2*	2,4	flagellar motor protein MotA	Signal transduction: Two-component system; chemotaxis protein MotA
YPK_2003	*rtxD*	2,4	type I secretion membrane fusion protein, HlyD family	Signal transduction: TCS; membrane fusion protein, RTX toxin transport system
YPK_2004	*rtxB*	2,2	type I secretion system ATPase	Signal transduction: Two-component system; ATP-binding cassette, subfamily B, bacterial RtxB
LCR-repressed loci				
YPK_3398	*yphF-5, ytfQ-5*	-2,4	carbohydrate ABC transporter periplasmic-binding protein	Structural complex: Environmental information processing; Saccharide, polyol, and lipid transport system; Putative simple sugar transport system; simple sugar transport system substrate-binding protein
YPK_3452	*degP, htrA*	-2,4	serine endoprotease	Signal transduction: Two-component system; serine protease Do
YPK_4109	*raxA, cvaA*	-2,3	secretion protein HlyD family protein	Membrane transport: Transporters; membrane fusion protein; Secretion system
YPK_2996	*nagE*	-2,1	PTS system N-acetylglucosamine-specific transporter subunit IIBC	Membrane transport: Phosphotransferase system (PTS)
YPK_3653	*lsrB*	-2,0	autoinducer AI-2 ABC transporter periplasmic AI-2-binding protein	Membrane transport: ABC transporters; AI-2 transport system substrate-binding protein

Transporters

LCR-activated loci

YPK_2914	*betT*	3,1	choline transport protein BetT	Other Transporters: Electrochemical potential-driven transporters [TC:2]
YPK_2649	*ompF*	2,9	porin	Other Transporters: Pores ion channels; outer membrane pore protein F
YPK_0423	*ssuC*	2,6	binding-protein-dependent transport systems inner membrane component	ABC Transporters, Prokaryotic Type: Mineral and organic ion transporters; Sulfonate transporter; sulfonate transport system permease protein
YPK_0495	*treB*	2,4	PTS system trehalose(maltose)-specific transporter subunit IIBC	Phosphotransferase System (PTS): Enzyme II; Trehalose-specific II component; PTS-Tre-EIIC; PTS system, trehalose-specific IIC component
YPK_1748	*motB-2*	2,4	flagellar motor protein MotB	Other Transporters: Pores ion channels; chemotaxis protein MotB
YPK_1747	*motA-2*	2,4	flagellar motor protein MotA	Other Transporters: Pores ion channels; chemotaxis protein MotA
YPK_2003	*rtxD*	2,4	type I secretion membrane fusion protein, HlyD family	Other Transporters: Accessory factors involved in transport; membrane fusion protein, RTX toxin transport system

LCR-repressed loci

YPK_3398	*yphF-5, ytfQ-5*	-2,4	carbohydrate ABC transporter periplasmic-binding protein	ABC Transporters: Saccharide, polyol, and lipid transporters; Putative simple sugar transporter; galactofuranose ABC transporter periplasmic binding protein; simple sugar transport system substrate-binding protein
YPK_3653	*lsrB*	-2,0	autoinducer AI-2 ABC transporter periplasmic AI-2-binding protein	ABC Transporters, Prokaryotic Type: Saccharide, polyol, and lipid transporters; AI-2 transporter; AI-2 transport system substrate-binding protein

Genetic Information Processing

LCR-activated loci

Ysr164		3,6	Synonym: Ysr164; Class: transRNA	RNA family: Non-coding RNAs
YPK_2915	*betI*	3,5	transcriptional regulator BetI	Transcription: Transcription factors; TetR/AcrR family transcriptional regulator,

				transcriptional repressor of *bet* genes
Ysr290		3,3	Synonym: Ysr290; Class: asRNA	RNA family: Non-coding RNAs
YPK_0217		3,0	putative transcriptional regulator, Nlp	Transcription
Ysr298		2,8	Synonym: Ysr298; Class: asRNA	RNA family: Non-coding RNAs
YPK_0888	*dam-2*	2,7	DNA adenine methylase	Replication and repair: mismatch repair; DNA adenine methylase
Ysr299		2,5	Synonym: Ysr299; Class: asRNA	RNA family: Non-coding RNAs
LCR-repressed loci				
YPK_R0037	*tRNA-Phe*	-3,0	tRNA Phe	Translation: Transfer RNA biogenesis
YPK_3452	*degP, htrA*	-2,4	serine endoprotease	Folding, sorting and degradation: Chaperones and folding catalysts; serine protease Do
YPK_R0034	*tRNA-Leu*	-2,2	tRNA Leu	Translation: Transfer RNA biogenesis
YPK_R0016	*tRNA-Val*	-2,1	tRNA Val	Translation: Transfer RNA biogenesis
YPK_0504	*yhbH*	-2,1	putative sigma(54) modulation protein	Translation: Ribosome biogenesis; putative sigma-54 modulation protein
YPK_R0037	*tRNA-Phe*	-3,0	tRNA Phe	Translation: Transfer RNA biogenesis

Hypothetical Proteins

LCR-activated loci

pYV0002	6,4	hypothetical protein
pYV0099	6,4	hypothetical protein
pYV0078	4,8	hypothetical protein
pYV0097	4,6	hypothetical protein
pYV0035	4,5	hypothetical protein
pYV0048	4,1	hypothetical protein
pYV0049	3,6	hypothetical protein
pYV0044	3,5	hypothetical protein
YPK_2588	2,9	hypothetical protein
pYV0051	2,9	hypothetical protein
YPK_2682	2,6	hypothetical protein
YPK_0912	2,3	hypothetical protein
YPK_1487	2,0	hypothetical protein

LCR-repressed loci

YPK_3773	*ytfK*	-3,8	hypothetical protein
YPK_3567	*rovC*	-2,1	hypothetical protein
YPK_0631		-2,0	hypothetical protein

Others

LCR-activated loci

pYV0038	8,5	pseudogene
pYV0039	7,1	putative transposase
pYV0014	5,2	pseudogene
pYV0092	4,5	transposase
pYV0037	4,2	pseudogene
pYV0091	4,1	transposase
pYV0008	3,2	possible transposase remnant
YPK_1991	2,5	pseudogene
pYV0015	2,5	pseudogene
pYV0090	2,5	transposase
pYV0046	2,4	putative transposase remnant
YPK_2286	2,4	putative transposase
pYV0093	2,4	transposase
pYV0096	2,3	IS630 family transposase
pYV0017	2,2	resolvase

Danksagung

Mein größter Dank geht an meine Mentorin Prof. Dr. Petra Dersch. Danke für das tolle Projekt, die gute Betreuung meiner Arbeit, die grenzenlose Unterstützung in allem und dein Vertrauen in meine Fähigkeiten!

Des Weiteren danke ich ganz herzlich Prof. Dr. Michael Steinert für die Unterstützung meines Projektes im Rahmen des *Thesis Committees* sowie für die Übernahme des Koreferates meiner Doktorarbeit. Bei apl. Prof. Dr. Michael Hust bedanke ich mich für die Übernahme des Prüfungsvorsitzes. Ein weiterer Dank geht an Prof. Dr. Marc Erhardt für die Teilnahme und Diskussionen bei meinen *Thesis Committees*.

Bei der „Helmholtz International Graduate School for Infection Research“ möchte ich mich für die Teilfinanzierung meiner Promotion bedanken. Ein großer Dank auch für die Möglichkeit, an den nationalen und internationalen Konferenzen teilzunehmen.

Zudem möchte ich unseren Kooperationspartnern Erik Holmqvist und Lars Barquist aus dem Institut für Molekulare Infektionsbiologie an der Julius-Maximilians-Universität Würzburg für die gute Zusammenarbeit und den Gedankenaustausch bezüglich der Anwendung der CLIP-seq Methode für Yersinien danken.

Ein ganz großes Dankeschön gilt den liebsten PostDocs (Kathi, Sabrina, Franzi). Ich danke euch dafür, dass ihr immer für mich da wart, wenn ich meine Zweifel hatte und mich immer mit Rat und Tat unterstützt habt sowohl in wissenschaftlichen als auch in weniger wissenschaftlichen Fragen :-*

Ein besonderer Dank geht an Claudia, ohne der die bürokratische und organisatorische Kriege nicht zu gewinnen gewesen wären.

Vielen Dank auch an alle TAs (Tanja, Sandra, Jenny, Amrei, Karin, Bettina) für die Erleichterungen im Laboralltag. Bei Sandra bedanke ich mich extra für das Beibringen der deutschen Ironie. Die Schule war hart, dafür verwende ich aber die gelernte *skills* nun auch sehr gerne :D

Ich danke auch meinen „Büromitbewohnern“ (Vanessa und Carina) für die schönen Jahre in unserer Arbeits-WG, für die wissenschaftlichen und manchmal auch nicht wissenschaftlichen Diskussionen - und dass ihr immer für meine Probleme, oder, besser gesagt, Panikattacken ein offenes Ohr hattet und mich rechtzeitig in den Ruhezustand bringen konntet ;-)

Dem besten Doktorandenteam der Welt (Paweena, Ines, Vanessa, Carina und Marcel) danke ich ganz herzlich für die zahlreichen „nebenbei“-Aktivitäten, die mir immer sehr viel Spaß gemacht haben!

Bei Jörn bedanke ich mich dafür, dass er mir die Überlebenskünste im dunklen Wald der Regulation des T3SSs beigebracht hat.

Besonderer Dank gilt meinen Korrekturlesern (Sabrina, Vanessa und Ines) für ihre Tapferkeit beim Eintauchen in die spannende aber äußerst komplizierte und für den mentalen Zustand gefährliche Welt der Regulation.

Der gesamten MIBI Arbeitsgruppe danke ich für die beste Arbeitsatmosphäre, die ich mir nur wünschen konnte. Auch dafür, dass ich in vielen von euch gute Freunde gefunden habe, die ich nicht mehr missen will.

Mein allergrößter Dank gilt natürlich meiner Familie. Ein ganz großes Dankeschön geht an meinen Ehemann Marius, der mich immer grenzenlos unterstützt hat, ein großes Verständnis für meine manchmal schlechte Laune hatte und mir sehr viel Rückhalt gegeben hat. Ein besonderes Dankeschön geht an meinen Vater Stephan, ohne den ich niemals da gewesen wäre, wo ich jetzt bin. Aus tiefsten Herzen danke ich meiner Mutter Nelli für ihre Liebe, ihre Unterstützung und die Kraft, die sie mir immer gegeben hat und die mir unglaublich geholfen hat, immer weiter zu machen und nie aufzugeben. Mit Euch an meiner Seite kann ich alles schaffen!

Curriculum vitae

Personal information

Name:	Maria Kusmierek née Pimenova
Date of birth:	9 May 1988
Place of birth:	Moscow
Nationality:	Russian
Material status:	married
Private address:	Am Bennevoß 35 38259 Salzgitter, Germany
Phone:	+49 (0)151-51891246
e-mail:	m.pimenova88@gmail.com

Scientific education and academic appointments

2014 May	**Doctoral student, Helmholtz Centre for Infection Research, Department of Molecular Infection Biology, Braunschweig, Germany** Department of Molecular Infection Biology of Prof. Dr. Petra Dersch Thesis on *Yersinia pseudotubrculosis* Type III secretion system: Identification of regulatory mechanisms important to control *Yersinia pseudotuberculosis* Type III secretion and virulence.
2012-2014	**Master Degree in Biology, TU Braunschweig, Braunschweig, Germany** Department of Molecular Infection Biology of Prof. Dr. Petra Dersch Thesis on *Yersinia pseudotubrculosis* LcrF: Regulation of the cell contact-dependent expression of the major virulence activator LcrF in *Yersinia pseudotuberculosis*.
2010-2011	**Doctoral student, Lomonossov Moscow State University, Moscow, Russia** Department of microbiology Project: Kefir grains as a promising source for novel probiotics.
2010	**Research internship at Institute of Immunological Engineering of the State Concern "Biopreparation", Lyubuchany, Chekhov, Russia** Project: Genotyping and Analysis of Lactic Acid Bacteria Isolated from National Sour Milk Produce Included into Functional Nutrition Rations in the Residence Regions of Persons with Active Longevity in the CIS Countries.
2005-2010	**Diplom Degree with distinction in Biology, Lomonossov Moscow State University, Moscow, Russia** Department of microbiology Project: Isolation, identification and characterisation of new promising probiotic bacteria.
1994-2005	**School Nr. 875 Moscow, Russia** General qualification for university entrance, grade 'with distinction'

Awards

2016	**1st one minute presentation prize**, Annual PhD retreat, HZI International Graduate School for Infection Research (GS-FIRE)
2015	**3d Poster prize**, Annual PhD retreat, HZI International Graduate School for Infection Research (GS-FIRE)

Teaching

2015	**Supervision of the scientific master project including the revision of the project report (3 months)** Project: The role of Degradosome in regulation of *Yersinia pseudotubrculosis* Type III secretion system
2014-2018	**Annual supervision of the practical courses of the TU Braunschweig** Topic: Molecular Infection Biology

Conference Presentation

2018 Aug	Young Microbiologists Symposium 2018, Belfast (Talk)
2018 Jul	RNA Meeting on Sensory and Regulatory RNA, Gießen (Poster)
2018 Apr	Annual Conference 2018 of the Association for General and Applied Microbiology, Wolfsburg (Poster)
2017 Mar	5th Joint Conference of the DGHM & VAAM 2017, Würzburg (Talk)
2016 Jul	Workshop on Sensory and regulatory RNAs in Prokaryotes, Münich (Poster)
2016 May	5th National Yersinia Meeting, Münster (Talk)
2015 Sep	Follow-up meeting of the members of DFG priority program SPP1258: "Sensatory and Regulatory RNAs in Prokaryotes and CRISPR-Cas", Braunschweig (Poster)
2014 Sep	Follow-up meeting of the members of DFG priority program SPP1258: „Sensory and regulatory RNAs in Prokaryotes“, Jena (Talk)
2014 May	4th National Yersinia Meeting, Hamburg (Poster)

Work Experience

2015 Oct – 2018 Sep	**Helmholtz Centre for Infection Research** Scientific assistant, PhD student
2010 Jan – 2010 Dec	**Research internship at Institute of Immunological Engineering of the State Concern "Biopreparation", Lyubuchany, Chekhov, Russia** Scientific assistant

List of publications

Kusmierek M, Hoßmann J, Steinmann R, Vollmer I, Volk M, Opitz W, Heroven AK, Wolf-Watz H, Dersch P. A bacterial translocator hijacks riboregulators to control type III secretion in response to host cell contact. PLoS pathog. *Expected to be submitted in September 2018*

Kusmierek M*, Heroven AK*, Beckstette M, Nuss AM, Dersch P. (2018) Discovering *Yersinia*-Host Interactions by Tissue Dual RNA-seq. Biology of *Yersinia* Infection. *Methods and Molecular Biology Protocols*. Springer. *Accepted*. * equal contribution

Kusmierek M, Dersch P. (2018) Regulation of host-pathogen interactions via the post-transcriptional Csr/Rsm system. **Current Opinion in Microbiology** 41: 58-67. doi: 10.1016/j.mib.2017.11.022. Epub 2017 Dec 5.

Nuss AM, Beckstette M, **Pimenova M**, Schmühl C, Opitz W, Pisano F, Heroven AK, Dersch P. (2017) Tissue dual RNA-seq: a fast discovery path for infection-specific functions and riboregulators shaping host-pathogen transcriptomes. **PNAS** 114(5): E791-E800. doi: 10.1073/pnas.1613405114. Epub 2017 Jan 17.